

Handbook T-II

Science of Technology and Innovation

LEDESMA-ALBERT, Aida

Coordinator

ECORFAN®

ECORFAN®

Coordinator

LEDESMA-ALBERT, Aida. PhD

Editor in Chief

VARGAS-DELGADO, Oscar. PhD

Executive Director

RAMOS-ESCAMILLA, María. PhD

Editorial Director

PERALTA-CASTRO, Enrique. MSc

Web Designer

ESCAMILLA-BOUCHAN, Imelda. PhD

Web Diagrammer

LUNA-SOTO, Vladimir. PhD

Editorial Assistant

TREJO-RAMOS, Iván. BsC

Translator

DÍAZ-OCAMPO, Javier. BsC

Philologist

RAMOS-ARANCIBIA, Alejandra. BsC

ISBN: 978-607-8695-89-8

ECORFAN Publishing Label: 607-8695

HSTI Control Number: 2022-003

HSTI Classification (2022): 281122-0003

©ECORFAN-México, S.C.

No part of this writing protected by the Federal Copyright Law may be reproduced, transmitted or used in any form or by any means, graphic, electronic or mechanical, including, but not limited to, the following: Quotations in radio or electronic journalistic data compilation articles and bibliographic commentaries. For the purposes of articles 13, 162, 163 fraction I, 164 fraction I, 168, 169, 209 fraction III and other relative articles of the Federal Copyright Law. Infringements: Being compelled to prosecute under Mexican copyright law. The use of general descriptive names, registered names, trademarks, or trade names in this publication does not imply, even in the absence of a specific statement, that such names are exempt from the relevant protection in laws and regulations of Mexico and therefore free for general use by the international scientific community. SRS is part of ECORFAN Media (www.ecorfan.org)

Handbooks

Definition of Handbooks

Scientific Objectives

To support the International Scientific Community in its written production of Science, Technology and Innovation in the CONACYT and PRODEP research areas.

ECORFAN-Mexico, S.C. is a Scientific and Technological Company in contribution to the formation of Human Resources focused on the continuity in the critical analysis of International Research and is attached to the RENIECYT of CONACYT with number 1702902, its commitment is to disseminate research and contributions of the International Scientific Community, academic institutions, agencies and entities of the public and private sectors and contribute to the linkage of researchers who perform scientific activities, technological developments and training of specialized human resources with governments, businesses and social organizations.

To encourage the interlocution of the International Scientific Community with other study centres in Mexico and abroad and to promote a wide incorporation of academics, specialists and researchers to the serial publication in Science Niches of Autonomous Universities - State Public Universities - Federal IES - Polytechnic Universities - Technological Universities - Federal Technological Institutes - Teacher Training Colleges - Decentralised Technological Institutes - Intercultural Universities - S&T Councils - CONACYT Research Centres.

Scope, Coverage and Audience

Handbooks is a product edited by ECORFAN-Mexico S.C. in its Holding with repository in Mexico, it is a refereed and indexed scientific publication. It admits a wide range of contents that are evaluated by academic peers by the double-blind method, on topics related to the theory and practice of the CONACYT and PRODEP research areas respectively with diverse approaches and perspectives, which contribute to the dissemination of the development of Science, Technology and Innovation that allow arguments related to decision-making and influence the formulation of international policies in the field of Science. The editorial horizon of ECORFAN-Mexico® extends beyond academia and integrates other segments of research and analysis outside that field, as long as they meet the requirements of argumentative and scientific rigour, in addition to addressing issues of general and current interest of the International Scientific Society.

Editorial Board

ROCHA - RANGEL, Enrique. PhD
Oak Ridge National Laboratory

CARBAJAL - DE LA TORRE, Georgina. PhD
Université des Sciences et Technologies de Lille

GUZMÁN - ARENAS, Adolfo. PhD
Institute of Technology

CASTILLO - TÉLLEZ, Beatriz. PhD
University of La Rochelle

FERNANDEZ - ZAYAS, José Luis. PhD
University of Bristol

DECTOR - ESPINOZA, Andrés. PhD
Centro de Microelectrónica de Barcelona

TELOXA - REYES, Julio. PhD
Advanced Technology Center

HERNÁNDEZ - PRIETO, María de Lourdes. PhD
Universidad Gestalt

CENDEJAS - VALDEZ, José Luis. PhD
Universidad Politécnica de Madrid

HERNANDEZ - ESCOBEDO, Quetzalcoatl Cruz. PhD
Universidad Central del Ecuador

Arbitration Committee

GAXIOLA - PACHECO, Carelia Guadalupe. PhD
Universidad Autónoma de Baja California

GONZÁLEZ - JASSO, Eva. PhD
Instituto Politécnico Nacional

FLORES - RAMÍREZ, Oscar. PhD
Universidad Politécnica de Amozoc

ARROYO - FIGUEROA, Gabriela. PhD
Universidad de Guadalajara

BAUTISTA - SANTOS, Horacio. PhD
Universidad Popular Autónoma del Estado de Puebla

GUTIÉRREZ - VILLEGAS, Juan Carlos. PhD
Centro de Tecnología Avanzada

HERRERA - ROMERO, José Vidal. PhD
Universidad Nacional Autónoma de México

MARTINEZ - MENDEZ, Luis G. PhD
Universidad Autónoma de Baja California

LUGO - DEL ANGEL, Fabiola Erika. PhD
Instituto Tecnológico de Ciudad Madero

NÚÑEZ - GONZÁLEZ, Gerardo. PhD
Universidad Autónoma de Querétaro

Handbooks

Definition of Handbooks

Scientific Objectives

To support the International Scientific Community in its written production of Science, Technology and Innovation in the CONACYT and PRODEP research areas.

ECORFAN-Mexico, S.C. is a Scientific and Technological Company in contribution to the formation of Human Resources focused on the continuity in the critical analysis of International Research and is attached to the RENIECYT of CONACYT with number 1702902, its commitment is to disseminate research and contributions of the International Scientific Community, academic institutions, agencies and entities of the public and private sectors and contribute to the linkage of researchers who perform scientific activities, technological developments and training of specialized human resources with governments, businesses and social organizations.

To encourage the interlocution of the International Scientific Community with other study centres in Mexico and abroad and to promote a wide incorporation of academics, specialists and researchers to the serial publication in Science Niches of Autonomous Universities - State Public Universities - Federal IES - Polytechnic Universities - Technological Universities - Federal Technological Institutes - Teacher Training Colleges - Decentralised Technological Institutes - Intercultural Universities - S&T Councils - CONACYT Research Centres.

Scope, Coverage and Audience

Handbooks is a product edited by ECORFAN-Mexico S.C. in its Holding with repository in Mexico, it is a refereed and indexed scientific publication. It admits a wide range of contents that are evaluated by academic peers by the double-blind method, on topics related to the theory and practice of the CONACYT and PRODEP research areas respectively with diverse approaches and perspectives, which contribute to the dissemination of the development of Science, Technology and Innovation that allow arguments related to decision-making and influence the formulation of international policies in the field of Science. The editorial horizon of ECORFAN-Mexico® extends beyond academia and integrates other segments of research and analysis outside that field, as long as they meet the requirements of argumentative and scientific rigour, in addition to addressing issues of general and current interest of the International Scientific Society.

Assignment of Rights

By submitting a Scientific Work to ECORFAN Handbooks, the author undertakes not to submit it simultaneously to other scientific publications for consideration. To do so, the author must complete the Originality Form for his or her Scientific Work.

The authors sign the Authorisation Form for their Scientific Work to be disseminated by the means that ECORFAN-Mexico, S.C. in its Holding Mexico considers pertinent for the dissemination and diffusion of their Scientific Work, ceding their Scientific Work Rights.

Declaration of Authorship

Indicate the name of 1 Author and a maximum of 3 Co-authors in the participation of the Scientific Work and indicate in full the Institutional Affiliation indicating the Unit.

Identify the name of 1 author and a maximum of 3 co-authors with the CVU number -PNPC or SNI-CONACYT- indicating the level of researcher and their Google Scholar profile to verify their citation level and H index.

Identify the Name of 1 Author and 3 Co-authors maximum in the Science and Technology Profiles widely accepted by the International Scientific Community ORC ID - Researcher ID Thomson - arXiv Author ID - PubMed Author ID - Open ID respectively.

Indicate the contact for correspondence to the Author (Mail and Telephone) and indicate the Contributing Researcher as the first Author of the Scientific Work.

Plagiarism Detection

All Scientific Works will be tested by the PLAGSCAN plagiarism software. If a Positive plagiarism level is detected, the Scientific Work will not be sent to arbitration and the receipt of the Scientific Work will be rescinded, notifying the responsible Authors, claiming that academic plagiarism is typified as a crime in the Penal Code.

Refereeing Process

All Scientific Works will be evaluated by academic peers using the Double Blind method. Approved refereeing is a requirement for the Editorial Board to make a final decision which will be final in all cases. MARVID® is a spin-off brand of ECORFAN® specialised in providing expert reviewers all of them with PhD degree and distinction of International Researchers in the respective Councils of Science and Technology and the counterpart of CONACYT for the chapters of America-Europe-Asia-Africa and Oceania. The identification of authorship should only appear on a first page, which can be removed, in order to ensure that the refereeing process is anonymous and covers the following stages: Identification of ECORFAN Handbooks with their author occupancy rate - Identification of Authors and Co-authors - PLAGSCAN Plagiarism Detection - Review of Authorisation and Originality Forms-Assignment to the Editorial Board - Assignment of the pair of Expert Referees - Notification of Opinion - Statement of Observations to the Author - Modified Scientific Work Package for Editing - Publication.

ECORFAN Science of Technology and Innovation

Volume II

The Handbook will offer volumes of selected contributions from researchers who contribute to the scientific dissemination activity Tecnológico de Estudios Superiores de Jocotitlán in their areas of research in Technology and Innovation. In addition to having a total evaluation, in the hands of the directors of the Tecnológico de Estudios Superiores de Jocotitlán, the quality and timeliness of its chapters, each individual contribution was refereed to international standards (RESEARCH GATE, MENDELEY, GOOGLE SCHOLAR and REDIB), the Handbook thus proposes to the academic community, recent reports on new developments in the most interesting and promising areas of research in the Technology and Innovation.

Ledesma-Albert, Aida

Coordinator

Science of Technology and Innovation **T-II** *Handbooks*

Tecnológico de Estudios Superiores de Jocotitlán– México.

November, 2022

DOI: 10.35429/H.2022.3.1.181

Preface

López, Reyes, Antonio and Caballero seek to explain the main encryption techniques currently used, the fundamental basis of their encryption process, the importance of the most known standards in the computer era, the difference between symmetric and asymmetric encryption, when it can be considered hybrid encryption and where they are commonly used.

Reyes, Sánchez, López and Antonio, divide this project into two phases: the first is to determine the performance of the algorithm for a small sample of images and video analysis, and the second is to extend the data corpus for automatic analysis of new samples. It is worth mentioning that this work focuses on the development of the first phase, which is based on the development and training of the algorithm based on Convolutional Neural Networks using MobileNet for the correct identification and classification of the cob.

Bernal, Sanchez and Salazar, evaluate the Diagnosis of Urban Solid Waste (USW) in the State of Mexico, through the sustainability framework. Urban areas represent a focus of attention for local administrations since they represent spaces of economic importance in the Gross Domestic Product.

Oguri, Escobar, Pretel and García, present the partial results of a research project whose objective is to develop an innovative solution for gypsum boards with plastic aggregates such as pet and natural Ixtle fibers.

Soriano, Lopez, Cayetano and Castrejon study the spinodal decomposition during aging of Fe-Cr alloys by numerical solution of the linear and nonlinear partial differential Cahn-Hilliard equations using the explicit finite difference method.

Caballero, Muñoz, Ramos and López refer to a literature review of the research carried out on the development of proposals to identify fire situations in natural ecosystems. The presence of fire is identified by means of computational systems that combine computer vision, artificial intelligence and sophisticated monitoring variables that can indicate the presence of fire in a natural area.

Vargas & Rodriguez present an empirical analysis to observe the influence of industrial property, measured as Patents, on the Gross Domestic Product (GDP) of two Latin American countries: Mexico - Brazil in the period 2000 - 2015 as a phase I study on patents and their effects. A unit root test is applied. The results show the existence of a positive relationship between the level of innovation and GDP.

Salazar, Pichardo, Sanchez and Pichardo present the basic techniques for the preparation of specimens to be evaluated metallographically, addressing the following topics: Generalities, Atomic structure: Nucleation and atoms, Crystalline structure: Perfect crystals and crystals with imperfections. Substructure: Subgrains and other cellular structures, Microstructure: Grains of single metallic phases and arrangements of the configuration of alloys with multiple phase systems, Texture. Macrostructure. and Metallographic practice applicable to all metals. It is concluded that this study lays the foundation for further and specific metallographic studies of ferrous and non-ferrous alloys.

Mastache, López, Viguera and Hermenegildo show the results of experiments related to the obtaining of zinc (Zn) nanoparticles, on glass or alumina substrates by the thermal evaporation process in a high temperature tubular furnace at 800°C, with a flow of 400 sccm of inert gas (Argon) used as carrier gas, to deposit the metallic Zn particles in the cold zone of the furnace.

Sanchez, Bernal, and Salazar simulated a sustainable process for the production of ethanol from the monosaccharide glucose. The thermodynamic model used for the process was NRTL-RK (based on activity coefficients) due to the polar nature and non-ideal behavior of the species involved. The process was carried out in three steps. First, glucose in aqueous solution was subjected to a fermentation process using a stoichiometric reactor. The second stage consisted of carbon dioxide degassing using two flash tank systems. In the third stage, a RadFrac distillation column was used to facilitate the separation of ethanol and water.

LEDESMA-ALBERT, Aida. PhD

Content

	Page
1 Analysis of the main encryption systems and their applicability LÓPEZ-GONZÁLEZ, Erika, REYES-NAVA, Adriana, ANTONIO-VELÁZQUEZ, Juan A. and CABALLERO-HERNÁNDEZ, Héctor	1-15
2 Classification of mature corn cobs using Convolutional Neural Networks REYES-NAVA, Adriana, SANCHEZ-FLORES, Diego, LÓPEZ-GONZÁLEZ, Erika and ANTONIO-VELAZQUEZ, Juan Alberto	16-31
3 Diagnosis of municipal solid waste (MSW), in the State of Mexico BERNAL-MARTÍNEZ, Lina Agustina, SÁNCHEZ-OROZCO, Raymundo and SALAZAR-PERALTA Araceli	32-48
4 Ecological panel based on plastic aggregates, natural fibers, and plaster OGURI, Leticia, ESCOBAR, Marlem Guadalupe, PRETEL, Ana María and GARCIA, Nidia Miriam	49-64
5 Phase simulation of the Fe-Cr alloy system SORIANO-VARGAS, Orlando, LOPEZ-HIRATA, Víctor M., CAYETANO-CASTRO, Nicolas, CASTREJON-SANCHEZ, Víctor H.	65-83
6 Hot Spot Identification Systems for Wildfire Control CABALLERO-HERNÁNEZ, Héctor, MUÑOZ-JIMÉNEZ, Vianney, RAMOS-CORCHADO, Marco A. and LÓPEZ-GONZALEZ, Erika	84-94
7 Influence of patents on economic growth: An empirical analysis Mexico-Brazil VARGAS-GONZÁLEZ, Jaqueline & RODRIGUEZ-HERNÁNDEZ, Gloria Patricia	95-105
8 Introduction to Metallographic Study SALAZAR-PERALTA, Araceli, PICHARDO-SALAZAR, José Alfredo, SÁNCHEZ-OROZCO Raymundo and PICHARDO-SALAZAR Ulises	106-129
9 Obtaining Process of Zinc Oxide (ZnO) in laboratory with Evaporation and Thermal Oxidation MASTACHE-MASTACHE, Jorge Edmundo, LÓPEZ-RAMÍREZ, Roberto, VIGUERAS-SANTIAGO, Enrique and HERMENEGILDO-MEJÍA, Francisco Javier	130-143
10 Sensitivity analysis of ethanol production process using Aspen Plus SÁNCHEZ-OROZCO, Raymundo, BERNAL-MARTÍNEZ, Lina Agustina and SALAZAR-PERALTA Araceli	144-160

Chapter 1 Analysis of the main encryption systems and their applicability

Capítulo 1 Análisis de los principales sistemas de cifrado y su aplicabilidad

LÓPEZ-GONZÁLEZ, Erika†*, REYES-NAVA, Adriana, ANTONIO-VELÁZQUEZ, Juan A. and CABALLERO-HERNÁNDEZ, Héctor

Tecnológico de Estudios Superiores de Jocotitlán, Carretera Toluca-Atacomulco km 44.8, Ejido de San Juan y San Agustín, Jocotitlán, Edo.

ID 1st Author: *Erika, López-González* / **ORC ID:** 0000-0001-7279-5111, **CVU CONACYT ID:** 289386

ID 1st Co-author: *Adriana, Reyes-Nava* / **ORC ID:** 0000-0002-4440-909X

ID 2nd Co-author: *Juan A., Antonio-Velázquez* / **ORC ID:** 0000-0003-3052-3171

ID 3rd Co-author: *Hector, Caballero-Hernandez* / **ORC ID:** 0000-0002-2790-833X, **CVU CONACYT ID:** 445998

DOI: 10.35429/H.2022.3.1.15

E. López, A. Reyes, J. Antonio and H. Caballero

*erika.lopez@tesjo.edu.mx

A. Ledesma (AA.). Science of Technology and Innovation. Handbooks-TII-©ECORFAN-Mexico, 2022.

Abstract

Virtual work, e-commerce, digital health, distance, or virtual education grew exponentially thanks to the confinement due to the Covid-19 pandemic. As a result, the same happened with attacks and security incidents, caused by various circumstances. Personal data is generally the main target of hackers, this includes financial institutions. In 2020 alone, 12 known cybersecurity events occurred in Mexico that included institutions such as Condusef, SAT, Banxico, the secretary of public function, among others, in the last one personal data of public officials were violated and exposed (Riquelme, 2021).

With the evolution of technology, attacks become increasingly sophisticated. However, one of the most used and effective systems to protect data is encryption that is related to computer security offers solutions to this problem since it is a discipline that addresses various techniques, applications and devices responsible for ensuring the integrity and privacy of the information of both the computer system and its users. This work seeks to explain the main encryption techniques currently used, the fundamental basis of its encryption process, the importance of the best-known standards in the computer age, the difference between symmetric encryption and asymmetric encryption, when it can be considered hybrid encryption and where they are commonly used.

Asymmetric, Encrypted, Symmetric, Systems, Integrity

Resumen

El trabajo virtual, comercio electrónico, la salud digital, la educación a distancia o virtual, crecieron exponencialmente gracias al confinamiento por la pandemia de Covid-19. Como consecuencia lo mismo sucedió con los ataques e incidentes de seguridad, provocados por diversas circunstancias. Los datos personales generalmente son el principal objetivo de los hackers, esto incluye a las entidades financieras. Tan sólo en el año 2020 ocurrieron 12 eventos de ciberseguridad conocidos en México que incluía a instituciones como Condusef, SAT, Banxico, La secretaria de función pública, entre otras, en la última se vulneraron y expusieron datos personales de los funcionarios públicos (Riquelme, 2021).

Con la evolución de la tecnología, los ataques se vuelven cada vez más sofisticados. Sin embargo, uno de los sistemas más usados y efectivos para proteger los datos es el encriptado que se relaciona con la seguridad informática ofrece soluciones a esta problemática ya que es una disciplina que aborda diversas técnicas, aplicaciones y dispositivos encargados de asegurar la integridad y privacidad de la información tanto del sistema informático y sus usuarios. Este trabajo busca explicar las principales técnicas de cifrado utilizadas actualmente, la base fundamental de su proceso de cifrado, la importancia que tienen en la era informática los estándares más conocidos, la diferencia entre el cifrado simétrico y el cifrado asimétrico, en qué momento puede considerarse cifrado híbrido y dónde comúnmente son empleados.

Asimétrico, Cifrado, Simétrico, Sistemas, Integridad

1. Introduction

Various public and private institutions have suffered attacks and security incidents, putting the information of hundreds of thousands of people at risk and/or vulnerability (Gil Vera, 2017). Where those affected by the personal data breach can do little to protect their information.

Therefore, security strategies applied at the national level must be sought, as mentioned by Romero, there are different attacks that are perpetrated directly or indirectly in the financial sector, in public or private institutions by organized crime organizations, this makes it important to increase security in the various sectors of the country to avoid risks (Romero, 2018), especially economic that can cause a high impact, this is a task that not only concerns the ICT infrastructures that support the different business processes. It is an activity that involves everyone, including industrial control systems. Therefore, it must seek to address threats to national, local and personal security that guarantee the stability, integrity, availability and control of information.

The study of security depends on the origins or sources of threats to systems. (Haro, 2011) In the field of logical security, information is protected within its own environment with the use of security tools, and can be defined as a set of operations and techniques aimed at protecting information against destruction, modification, improper disclosure. gives or simply delays in its gestation; That is, it applies barriers and procedures that safeguard access to data and only access them, the people authorized to do so. Depending on the application required for the processing of information or the means by which it is transmitted, so will be the services to be covered and/or the objectives of all security services.

The goals of logical security are to restrict access to data, programs, or files, to ensure that users can work with confidence that they won't modify information or resources that don't belong to them. Ensure the correct use of information resources with the appropriate procedures and if the information is transmitted it is received guaranteeing security. Some of the objectives of security are to guarantee some services, table 1.

Table 1 Security Objectives

Objective	Service
Keep information secret, for everyone except those who have access authorization.	Confidentiality
Ensure that the data has not been altered in any way, and if it was correctly altered by the right person	Integrity
Have the information at the required and authorized time	Availability
Check the source of the message.	Authentication
Verify the identity of a participating entity.	Identification
Be able to relate a message to an entity.	Company digital
Approval of certain information by a trusted entity.	Certificate
Prevent the denial of previous agreements or actions. Not being able to deny actions	Non-repudiation
Being able to hide the identity of an entity involved in some process	Anonymity

Source: Own Work

One of the sciences responsible for safeguarding security is cryptology whose main objective is to offer security to data, hiding information, using different techniques. This is derived from cryptography, which is responsible for studying the algorithms, protocols and systems that are used to protect information and provide security to communications and entities that need it. Currently, cryptography is the only method capable of ensuring the correct use and protection of data, guaranteeing confidentiality, availability, integrity and authentication of data. Therefore, it is important to know the operation of the various encryption systems that will be described below.

2. Basis of encryption systems

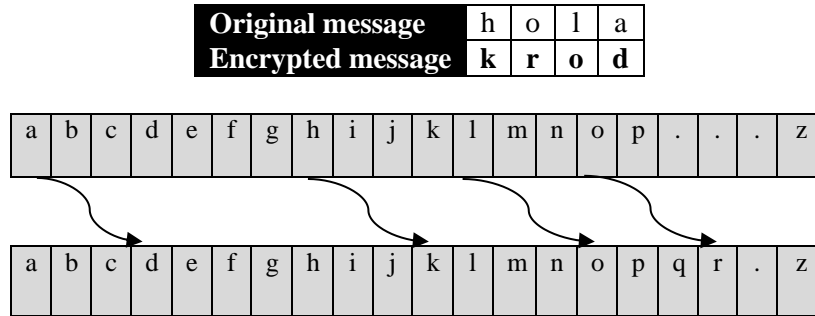
2.1 Replacement

The substitution technique is used as a base process in various systems of cryptography, where its main objective is only to replace an occupied character, by another, it is often done by a character that belongs to the same system used; either numeric or alphanumeric, depending on the encryption system, however it takes different variants, currently it is used by standards such as DES, AES.

An example of the operation of substitution encryption can be seen in Figure 1 that describes one of the oldest forms of cipher and consists of replacing one character with another of the alphabet considering a number as a key (k), this key will indicate how many characters will have to be advanced in the previously ordered alphabet. In this example, the key k is 3 so for each letter of the message will advance 3 positions of the alphabet, finding a different character from the original. If the word "hello" is considered taken from the alphabet that already has a defined order as shown in figure 1 shaded part, the letter h is replaced by the d, having traveled the 3 positions indicated by the key; for example, the letter o is replaced by the r, the letter l by the letter o, and a for d; thus having a surrogate encrypted message; Then the word hello of the original message is replaced by the letters krod which would be the encrypted message by substitution, as marked in Figure 1.

In the example of figure 1, the decryption will consist of placing the encrypted message and now instead of advancing the 3 positions of the value of k (key), in the array of the alphabet, those same positions will be regressed, in such a way that the original characters of the message are located, if the value of **k** is not correct the original message can not be deciphered.

Figure 1 Substitution Encryption



Source: Own Work

It is important to mention that cipher systems occupy this principle, but considering other elements or characteristics, for example, with bits, or hexadecimal numbers and will be described later with encryption standards.

2.2 Transposition

Transposition encryption consists of hiding the original message, but placing the characters in different positions or order, there are different techniques and ways to perform it, usually a key is used, for example, the transposition by columns with key works as shown in table 2. This technique basically consists of choosing a word that will be the key to encrypt the message, in the example the key is "secret", and of course the message, which in this case is "hello as you are today". The operation is described in the following steps:

1. First it will be necessary to place in an array the keyword "secret", considering a character by position of the array, as shown in Table 2,
2. The letters of the key are numbered according to the order in which they appear in the alphabet. In case a letter is repeated, it will be assigned the number following the first, as is the case with the letter e in the example.
3. Once the key values have been assigned, the message to be encrypted is written by placing letter by letter at the same height of the calve occupying one cell at a time and according to the length of the key, if the message is long it will continue in the next row, until all the columns are completed (according to the key) and finish writing the message.
4. If the characters in the message are not enough, some other character known as "*" is added.
5. To obtain the encrypted message, the letters will be written considering the columns according to the consecutive order of numbers, that is, first all the characters that seem in the column numbered with 1, then those of column 2, and so on, you have to obtain the encrypted message, as seen in the example, table2. In this case column 1 corresponds to the letter a and is marked with red, column 2 is c, etc. So the encrypted message is "oa*I hoo syaehmsct*".

Table 2 Substitution encryption

Key	s	e	c	r	e	t	a
Position and/or order	6	3	2	5	4	7	1
Original message	h	o	l	a	c	o	*
	m	o	e	s	t	a	*
	s	h	o	y	*	*	*
Encrypted message	oa*I hoo syaehmsct*						

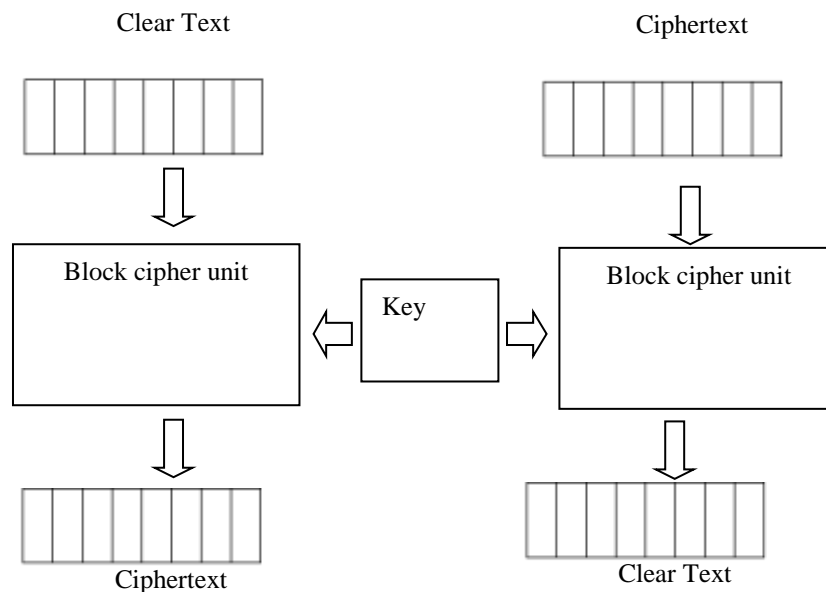
Source: Own Work

The decryption process is reversed, that is, it is necessary to know the key and having the length of the encrypted message you can know the appropriate rows to the table to build the array. Starting by placing the characters in the column with the number 1, the same for the 2, so on, until you get all the columns and find the original message, which will be read by rows

3. Symmetric encryption

This symmetric encryption uses a key to encrypt and with the same key the original message is decrypted, normally it works in blocks of data, binary or hexadecimal. Generally, in the encryption algorithm, does divide the clear text into blocks of equal length, operating on each of these considered as a unit, as can be seen in figure 2. It is important to consider that the encryption process, like the decryption process, is the same. The block length is preset by the encryption algorithm such as the DES or IDEA standard.

Figure 2 Block Cipher



Source: Own Work

3.1 DES Y Triple DES

DES (Data Encryption Standard), is the most studied and widely used data encryption standard, developed by Horst Feistel of IBM, published in March 1975 (Hernández Díaz, 2016). This algorithm works with 64-bit blocks and keys of the same length, described in the following steps, which are also shown in Figure 3:

Data processing

1. To develop the standard encryption process, this is made up of 19 stages, in the first and last, processes called transposition known as initial permutation (IP) and inverse permutation (IP-1) respectively, which are observed in the table 3. This is that the bits are reordered considering the positions marked by each table.

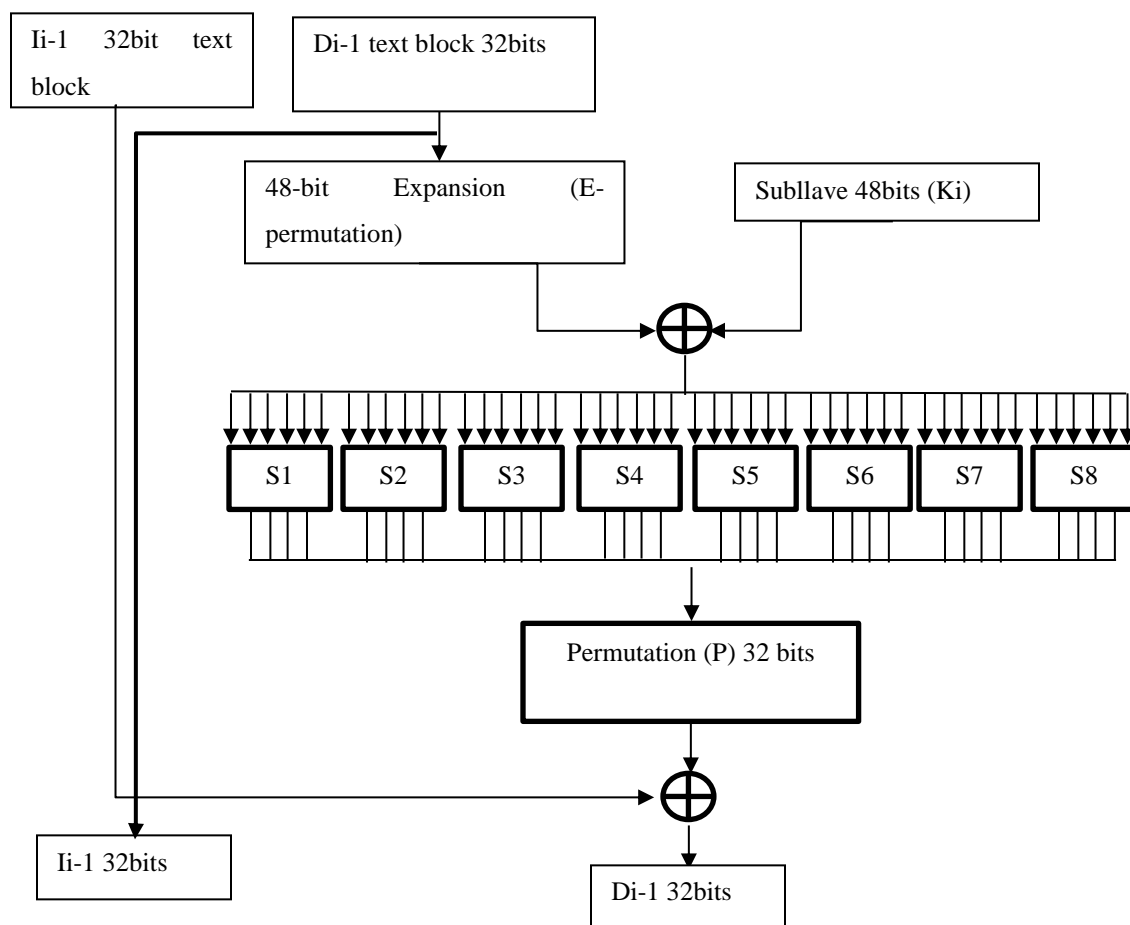
Table 3 Initial permutation (IP) Reverse permutation (IP-1)

58	50	42	34	26	18	10	2	40	8	48	16	56	24	64	32
60	52	44	36	28	20	12	4	39	7	47	15	55	23	63	31
62	54	46	28	30	22	14	6	39	6	46	14	54	22	62	30
64	56	48	40	32	24	16	8	37	5	45	13	53	21	61	29
57	49	41	33	25	17	9	1	36	4	44	12	52	20	60	28
59	51	43	35	27	19	11	3	35	3	43	11	51	19	59	27
61	53	45	37	29	21	13	5	34	2	42	10	50	18	58	26
63	55	47	39	31	23	15	7	33	1	41	9	49	17	57	25

Source: Own Work

2. Subsequently, the information is processed in 64-bit blocks, which will be subdivided into 2 32-bit blocks, so that one 32-bit block will take the left part (I) and the other, the right part (R). This process will be carried out in 16 intermediate stages, considering for the first stage of the 16 the first data right block to which the party function is applied, figure 3, which is used in the 16 stages.
3. The Fiestel function figure 3, expands and reduces the processed data block (right), all this based on permutation tables and substitution boxes, that is, it is composed of an expansion permutation (E), which converts the right block of 32 bits into one of 48 bits and is observed in table 4. For the expansion it is necessary, as indicated in the standard table, to repeat 16 bits, which are already marked in it. Subsequently, an exclusive-or is performed with the data block and the subkey block, the respective K_i value. The result will be a 48-bit data block; then it is necessary to reduce the result of the x-o again to a 32-bit block, eight 6x4-bit boxes are used (S-Box established by the standard). For this, groups of 6 bits must be condensed, the 1st and 6th bits of the block are taken and they form a 2-bit number called m. This value will indicate the row in the corresponding substitution table S (j), with the 2nd to 5th bits another number called n is formed, with four bits that will indicate the column of S (j) so that the intersection between these two numbers in the S boxes they will indicate the number by which the previous group of 6 bits will be replaced in bits, thus reducing the value of the bits, which is observed in Table 5. Considering that the maximum value for the rows is a binary number of 2 digits, where the largest value would be 3, and the maximum number for the columns would be a binary number of 4 that would be represented as greater than 15. This intermediate phase is completed with a permutation (P) that is shown in the second part of table 4 (Publication F. I., 1999), obtaining a processed right block that for the next round will take the place of the left. The resulting 32-bit blocks will swap positions until the required 16 rounds are obtained. As indicated in the general figure 4.

Figure 3 Fiestel function



Source: Own Work

Table 4 Expansion Function (E) and Permutation Function (P)

32	1	2	3	4	5	4	5	16	7	20	21	29	12	28	17
6	7	8	9	8	9	10	11	1	15	23	26	5	18	31	10
12	13	12	13	14	15	16	17	2	8	24	14	32	27	3	9
16	17	18	19	20	21	20	21	19	13	30	6	22	11	4	25
22	23	24	25	24	25	26	27								
28	29	28	29	30	31	32	1								

*Source: Own Work***Table 5** Replacement boxes S

Row	Column															S-boxes	
	0	1	2	3	4	5	6	7	8	9	10	11	12	13	14		15
0	14	4	13	1	2	15	11	8	3	10	6	12	5	9	0	7	S1
1	0	15	7	4	14	2	13	1	10	6	12	11	9	5	3	8	
2	4	1	14	8	13	6	2	11	15	12	9	7	3	10	5	0	
3	15	12	8	2	4	9	1	7	5	11	3	14	10	0	6	13	
0	15	1	8	14	6	11	3	4	9	7	2	13	12	0	5	10	S2
1	3	13	4	7	15	2	8	14	12	0	1	10	6	9	11	5	
2	0	14	7	11	10	4	13	1	5	8	12	6	9	3	2	15	
3	13	8	10	1	3	15	4	2	11	6	7	12	0	5	14	9	
0	10	0	9	14	6	3	15	5	1	13	12	7	11	4	2	8	S3
1	13	7	0	9	3	4	6	10	2	8	5	14	12	11	15	1	
2	13	6	4	9	8	15	3	0	11	1	2	12	5	10	14	7	
3	1	10	13	0	6	9	8	7	4	15	14	3	11	5	2	12	
0	7	13	14	3	0	6	9	10	1	2	8	5	11	12	4	15	S4
1	13	8	11	5	6	15	0	3	4	7	2	12	1	10	14	9	
2	10	6	9	0	12	11	7	12	15	1	3	14	5	2	8	4	
3	3	15	0	6	10	1	13	8	9	4	5	11	12	7	2	14	
0	2	12	4	1	7	10	11	6	8	5	3	15	13	0	14	9	S5
1	14	11	2	12	4	7	13	1	5	0	15	10	3	9	8	6	
2	4	2	1	11	10	13	7	8	15	9	12	5	6	3	0	14	
3	11	8	12	7	1	14	2	13	6	15	0	9	10	4	5	3	
0	12	1	10	15	9	2	6	8	0	13	3	4	14	7	5	11	S6
1	10	15	4	2	7	12	9	5	6	1	13	14	0	11	3	8	
2	9	14	15	5	2	8	12	3	7	0	4	10	1	13	11	6	
3	4	3	2	12	9	5	15	10	11	14	1	7	6	0	8	13	
0	4	11	2	14	15	0	8	13	3	12	9	7	5	10	6	1	S7
1	13	0	11	7	4	9	1	10	14	3	5	12	2	15	8	6	
2	1	4	11	13	12	3	7	14	10	15	6	8	0	5	9	2	
3	6	11	13	8	1	4	10	7	9	5	0	15	14	2	3	12	
0	13	2	8	4	6	15	11	1	10	9	3	14	5	0	12	7	S8
1	1	15	13	8	10	3	7	4	12	5	6	11	0	14	9	2	
2	7	11	4	1	9	12	14	2	0	6	10	13	15	3	5	8	
3	2	1	14	7	4	10	8	13	15	12	9	0	3	5	6	11	

Source: Eown Work

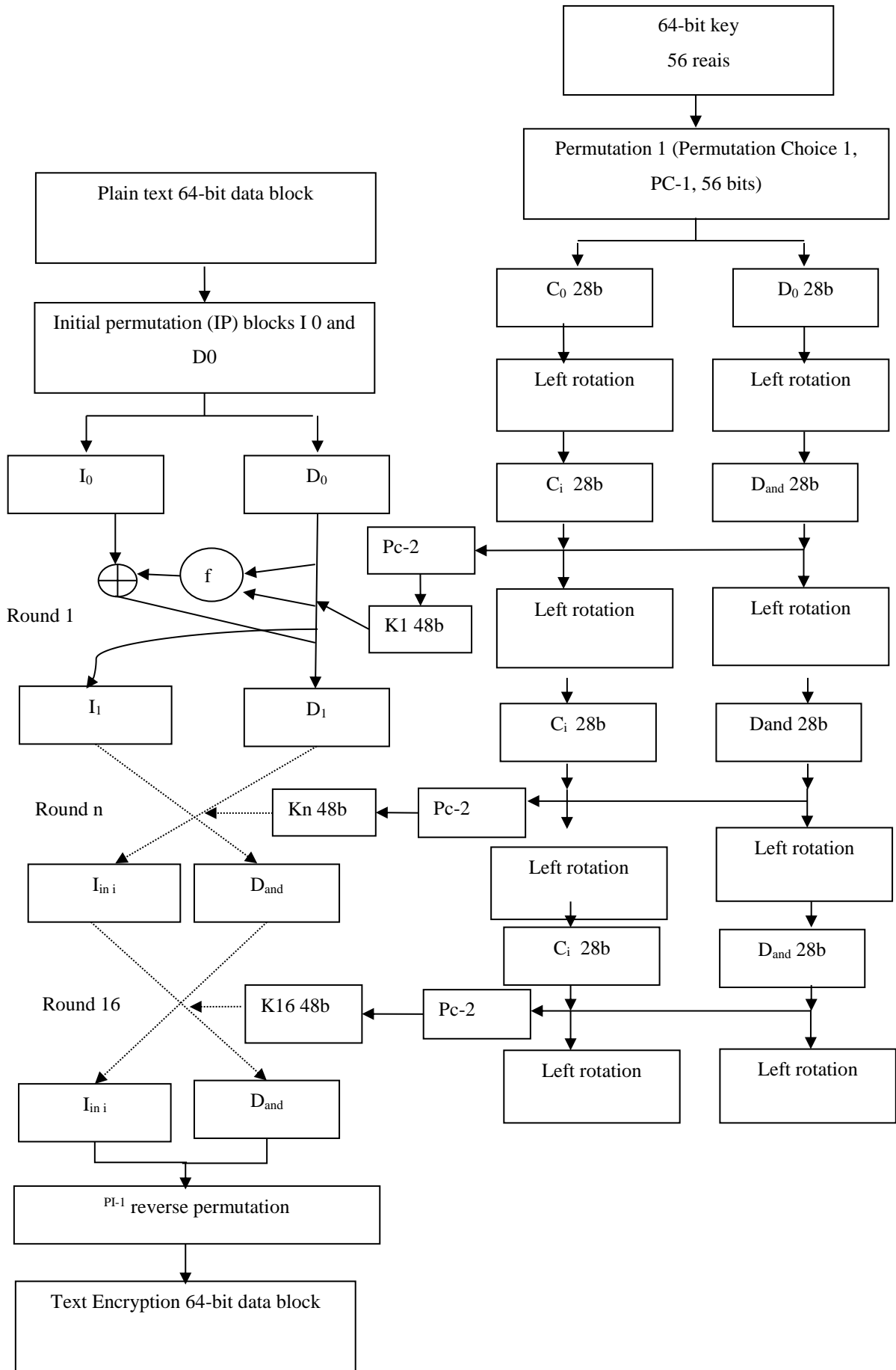
4. In the penultimate stage, the exchange of left and right blocks of 32 bits each is carried out, as shown on the left of figure 4.

Working the keys

1. First for key processing: initially the key block is 64 bits, however, it is reduced in the process to 56 bits that guarantee the effectiveness of encryption, that is, the least significant bits of each byte are eliminated.
2. 16 different subkeys of 48 bits each, obtained from the original 56-bit key, are processed. To obtain the first subkey, an initial permutation (PC-1) is performed, which is shown in Table 6 First Part
3. The subkey is divided into 28-bit blocks which are rotated to the left a certain number of bits depending on the round, for this a table of shift bits provided by the standard is used, table 7.

- Subsequently, the permuted choice is made (PC-2) as a reference to table 6 part 2, of the two halves already rotated; the process is cycled from the rotation of bits to obtain the 16 necessary subkeys, (Sánchez Arriazu, 1999).

Figure 4 DES encryption diagram



Source: Own work

Table 6 Permutation (PC-1) and Permutation (PC-2)

57	49	41	33	25	17	9	1	14	17	11	24	1	5	3	28
28	50	42	34	26	18	10	2	15	6	21	10	23	19	12	4
29	51	43	35	27	19	11	3	26	8	16	7	27	20	13	2
60	52	44	36	63	55	47	39	41	52	31	37	47	55	30	40
31	23	15	7	62	54	46	38	51	45	33	48	44	49	39	56
30	22	14	6	61	53	45	37	34	53	46	42	50	36	29	32
29	21	13	5	28	20	12	4								

Source: Own Work

Table 7 Offset bits according to round

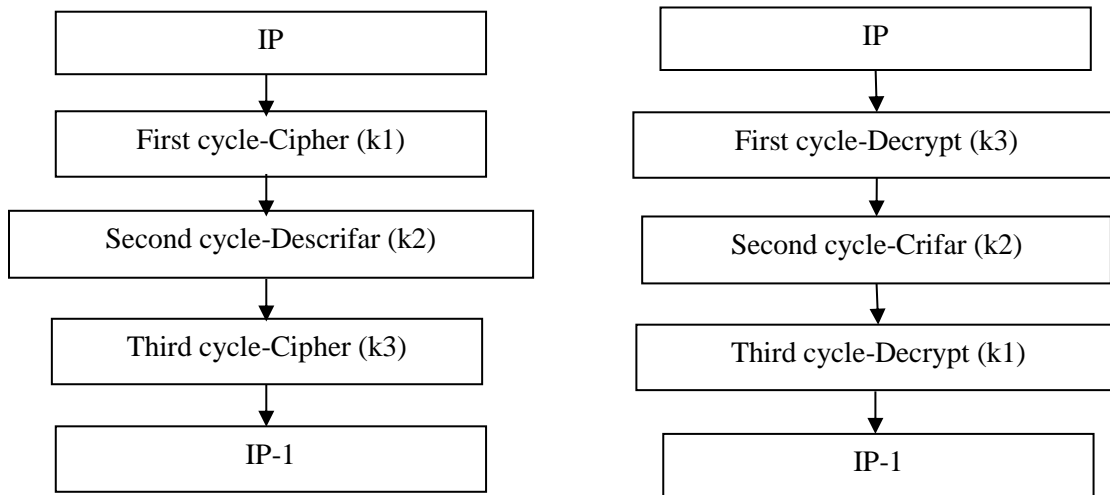
Round	1	2	3	4	5	6	7	8	9	10	11	12	13	14	15	16
Bits	1	1	2	2	2	2	2	2	1	2	2	2	2	2	2	1

Source: Own Work

The decryption process uses the same algorithm that is used to encrypt, only the keys are used in the reverse order, although this standard has already been violated by brute force, it is still used in its Triple DES version.

The Triple DES algorithm consists of applying, as its name indicates, 3 DES cycles. To encrypt, use the CDC process (Encrypt-Decrypt-Encrypt) and to decrypt DCD (Decrypt-Encrypt-Decrypt). There is another less used variant which consists of CCC (Encrypt-Encrypt-Encrypt) for encryption and DDD (Decrypt-Decrypt-Decrypt) for decryption. In the algorithm described in the standard (Publication, 1999) 3 different keys are used (k1-k2-k3), which means that an effective 168-bit key called 3DDEA is used. You can also use 2 different keys (k1-k2), where the key effectiveness would be 112 known as 2TDEA. The technique known as 3TDEA can be seen in Figure 5, where you can see from the first to the last stage described in the previous DES.

Figure 5 Encryption and decryption Triple DES



Source: Own Work


3.2 Advanced Encryption Standard (AES)

The Advanced Encryption Standard officially adopted by the United States National Institute of Standards and Technology (NIST) in October 2000, also known as Rijnda, an acronym formed by the surnames of its authors Joan Deamen and Vincent Rijmen (Diaz, 2012). This encryption system works on data blocks in a 4x4 arrangement with 128 bits in hexadecimal notation, the keys can be 128, 192 and 256. The higher the key, the more secure it will be. Figure 6 shows an example of how the data is stored on the left and the key on the right of the aforementioned image, both represented by tables.

Figure 6 AES Data Block

Flat text				Encryption key			
52	78	A1	11	21	56	89	C2
89	B2	C3	33	41	87	34	F3
22	34	67	F1	59	E4	6D	1C
D2	55	9B	1C	44	6A	2B	11

Hexadecimal notation

Example **0101 0010**


5hex 2hex

Source: Own Work

AES works with substitution and permutation processes in 4 transformation operations called: SubBytes, ShiftRows, MixColumns, and AddRoundKey, applied in 10 rounds, for data encryption shown in Figure 9, general diagram of AES.

The first operation that is applied in AES, is SubBytes which consists of replacing each byte with another according to the S-Box box (provided by the standard) considering row by column, example shown in table 8, where the unit of the hexadecimal number will determine the column and the ten of the hexadecimal number determine the row, being that the intersection of both numbers will be the one taken in the new data set, example for the number 52 of the plain text of figure 6, this would be replaced by 00.

Table 8 Substitution table SubBytes

HEX	0	1	2	3	4	5	6	7	8	9	A	B	C	D	E	F
0	63	7C	77	7B	F2	6B	6F	C5	30	01	67	2B	FE	D7	AB	76
1	CA	82	C9	7D	FA	59	47	F0	TO	D4	A2	OF	9C	A4	72	C0
2	B7	FD	93	26	36	3F	F7	CC	34	A5	E5	F1	71	D8	31	15
3	04	C7	23	C3	18	96	05	9A	07	12	80	E2	EB	27	B2	75
4	09	83	2C	1A	1B	6E	5A	A0	52	3B	D6	B3	29	E3	2F	84
5	53	D1	00	ED	20	FC	B1	5B	6A	CB	BE	39	4A	4C	58	CF
6	D0	1F	AA	FB	43	4D	33	85	45	F9	02	7F	50	3C	9F	A8
7	51	A3	40	8F	92	9D	38	F5	BC	B6	DA	21	10	FF	F3	D2
8	CD	0C	13	EC	5F	97	44	17	C4	A7	7E	3D	64	5D	19	73
9	60	81	4F	DC	22	2A	90	88	46	EE	B8	14	DE	5E	0B	DB
A	E0	32	3A	0A	49	06	24	5C	C2	D3	AC	62	91	95	E4	79
B	E7	C8	37	6D	8D	D5	4E	A9	6C	56	F4	EA	65	7A	AE	08
C	BA	78	25	2E	1C	A6	B4	C6	E8	DD	74	1F	4B	BD	8B	8A
D	70	3E	B5	66	48	03	F6	0E	61	35	57	B9	86	C1	1D	9E
E	E1	F8	98	11	69	D9	8E	94	9B	1E	87	E9	CE	55	28	DF
F	8C	A1	89	0D	BF	E6	42	68	41	99	2D	0F	B0	54	BB	16

Source: Own Work

In ShiftRows one byte is rotated to the left according to the row of the array, where row 0 has no rotation, row 1 rotates 1 byte, row 2 rotates two bytes and the third row 3 bytes to the left, figure 7.

Figure 7 AES ShiftRows

DATA to process ShiftRows				DATA processed ShiftRows			
66	32	45	23	66	32	45	23
04	1f	89	0f	1f	89	0f	04
E5	DC	5F	DF	5F	DF	E5	DC
81	A1	FD	FC	FC	81	A1	FD

Source: Own Work

MixColumns will multiply the 4 bytes of each column by a given matrix, using a linear transformation, obtaining new data for the matrix.

While AddRoundKey does an x-or with column0 of the datablock and column0 of the key, column1 of the datablock with column1 of the key and so on with the 3 columns, figure 8.

These four operations are carried out in the 9 intermediate rounds, while for the last one only SubBytes, ShiftRows and AddRoundKey will be used, an encryption process consulted in the official publication ((Publication F. I., 2001)).

Figure 8 AES AddRoundKey

66	x-or	Ago	=	9C
04		A0		A4
E5		17		F2
81		FE		7F

DATA (column1-3)			KEY (column1-3)		
32	45	23	47	8F	AA
If	89	Of	5F	DC	Ff
DC	5F	DF	E2	A1	D9
A1	FD	FC	D6	C7	E3

Source: Own Work

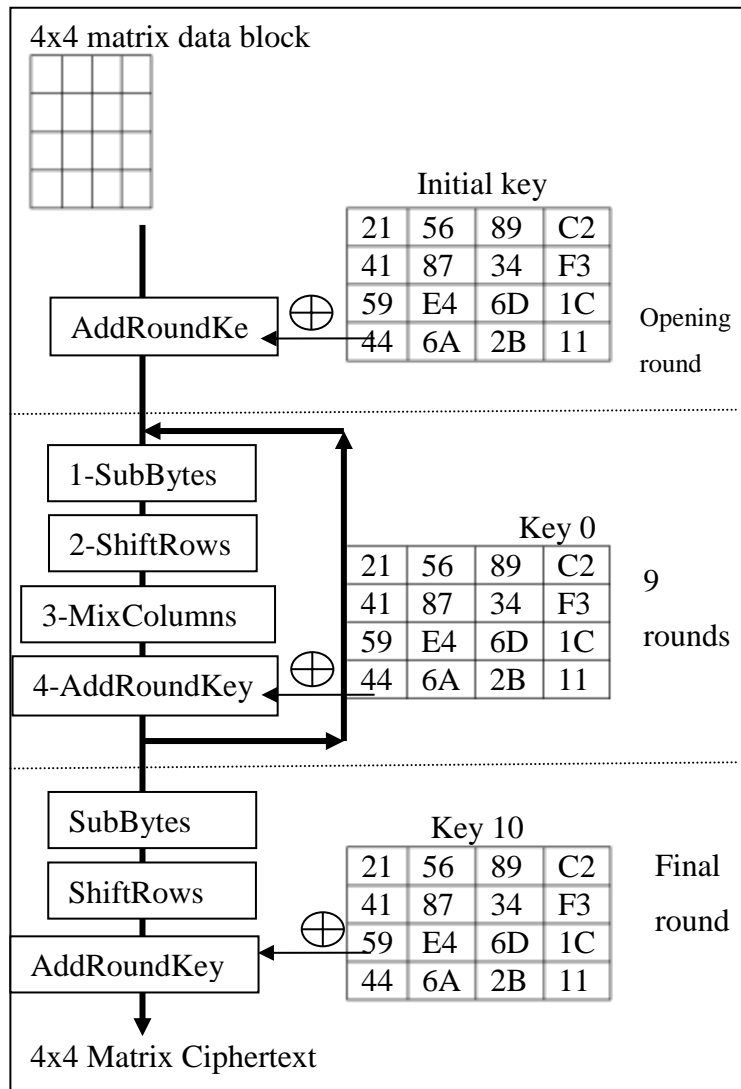
For the generation of subkeys in AES, the original key block is considered and the fourth column from the left or the first from the right, marked in the key table of figure 6, is processed. This consists of rotating the first byte downwards, with the rotated bit.

The SubBytes transformation function (Boxes-S, table 8) is applied to the entire column, that is, new data will be obtained, according to the substitution of table S. Subsequently, a logical operation is performed on this column x-or with column 1 from the left of the original key, in the same way another x-or will be applied with the first column of a constant matrix (Rcon of the standard), assigned one for each subkey, in this way the first column is processed.

The complete key is made up of a 4x4 matrix. In the previous iteration, only the first column of the subkey was worked. For the second column of the subkey, an X-OR will be applied with the second column of the previous key and the first column of the already processed subkey.

Then, for the third column, the third column of the previous key will be taken with the second column of the subkey already processed, performing an X-OR. Finally the fourth column of the subkey will be obtained from the X-OR operation of the fourth column of the previous key and the third column of the subkey already preceded of course. The iterations from the generation of the first column are repetitive, which allows generating the necessary 10 subkeys in AES.

Figure 9 AES cipher diagram



Source: Own Work

4. Asymmetric encryption

This type of encryption works using a key to encrypt and another key to decrypt, generally each user who wishes to work with this technique must have two keys one that is public, and that any other user can use to transmit a message; and a private one that is only known by the owner and is used to recover the original encrypted messages, by asymmetric encryption

4.1 RSA

In 1978, Ronald Rivest, Len Adleman and Adi Shamir proposed the first (probably the best known) public-key cryptographic system. RSA, whose name derives from the initials of each of the authors. It is a cryptographic system that complies with the Diffie–Hellman conditions. Its security is based on the factorization of composite numbers as a product of primes. It also allows the exchange of secret keys and mathematically signing.

RSA work with modular arithmetic using the notation "mod" where the number you want to rescue is the residue of a division. The public key (n) equation 1, is obtained by multiplying 2 prime numbers large enough to guarantee its security, named p and q , it is convenient to clarify that p and q are not public. An F -value, equation 2, is also obtained. From F , a number e is selected, where e and F are relative primes, that is, they have no divisors in common and that their greatest common divisor is one. Finally, a number d that satisfies equation 3 and that is the inverse (multiplicative) of e modulo F , (R. Rivest, 1978).

$$n = p * q \quad (1)$$

$$F = (p - 1) * (q - 1) \quad (2)$$

$$e * d \text{ mod } F = 1 \quad (3)$$

To encrypt, s emust use e and n , considering the plaintext M equation 3.

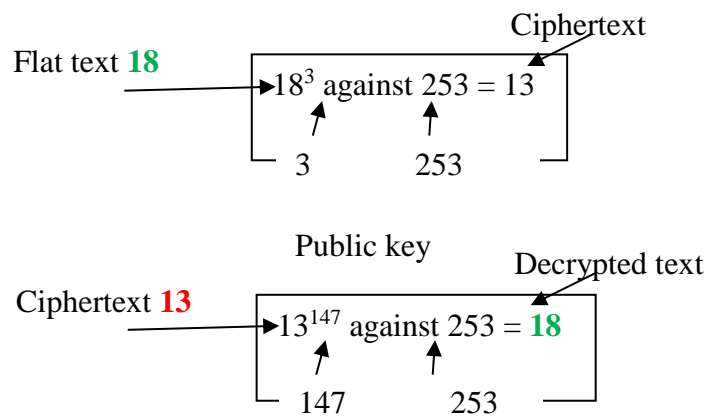
$$C = (M^e) \text{ mod } n \quad (4)$$

To decrypt, consider the value d, the ciphertext value and use equation 5.

$$M = (C^d) \text{ mod } n \quad (5)$$

To better observe this process of encryption with RSA, Figure 8 exemplifies encryption, using the equations.

Figure 8 RSA Encryption Process



Source: Own Work

5. Other forms of encryption

5.1 Hybrid encryption

A hybrid cipher uses both symmetric encryption and asymmetric encryption. That is, a hybrid encryption scheme, an encryption mechanism that can be built from a key encryption scheme or KEM (Key Encapsulation Mechanism) based on a public key scheme, i.e. asymmetric encryption is used to encrypt the key available to encrypt the data in a data encryption scheme or DEM (Data Encapsulation Mechanism) based on a private key scheme.

5.2 Quantum cryptography

"Quantum cryptography solves the problems of encrypting messages to hide information, as well as key distribution, where each bit can be in a discrete and alternate state at the same time; The fundamental unit of storage is the quantum bit, each of which can have multiple states simultaneously at a given instant, reducing the execution time of some algorithms from thousands of OS to just seconds. Quantum cryptography is based on the interactions of the sub-atomic world, and has elements such as the quantum bit, quantum gates, confusing states, quantum teleportation, quantum parallelism, and quantum computing (Molina Vilchis, Silva Ortigoza, & Bracho Molina, 2007)."

Therefore, we must consider that this is a paradigm that must be studied in depth because the most recognized research centers already have and/or are working on quantum computers, hence the weakness of the numbers used in the encryption processes, meaning that in order to crack a key used to encrypt data, less time and effort will be spent with quantum computers, so it is important to start working on quantum encryption and cryptography.

6. Discussion

It is clear that there are many symmetric encryption algorithms, such as: DES, 3DES, AES, IDEA, RC4, among others. Currently several institutions use AES combined with other ciphers. Also, in asymmetric cryptography there is variety such as: Diffie-Hellman, RSA, ElGamal Cipher, Elliptic curve cryptography, Merkle-Hellman cryptosystem, which can also be combined with symmetric encryption to ensure security or privacy. Table 9 describes some advantages and disadvantages of the systems.

Table 9 Comparison of encryption systems

Systems by type		
Type of encryption	Advantages	Disadvantages
Symmetric encryption	<ul style="list-style-type: none"> – Fast encryption – Easy to set up – Easy to understand – Suitable for encrypting big data – Only one key is memorized 	<ul style="list-style-type: none"> – Same key to encrypt as to decrypt – Key exchange is not secure – If the key is shared several times, non-repudiation is not guaranteed
Asymmetric encryption	<ul style="list-style-type: none"> – No keys are shared – Keys must be larger than symmetric keys – Support digital signatures – Ensures recipient authentication 	<ul style="list-style-type: none"> – Must have experience with encryption – If the private key is lost, it will never be recovered – Time consuming
Analyzed encryption systems		
Some	<ul style="list-style-type: none"> – Security of 2^{64} 	<ul style="list-style-type: none"> – Obsolete – Shared key
Triple DES	<ul style="list-style-type: none"> – Security of 2^{128} and 2^{192} since it accepts 2 keys of 64 or 3 also of 64 	<ul style="list-style-type: none"> – May become sluggish – Shared key
AES	<ul style="list-style-type: none"> – Accepts 128, 192, 256-bit keys, minimum security of 2^{128} 	<ul style="list-style-type: none"> – Shared key – Relatively fast
RSA	<ul style="list-style-type: none"> – Can be combined with asymmetric and forms a hybrid cipher 	<ul style="list-style-type: none"> – Slow – Using a random number system for encryption

Source: Own Work

Now, it is important to consider that encryption systems are not only used to protect information. There are also forms of attack such as ransomware, which is a type of cyberattack through malicious software that encrypts files preventing the legitimate user from accessing them, generating a kind of computer hijacking. This type of attack is very common and has great effects, as Ruiz and Jairo comment. Therefore, it is important to document yourself and know both the advantages and risks of encryption systems (Pinzón Ruiz, 2021).

7. Conclusions

Encryption is intended to hide information using cryptographic techniques to prevent it from being readable by those who are not authorized to see it. Encryption is a solution for storing and transmitting sensitive information, since it allows you to control access to information; Restricts unauthorized dissemination in case of loss or theft.

We recommend that you use symmetric encryption when you want to send a fast encrypted message. Asymmetric encryption can be used when you have the public key verified, which complies with a security standard such as OpenPGP of your recipient. It is often complemented by digital signatures to avoid taking risks.

Asymmetric encryption is considered to be more secure since there is no sharing of keys, the public key is already publicly available. With symmetrical encryption, you have to share the password in one way or another, so there is a risk of leakage and you can potentially compromise the encrypted message. In addition to this, the decryption key must be strong enough to prevent unauthorized access to the information that is protected; if this key is lost the information will not be accessible; in the event of a failure of the physical storage device, the information may not be recovered, even if it is encrypted or not.

Finally, it is concluded that symmetric, asymmetric or hybrid data encryption is used depending on the needs of the computer system, the objective is to comply with the characteristics of computer security, which includes protecting the integrity and privacy of the information stored, in process or transaction. Unquestionably, cryptography and the various encryption systems complement computer security and are a preventive measure for data processing and information protection.

Acknowledgement

We are grateful to the Tecnológico de Estudios Superiores de Jocotitlan for the support given in carrying out this research project.

References

- Díaz, L. P. (2012). Algoritmo de encriptación híbrido: cifrado simétrico AES (Advanced Encryption Standard) en combinación con curva elíptica. México. IPN, ESIME. <https://tesis.ipn.mx/handle/123456789/17679?show=full>
- Gil Vera, V. D. (2017). Seguridad informática organizacional: un modelo de simulación basado en dinámica de sistemas. (I. 0122-1701, Ed.) *Scientia Et Technica [en línea]* 22(2), 193-197. Obtenido de <https://www.redalyc.org/>, <https://www.redalyc.org/pdf/280/28010209.pdf>
- Haro, R. (2011). La Seguridad Informática. C. A. <https://www.redalyc.org/pdf/5826/582663867004.pdf>
- Hernández Díaz, E. A. (2016). Cifrado de audio por medio del algoritmo Triple DES-96. México: IPN, CIDETEC. <https://n9.cl/dimaa>
<https://tesis.ipn.mx/bitstream/handle/123456789/20140/Cifrado%20de%20audio%20por%20medio%20del%20algoritmo%20Triple-DES-96.pdf?sequence=1&isAllowed=y>
- Molina Vilchis, M. A., Silva Ortigoza, R., & Bracho Molina, E. (2007). Criptografía Cuántica: Un Nuevo Paradigma. *Polibits*, núm. 36, Instituto Politécnico Nacional, México, 30-35. <https://www.redalyc.org/articulo.oa?id=402640449006>
- Pinzón Ruiz, J. J. (2021). *Análisis del impacto de los ataques de Ransomware en las organizaciones colombianas como base de conocimiento para la determinación de nuevos mecanismos de protección y minimización de riesgos cibernéticos*. <https://repository.unad.edu.co/handle/10596/50093>
- Publication, F. I. (1999). “FIPS PUB 46-3”. <https://csrc.nist.gov/csrc/media/publications/fips/46/3/archive/1999-10-25/documents/fips46-3.pdf>
- Publication, F. I. (2001). Advanced Encryption Standard (AES). “FIPS PUB 197”. <https://nvlpubs.nist.gov/nistpubs/fips/nist.fips.197.pdf>
- R. Rivest, A. S. (1978). A Method for Obtaining Digital Signatures and Public-Key Cryptosystems. *Communications of the ACM*, Vol. 21 (2). <https://people.csail.mit.edu/rivest/Rsapaper.pdf>
- Riquelme, R. (2021). 2020 en 12 hackeos o incidentes de seguridad en México. *El economista*. <https://www.economista.com.mx/tecnologia/2020-en-12-hackeos-o-incidentes-de-seguridad-en-Mexico-20210102-0007.html>
- Romero, G. J. (2018). Conceptualización De Una Estrategia De Ciberseguridad Para La Seguridad Nacional De México. *Revista Internacional de Ciencias Sociales y Humanidades, SOCIOTAM*, XXVIII (2), 1-26. <https://www.redalyc.org/articulo.oa?id=65458498003>
- Sánchez Arriazu, J. (1999). *Descripción del algoritmo DES, (Data Encryption Standard)*. México. <https://docplayer.es/9888866-Descripcion-del-algoritmo-des-data-encryption-standard.html>

Chapter 2 Classification of mature corn cobs using Convolutional Neural Networks

Capítulo 2 Clasificación de mazorcas de maíz maduro mediante Redes Neuronales Convolucionales

REYES-NAVA, Adriana†*, SANCHEZ-FLORES, Diego, LÓPEZ-GONZÁLEZ, Erika and ANTONIO-VELAZQUEZ, Juan Alberto

Tecnológico de Estudios Superiores de Jocotitlán, Division of Engineering in Computer Systems.

ID 1st Author: *Adriana, Reyes-Nava* / **ORC ID:** 0000-0002-4440-909X

ID 1st Co-author: *Diego, Sanchez-Flores* / **ORC ID:** 0000-0002-9280-7287

ID 2nd Co-author: *Erika, López-González* / **ORC ID:** 0000-0001-7279-5111, **CVU CONACYT ID:** 289386

ID 3rd Co-author: *Juan Alberto, Antonio-Velazquez* / **ORC ID:** 0000-0003-3052-3171

DOI: 10.35429/H.2022.3.16.31

A. Reyes, D. Sánchez, E. López and J. Antonio

*adriana.reyes@tesjo.edu.mx

A. Ledesma (AA.). Science of Technology and Innovation. Handbooks-TII-©ECORFAN-Mexico, 2022.

Abstract

The aim of this study is to analyze an algorithm capable of classifying mature corn cobs for the detection of diseases, including *Aspergillus*, *Gibberella* and *Fusarium* fungi, in addition to the common charcoal that these elements may have. The process was carried out through a Convolutional Neural Network associated to a classification algorithm, based on deep learning techniques using MobileNet. This work is divided into two phases, the first one is to determine the performance of the algorithm for a small sample of images and videos analysis and the second one is the extension of the data corpus for the automatic analysis of new samples. It is necessary to mention that this work focuses on the development of the first phase, in which the identification and classification of the cob has had promising results.

Convolutional Neural Network, MobileNet, Classification Mature corn cob

Resumen

En el presente trabajo se genera un algoritmo con la capacidad de clasificar mazorca de maíz maduro para la detección de enfermedades, entre los cuales se encuentran *Aspergillus*, *Gibberella*, *Fusarium* y Carbón común que pudieran tener dichos elementos, este proceso se hará mediante una Red Neuronal Convolutiva asociada a un algoritmo de clasificación, basadas en técnicas de aprendizaje profundo. Este trabajo se divide en dos fases la primera es determinar el funcionamiento del algoritmo para una muestra pequeña de imágenes y análisis mediante video y la segunda la ampliación del corpus de datos para análisis automático de nuevas muestras. Es preciso mencionar que este trabajo se enfoca en el desarrollo de la primera fase, la cual se basa en el desarrollo y entrenamiento del algoritmo basado en Redes Neuronales Convolutivas haciendo uso de MobileNet para la correcta identificación y clasificación de la mazorca.

Red Neuronal Convolutiva, MobileNet, Clasificación de mazorca de maíz maduro

1. Introduction

Image classification in the field of artificial intelligence (AI) is considered by many as one of the most outstanding for the progressive development of this science (Ponce Cruz, P, 2011). The classification techniques of products, species, objects among others have had a great acceptance and more and more research is being done around these case studies, having as main objectives, solve a problem, provide knowledge and tools to different fields of study, as well as provide technological assistance to anyone looking for some kind of solution to a specific task.

In this work, a solution of classification of mature corn cobs is presented to determine the class to which it belongs, these results can be: healthy corn, or diseased corn containing the fungi *Aspergillus*, *Gibberella*, *Fusarium* and Common Charcoal. The classification results will be obtained through the application of Convolutional Neural Networks, in order to make the grouping process more efficient and will be useful to farmers in the northern region of the State of Mexico. It is worth mentioning that currently the classification is carried out by people who know about the identification of corn diseases, and who are usually people over 50 years old, while the younger population does not know how to determine the type of disease and its spread. It should be noted that the state of the art does not mention that there are works fully identified in the analysis of diseased corn and that use artificial intelligence algorithms, since the literature mentions applications that have been used more in the study of fruits, plants, objects and people, so the scope is new in this field.

Regarding the detection and classification of diseases in different plants and fruits (Mora, E. A. H., Huitrón, V. G., Rangel, H. R., & Sosa, L. E. A., 2021), present a work where pests are detected through transfer learning with fine tuning, using the Plant Village dataset, which contains 38 classes, including diseased and healthy leaves. The measures to evaluate the models were precision, sensitivity, F-Score and accuracy, where the results obtained by the VGG16 technique were 90% sensitivity and accuracy. While (Ferreira, U. E. C., & Camacho, J. M. G., 2021), implement a machine learning model with a database of digital images of fruits collected in the field, through the creation of a convolutional neural network (CNN) classifier, training and validating it to identify healthy avocado fruits and fruits infected with scab, this was trained through a hold-out of 80% and validated with the remaining 20%, finally obtaining an accuracy of 87% correct classification.

Likewise (Arévalo, M. D., Ayala, J., & RUIZ CASTILLA, J. S., 2007), they applied a convolutional neural network programmed in Python, using Keras and TensorFlow to classify peaches, obtaining an accuracy of 95.31% in the classification between ripe and immature, when classifying between healthy and damaged, 92.18% was obtained, while when classifying the three categories (damaged, immature and mature), 83.33% accuracy was obtained. On the other hand (Salazar Campos, J. O., 2020), they implement a parameterized model where a correct identification of Hass avocado images was achieved with an accuracy of 87.5%.

There are also applications of the deep learning algorithm in the recognition of people, for example, (Araujo, A., Pérez, J., & Rodríguez, W., 2018), presents a work where, through voice spectrograms analyzed by a Convolutional Neural Network recognizes a person with an accuracy of 93%. On the other hand, a broader application is presented in (Aramendiz, C., et al., 2020), where the development of a mobile application that supports people with visual disabilities is proposed. This application will have the ability to recognize objects from a mobile camera and will provide this information to the person audibly, the information used for recognition is provided to a YOLO convolutional network to have prior knowledge of the objects and capture them in real time. In the same way, the use of convolutional neural networks has been extended to the analysis of sign language, where (Ortiz García, C. D., 2021), where they apply the ResNet50 model for the interpretation and translation of the sign through a webcam.

This work is organized into 5 sections, where the points related to the research topic are treated, organized as follows:

Section 1. Introduction, the focus of the work is presented, and an analysis is made on the fields that have been covered with Convolutional Networks.

Section 2. Theoretical basis, here are presented the fundamental concepts of classification by Convolutional Neural Networks and the development algorithm as well as its architecture.

Section 3. Development, this section shows the steps to follow to carry out the classification of ripe corn cobs.

Section 4. Results, the results obtained based on the experimentation carried out are shown.

Section 5. Conclusions, the conclusion reached based on the results obtained is presented and the future work that is planned to be carried out is shown.

2. Theoretical bases

2.1. Convolutional neural networks

Currently the use of Convolutional Neural Networks (CNN) has practical applications in any field, it is considered as a variation of the Multilayer Perceptron that works with flat or one-dimensional data, while CNN works with two-dimensional data, such is the case of images, voice and video signals mainly.

A convolutional neural network is a network architecture for deep learning that learns directly from data, without the need to extract functions manually. That is, the network takes as input the pixels of an image (Lugo Sanchez, Omar E., et al, 2020). For example, if you have an image of 50×50 pixels in height and width, that is equivalent to 2500 neurons, considering a single color (grayscale), if on the other hand you have a color image, you will need 3 channels (red, green and blue) and then you would have $50 \times 50 \times 3 = 7500$ input neurons.

The use of CNNs is highly recognized for three main factors (Convolutional Neural Networks, 2022):

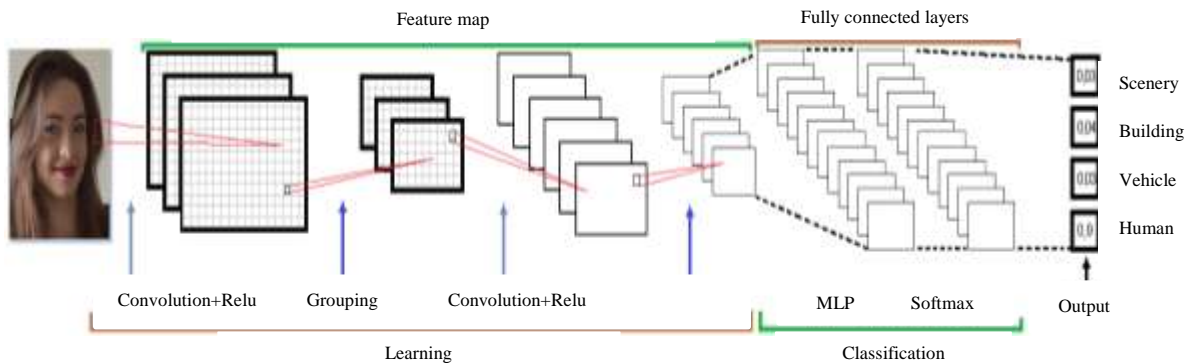
- They learn features directly without having to extract them manually.
- They generate highly accurate recognition results.

- They can retrain themselves for new recognition tasks, allowing them to leverage pre-existing networks.

One of the first works where a CNN is used to classify images of handwritten postal digits is in (LeCun, Y., et al, 1989), obtaining a 99.3% correct classification, but it is not until later years that in 2012 the power of CNNs for image analysis was demonstrated.

The CNN structure is basically composed of 3 different layers, the first is one or more convolutional layers, the second is the clustering layer and the classifier layer, as shown in figure 1. (CNN-RNA Convolutional, 2022).

Figure 1 Layers of a CNN

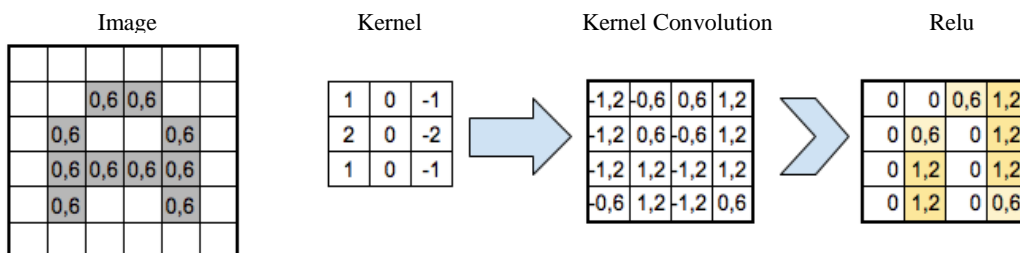


2.1.1. Convolution layer

Here the first convolution layer is not connected to all the pixels of the input image, only to those belonging to its receiving area, in the second layer the neurons are connected to the neurons of the area of the first layer and so on. The purpose of this layer is to extract the features of each image by compressing it to reduce the initial image size.

This layer takes a group of pixels from the input image and makes a scalar product with a kernel, the kernel is the filter responsible for extracting the most important features from the image. The kernel will go through all the inputs and get a new matrix, which will be one of the hidden layers. In case the image is colored, there will be 3 kernels of the same size that will be added to obtain an output figure 2.

Figure 2 Convolution layer

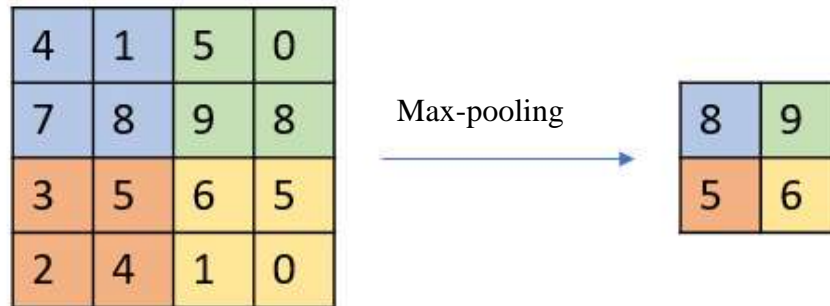


2.1.2 Grouping-pooling layer

This layer is responsible for subsampling the image to reduce the number of parameters and memory usage, in this layer like the previous one the connections are only made to a certain number of neurons of the previous layer, its objective is to obtain the maximum and average values of the sampling window. The pooling layers in a convolutional neural network are used to reduce the size of the activation maps that are being worked on, there are two types of pooling layers in a convolutional neural network which are (Arroyo, D. E., 2019):

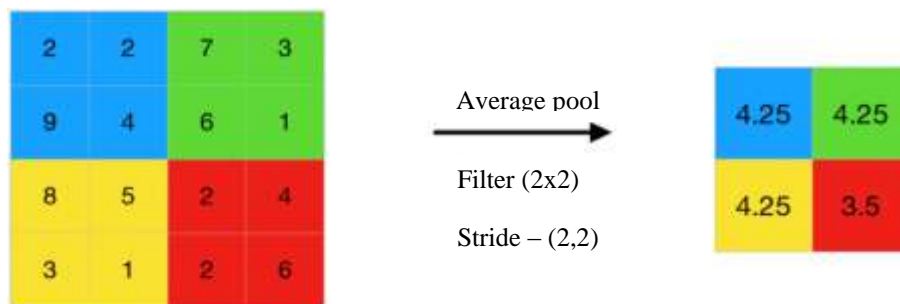
- Max-pooling: it is the most common and is responsible for calculating the maximum of the elements. On the other hand, we must bear in mind that this is done for each map of activations of our volume, that is, the depth dimension does not intervene at all in the calculations. As shown in Figure 3.

Figure 3 Max-pooling



- Average-pooling: It is responsible for calculating the average of the elements that are being studied in a certain image. As shown in Figure 4.

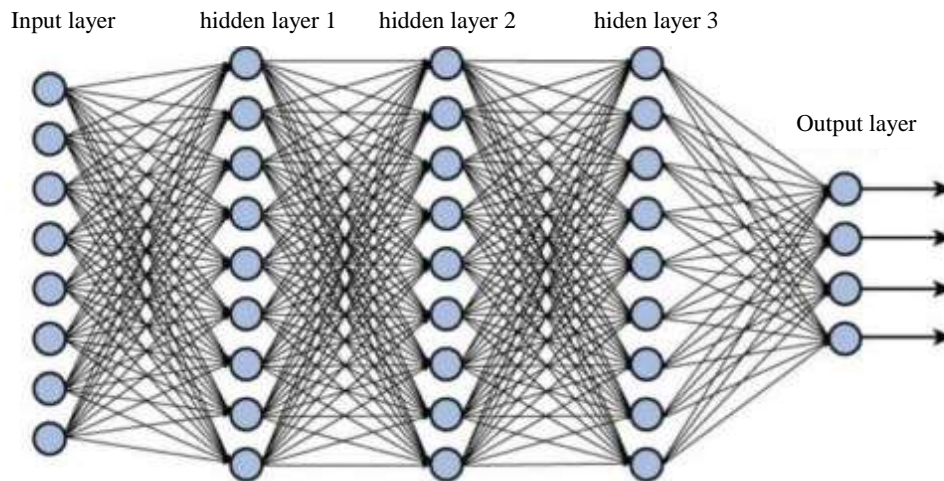
Figure 4 Average-pooling



2.1.3. Sorting layer

It combines the features found by the previous layers to classify the image. In this case, unlike the previous layers, the neurons of the previous layer are fully connected to the next layer. It is based on a deep neural network, these have several hidden layers with millions of artificial neurons connected to each other. A number, called a weight, represents the connections between one node and another. The weight is a positive number if one node stimulates another, or negative if one node suppresses another. Nodes with higher weight values have a greater influence on other nodes.

In theory, deep neural networks can map any type of input to any type of output. However, they also need much more training compared to other machine learning methods. They need millions of examples of training data instead of the hundreds or thousands they might need in a simpler network.

Figure 5 Deep Neural Network

2.2. MobileNet

MobileNet is a CNN capable of classifying images, detecting objects and extracting features, based on an architecture of separable elements in depth with factored convolutions that are by dimensions 1×1 to optimize latency performances. The factorization of convolutions is called point convolution.

A standard convolutional layer takes as input to feature map $D_F \times D_F \times MF$ and produces a feature map $GD_F \times D_F \times N$ where G is the *width and spatial height of a square input feature map* D_F M is the input number channels (input depth) N is the *channel output number (output depth)*. The map of output characteristics for standard convolution assuming stride one and the fill is calculated as (Howard, A. G., et al., 2017):

$$G_{k,l,n} = \sum_{i,j,m} K_{i,j,m,n} \cdot F_{k+i-1, l+j-1,m}$$

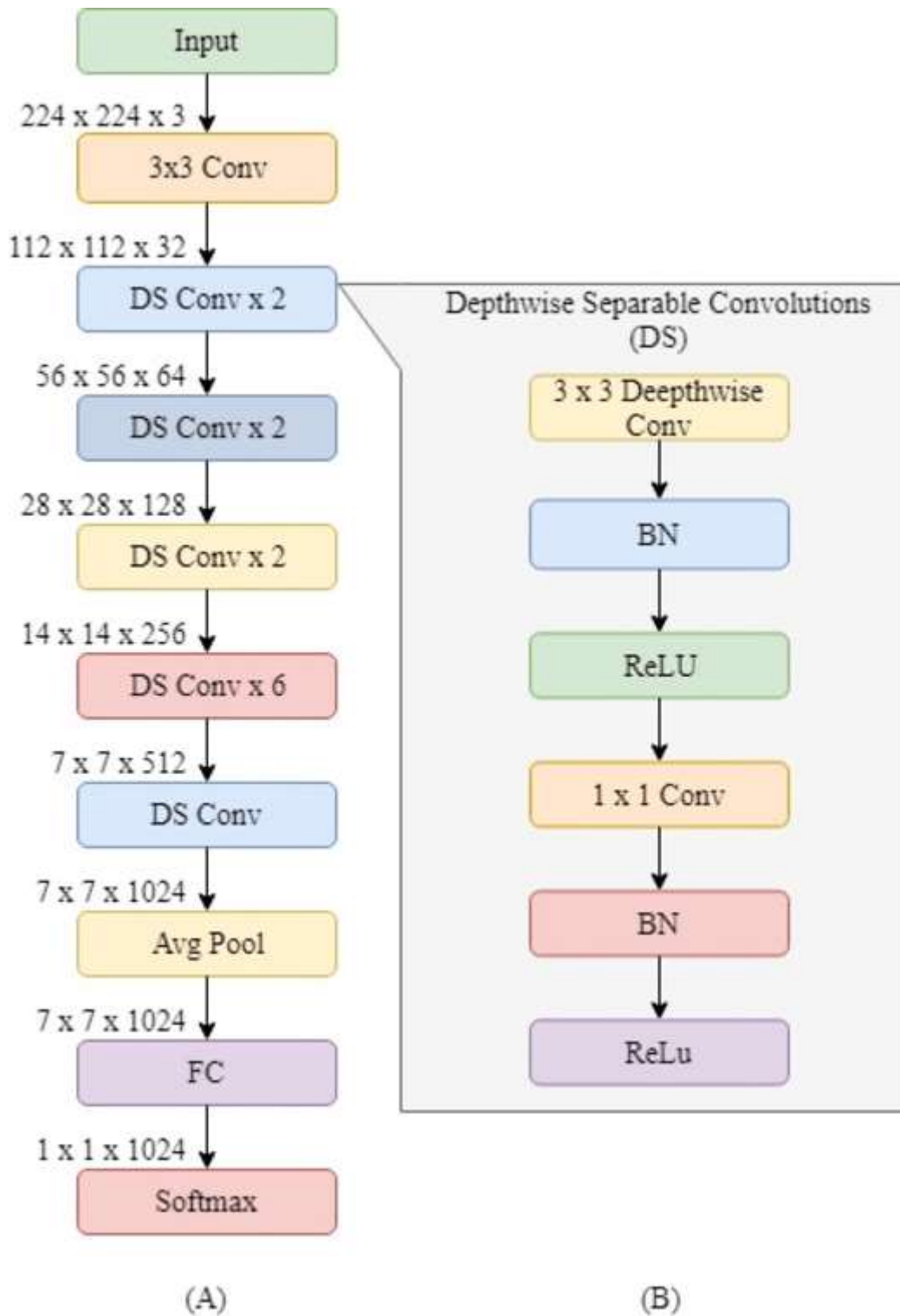
The mobileNet architecture is based on factoring traditional convolutions into 2 types of layers, a first convolutional layer "depthwise" and a convolutional layer 1×1 "pointwise". This division allows to reduce the computational cost and the size of the model.

Standard convolutional layers have a computational cost between 8 and 9 times higher than the computational cost of both "depthwise" and "pointwise" layers. In addition, 2 parameters are added to reduce the size and speed of the neural network. Both parameters allow to reduce even more the size and response time of the neural network:

- The α parameter is a factor that reduces the number of filters/channels applied to each layer by multiplying them $\alpha \in \langle 0.1 \rangle$.
- The β parameter is a factor that reduces the size of the inputs by multiplying it by $\beta \in \langle 0.1 \rangle$.

The MobileNet architecture is shown below:

Figure 6A) General MobileNet architecture (B) detailed DS explanation obtained from (Phiphitphatphaisit, Sirawan & Surinta, Olarik. 2020)



2.3. K—NN algorithm

One of the algorithms for the classification of large amounts of data is K-NN (k- Nearest Neighbors) or k – close neighbors, conceived by (Fix, E., & Hodges, J. L., 1989), this algorithm is based on the fundamental concepts of deep learning, such as the *dataset* and the *model*. These two fields are within the learning stages, where: the model is built from a set of examples *or data* already classified, the model obtained is represented as a set of classification rules, decision trees, mathematical formula, etc. And in the validation: the estimation of the precision of the model, the model is tested with a set of examples different from the one used for the construction of the model. For each example, its real class is compared with the class predicted by the classifier, the accuracy ratio is the percentage of examples that the model correctly classifies (Berastegui, A. G., & Galar, I. M., 2018).

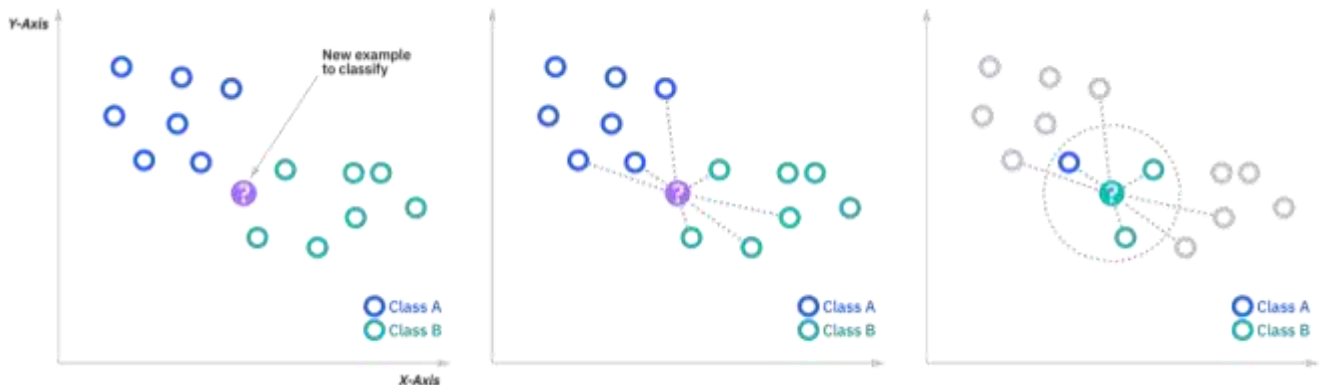
KNN is more of a predictive method than a classification technique, which is relevant, because in order for the algorithm to classify, the most general neighborhood classification rule is based on the assumption that the nearest prototypes have a similar a posteriori probability.

If $K_i(X)$ is the number of samples of the class present in the k closest neighbors to X , this rule can be expressed as:

$$d(X) = w_c \text{ si } K_c(X) = \max_{i=1 \rightarrow j} K_i(K)$$

The general model of representation of the algorithm is shown in the following figure:

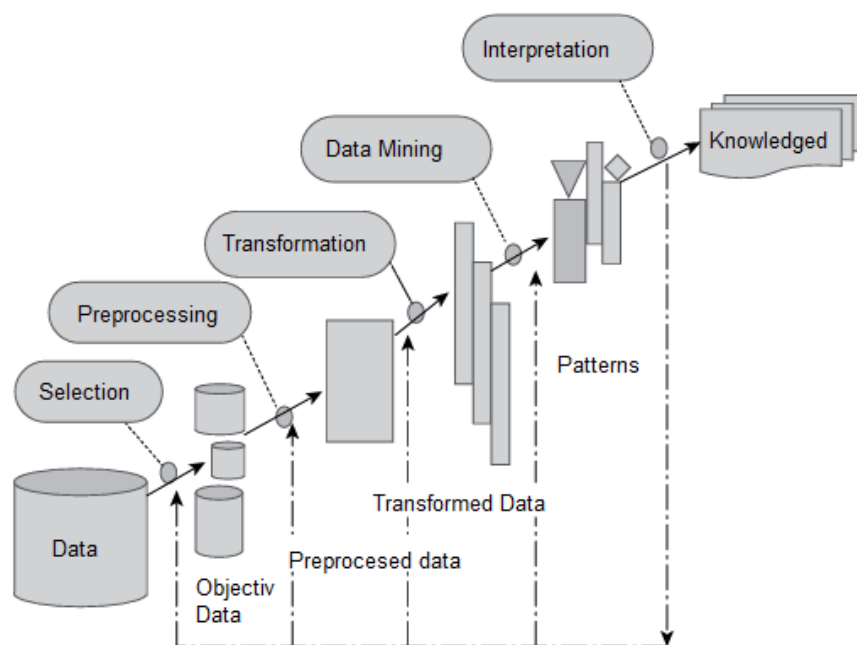
Figure 7 K-NN algorithm obtained from (What is the nearest neighbors k algorithm? | IBM., 2022)



2.4. KDD (Knowledge Discovery in Databases)

The process that is followed to obtain knowledge of a database through the application of data mining algorithms is shown in figure 8, this process is known as KDD for its acronym in English (Knowledge Discovery in Databases), refers to the analysis of large databases through different algorithms to obtain useful information for the organization (Tangarife Morales, 2016).

Figure 8 Stages of the KDD process obtained from (Timarán-Pereira, S. R., et al, 2016)



The description of the stages of the knowledge extraction process according to (Timarán-Pereira, S. R., *et al*, 2016) are:

- Selection: once the relevant and priority knowledge has been identified and the goals of the kdd process defined, from the point of view of the end user, an objective data set is created, selecting the entire dataset or a representative sample of it, on which the discovery process is carried out.
- Pre-processing: data quality is analyzed, basic operations such as noisy data removal are applied, strategies are selected for the handling of unknown data (missing and empty), null data, duplicate data and statistical techniques for its replacement.
- Transformation: useful characteristics are sought to represent the data depending on the goal of the process. Dimension reduction or transformation methods are used to decrease the effective number of variables under consideration or to find invariant representations of the data.
- Data mining: is the search and discovery of unsuspected patterns and interest, applying discovery tasks as classification.
- Interpretation: the discovered patterns are interpreted and the classification is made.

3. Development

In this stage, the application of the KDD process is presented to analyze and classify the cobs by video in real time, considering the training stage of the algorithm based on a deep neural network.

3.1. Selection and pre-processing of data.

In the first instance for this work, it consisted of looking for specimens that will meet the characteristics of a healthy ripe corn cob, in this work only ears with white grain (figure 9) and elements that had an impact on diseases (figure 10, 11, 12, and 13) on the cob were considered, such as: *Aspergillus*, *Gibberella*, *Fusarium* and Common Charcoal, respectively.

To determine to which class the cob belongs, the following aspects should be considered according to (Taba, S., 2004 and Varón de Agudelo, F., & Sarria Villa, G. A., 2007):

- Healthy: does not change the color of the grains and the corn is in good condition. (Figure 9).
- *Aspergillus*: occurs when infected ears with high moisture content are stored, may contain yellow-green, ivy green or black masses on the grain or on the olote. (Figure 10).
- *Gibberella*: is more common in cold and humid areas. The first signs of infection are the formation of white mycelia, which descend from the tip of the cob and give a reddish and pink coloration to the infected grains, this type of infection can be poisonous to some species of animals, (see figure 11).
- *Fusarium*: is the most common disease, causes infected grains to develop cottony mold and can be toxic to animals, (see figure 12).
- Common Charcoal: this disease can be detected in the young plant since the corn is germinating when it is produced in mushroom "huitlacoche" consumed by some people, when it reaches the state of maturation it produces a black color similar to the coal polvo hence its name, (figure 13).

Figure 9 Healthy cob



Figure 10 Cob with Aspergillus



Figure 11 Cob with Gibberella



Figure 12 Cob with Fusarium



Figure 13 Cob with common charcoal

3.2 Algorithm transformation and implementation

The transformation of the data is carried out once it has been defined how the classifier will operate, for this it has been contemplated that the functions of the classifier both for training and for the evaluation phase are in real time. Since in this way you can take full advantage of the capabilities of Mobile Net.

The CreateCaptutre method, is created to make use of the webcam, this will be the way for the classifier to receive the data in real time and thus can also transform them from their original input, and store these elements, in a general basis for knowledge. A white filter (Threshold) will be applied, this is to lighten the information of the images that are being sent to CNN.

Image 14 Transformation using threshold

All the information obtained from the training will be contained in a file called Base_MEC.json, this file will host the transformed data, in a JSON format, which is the way in which ML5 supplies the information to Mobile Net. What Base_MEC.json stores is basically the data set or corpus, which is composed of a valid format for CNN, where it contains the value of the images.

Figure 15 Preview transformed data

index.js	app.js	index.html	Base_MEC.json
			<pre>[{"dataset":{"0":{"kept":true,"isDisposedInternal":false,"shape":[100,256],"dtype":"float32","size":25600,"strides":[256,criollo]},"2":{"kept":true,"isDisposedInternal":false,"shape":[100,256],"dtype":"float32","size":25600,"strides":[256,criollo]},"4":{"kept":true,"isDisposedInternal":false,"shape":[100,256],"dtype":"float32","size":25600,"strides":[256,Fusarium]},"6":{"kept":true,"isDisposedInternal":false,"shape":[42,256],"dtype":"float32","size":10752,"strides":[256,</pre>

3.3 Evaluation of the algorithm

The implementation of a KNN classification algorithm provided by ML5, which is stored in the KNN classifier, will help to form a prediction about the classification processes with the information contained in the data set, to obtain the final results.

Figure 16 Optimal parameters of CNN

```
const ValoresD = {
  version: 1,
  alpha: 0.25,
  topk: 3,
  learningRate: 0.0001,
  hiddenUnits: 100,
  epochs: 60,
  numLabels: 2,
  batchSize: 0.4,
  layer: 'conv_pw_13_relu',
};
```


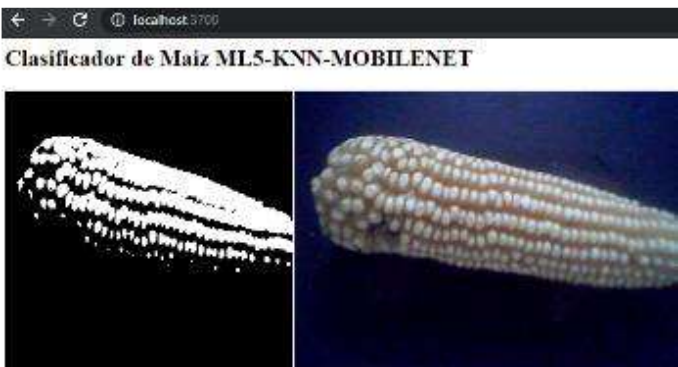


For the training of the algorithm it is necessary that for each specimen of cob is shown in different positions the button of Train, placed on the text box, the label with which the specimen shown will be designated, repeating this process in all healthy corn cobs and the ears of corn with disease are obtained and the following count that can be visualized in the browser console as shown in the following image.



Figure 17 Classifier interface

In this way, the network training process is carried out in real time and continues to learn from the new samples that are introduced, since the generated data is stored in a database in the MobileNet reading format for the subsequent classification of the new cobs.

4. Results

Based on the implementation and analysis of the results obtained by measuring the accuracy of the algorithm to correctly or incorrectly classify the species introduced in the training and validation of the algorithm, the following table shows two columns, the first corresponds to the analyzed specimen and its white filter and the second corresponds to the labeling assigned to the cob and the level of confidence obtained by the algorithm used.

Specimens analyzed	Results
<p>Figure 18 Specimen 1</p> 	<p>Result: cob 4 healthy creole Confidence: 100%</p>
<p>Figure 19 Specimen 2</p> 	<p>Result: cob 2 healthy creole Confidence: 80%</p>
<p>Figure 20 Specimen 3</p> 	<p>Result: cob with Gibberella Confidence: 100%</p>
<p>Figure 201 Specimen 4</p> 	<p>Result: cob with Fusarium Confidence: 100%</p>

<p style="text-align: center;">Figure 212 Specimen 5</p> 	<p>Result: cob with common charcoal Confidence: 100%</p>
<p style="text-align: center;">Figure 223 Specimen 6</p> 	<p>Result: cob with Gibberella Confidence: 100%</p>

The results obtained, show that the classification is done correctly with the specimens shown, however, the problems presented in the analysis must be taken into account, such as the quality of the camera of which it was used, a more controlled environment to manipulate the levels of luminosity, position of the camera and distance when taking the images in real time, which can affect image quality.

This work has been funded by Tecnológico de Estudios Superiores de Jocotitlán.

5. Conclusions

With the analysis of the ripe corn cobs it was determined that the accuracy of the algorithm is 100% in most cases, however, there are deficiencies in the classification of some specimens, derived from issues of luminosity and the analysis environment, in addition the number of classified images is low, so it is considered to work in a second stage where the number of images is greater to make a More extensive training of the classifier and a greater number of samples are taken for sorting.

The process of classification in the ear of mature corn, is an activity with great antecedents, which until recently was done in light or large amounts of elements, manually. To which opens a possibility of extending this work, implementing the same classification system presented, to a device that has the necessary actuators to optimize in its entirety the classification of the ear of mature corn in the area from where the specimens were obtained. Having as consideration and recommendations the following:

- Extend the dataset: Generate a much larger dataset with more instances by varying the characteristics.
- Have better control of environmental variables: contemplate a camera of higher resolution in the quality of the image and take into account variations in luminosity.

References

- ¿What is a neural network? IA y ML guide - AWS. (2022). Retrieved September 18, 2022, from: <https://aws.amazon.com/es/what-is/neural-network/>
- Aramendiz, C., Escorcía, D., Romero, J., Torres, K., Triana, C., & Moreno, S. (2020). Sistema basado en reconocimiento de objetos para el apoyo a personas con discapacidad visual. *Investigación y desarrollo en TIC*, 11(2), 75-82. From: <https://revistas.unisimon.edu.co/index.php/identific/article/view/4940>
- Araujo, A., Pérez, J., & Rodríguez, W. (2018). Aplicación de una Red Neuronal Convolutiva para el Reconocimiento de Personas a Través de la Voz. In *Proc. Sexta Conferencia Nacional de Computación, Informática y Sistemas* (pp. 77-81). From: <https://cutt.ly/FMzpYJ6>
- Arévalo, M. D., Ayala, J., & RUIZ CASTILLA, J. S. (2007). Clasificación del fruto del durazno en maduros, no maduros y dañados hacia la cosecha automatizada. From: <http://hdl.handle.net/20.500.11799/111780>
- Arroyo, D. E. (2019). Visualizando neuronas en redes neuronales convolucionales. Public Univ. Navarra, Pamplona, Spain, Tech. Rep, 2454, 33694. From: <https://hdl.handle.net/2454/33694>
- Berastegui, A. G., & Galar, I. M. (2018). Implementación del algoritmo de los k vecinos más cercanos (k-NN) y estimación del mejor valor local de k para su cálculo. (Trabajo Fin de Grado). from: <https://academicae.unavarra.es/bitstream/handle/2454/29112/Memoria.pdf>.
- CNN-RNA Convolutional (2022). Retrieved September 18, 2022, from: <https://numerentur.org/convolucionales/>
- Convolutional Neural Network. (2022). Retrieved September 18, 2022, from: <https://la.mathworks.com/discovery/convolutional-neural-network-matlab.html>
- Ferreira, U. E. C., & Camacho, J. M. G. (2021). Clasificador de red neuronal convolutiva para identificar enfermedades del fruto de aguacate (*Persea americana* mill.) a partir de imágenes digitales. *Agrociencia*, 55(8), 695-709. From: <https://www.agrociencia-colpos.org/index.php/agrociencia/article/view/2662>. DOI: <https://doi.org/10.47163/agrociencia.v55i8.2662>
- Fix, E., & Hodges, J. L. (1989). Discriminatory analysis. Nonparametric discrimination: Consistency properties. *International Statistical Review/Revue Internationale de Statistique*, 57(3), 238-247. DOI: <https://doi.org/10.2307/1403797>. From: <https://www.jstor.org/stable/1403797>
- Howard, A. G., Zhu, M., Chen, B., Kalenichenko, D., Wang, W., Weyand, T., ... & Adam, H. (2017). Mobilenets: Efficient convolutional neural networks for mobile vision applications. *arXiv preprint arXiv:1704.04861*. DOI: <https://doi.org/10.48550/arXiv.1704.04861>
- LeCun, Y., Jackel, L. D., Boser, B., Denker, J. S., Graf, H. P., Guyon, I., ... & Hubbard, W. (1989). Handwritten digit recognition: Applications of neural network chips and automatic learning. *IEEE Communications Magazine*, 27(11), 41-46. DOI: 10.1109/35.41400 From: <https://ieeexplore.ieee.org/abstract/document/41400>.
- Lugo Sánchez, Omar E., Sossa, Humberto, & Zamora, Erik. (2020). Reconocimiento robusto de lugares mediante redes neuronales convolucionales. *Computación y Sistemas*, 24(4), 1589-1605. Epub 11 de junio de 2021. DOI: <https://doi.org/10.13053/cys-24-4-3340>
- Mora, E. A. H., Huitrón, V. G., Rangel, H. R., & Sosa, L. E. A. (2021). Detección de enfermedades foliares con arquitecturas de redes neuronales convolucionales. *RINDERESU*, 5(1). From: <http://rinderesu.com/index.php/rinderesu/article/view/46>

Ortiz Garcia, C. D. (2021). TRADUCTOR DE LETRAS EN LENGUAJE DE SENAS? CON REDES NEURONALES CONVOLUCIONALES. Universidad de los Andes. From: <http://hdl.handle.net/1992/53437>

Phiphatphaisit, S., & Surinta, O. (2020). Food image classification with improved MobileNet architecture and data augmentation. In Proceedings of the 2020 The 3rd International Conference on Information Science and System (pp. 51-56). DOI: <https://doi.org/10.1145/3388176.3388179>

Ponce Cruz, P. (2011). Inteligencia artificial con aplicaciones a la ingeniería (2nd ed.). Barcelona: Marcombo. From: <https://cutt.ly/jMzpyWp>

Salazar Campos, J. O. (2020). Diseño de un modelo basado en redes neuronales artificiales para la clasificación de palta hass. (Trabajo Fin de Grado). From: <http://hdl.handle.net/20.500.12404/17400>.

Taba, S. (2004). Enfermedades del maíz: una guía para su identificación en el campo. Cimmyt.

Tangarife Morales, C. (2016). Estudio comparativo de metodologías para la detección de áreas de control de tensión. Colombia: Universidad Tecnológica de Pereira. Facultad de Ingenierías Eléctrica, Electrónica, Física y Ciencias de la Computación. Ingeniería Eléctrica. From: <https://hdl.handle.net/11059/7078>

Timarán-Pereira, S. R., Hernández-Arteaga, I., Caicedo-Zambrano, S. J., Hidalgo-Troya, A. y AlvaradoPérez, J. C. (2016). El proceso de descubrimiento de conocimiento en bases de datos. En Descubrimiento de patrones de desempeño académico con árboles de decisión en las competencias genéricas de la formación profesional (pp. 63-86). Bogotá: Ediciones Universidad Cooperativa de Colombia. doi: <http://dx.doi.org/10.16925/9789587600490>

Varón de Agudelo, F., & Sarria Villa, G. A. (2007). Enfermedades del maíz y su manejo: compendio ilustrado. Instituto Colombiano Agropecuario-ICA. From: <https://cutt.ly/wMzagpP>

What is the nearest neighbors k algorithm?| IBM. (2022). Retrieved September 18, 2022, from: <https://www.ibm.com/co-es/topics/knn>

Chapter 3 Diagnosis of municipal solid waste (MSW), in the State of Mexico

Capítulo 3 Diagnóstico de los residuos sólidos urbanos (RSU), en el Estado de México

BERNAL-MARTÍNEZ, Lina Agustina†*, SÁNCHEZ-OROZCO, Raymundo and SALAZAR-PERALTA Araceli

Tecnológico de Estudios Superiores de Jocotitlán, Chemical Engineering Division, Carretera Toluca Atlacomulco km 44.8, Ejido de San Juan y San Agustín, Jocotitlán, Mexico.

ID 1st Author: *Lina Agustina, Bernal-Martínez* / **ORC ID:** 0000-0002-4922-043X, **CVU CONACYT ID:** 173701

ID 1st Co-author: *Raymundo, Sánchez-Orozco* / **ORC ID:** 0000-0003-0006-1711, **CVU CONACYT ID:** 169684

ID 2nd Co-author: *Araceli, Salazar-Peralta* / **ORC ID:** 0000-0001-5861-3748, **Researcher ID Thomson:** U-2933-2018, **CVU CONACYT ID:** 300357

DOI: 10.35429/H.2022.3.32.48

L. Bernal, R. Sánchez and A. Salazar

*lina.bernal@tesjo.edu.mx

A. Ledesma (AA.). Science of Technology and Innovation. Handbooks-TII-©ECORFAN-Mexico, 2022.

Abstract

The purpose of this paper is to evaluate the diagnosis of urban solid waste (USW) in the State of Mexico, through the framework of sustainability. Urban areas represent a focus of attention for local administrations since they represent spaces of economic importance in the Gross Domestic Product. At the same time, these areas favor the concentration of population and air, water and soil pollution in these areas. The analysis included documentary review and diagnosis of urban solid waste (USW) in the State of Mexico, for which it is necessary to investigate different aspects of utmost importance, as well as some background information that involves not only the state, since in order to compare it is necessary to know the management of USW in Mexico at a national level first and then focus on the State of Mexico. As we know, MSW has increased over time due to the demographic and industrial growth of the country, the change in consumption habits of the population, the increase in welfare levels, and the tendency to abandon rural areas to concentrate in urban centers. This has substantially modified the quantity and composition of MSW.

Urban, Sustainability, Demographic analysis, Composition, Tendency

Resumen

Este trabajo tiene el propósito de evaluar el Diagnóstico de los residuos sólidos urbanos (RSU) en el Estado de México, a través del marco de la sustentabilidad. Las áreas urbanas representan un foco de atención para las administraciones locales ya que representan espacios de importancia económica en el Producto Interno Bruto. Al mismo tiempo, en estas áreas se favorece la concentración de población y la contaminación del aire, agua y suelo en estas áreas. El análisis comprendió revisión documental y diagnóstico de los residuos sólidos urbanos (RSU) en el Estado de México, para lo cual es necesario investigar diferentes aspectos de suma importancia, así como algunos antecedentes que involucran no solo al estado, ya que para poder comparar es necesario conocer la gestión de RSU en México a nivel nacional primero para posteriormente enfocarnos en el Estado de México. Como sabemos, los RSU han aumentado con el paso del tiempo debido al crecimiento demográfico e industrial del país, al cambio de hábitos de consumo de la población, la elevación de los niveles de bienestar, y la tendencia a abandonar las zonas rurales para concentrarse en los centros urbanos. Lo anterior ha modificado de manera sustancial la cantidad y composición de los RSU.

Urbano, Sustentabilidad, Análisis demográfico, Composición, Tendencia

1. Introduction

At present, most of the world's inhabitants are focused on urban regions, presenting increasingly greater challenges to solve urban-environmental and governance problems, this is due to a hurried urbanization initiated since the mid-twentieth century, which formed localities that were not prepared for the requests of their inhabitants and its increase acquired a disorderly character, a problem that is causing a social, economic and environmental imbalance is the issue of urban solid waste that constitutes one of the greatest concerns of contemporary communities and a global challenge for public administration, and this problem is expressed as a global trend in the generation of urban solid waste, where the highest levels correspond to nations with economic incomes. Such is the situation of the territory of North America, consisting of the USA, Canada and Mexico.

According to a study in the 2010 population census (INEGI 2010), it is suggested that 72% of the population of the territory inhabits more than 15,000 inhabitants. Recent projections of the urban phenomenon in Mexico, estimate that the population will reach 121 million individuals in the next 18 years, who will live in metropolises of more than one million inhabitants in 2030, growth and concentration will demand various inputs for its sustenance such as water, energy and materials, as well as the adequate disposal of waste discharged into water, air and soil, where inadequate dumping of solid waste alters the quality of these three resources, as well as their impact on human health and ecosystems. In Mexico, the transition from rural to urban changed the consumption patterns of a society that produced mostly organic waste, to one that generates primarily inorganic waste derived from the usual consumption patterns of urban industrial communities (SEDESOL, 2011) and in 2010 alone, the territory generated 109,750 tons of solid waste daily, of which 64% were deposited in landfills, 9% in controlled landfills, and the remaining 27% was disposed of in uncontrolled sites.

The management of municipal solid waste in most developing nations rests with local authorities, such as China, Turkey, India, Ethiopia, Uganda, Greece and Spain among others, (Kanat, 2010; Lohri *et al.*, 2017; Okot-Okumo and Nyenje, 2011; Papachristou *et al.*, 2009) where the situation in Mexico does not flee to this condition, the "Political Constitution of the United Mexican States" points out that it is the responsibility of the municipal authorities to collect and operate it, since, although there are different policies, laws and programs aimed at providing a convenient operation, the lack of tools for its proper use and administration has made it possible to these programs are political-environmental discourses, where society is a scarcely participating observer. In this research, in order to know the administration of Urban Solid Waste (MSW) in the State of Mexico in conjunction with the Ministry of Environment and Natural Resources, SEMARNAT, information collection tools were used, such as observation, qualitative and quantitative research, focused on detecting the specific reasons for the incongruity between the formal and hence this chapter is divided into the following sections:

Section 1.1: Waste Management

Section 1.2: General Law for the Prevention and Integral Management of Waste (LGPGIR)

Section 1.3: Municipal Solid Waste (MSW)

Section 1.4: Management of municipal solid waste (MSW), special handling waste (SHW) and hazardous waste (HW) in Mexico.

Likewise, in section 2, the methodology is mentioned and in section 3 the results obtained during the research are presented.

1.1 Waste Management

The management of solid waste in Mexico goes through three moments in its history: it begins in 1964 under a predominant approach of sanitary regulation, in 1988 from the creation of national environmental legislation a step is taken towards the basic management of waste and in 2003 the creation of the General Law for the Prevention and Integral Management of Waste (DOF, 2003), by incorporating some aspects of sustainable management of municipal solid waste, in Table 1.1. The different approaches established in Mexican legislation are shown.

Table 1.1. Enghouse established in Mexican legislation: sanitary regulation, basic management and integral management of MSW, with respect to the conceptual framework of sustainable management.

Conceptual framework: sustainable MSW management	Waste sanitary regulation (1964 -1987)	Basic waste management (1988 -2002)	Comprehensive MSW Management (lowercase m) (2003-2012)
Production of goods and environment	Environment and development	The environmental issue is involved in the production of goods and services	Environmental responsibility is involved
Urban metabolism	Linear metabolism	Circular metabolism	Circular metabolism
Material Recovery	Recovery	Diversity of recovered by-products	Highlights the hierarchical management of waste through reduction, reuse and recycling
Infrastructure	Scarce physical and human resources	Scarce resources, with deployments for recovery	Scarce resources, with improvements in material collection
Legal framework	General legal framework for health management	Environmental legal framework for operational management	Sectoral legal framework for operational management
Public policies	Short-term operational actions	Operational and short-term public policies	Operational public policies for short-term pollution prevention
Innovation and research	Research is minimal and health-oriented	Preparation of technical studies, in accordance with official standards	Preparation of technical studies, and audits
Education and training	Educational axes if Environmental content and minimum training	Education activities Formal informal environment budding training	The contents are extended in the Basic educational axes and localized training

Source: Diagnosis of Urban Solid Waste Management in the Municipality of Mexicali, Mexico. Challenges for the Achievement of Sustainable Planning.

Consequently, the sanitary regulation considered solid waste as an urban sanitation problem that was in charge of the public health authorities, its operation was specified in the collection and removal of waste from urban centers for disposal in rural areas with the traditional management of burning, on the other hand, the period of sanitary regulation includes from the appearance of the first federal rules of operation by the Ministry of Health and Assistance (SSA) in 1964, until the assignment of functions to public services in the municipalities in 1985, and that is modified with the publication of the General Law of Ecological Balance and Environmental Protection in 1988 (DOF, 1988), when establishing the official Mexican standards for final disposal sites.

In such a way that the basic annex assumes not only an operational policy of collection and final disposal, but also tasks of prevention of pollution by MSW, with the publication of the Law of Ecological Balance and Environmental Protection, in 1988, the first type of waste was built and rum was distributed. competences for the three levels of government, ratifying the formulation of environmental policy, the provision of the service of collection and management of MSW, to the municipalities, to itself also, appears the Official Mexican Standard specific in 1996 the sites of final disposal, and the construction of infrastructure by the federal government is accentuated, by manifesting the budgetary limitations that the municipalities had to build this type of infrastructure, the validity of this approach extends until before the publication of the first federal sectoral law (Gil, 2009).

Finally, the integral management of Urban Solid Waste is an approach that presents a comprehensive vision through the publication of the General Law for the Prevention and Integral Management of Waste (DOF, 2003), has a categorization into three groups of waste: municipal solid waste (MSW) of municipal competence, special handling waste (SHW) of state competence and hazardous waste (HW) of federal competence, based on this categorization local governments assume responsibility for municipal management, management that requires coordination and concurrence with other levels of government for pollution control under the signing of agreements. Thus, the integral management considers, attend the waste management system that includes the generation, storage, sweeping, collection, transfer, treatment, use of materials and final disposal, as well as include regulatory actions for the issuance of cleaning regulations, incentives for the reduction of garbage, the promotion of collection centers, management of resources and support, training, as well as impact assessments on the natural and social environment.

The State of Mexico ranks first nationally, by the number of its inhabitants 15,175,862, according to the 2010 population census, also has 13.5% of the national industry, highlighting the production of food, beverages, tobacco, among others, coupled with it social and commercial activities have increased; thereby generating a considerable increase in waste generation, A situation that is complicated by inadequate practices during the collection, separation and lack of use of recoverable materials that can be reincorporated into the production chain and used as raw material in production processes, a situation that is neglected by the high costs they require for their treatment, derived from the poor conditions in which they are found. (SEMARNAT, General Directorate of Solid Waste Management).

Similarly, the State of Mexico is the most populous entity in Mexico, with 16,187,608 inhabitants (INEGI, 2015), it is the territory with the highest generation of MSW in the country, around 10% of the total, its production is 1,046kg / inhabitant / day, above the national average of 0.852 kg (GEM, 2009). In addition, due to its geographical location, it experiences a variability of climates with strong variations in temperature and precipitation, which affect the processes of decomposition of organic matter, as well as the diffusion of water-soluble substances, which when available on slopes or landfills in the "open sky" are typical to spread the contamination of the same, These data show the magnitude of the problem, by dimensioning that each person produces about 1kg of waste, the excessive consumption of products is inferred or that they contain waste materials in excess, any of the cases speak of an irrational behavior before consumption.

1.2 General Law for the Prevention and Integral Management of Waste (LGPGIR)

The LGPGIR, defines MSW as those generated in dwelling homes, resulting from the elimination of materials used in their domestic activities, the products they consume and their containers, packaging and packaging; waste that comes from any other activity within establishments or on public roads and those resulting from the cleaning of roads and public places (LGPGIR, Article 5, section XXXIII).

On the other hand, the activities associated with the solid waste management process, from the point of generation to the final disposal, have been grouped into six functional elements Tchobanoglous (1997): a) Waste generation, b) Handling and separation of waste, storage and processing at source, c) Collection, d) Separation, processing and processing of solid waste; (e) Transfer and transport and (f) Emptying.

The Integrated Management of Municipal Solid Waste can be defined as the selection and application of techniques, technologies and management programs suitable to achieve specific waste management goals and objectives. The problems associated with MSW management in today's society are complex due to the amount and diverse nature of waste, the development of dispersed urban areas, the limitations of funds for the provision of the municipal public cleaning service, as well as the impacts of technology and emerging limitations of energy and raw materials (Tchobanoglous, 1997).

Consequently, the Integral Management of MSW must be carried out in an effective and orderly manner, identifying the relationships and the fundamental aspects involved, to obtain information with uniform data to support the design of both federal and state and municipal programs, in order to optimize resources, staff training, restructuring of operational and administrative methods and procedures, environmental awareness to achieve the committed participation of the population and the establishment of mechanisms to give continuity to projects and programs through institutional changes in the current municipal administration in the context of Integral MSW Management. Integrated MSW Management has to be considered as an integral part of Environmental Management.

The steps of this management are: reduction in the source, reuse, recycling, sweeping, storage, collection, transfer, treatment and final disposal. Within its local scope, this management must include all administrative, financial, legal, planning and engineering functions (technical aspects) involved in solving all problems associated with inadequate management.

1.3 Municipal Solid Waste (MSW)

Urban solid waste (MSW) is those that are produced in homes, whether houses, offices or small businesses, as well as those that come from any other activity that is carried out in establishments or on public roads, with domiciliary characteristics and those that occur in public places, provided that they are not considered as waste of another nature (DOF, 2003).

In Mexico, according to the most recent figures, published in 2017, MSW generation reached 44.6 million tons, which represented an increase of 35.6% compared to 2003 (11.73 million tons more generated in that period). If expressed per inhabitant, it reached 0.98 kilograms on average daily in the same year (Presidency of the Republic, 2017).

The amount of municipal solid waste generated can be explained as a result of multiple factors, recognizing among the most important urban growth, industrial development, technological modifications and changes in the consumption patterns of the population, among others.

In Mexico, as in the case of many other countries, the growth of MSW generation goes hand in hand with private final consumption expenditure and national, this relationship, which has also been observed in other regions of the world, means that, with higher incomes, the level of consumption increases and, as a result, a greater volume of waste is produced.

The generation of waste is also closely linked to the urbanization process, and it is generally recognized that this is accompanied by a greater increase in the purchasing power of the population, which leads to living standards with high levels of consumption of goods and services, which produces a greater volume of waste. By contrast, in small or rural communities, inhabitants base their consumption mainly on less manufactured products that generally lack materials that end up as waste.

Using the size of the population and the characteristics of the localities, the states that would be generating the most MSW would be the state of Mexico (6.98 million t; 15.7% of the national total), Mexico City (3.98 million t; 9%), Jalisco (3.2 million t; 7.1%) and Veracruz (2.4 million) Colima (241 955 t; 0.5%), Baja California Sur (301 640 thousand t; 0.7%), Tlaxcala (301 759 t; 0.7%) and Campeche (313 317 t; 0.7%).

1.4 Management of municipal solid waste (MSW), special handling waste (SHW) and hazardous waste (HW) in Mexico

In Mexico there are legal instruments that regulate the integral management of waste and that involve generators, those who transport them and those who process them, or not of these legal instruments is the General Law for the Prevention and Integral Management of Waste (LGPGIR; DOF, 2003), the National Program for the Prevention and Integral Management of Waste and the state and municipal programs for Prevention and Integral Management of Waste, however in the case of hazardous waste or another type of instruments to manage waste are inventories, which provide information for decision-making, in addition to collecting and integrating information on the sites where this type of material is collected, including those that no longer operate or are even clandestine, nevertheless solid waste management plans, through which generators (whether in the public, private or social sector) must adopt measures to reduce the generation of MSW, SHW and HW, take advantage of those susceptible to reuse, recycling or energy production, or to treat or confine those that cannot be recovered. Several instances are involved in waste management, see Table 1.2.

Table 1.2 Waste management according to the instance involved.

Instance	Responsibilities and roles
Secretary of Environment and Natural Resources (SEMARNAT)	Develop policies and strategies for environmental control. Regulate and supervise the environmental regulatory framework. Coordinate national programs for environmental management. Promote the creation of infrastructure (in collaboration with Sedatu).
Secretary of Health (SSA)	Develop policies and strategies for health control. Regulate and supervise health. Develop plans for the prevention of occupational risks and risks to public health in the different stages of MSW management. Coordinate national programs for environmental sanitation.
Secretary of Agrarian, Territorial and Urban Development (Sedatu)	Promote the creation of infrastructure (in collaboration with Semarnat).
Other secretaries	Support the management of MSW in their respective areas (tourism, industry, fisheries, energy and mines, transport, housing, others). Regulation of MSW management in their respective areas of intervention.
Municipal governments	MSW management: sweeping, collection and final disposal. Formulation of the local regulatory framework. Application of penalties for non-compliance in the handling of MSW. Formulation and implementation of mandatory fees for the services provided.

Source: Report on the Situation of the Environment in Mexico

2. Methodology to be developed

2.1 Sustainable MSW planning

The proposal in general is built from the circular approach for solid waste that integrates compatible forms of production and consumption that consider the flows of matter and energy in the system, which refers to the use of waste via the reduction in consumption, reuse and recycling (Dálisa *et al.*, 2012; Marshall and Farahbakhsh, 2013; Pires *et al.*, 2011; Seadon, 2010).

2.2 MSW management in the State of Mexico

Currently, most rural municipalities limit the management of their solid waste to basic elements, so the generation, collection and final disposal should be monitored; in some cases, manual sweeping is also carried out in streets of the municipal capital, in Figure 2.1, the diagram of the management of the general MSW is observed.

Figure 2.1 General diagram of MSW management



Source: Program for the prevention and Integral Management of MSW and Special management of the State of Mexico

2.3 Types of MSW Treatment

In this section, the identification of the different types of treatment of MSW in the State of Mexico was carried out, with respect to current regulations.

2.4 MSW generation in the State of Mexico

Based on the documentary research, the total amount of waste generated in the State of Mexico tons / month was estimated.

2.5 Regulations applied to MSW in the State of Mexico

The regulations covered by MSW within the State of Mexico, on which this study was based, are:

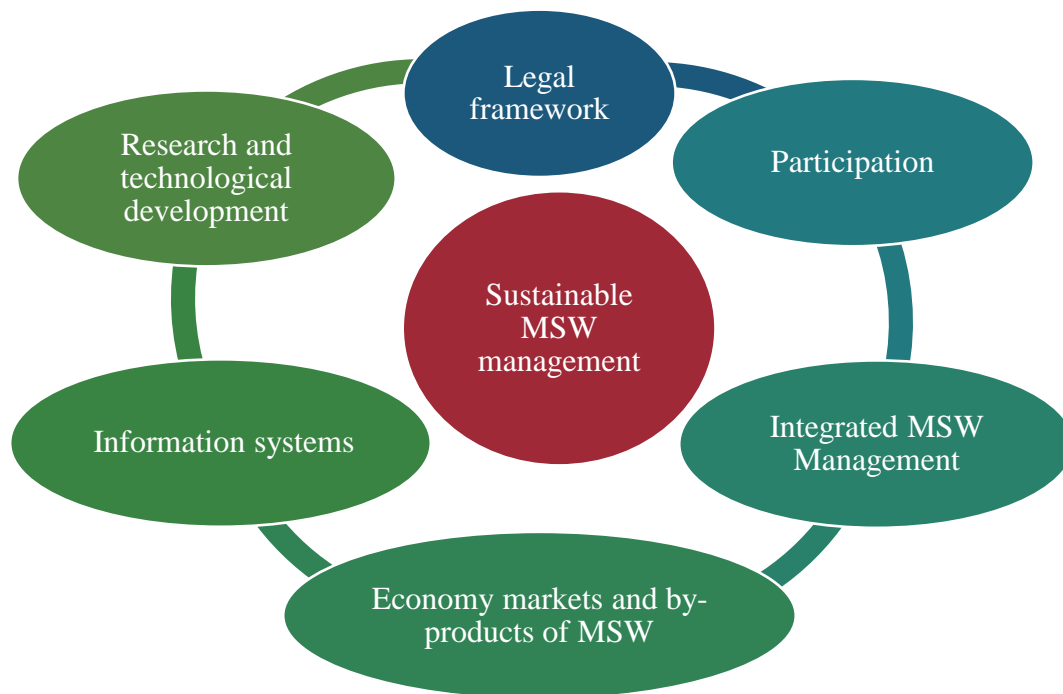
- Regulation of book 4 of the code for biodiversity of the state of Mexico.
- General Law of Ecological Balance and Environmental Protection
- General Law of Ecological Balance and Environmental Protection
- Code of Administrative Procedures of the State of Mexico
- Administrative Code of the State of Mexico
- Code for Biodiversity of the State of Mexico
- Rules of Procedure of PROPAEM.

3. Results

3.1 Sustainable MSW planning

The planning of MSW contemplates environmental restoration that involves the integration of new administrative and regulatory forms, the reengineering of public policies; the incorporation of technological innovation and the development of research, the promotion of educational and training cycles, the formation of market circuits, the formation of clusters, the participation of private initiative, the management and promotion of finances to the sector, investment funds; public participation; as well as the implementation of monitoring and evaluation (ICLEI, 2005, AUMA, 2006; Centro Complutense de Studio's e Información Ambiental, 2009), which implies analyzing the forms of management that have been carried out in Mexico, an example is the study carried out in the municipality of Mexicali, in Figure 3.1, the elements that form the framework for the planning of Urban Solid Waste from the approach of sustainability are presented.

Figure 3.1 Diagram of the framework for planning Municipal Solid Waste from the approach of sustainability



Source of Consultation: Own Elaboration

According to the previous diagram, the competences and attributions of the orders of the government in the sector are described, referencing the federal, state and municipal regulatory structure; Institutional framework, presents the policies and actions concerning plans and programmers carried out by the council through the units related to the subject; Participation, integrates the different forms of participation in planning and management activities carried out by the actors, as well as the rights they have of access to information and mechanisms for disseminating actions for monitoring and evaluating the performance that should be carried out by the assembly, on the other hand, the groups involved in waste management, this analysis facilitates the identification of diverse profiles and opinions on the management system in which they participate: responsible, groups and organizations of the public, private and social sectors linked to the subject; Integrated MSW Management, provides basic information on generation, transfer and disposition; Infrastructure, reports the material resources and facilities available to carry out the work of waste management by the council; interactions, shows the actions of concurrence that the conjuncture has with the other levels of government, the waste of special handling and dangerous; Finance, provides the budgetary information for the operation of the service by the council; economy, considers the opportunities of new market niches for the use of solid waste by-products and of the economic and financial instruments available to enterprises.

The information systems creates databases associated with the planning and management of solid waste for better decision-making and actions for evaluation and monitoring of its performance and communication to society; Research and development, incorporates scientific and technological contributions aimed at the sustainable management of solid waste, as well as considers environmental education as the basis of cultural changes, such as the importance of the dissemination and communication of actions to society and the feedback they make to management and; Education and training, provides non-formal environmental education, trains its staff and implements technological innovation actions in the management of MSW.

3.2 MSW management in the State of Mexico

Currently, a large part of rural municipalities limits the management of their solid waste to the basic elements: generation, collection and final disposal; In some cases, manual sweeping is also carried out in the streets of the municipal capital.

- a) **Generation:** The generation of waste is directly associated with the amount of population and the economic dynamics that characterize a community, municipality or region. According to INEGI, in 2010, the State of Mexico had a total population of 15,175,862 inhabitants, contributing 13.5% to the national total. As for the distribution of the population in the state, 87% is located in urban areas and 13% in rural areas. As a result of the amount of population accumulated by the State of Mexico and the diversity of economic activities, the demand for goods and services is very high, which leads to the generation and management of large amounts of urban solid waste. On the other hand, the INEGI, 2010. The State of Mexico generates approximately 6,798,100 tons of municipal solid waste per year, which represents 16% of the total waste generated nationwide.
- b) **Collection:** Of all the processes that make up the Integrated Management of Urban Solid Waste collection regularly is the one that generates the highest costs and depends, to a large extent, on the type of collection that is carried out (mixed or separated waste) since this determines the type of subsequent treatment. Obviously, the collection of separated waste reduces costs. In Table 3.1, the municipalities that provided information have high percentages of waste collection in their localities.

Table 3.1 Collection in municipalities of the State of Mexico

Municipalities	Localities by municipality	Locations with Collection %
Temascalcingo	66	91
San Felipe del Progreso	105	Sd
Acambay, Ruíz Castañeda	103	85
Municipalities	Localities by municipality	Locations with collection service %
Aculco	67	61.19
Atlacomulco	66	90
Jilotepec	66	63.63
San Jose del Rincon	139	86.33
Timilpan	27	70
Gold	44	93
Ixtlahuaca	64	85
Jocotitlan	60	Sd
Total	807	80.57%

- c) **Transfer:** When the final disposal sites are located at very long distances from the collection areas, transfer plants are installed. The complexity of the plants depends on where it is located, since it is necessary to comply with the sanitary rules, as well as with the NTEA-010-SMA-RS-2008. The use of transfer centers is low in the region that integrates the program, since most municipalities have a final disposal site and in which they dispose of their waste without the need to make use of a transfer center
- d) **Separation of by-products for recycling:** The separation of waste into by-products, for treatment, protects the environment since the number of tons of waste for final disposal is reduced. In addition, the sale of recyclable waste can help municipalities economically, however, the industry is usually interested in large volumes, which small municipalities cannot meet, so the creation of an intermunicipal system is recommended. The General Law for the Prevention and Integral Management of Waste provides for at least two types of separations, primary and secondary, the first is to separate organic waste from inorganic waste and secondary refers to separate from inorganic waste those that are likely to be recycled. In some municipalities, with regard to the separation of by-products for recycling, there is a "Program municipal are la prevention and gestion integral of MSW and special handling", within which it is known that: "the municipality during the work of collection of urban solid waste, the recovery of certain by-products with commercial value is practiced by the operators of the service within collection vehicles, being the materials with greater demand the PET, glass, metals and cardboard. Once these materials are separated, operators go to collection centers for direct sale.

- e) Final disposal: at this stage the waste would be deposited or permanently confined in sites and facilities whose characteristics allow preventing its release into the environment and the consequent effects on the health of the population and ecosystems and their elements, it is important to mention that the Official Mexican Standard NOM-083-SEMARNAT-2003, establishes the terms to which the location of the sites, the design, construction and operation of the facilities destined to the final disposal of urban solid waste and special handling, in landfills or in controlled confinements, must be subject, in this way the LGPGIR, points out that municipalities must regulate land uses in accordance with ecological planning and urban development programs, in which the areas in which the final disposal sites of urban solid waste and special management will be established will be considered. The landfill is the main option for the final disposal of waste used in the State of Mexico, and which consists of an infrastructure work that limits the impacts caused to the environment due to poor waste disposal, also in the State of Mexico according to the information obtained in the Consultation Portal of the Integral Waste System of the State of Mexico, the disposal of this waste is carried out both in landfills and in integral waste centers, each of these places depends on the municipality, in Table 3.2 they mention the municipalities that have a sanitary landfill and those that have an integral waste center are shown in Table 3.3, which would be the most prominent in the State of Mexico.

Table 3.2 Municipalities of the State of Mexico that have a landfill.

Name or business name	Municipality
Tecnosilicatos de México S.A. de C.V.	Ixtapaluca
Mexican waste concentrator S.A. de C.V.	Ixtapaluca
Constructora y operadora de rellenos sanitarios, S.A. de C.V.	Tenango del Valle
Chicoloapan landfill	Chicoloapan
Grupo contadero, S.A. de C.V. (Xonacatlán)	Xonacatlán
Tersa del golfo, S. de R.L. de C.V	Cuautitlan izcalli
Vigue relleno sanitario, S.A. de C.V	San Antonio de la Isla
RS Wast, S.A. de C.V.	Tecámac
MA. Carolina Villalobos Hernandez	Zumpango
Environmental Maintenance and Services, S.A de C.V.	Zinacantepec
Esmenra, S.A. de C.V.	Teoloyucán
Pro-faj hidrolimpieza, S.A. de C.V	Naucalpan de Juarez
H. city council of Tlalnepantla de Baz	Tlalnepantla de Baz
H. Atlacomulco city council	Atlacomulco

Table 3.3 Municipalities of the State of Mexico that have a comprehensive waste center

Name or business name	Municipality
Tecnosilicatos de México S.A. de C.V.	Ixtapaluca
RS wast, S.A. de c.v.	Tecámac

The final disposal of MSW in region II of the State of Mexico, there are final disposal sites, however, not all municipalities control the disposal.

3.3 Types of treatment

The treatments used in the State of Mexico are:

Biological treatment: This type of treatment is used for the elimination of gas and bad odor in the final disposal sites that is originated by organic waste, they are based on the degradation of organic matter present in the waste by the action of microorganisms, altering the molecular structure of the compounds eliminating toxic and dangerous compounds.

Other treatments currently used are the following:

- a) **Composted:** This type of treatment according to the information obtained in, has only been reported by the municipality of Atlacomulco, however, it is not followed to the letter according to the stipulations of current regulations mainly consist of 20% waste by pruning, 60% organic waste and 20% manure.

- b) Methanization: there is a biogas plant in the municipality of Atlacomulco that aims to provide municipal authorities with a tool to dispose of their urban solid waste in a sustainable ecological way, and thus also obtain economic benefit with the sale of the products obtained in this process. Fresh organic waste and municipal wastewater are treated which, through anaerobic fermentation, will produce biogas (liquid fertilizer) biosolid (solid fertilizer) and biogas as a product.
- c) Mechanical-biological treatment: it is a treatment that improves the properties of the waste that you want to deposit to reduce environmental impacts. It is a process that converts waste into semi-inert material through a broad stabilization phase, before final disposal, consists of two treatment stages: mechanical, to condition the MSW to its subsequent treatment and biological, through controlled fermentation or aerobic digestion.

There are also other types of treatment that are applied in many regions of the world, however, in Mexico there is little application mainly due to the high costs associated with these technologies. It refers to the chemical degradation of waste due to the increase in temperature caused by the combustion of most materials.

In the State of Mexico there are no plants of this type, due to the high cost of their installation and operation. Some of the heat treatments used in Mexico are:

1. Drying: it is the decrease in the weight of the waste, and increases the temperature so that the water evaporates and thus reduces up to 50% the weight of the waste, however, by increasing the temperature the volatile compounds are released causing an impact on the environment.
2. Incineration: process to reduce the volume and decompose or change the physical, chemical or biological composition of a solid, liquid or gaseous waste, by thermal oxidation, in which all combustion factors can be controlled. The incineration of MSW can reduce the volume by 70 to 90%.
3. Pyrolysis: thermal decomposition of a material in the absence of oxygen or any other reactant. This decomposition occurs through a complex series of chemical reactions and processes of transfer of matter and heat.
4. Gasification: optimized pyrolytic process, by which a solid or liquid substance with high carbon content, is transformed into a gaseous mixture of fuel, by partial oxidation with application of heat, process technology designed to obtain a synthesis gas; that is, a product that can be used to produce fuels, chemicals or energy.
5. Biomass reforming: heat treatment process, which with the help of a catalyst produces a hydrogen-rich gas from organic matter.

3.4 MSW generation in the State of Mexico

Table 3.4 shows the total amount of waste generated in the State of Mexico.

Table 3.4 Waste generated: Integral Waste System of the State of Mexico (SIREM).

Waste Management Destination									
Description of the Waste	Quantity generated (Ton/Month)	Use		Treatment		Gathering		Final Provision	
		Ton/Month	%	Ton/Month	%	Ton/Month	%	Ton/Month	%
MSW-1 Solid organic waste (from food and gardening)	712.675	68.315	9.586	3.608	0.506	8.582	1.204	632.170	88.704
MSW-2 Recyclable solid waste, specify with form to classification	180.249	5.583	3.097	1.371	0.761	4.120	2.286	169.175	93.856
MSW-3 Medical waste	477.580	4.259	0.892	2.985	0.625	15.601	3.267	454.735	95.217
MSW-4 Other / specify	104.931	3.966	3.780	1.380	1.315	0.000	0.000	99.585	94.905
RME-1 Waste from health services generated by a large generator in Medical-assistance centers	86.292	7.241	8.391	0.054	0.063	0.269	0.312	78.728	91.234
RME-2 Agroplastic waste generated by intensive agricultural/forestry and forestry activities	0.000	0.000	0.000	0.000	0.000	0.000	0.000	0.000	0.000
RME-3 Organic residues from intensive agricultural/poultry activities / Livestock and fishing	67.892	14.400	21.210	0.000	0.000	0.000	0.000	53.492	78.790
RME-4 Waste from federal transport activities, which includes services in ports, airports, bus stations and motor transport stations and those of public transport, which includes service providers that have terminals, workshops or stations, which are included in The following list	42.166	0.000	0.000	0.000	0.000	0.000	0.000	42.166	100.000
RME-5 Sludge from wastewater treatment with the exception of those indicated in the NOM-052-SEMARNAT-2005	2,989.014	703.289	23.529	805.645	26.954	35.184	1.177	1,444.896	48.340
RME-6 Waste from department stores or shopping centers, including self-service stores, supply centers, public markets and Travelling.	10,905.351	8,842.732	81.086	50.000	0.458	0.000	0.000	2,012.619	18.455
RME-7 Construction waste / maintenance and demolition in general that is generated in a work in a quantity greater than 80 m ³	418.839	44.767	10.688	0.000	0.000	0.000	0.000	374.072	89.312
RME-8 Products that at the end of them Shelf life are discarded	17,923.980	6,822.301	38.062	1,000.403	5.581	4,553.970	25.407	5,547.306	30.949
RME-9 Others established in the General Law for Prevention and Management Integral Waste and Regulation	14.464	0.000	.000	0.000	0.000	0.000	0.000	14.464	100.000
RME-10 Other	10,594.455	1,987.168	18.757	2,125.346	20.061	44.332	0.418	6,437.609	60.764
Total	44,517.888	18,504.021	41.565	3,990.792	8.964	4,662.058	10.472	17,361.017	38.998

Source: Integral Waste System of the State of Mexico (SIREM)

With the data obtained previously, the result of the generation of MSW in the State of Mexico is 6,798,100 tons per year of municipal solid waste, representing 16% of the total waste generated nationwide with a population of 15,175,862. In Edo. Mexico has a population of approximately 16.99 million people, so it is estimated that, in 2021, there will be an increase in MSW generation of 7611,835 tons per year.

In this way it can be established that residue growth exists exponentially, given by the following formula: $P(t) = (P_0) e^{rt}$, where the growth rate is:

Starting amount (P_0): 15,175,862 people
 Time (t): 10 years
 Final quantity ($P(t)$): 169,924,18
 Growth rate: $0.0113061105282 = 1.13061105282\%$

Therefore, using the same formula, with respect to waste generation and growth rate, the final amount generated per year is sought:

Initial amount (P_0): 6798,100 tons per year
 Time (t): 10 years
 T growth rate: $0.0113061105282 = 1.13061105282\%$
 Final quantity ($P(t)$): 7611.835 Ton per year

In this way, the proposals in sustainable planning seek to reduce a large percentage in waste generation, so that together with the organizations and institutions responsible for the environment, greater impact must be generated to apply the management and regulations in force.

3.5 Proposal to improve MSW in the state of Mexico

In the country of Sweden, whose population is one of the largest in the Nordic countries, it is an exemplary country in the recovery of energy from waste, and this energy recovery is mainly based on the incineration of its waste, from which energy is provided for district heating of 20% of the country and for the electricity of some 250,000 families. Waste management in this country has become an industry and source of employment (Cali.gov.co, 2012).

However, the trend in Mexico is to increase the generation of waste, as well as its deficient final disposal, coupled with a lack of environmental culture and the clear devaluation that the majority of society gives to waste. On the other hand, the anaerobic conversion method is an environmentally safe option.

Likewise, the implementation of MSW treatment policies is a necessary alternative and improvement as an infrastructure for both society and the environment. The growing demand for MSW collection service requires an increase in the infrastructure with which it is able to properly handle MSW. However, with the passage of time, the location of the required infrastructure tends to move away from urban centers, so it is convenient to carry out comprehensive regional planning with long-term perspectives that allows the strengthening of the infrastructure for the management of MSW.

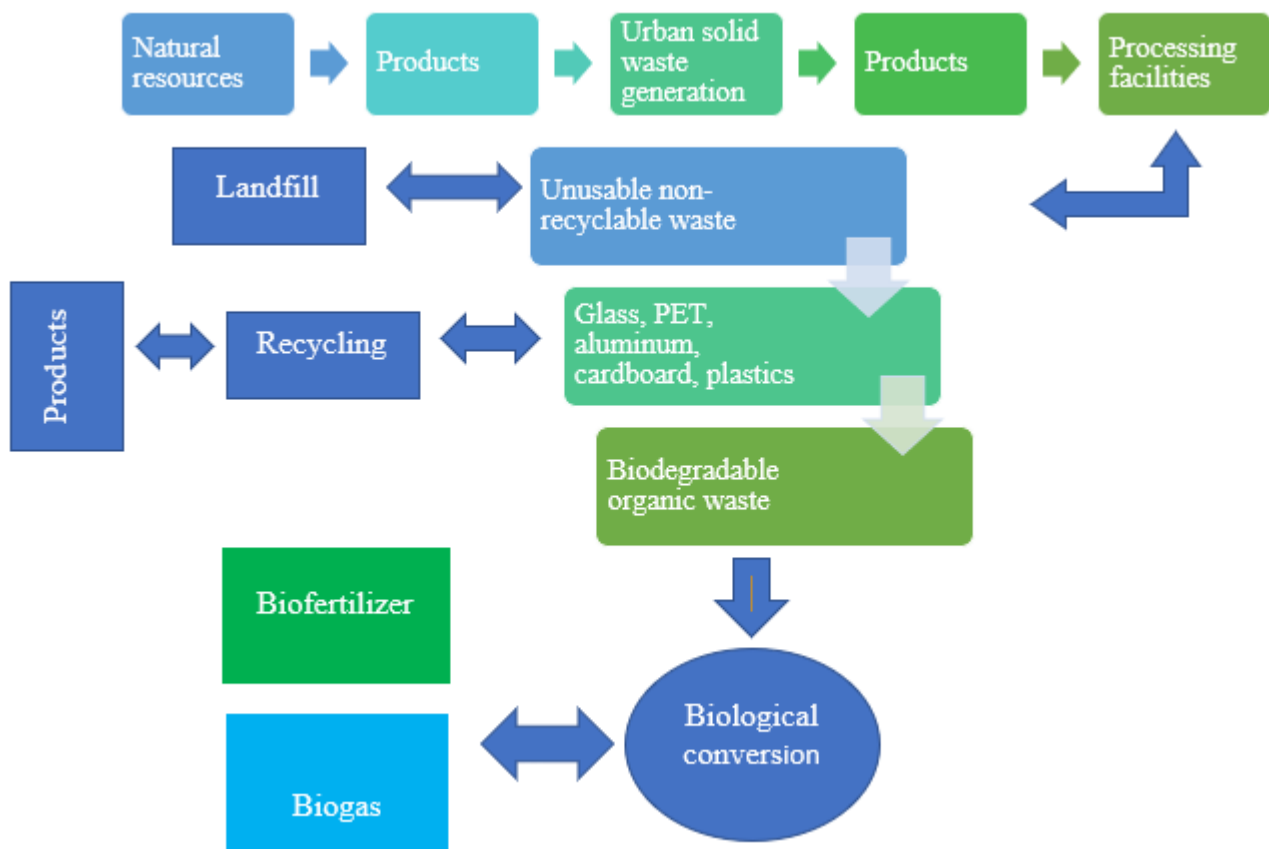
Comprehensive systems require collection and transportation systems, as well as infrastructure for waste treatment and separation. Currently, separation and treatment plants for MSW are becoming a necessary installation in large cities. In Mexico, growth rates are below expectations, as only 10% of the total MSW generated is recycled.

The capture of biogas is done through the biological conversion of organic waste by which different bacterial groups use this material to feed. This process of decomposition of matter generates a significant amount of methane gas, carbon dioxide, some nitrogen, hydrogen and hydrogen sulfide. The gas generated, biogas, can be used for heating or in electric generators. Through this process it is estimated that for each ton of organic waste, up to 175kWh can be generated, enough energy to power a standard refrigerator for two months (SENER, 2014).

At the global level, Germany and Sweden have set an example on this issue. In Germany there are more than 5,000 biogas plants throughout the country. In 2010 alone, these plants generated more than 13 TWh (billion kilowatt hours), representing approximately 2% of all renewable energy generated in the country. (IMCO, 2012).

On the other hand, the digested residue can also be very useful as a biofertilizer, since it has no odor and has characteristics similar to humus, favors the fixation of carbon in soils, and can improve the capacity of water absorption. Therefore, it is proposed to install an integrated MSW treatment plant with the capacity to capture biogas and biofertilizer production through anaerobic conversion. This treatment method favors the recycling and recovery of the materials that make up the MSW throughout the process: in the separation stage, inorganic waste is recovered to be recycled, which reduces the pressure on natural resources (extraction, production and transport of new products) and reintroduces these materials into the production system; In the stage of anaerobic digestion of the organic fraction, in addition to producing biofertilizer, methane emissions are reduced. Figure 3.2 shows a diagram of the conversion process of MSW to biofertilizer and biogas. Thus, from the primary products obtained with this waste treatment technology, a recovery of products or energy can be made at a later stage, and in this way a direct impact is achieved in the reduction of greenhouse gas emissions.

Figure 3.2. Process of conversion of MSW to biofertilizer and biogas



Source of Consultation: Own Elaboration

Acknowledgements

This work has been funded by the Technologic of Studio's Superiors of Jocotitlán and the Secretary of the Ministry of Mexico with the project: Study, evaluation and treatment of pollutants present in environmental matrices through sustainable processes for technological development, PI202022, 2020-2022.

Conclusions

The generation of MSW in Mexico and in particular the State of Mexico, highlighting the different processes that are applied for the reduction of these through different processes by previously defined category are important for an improvement of life not only municipal, state and national.

Carrying out this research is a reflection and is an awareness to reduce individually the garbage generated day by day, since, according to the statistics published by the government, the numbers are really high and although it seems that we have the opportunity and the obligation to create solutions to these problems, A high potential is really needed, since controlling waste generation is an unstable parameter at this time. The purpose is that the proposal of a turn of change in people so that they can and know what to do with waste.

The generation of Urban Solid Waste (MSW) is already becoming a serious problem for society, the environment for example in the pollution of seas, rivers and mainly in the quality of drinking water. According to the diagnosis made to the MSW generated in the State of Mexico, data is obtained where it has not been intended to reduce it, although there are laws and institutions, the legal framework in charge of applying is not reflected 100% for various reasons (politics, corruption, bad habits, lack of responsibility, etc.), this can be clearly observed in the final disposal sites since of the few sites that exist in the State of Mexico these do not comply with the stipulations of the rules, that is, they are not controlled, it was also realized that the treatments that must be used in the different types of waste, as mentioned in the document, are not used in most cases, and the only municipality that has reported the use of one of them, is the treatment by composting in the municipality of Atlacomulco, Edo. of Mexico, so it is really necessary to look for alternatives that can be used effectively and thus reduce the generation of waste in the State of Mexico, which surprisingly is the state with the highest generation of MSW in Mexico and is something really worrying. It is important to mention that it is everyone's task from the municipalities where planning should be applied mainly, to the citizens.

References

Calva Alejo and Rojas Caldelas. Diagnosis of Urban Solid Waste Management in the Municipality of Mexicali, Mexico: Challenges for the Achievement of Sustainable Planning: <https://scielo.conicyt.cl/pdf/infotec/v25n3/art09.pdf> (February 11, 2014). DOI: 10.4067/S0718-07642014000300009

Cali.gov.co, 2012. Plan de Desarrollo Municipal 2012-2015. https://www.cali.gov.co/planeacion/publicaciones/44418/plan_desarrollo_municipal_2012_2015/

Contreras Mendoza, A. Intermunicipal Program for the Prevention and Integral Management of Urban Solid Waste for Region II, State of Mexico. Autonomous University of the State of Mexico. Faculty of Urban and Regional Planning. <http://ri.uaemex.mx/bitstream/handle/20.500.11799/67520/UAEMFaPURPrograma%20Intermunicipal%20para%20la%20Preveni%C3%B3n%20y%20Gest.pdf> (September 2017).

Dálisa, G., M.F. Di Nola, M. Giampietro, A multi-scale analysis of urban waste metabolism: density of waste disposed in Campania, *Journal of Cleaner Production*: 35, 59-70 (2012). <https://www.sciencedirect.com/science/article/abs/pii/S0959652612002405>, DOI: 10.1016/j.jclepro.2012.05.017

Gil, M. Á, Crónica del Instituto Nacional de Ecología, SEMARNAT. INE- SEMARNAT, Mexico City, (2009). https://apps1.semarnat.gob.mx:8443/dgeia/informe15/tema/pdf/Informe15_completo.pdf <http://cambioclimatico.gob.mx:8080/xmlui/handle/publicaciones/261>

Government of the State of Mexico (GEM) (2009) Program for the integral prevention of urban solid waste and special management of the State of Mexico. *Gaceta de Gobierno del Estado de México*. <https://legislacion.edomex.gob.mx/sites/legislacion.edomex.gob.mx/files/files/pdf/gct/2009/mar103.pdf>

IMCO, 2012, Índice de competitividad urbana 2012. <https://imco.org.mx/indice-de-competitividad-urbana-2012/>

INEGI. 2010. Population and housing censuses, 1990, 2000 and 2010. Databases: <https://www.inegi.org.mx/rnm/index.php/catalog/71> (May 11, 2021).

- Kanat Gurdal, Municipal solid-waste management in Istanbul. *Waste Management*, Vol 30, Issues 8-9, 2010, 1737-1745. <https://www.sciencedirect.com/science/article/abs/pii/S0956053X10000826>
DOI: 10.1016/j.wasman.2010.01.036
- Lohri C., R., Diener, S., Zabaleta I., Mertenat A., Treatment technologies for urban solid biowaste to create value products: a review with focus on low- and middle- income settings, *Reviews in Environmental Science and Bio/Technology* 16(1). <https://link.springer.com/content/pdf/10.1007/s11157-017-9422-5.pdf>, <https://doi.org/10.1007/s11157-017-9422-5>, DOI: 10.1007/s11157-017-9422-5
- Marshall, R.E. and Farahbakhsh, K. (2013) Systems Approaches to Integrated Solid Waste Management in Developing Countries. *Waste Management*, 33, 988-1003. https://edisciplinas.usp.br/pluginfile.php/4448762/mod_resource/content/1/Texto%20%20Systems%20approaches%20to%20integrated%20solid%20waste%20management.pdf
<http://dx.doi.org/10.1016/j.wasman.2012.12.023>, DOI: 10.1016/j.wasman.2012.12.023
- Montesillo, R. Proposal for the sustainable management of urban solid waste in the central zone. *Revista Legado de Arquitectura y Diseño*. <https://www.redalyc.org/articulo.oa?id=477948279059>
- Okot-Okumu, J., R. Nyenje, Municipal solid waste management under decentralization in Uganda, *Habitat International*: 35, 537-543. <https://www.sciencedirect.com/science/article/abs/pii/S0197397511000178>, <https://doi.org/10.1016/j.habitatint.2011.03.003>, DOI : 10.1016/j.habitatint.2011.03.003
- Official Journal of the Federation (DOF) General Law for the Prevention and Integral Management of Waste (2003). <https://www.gob.mx/profepa/documentos/ley-general-para-la-prevencion-y-gestion-integral-de-los-residuos-62914>
- Official Journal of the Federation (DOF), General Law of Ecological Balance and Environmental Protection (1988). https://dof.gob.mx/nota_detalle.php?codigo=4718573&fecha=28/01/1988#gsc.tab=0
- Papachristou, E., H. Hadjianghelou, E. Darakas, K. Alivanis, A. Belou, D. Ioannidou, E. Paraskevopoulou, K. Poulis, A. Koukourikou, K. Sortikos, Perspectives for integrated municipal solid waste management in Thessaloniki, Greece, *Waste Management*: 29, 1158-1162 (2009). <https://www.sciencedirect.com/science/article/abs/pii/S0956053X0800161X?via%3Dihub>, <https://doi.org/10.1016/j.wasman.2008.04.015>, DOI: 10.1016/j.wasman.2008.04.015
- Pires, Ana, G. Martinho, N. Chang, Solid waste management in European countries: A review of systems analysis techniques, *Journal of Environmental Management*: 92, 1033-1050 (2011). <https://www.sciencedirect.com/science/article/pii/S0301479710004275?via%3Dihub>, DOI: 10.1016/j.jenvman.2010.11.024
- Portal of Consultation of the Integral System of Waste of the State of Mexico. Ministry of the Environment. <http://189.195.154.174:8095/portal-sirem/>
- Seadon, J.K., Sustainable waste management systems, *Journal of Cleaner Production*: 18, 1639-1651 (2010). <https://www.sciencedirect.com/science/article/abs/pii/S0959652610002672?via%3Dihub>, DOI: 10.1016/j.jclepro.2010.07.009
- SEDESOL, Estado de las Ciudades de México 2011, Mexico City, Secretary of Social Development United Nations Human Settlements Programme, UN-HABITAT. http://www.ampres.com.mx/assets/estado_de_las_ciudades_de_mexico_2011-1-.pdf (May 15, 2021)
- SENER, 2014. Balance nacional de energía. https://www.gob.mx/cms/uploads/attachment/file/44353/Balance_Nacional_de_Energ_a_2014.pdf
- SEMARNAT. 2009. The environment in Mexico, in summary. Municipal solid waste generation: https://apps1.semarnat.gob.mx:8443/dgeia/informe15/tema/pdf/Cap7_Residuos.pdf (May 10, 2021)

Sosdf. 2007a. Actions for the management of solid waste in Mexico City. <https://www.sedema.cdmx.gob.mx/storage/app/uploads/public/577/2a0/df3/5772a0df3469a516268603.pdf> (May 14, 2021).

Tchobanoglous George, Hilary Theisen y Samuel Vigil (1994). *Gestión Integral de Desechos Sólidos*. Madrid: Editorial McGraw Hill.

Chapter 4 Ecological panel based on plastic aggregates, natural fibers, and plaster

Capítulo 4 Panel ecologico a base de agregados plasticos, fibras naturales y yeso

OGURI, Leticia†*, ESCOBAR, Marlem Guadalupe, PRETEL, Ana María and GARCIA, Nidia Miriam

Tecnológico de Estudios Superiores de Jocotitlán, Licenciatura en Arquitectura

ID 1st Author: *Leticia, Oguri* / **ORC ID:** 0000-0003-3723-9202, **Researcher ID Thomson:** AAX-2427-2021

ID 1st Co-author: *Marlem Guadalupe, Escobar* / **ORC ID:** 0000-0003-3079-3462

ID 2nd Co-author: *Ana María, Pretel* / **ORC ID:** 0000-0002-8508-8114

ID 3rd Co-author: *Nidia Miriam, Garcia* / **ORC ID:** 0000-0001-6303-8418

DOI: 10.35429/H.2022.3.49.64

L. Oguri, M. Escobar, A. Pretel and N. García

*leticia.oguri@ tesjo.edu.mx

A. Ledesma (AA.). Science of Technology and Innovation. Handbooks-TII-©ECORFAN-Mexico, 2022.

Abstract

Today, there is a growing need for alternative construction technologies that allow, among other things, to reduce of plastic waste and energy consumption during the life cycle of buildings. In this context, this article presents the partial results of a research project whose objective is to develop an innovative solution for plasterboard with plastic aggregates such as pet and Ixtle natural fibers. This solution is based on a plasterboard made with a mixture of eco-efficient composite materials. The composite material used in the production of the plates or panels results from the combination of two industrial by-products: commercial plaster; crushed or laminated pet, and natural “ixtle” textile fibers resulting from the “carving” process of the maguey leaves. In addition to the raw materials, the innovation of the solution also results from new future proposals for experimentation with different recycling materials. In this work, details of the process of elaboration of the plates and both the optimization of the composition of the material and the construction technology are provided, within the long strategies, the tests and validation of the mixtures will be carried out for the elaboration of plates from the point of view of mechanical, thermal and acoustic behavior, which from the results obtained can be concluded in the feasibility that meets all the structural stability requirements suitable for this type of construction element.

Panel Ixtle, Innovation, Experimentation

Resumen

Hoy en día, existe una creciente necesidad de tecnologías de construcción alternativas que permitan, entre otras cosas, reducir los residuos plásticos y el consumo de energía durante el ciclo de vida de los edificios. En este contexto, este artículo presenta los resultados parciales de un proyecto de investigación cuyo objetivo es desarrollar una solución innovadora para placas de yeso con agregados plásticos como el pet y las fibras naturales de Ixtle. Esta solución se basa en una placa de yeso realizada con una mezcla de materiales compuestos ecoeficientes. El material compuesto utilizado en la producción de las placas o paneles resulta de la combinación de dos subproductos industriales: el yeso comercial; pet triturado o laminado, y fibras textiles naturales de “ixtle” resultantes del proceso de “tallado” de las hojas de maguey. Además de las materias primas, la innovación de la solución también resulta de nuevas propuestas de futuro para la experimentación con diferentes materiales de reciclaje. En este trabajo se brindan detalles del proceso de elaboración de las placas y tanto de la optimización de la composición del material como de la tecnología constructiva, dentro de las estrategias largas se realizarán las pruebas y validación de las mezclas para la elaboración de placas desde el punto de vista del comportamiento mecánico, térmico y acústico, lo que de los resultados obtenidos se puede concluir en la viabilidad que cumple con todos los requisitos de estabilidad estructural adecuados para este tipo de elemento constructivo.

Panel Ixtle, Innovación, Experimentación

1. Introduction

Betting on new construction materials that are friendly to the environment has led higher-level educational institutions, whether universities or technology, the construction industry, and all those actors involved in architecture to encourage students and researchers to reflect on the architecture commitment. And the impact of its architectural work on the natural or artificial context that surrounds it, as well as its influence on one of the most critical problems of humanity such as the climate crisis which includes climate change, the deterioration of farmland, the expansion of the urban sprawl, pollution and loss of biodiversity, it is necessary to understand and measure the responsibility of all these actors. That is, why it is essential to promote, analyze, innovate and experiment with new products for this great industry that is construction, but above all to look for new strategies for teaching architecture to make future architects aware of this great crisis, but above all as an agent generator of well-being with responsibility and social commitment. (see figure 1)

Figure 1 The Great Crash

Source (De la Madrid & Landeros, 2020)

One of the great concerns is the impact generated by these current construction products produced with renewable and non-renewable materials, their management and final disposal is a critical situation, which worsens as cities grow.

This article invites reflection and presents a research project developed from the classrooms of the degree in Architecture, which is mainly based on the elaboration of an ecological panel based on plaster and aggregates such as PET and ixtle as a constructive element. , with the use of natural materials such as maguey with its Ixtle fibers typical of the northern region of the state of Mexico, one of the objectives of the project is to verify its feasibility and effectiveness and thus be able to use them in construction as another alternative construction element, friendly to the environment and the use of this natural fiber and the recycling of PET.

Gypsum panels or commonly called in Mexico Tablaroca are generally composed of a center of plaster gypsum, cellulose and confined under pressure between two sheets of recycled paper, in Mexico there are in the current market, brands such as Tablaroca, Panel Rey, and Plaka Comex, among others, which within their characteristics have a good ecological balance due to their efficient use of raw materials, such as plaster and cellulose in the production process, within the construction sector they are commonly used for their excellent, acoustic and thermal insulation properties and its resistance to fire, in addition to its easy handling and flexibility.

However, although gypsum and cellulose are the natural raw material that is found in abundance, they must be treated as non-renewable materials to be aware of their care, which is why this proposal to make the prototype of the panel of plaster, is from the analysis of conventional or commercial plaster panels which the elaboration of the panel will be carried out a controlled production process from the selection of the material and the processing of the material such as Ixtle and PET, and thus by uniting these two elements to obtain a more environmentally friendly and sustainable product, an element with these characteristics will allow the construction sector to reduce the rate of pollution released during its practice, it will be a resistant and light element, which will serve within the design and construction of the interior space.

That is, why the reason for this research, it is of the utmost importance to be aware of the architectural work and one of them is the interest in creating innovative projects, benefiting a large part of society, based on the above, it was decided to propose the project called "Ecological plasterboard based on PET plastic aggregate and ixtle", to generate a sustainable ecological material using materials that reduce the impact on the environment, and have benefits such as fire resistance, acoustic insulation, thermal resistance to humidity, at a low cost in its production and thereby contribute to reducing pollution, global warming, and environmental impact. (Acosta, 2009)

Under this perspective, it is evident that the architect's profession, originally so linked to the land, has been modified in recent times due to social, political, economic, and educational changes, the introduction of new materials and new practices, today, it is done. It is necessary to propose awareness programs aimed at architecture students where they reflect on priority issues such as in this case, the shared responsibility with the great environmental problems, and as far as possible, the social co-responsibility that joint participation requires, coordinated and differentiated from producers, distributors, consumers, users of by-products, and from the three levels of government as appropriate, under a scheme of market feasibility and environmental, technological, economic, and social efficiency.

2. Developing

The consumption of plastic materials has increased notably in recent years worldwide, specifically PET (Polyethylene Terephthalate) due to the proliferation of containers of this material in the food industry. PET containers have added to the changing consumption habits of the population such as consuming more and more bottled water and carbonated drinks, which leads to producing more waste because the container has no useful value for the consumer. and that is why what continues to contribute to the contamination of the soil and water is discarded. (Cristian, et al 2003)

When PET is discarded, its disintegration effect is for a long time. According to calculations, it can take between 500 and 1000 years to decompose. And even if it stops being seen, it will have released thousands of micro PET fragments that are even more polluting. Currently, there must be sustainable materials that help minimize pollution on the planet, especially those materials that are used in the field of construction. (Hernández, 2008)

Innovation in new materials provides construction with the fluidity to build, in addition to the fact that architecture itself is increasingly focused on the use of sustainable materials that have a favorable impact on the environment and the economy of consumers. Such is the case of gypsum boards or panels that minimize time and costs when building and designing exterior and interior spaces, where the general purpose of companies is to seek short-term alternatives to increase their productivity.

However, it can be counterproductive when it comes to being transported and manageable for assembly since they can become heavy and fragile. These panels are mainly made up of plaster, cellulose, water, and cardboard. Gypsum is a natural and universal raw material that is found in abundance in nature and its residues are biodegradable, however, care must be taken for it. For this reason, it is proposed to make a plaster panel mixed with PET grinding, this is one of the most common wastes currently causing a notable acceleration of global warming and great pollution in rivers, seas, oceans, forests, etc.

PET offers high resistance, a good barrier to CO₂ and humidity, is compatible with other materials, is recyclable, low weight, and waterproof. That is, why it has been chosen as one of the materials that will be most present in the elaboration of the panel. In addition, it is decided to add a vegetable fiber (Ixtle) obtained from the maguey that will allow a panel with greater resistance, since this fiber is placed on the lateral faces of the panel providing greater rigidity. (Alesmar et al, 2001)

The composition of the chosen materials allows us to achieve a sustainable element that will be used to create interior spaces seen mainly in walls, ceilings, ceiling.

The research topic called "Ecological plasterboard based on PET plastic aggregate and ixtle" was selected according to the current problem of environmental pollution where plastic is one of the main wastes found in large volumes in different places. That is, why it is decided to reuse I, so that the pollution it generates by having a late degradation process in the environment can be avoided. Being thus an idea of innovation that seeks for our current quality of life and that of future generations.

The panel is made with plaster, recycled PET plastic, and ixtle, which includes the grinding of PET, this being a process that will convert the bottles into smaller particles until reaching the granulometry required for our product. Elaborating an element with these characteristics will allow the construction to reduce the rate of contamination that it releases during its practice, it will be a resistant and light element, in addition to having an accessible price for the public that will serve the interior design of spaces where it is necessary to divide or build a space in creatively ways with the best finish.

For this, the appropriate execution of recycling and the implementation of concrete actions that benefit ecological, economic, and accessible aspects to a large part of humanity is essential.

The composition of the mixture of these materials proposes to obtain a sustainable element that guarantees the reduction of pollution and has unique characteristics of resistance and durability as an alternative to be used in the construction of interior spaces in dividing and decorative walls, false ceilings, and furniture, among others, other uses, depending on the required need of the project to be implemented.

The materials that make up the innovative product are: plaster, grinding of PET plastic, ixtle, cellulose, and recycled cardboard. Gypsum is usually white, with a fine texture and low hardness. It is composed of crystallized calcium sulfate with two water molecules; It is obtained by calcination of hydrated calcium sulfate. Gypsum by itself does not have direct applications, however, it is a binder that hardens quickly. Its elasticity allows us to easily model various ornamental elements at a low cost. (Mayor, 1977)

Plastic grinding has properties that make it transparent, shiny, resistant to wear, has a good slip coefficient, is a good thermal barrier, against gases and moisture, etc. Its advantages include transformation through extrusion, injection, and perform blow molding, and thermoforming processes. (Cosmos O., 2021).

Recycled paper is a raw material that has a lower impact on the environment since its production represents a reduction of up to 60% in carbon dioxide emissions compared to other materials. It is cellulose, its decomposition time is short, in addition to the fact that, after recycling, recycled cardboard or paper does not lose quality or properties and is also cheaper. (London T., 2011).

And finally, the lechuguilla fiber (Ixtle) or Tampico fiber, as it is known internationally, has excellent quality due to its hardness, high strength, and durability given its high-water absorption capacity (65%) and its resistance to solvents, chemicals, heat, diluted and concentrated acids, abrasive products, petroleum distillates, alcohols, and vegetable oils. (Castillo et al, 2013)

3. Methodology

The research method is quasi-experimental, it is shown through the management of unproven experimental variables, in relatively controlled conditions, since being an experimental work where the participation of students is included to promote research, creativity, and innovation, but above all, raise awareness of major issues such as sustainability. Likewise, it is proposed to manage this research in three stages in the short, medium, and long term so that there is continuity both in the work and in the participating students during these periods.

The objective of this research is to study the feasibility of the module or construction element from something already created such as the plaster panel and its incorporation of PET and Ixtle fibers, which these elements will first undergo various tests, elementary physical in this way to know and demonstrate its physical properties, in addition, its comparison with similar elements, which will enable the detection of virtues or defects of the element, as well as the exploration of new forms of construction to detect its advantages in use, functionality, and sustainability within drywall standards.

Within the research strategies:

Short term

- Documentary and field research stage.
- Analyze information collected both bibliographic and field.
- Analyze and characterize existing and/or commercial prototypes.

Medium term

- Select plastic materials especially PET and recycled paper
- Select the plants for the elaboration of the Ixtle.
- Execute the experimentation of the materials to be used, as well as define the samples and the proportions with the plaster, PET, and ixtle.
- Submit to non-specialized conventional tests of the materials and the construction element (prototype),
- Analysis of results.

Long-term

- Determine the construction processes.
- Real-scale prototyping
- Submit the prototypes to specialized laboratory tests in terms of resistance and compression
- Compare the costs of the product in the current market.
- Analyze the function, resistance, and durability of the prototype.
- Identify the benefits of manufacturing ecological panels such as cost reduction and their functions.
- Integrate the ecological gypsum panel into the construction market, to achieve national recognition of the product.

4. Results and discussion

Experimental part

Next, part of the research strategies in its medium-term stage consists of the process for the preparation of the panel is described.

- The selection of plastic materials, especially PET, plaster, ixtle, and recycled paper
- Raw material manufacturing process.
- Execute the experimentation of the materials to be used, as well as define the samples and the proportions with the plaster, PET, and ixtle.

Materials

For the elaboration of the panel, a controlled production process will be carried out from the selection of the material and the processing of the materials.

PET plastic (*polyethylene terephthalate, polyethylene terephthalate, polyethylene terephthalate, or polyethylene terephthalate*), was chosen because we consider it the most common waste recorded daily.

In general, this material is characterized by its properties such as purity, high resistance, and toughness, it also has properties of transparency and chemical resistance; It is light, with high rigidity and hardness, as well as being recyclable. Through this last property of "recycling", we obtain the grinding through a process of cleaning and selecting the plastic so that it passes through a plastic materials mill where particles of between 4-10 mm are obtained.

This material will be used as mentioned before to obtain a granulometry or laminar product according to its properties, in order to integration with the plaster feasible, and ixtle to make the mixtures and able to form panels of 0.60 x 0.60 m and 12mm in diameter. Thickness according to NMX-C168-1977 "gypsum boards or blocks for interior walls" in section 5.4.

Figure 2 Pet

Source (Authors, 2022)

Gypsum (*calcium sulfate hemihydrate*) is originally a mineral called gypsum or gypsum stone. This rock is mainly made up of calcium sulfate with two water molecules ($\text{CaSO}_4 \cdot 2\text{H}_2\text{O}$), called calcium sulfate dehydrate. From this mineral, you can obtain a product called calcium sulfate hemihydrate ($\text{CaSO}_4 \cdot \frac{1}{2}\text{H}_2\text{O}$), also known as construction plaster. In this form it acquires the ability to set in the air, it has properties such as malleability, hygroscopic, and favorable thermal conditions for construction (Mayor, 1977).

The ixtle, a material that is obtained through the "carving" of the maguey leaves (Salmiana), the integration of this natural material, arises by offering more resistance to the panel, forming a protective mesh on its lateral faces as it is a plant predominant succulent in several areas of the State of Mexico, it will allow us to access with greater accessibility and make use of the plant, manually obtaining the ixtle according to the ancestral technique to take advantage of this natural fiber. (Castillo et al, 2013)

Figure 3 Maguey Salmiana

Source (Authors, 2022)

Recycled paper

Recycled paper, also called post-consumer waste, carries a process to obtain cellulose, which is a pulp extracted from wood from chopping until it is transformed into a paste or pulp, which is subjected to chemical processes where cellulose is obtained pure cellulose fibers, the Kraft paper process is based on a solution of sodium sulfide and sodium hydroxide in a 1:3 ratio for 2 to 6 hours at a temperature of 160 to 170 °C at the boiling point and that subsequently the sodium sulfide is eliminated (Budjiashvil, 2019)

The use of Kraft Paper has been considered since it is very resistant, and the paper guarantees stability between the composition of the materials that are part of the core of the panel. It can be said that this type of paper is integrated to give life to some multilayer materials since it is feasible to be combined with other diverse materials.

For the selection of these materials, it was possible to identify advantages and disadvantages of the requirements that could meet the technical properties, such as resistance, wear, absorption, and resistance, to be used in the panels, properties that would make it possible to build a panel with ecological characteristics and constructive.

Experimental part

The raw material manufacturing process

Obtaining PET plastic milling

- a. PET collection (figure 4). It is the most conventional type of plastic in our daily lives, so it is very easy to get it, you must ensure that the material is free of impurities or dirt.

Figure 4 Plastic bottles



Source (Authors, 2022)

- b. Cleaning of the collected PET material, in order to obtain a clean grinding of dirt that may affect the elaboration of the panel. If necessary, the PET will have to be washed to remove any type of contaminant. Here are the labels, caps, and mouth of the bottles that have been collected are also removed as seen in figure 5.

Figure 5 Removal of labels and caps from the collected bottles



Source (Authors, 2022)

- c. Reduction of the size of the plastic through a mill where particles between 4 mm and 10 mm will be obtained. Figure 6 shows how the plastic bottles enter the plastic materials mill. And figure 7 shows the expulsion through the output chamber of ground plastic.

Figure 6 Entry of bottles to the hopper of the plastic materials mill



Source (Authors, 2022)

Figure 7 Expulsion through the output chamber of ground plastic



Source (authors, 2022)

- d. A series of factors must be considered to obtain the grinding of plastic for verification of the desirable granulometry, once it is subjected to the grinding process, sieves must be used which will allow classifying the different sizes of plastics that were obtained, or, where appropriate, repeat the grinding process to obtain the appropriate granulometry for mixing with the materials used in the panel. (see figure 8)

Figure 8 Obtaining plastic milling for panel use



Source (authors, 2022)

Ixtle extraction

- a. The process for obtaining the ixtle is described below, first, a maguey stalk is cut, using a saw bow and gloves, since care must be taken because the sap causes an allergic reaction on contact with the skin such as itching, or redness. (see fig.9).

Figure 9 Cutting of the maguey stem to obtain the ixtle



Source (Authors, 2022)

Subsequently, the sap is removed from the maguey fiber with the help of a stick or wooden trunk to obtain the ixtle, as shown in figure 7.

Figures 10, 11, and 12. The sap is removed to see the vegetable fiber, which is what is wanted.



Source (Authors, 2022)

Once the sap has been removed from the fiber, as shown in figure 13, all the fiber obtained from the maguey is left to dry in the sun for a period of approximately 3 to 4 days.

Figure 13 The ixtle is dried in the sun



Source (Authors, 2022)

Finally, when the maguey or ixtle fiber dries (figure 14,15), it can be used to make the panel.

Figures 14, 15. Ixtle fibers



Source (Authors, 2022)

Preparation of mixtures

The experimentation of the first mixtures was carried out to analyze the behavior of the materials among themselves and a 60 x 60 cm mold built with plywood and $\frac{3}{4} \times \frac{1}{2}$ " wood strips was taken as a base, for the emptying of the mixtures.

Which were the following:

Table 1 mixture dosages

Materiales	Unidades	Mezcla 1	Mezcla 2	Mezcla 3
Water	mililitros	500	750	1000
Gypsum	gramos	500	750	1000
PET	gramos	250	300	500
Ixtle	Metros	.50	2	4

Source (Authors, 2022)

Mix 1

A mixture of 500 milliliters of water, 500 g of white plaster, ½ meter of ixtle fiber, and 250 g of plastic grinding was made, then they were spread over the mold. Analyzing this test, it was observed that the proportion of water, plaster, and plastic grinding should not be the same since the materials absorb water and the plaster dries quickly without achieving adequate accommodation of the material inside the mold. While the plaster was being mixed, it dried in less than a minute, so when it was poured into the mold it did not have a good consistency, as illustrated in figure 17.

Figure 17 The first test result of the panel



Source (Authors, 2022)

Mix 2

According to what was analyzed in the previous test, a release agent was applied to the wood to get the panel to unmold and the amount of water was increased to 750 milliliters that were added to the mixture made up of plaster 750 g was, 300 g plastic grinding and on this occasion we added 2 meters of ixtle with the intention of giving the panel greater resistance and drilling was done to observe a better homogeneity between the materials, the mixture was more manageable and allowed adequate accommodation inside the mold, The result of this test is displayed in Figure 18.

Figure 18 Placement of the Ixtle fibers in the pouring of the mixture on the wooden mold



Source (Authors, 2022)

Mix 3

A third test was carried out to improve the techniques or methods used in the previous tests, the dimensions are 60×60 cm with a thickness of 1.2 cm, the proportion of the materials is made up of 1000 ml of water, 1000 g of plaster, 500 g of plastic grinding, 4 m of ixtle, before this test an improvement was observed in the result of uniformity in the panel, the materials integrate better, and it looks more aesthetically pleasing and thanks to the release agent we were allowed to remove the panel without any complications. The results of this test can be seen in Figure 19.

Figure 19 Third test result



Source (Authors, 2022)

5. Thanks

To the Tecnológico de Estudios Superiores de Jocotitlán for the support received, for the realization of this investigation and experimentation of the prototype.

6. Conclusions

According to the test tests presented above and the panel manufacturing process of the materials and methods, it was found that mixture 3 is the most viable for the manufacturing of the ecological gypsum panel prototype.

However, it was realized that the amount of plastic and plaster depend a lot on their proportions for the malleability of the mixture and adherence. The setting time is very susceptible to climate changes; however, a favorable result was obtained since the materials reacted adequately when mixed.

The ecological plasterboard based on plastic aggregate and ixtle is a solution to current problems of contamination with PET since plastic is increasing day by day and the environmental impact causes serious damage to the lives of all living beings on the planet. The inclusion of plastic in a granulometry state, with the plaster, the ixtle and the recycled paper in the panel was finally a good compositional result in the panel as established in the general objective.

It was found that the project can be a sustainable construction element that replaces the current existing panels to raise awareness about caring for the environment and reduce pollution in the construction industry.

During the development of the investigation, no material similar to that of this proposal was found, which is why it has been considered to be an idea of product innovation since there are only conventional drywall panels and recycled paper without the use of plastic waste or any other type of waste that allows recycling. The materials we use in the panel make it a unique product, making use of natural raw materials from the State of Mexico, in addition to seeing PET recycling as the best alternative to reduce environmental impact.

Knowing the properties of each material used will allow us to investigate more about the results that we could obtain since each characteristic positively contributed to the panel benefits of stability, lightness, and aesthetics. This panel is based on the NMX-C-059-ONNCCE-2013 standard. And based on said standard, tests will be carried out with conventional materials, to observe the behavior of the material during its setting process, it is important to mention that resistance, humidity, and fire tests will be carried out by the standards to specify the functioning test methods. Made for panels which said samples will be tested according to the following standards:

ASTM C-367, Standard Test Methods for Strength Properties of Precast Architectural Acoustical Tiles or Overlay Ceiling Panels, describes the method for establishing the strength properties of acoustical ceiling tiles and panels.

ASTM E-413, Standard Classification for Rating Acoustic Insulation, provides criteria for establishing the ceiling sound transmission (CAC) rating of an acoustical ceiling, similar to the STC ratings for walls.

ASTM C-423, Standard Test Method for Sound Absorption and Sound Absorption Coefficients by the Reverberation Room Method, describes the method for establishing sound absorption coefficient (NRC) values.

ASTM C-635, Standard Specification for the Manufacture, Performance, and Testing of Metal Suspension Systems for Acoustical Tile Ceilings and Overlay Panels, provides classification criteria for load capacity, along with manufacturing tolerance, coatings, and inspection criteria for suspension systems.

Likewise, it is important to mention that the project can be feasible and viable in the field of construction, a sustainable construction element as an alternative to the current existing panels to raise awareness about caring for the environment and reduce the environmental impacts that the construction industry generates, nowadays. Therefore, the regulations were met in the tests carried out.

This panel is a product with radical innovation since there are only conventional plasterboard and cardboard panels without the use of plastic waste or any other type of waste that allows recycling. The materials that were used in the panel of this research make it a unique product, in addition to seeing the recycling of PET as the best alternative to reduce the environmental impact. It is important to mention that innovation allows the generation of new knowledge and proposes solutions to problems that can be related to multiple aspects, which, in the medium and long term, can mean economic growth, improvement in productivity, and the social development of a nation.

7. References

ASTM E-413, Clasificación Estándar para Clasificar Aislamiento Acústico, proporciona criterios para establecer clasificación de transmisión de sonido en cielorrasos (CAC) de un cielorraso acústico, similar a las clasificaciones STC para muros. <https://www.astm.org/e0413-22.html>

ASTM C-423, Método de Prueba Estándar para Absorción Acústica y Coeficientes de Absorción Acústica Mediante el Método de Cuarto de Reverberación, describe el método para establecer valores de coeficiente de absorción de sonido (NRC). <https://www.astm.org/e0413-22.html>

ASTM C-635, Especificación Estándar para la Fabricación, Funcionamiento y Prueba de Sistemas de Suspensión Metálica para Cielorrasos de Losetas Acústicas y Paneles de Sobreponer, proporciona criterios de clasificación por capacidad de carga, junto con tolerancia de fabricación, revestimientos y criterios de inspección para sistemas de suspensiones. <https://www.astm.org/e0413-22.html>

Alesmar, Luis, Rendón, Nalia, & Korody, María Eugenia. (2008). Diseños de mezcla de tereftalato de polietileno (pet) - cemento. *Revista de la Facultad de Ingeniería Universidad Central de Venezuela*, 23(1), 76-86. Recuperado en 06 de noviembre de 2022, de http://ve.scielo.org/scielo.php?script=sci_arttext&pid=S0798-40652008000100006&lng=es&tlng=es.

Acosta, D., (2009). *Arquitectura y construcción sostenibles: CONCEPTOS, PROBLEMAS Y ESTRATEGIAS*. Dearq, (4) ,14-23. [Fecha de Consulta 6 de Noviembre de 2022]. ISSN: Recuperado de: <https://www.redalyc.org/articulo.oa?id=341630313002>

Budjiashvil, Turkadze, Constantine, (2019) *Uso de celulosa y derivados de la madera en la construcción*, https://issuu.com/tfg_constantin/docs/tfg_uso_de_celulosas_y_derivados_de_madera

Castillo Quiroz, David, Sáenz Reyes, J. Trinidad, Narcia Velasco, Mariano, & Vázquez Ramos, José Antonio. (2013). Propiedades físico-mecánicas de la fibra de Agave lechuguilla Torr. de cinco procedencias bajo plantaciones. *Revista mexicana de ciencias forestales*, 4(19), 78-91. Recuperado en 07 de noviembre de 2022, de http://www.scielo.org.mx/scielo.php?script=sci_arttext&pid=S2007-11322013000500007&lng=es&tlng=es.

Cosmos O. (2021). *Información Técnica y Comercial del Plástico PET (molido, desperdicio)*. Obtenido de <https://www.cosmos.com.mx/wiki/plastico-PET-molido-desperdicio-cw1r.html>

Cristan Frias, Arturo. Izelema, Irina, Gavilan Garcia, Arturo, (2003) *La situación de los envases de plástico en México*, *Gaceta Ecologica* (69), 67-82. ISSN: 1405-2849, Recuperado de: <https://www.redalyc.org/pdf/539/53906905.pdf>

De la Madrid, Enrique y Landeros, Emma (2020) *Mario Molina dijo que estamos en emergencia y nosotros le creemos*, *Centro para el futuro de la ciudades Tecnológico de Monterrey*, <https://futurociudades.tec.mx/es/cambio-climatico>

Hernández Moreno, S., (2008). *Diseño sustentable de materiales de construcción; caso del concreto de matriz de cemento Pórtland*. *CIENCIA ergo-sum, Revista Científica Multidisciplinaria de Prospectiva*, 15(3) ,306-310. [Fecha de Consulta 6 de agosto de 2022]. ISSN: 1405-0269. Recuperado de: <https://www.redalyc.org/articulo.oa?id=10415308>

London T. (2011). *Ventajas del cartón para el medio ambiente*. Obtenido de <https://www.dssmith.com/es/tecnicarton/sobre-tecnicarton/noticias/2019/6/ventajas-del-carton-para-el-medio-ambiente>.

Mayor González, Gerardo, (1977) *Materiales de construcción*, México, Mc Graw-Hill

NMX-C-059-ONNCCE-2013

https://dof.gob.mx/nota_detalle.php?codigo=5510054&fecha=04/01/2018#gsc.tab=0

NMX-C367-1977

https://caisatech.net/uploads/XXI_2_MXD_C239_NMX-C-168-1977_R0_30JUN1977

Chapter 5 Phase simulation of the Fe-Cr alloy system

Capítulo 5 Simulación de las Fases del sistema de aleación Fe-Cr

SORIANO-VARGAS, Orlando †*, LOPEZ-HIRATA, Víctor M., CAYETANO-CASTRO, Nicolas and CASTREJON-SANCHEZ, Víctor H.

¹*Tecnológico de Estudios Superiores de Jocotitlán, Carretera Toluca Atlacomulco km 44.8, Ejido de San Juan y San Agustín, Jocotitlán, México.*

²*Instituto Politécnico Nacional (ESIQIE), Apdo. Postal 118-395, Mexico, D.F. 07300*

³*CNMN, Instituto Politécnico Nacional, Wilfrido Massieu s/n, UPALM, Gustavo A. Madero, Ciudad de México 07738, México.*

ID 1st Author: *Orlando, Soriano-Vargas* / **ORC ID:** 0000-0002-9331-7909

ID 1st Co-author: *Víctor M., López-Hirata* / **ORC ID:** 0000-0002-7781-3419

ID 2nd Co-author: *Nicolas, Cayetano-Castro* / **ORC ID:** 0000-0003-4827-795X

ID 3rd Co-author: *Victor H., Castrejón-Sanchez* / **ORC ID:** 0000-0002-0112-5388

DOI: 10.35429/H.2022.3.65.83

O. Soriano, V. Lopez, N. Cayetano and V. Castrejon

*orlando.soriano@tesjo.edu.mx

A. Ledesma (AA.). Science of Technology and Innovation. Handbooks-TII-©ECORFAN-Mexico, 2022.

Abstract

Spinodal decomposition was studied during aging of Fe-Cr alloys by means of the numerical solution of the linear and nonlinear Cahn-Hilliard differential partial equations using the explicit finite difference method. Results of the numerical simulation permitted to describe appropriately the mechanism, microstructure, and kinetics of phase decomposition during the isothermal aging of these Fe-Cr alloys. The growth kinetics of phase transition was observed to occur very slowly during the early stages of aging, and it increased considerably as the aging progressed. The nonlinear equation was observed to be more suitable for describing the early stages of spinodal decomposition than the linear one.

Fe-Cr alloy, Spinodal insufficiency, Cahn-Hilliard equivalence, Thermal aging

Resumen

Se estudió la descomposición espinodal durante el envejecimiento de aleaciones de Fe-Cr mediante la solución numérica de las ecuaciones parciales diferenciales lineales y no lineales de Cahn-Hilliard utilizando el método explícito de diferencias finitas. Los resultados de la simulación numérica permitieron describir adecuadamente el mecanismo, morfología y cinética de descomposición de fase durante el envejecimiento isotérmico de estas aleaciones. Se observó que la cinética de crecimiento de la descomposición de fase se producía muy lentamente durante las primeras etapas del envejecimiento y aumentaba considerablemente a medida que avanzaba el envejecimiento. Se observó que la ecuación no lineal era más adecuada para describir las primeras etapas de la descomposición espinodal que la lineal.

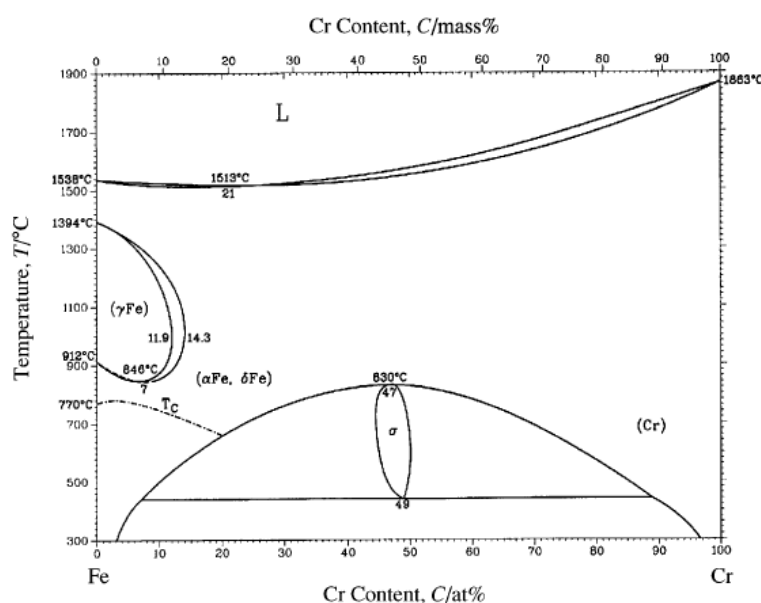
Aleación Fe-Cr, Descomposición espinodal, Ecuación Cahn-Hilliard, Envejecido térmico

1. Introduction

1.1 Phase Decomposition in the Fe-Cr Alloy System

Figure 1 illustrates the equilibrium diagram for the Fe-Cr alloy system, and it is characterized by an immiscibility gap above which there is a disordered solid solution and below which the solid solution decomposes into Fe-rich clusters and rich in Cr. The dome of the immiscibility gap is between 540 and 630° C. The Fe-Cr system is important in engineering materials, such as in the chemical and nuclear industries, where it is of perpetual interest by becoming brittle when aged at 475 °C (Weng *et al.* 2003). Zhu *et al.* 1986 were the first to suggest that the spinodal reaction occurs within the immiscibility gap at low temperatures. The morphology of the spinodal decomposition has been difficult to observe in its early stages of transformation, since due to the small elastic deformation between phases and the similarity of the atomic dispersion factors and lattice parameter between Fe and Cr.

Figure 1 Phase diagram of the Fe-Cr system



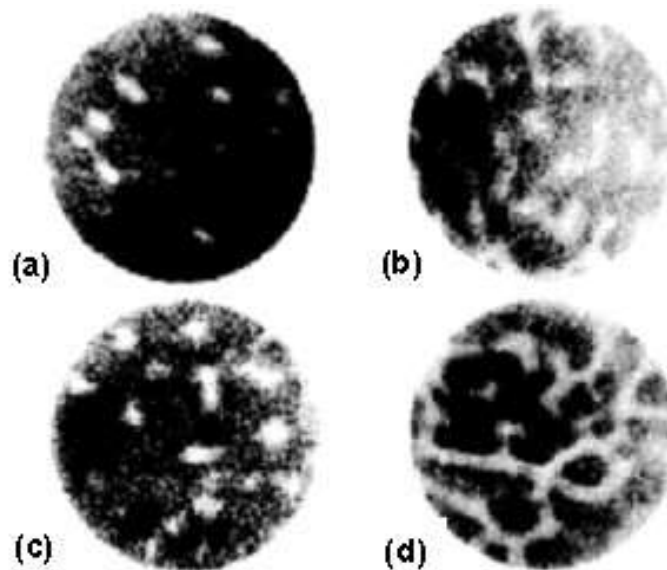
Source (Baker, 2000)

Therefore, the Fe-Cr system is considered as an ideal model system for the study of spinodal decomposition. However, the decomposition kinetics process of these alloys thermodynamically considers other decomposition mechanisms. For example, the decomposition of the alloy (Ustinovshikov *et al.* 2002):

- Fe-20 at 50% at. Cr at 475 °C is carried out by the spinodal decomposition mechanism, while at 550 °C by nucleation and growth.
- Fe-24% at. Cr aged at 475°C proceeds by nucleation and growth.
- Fe-60% at. Cr aged at 475 ° C proceeds by spinodal decomposition.

Hyde *et al.* 1995 carried out the analysis of spinodal decomposition in Fe-Cr alloys (see figure 2). The study has three parts: the first details the experimental techniques by ion microscopy, making a three-dimensional reconstruction of the atomic structure of a series of aging treatments at 500°C in Fe-24, 32 and 45% Cr alloys. The second part describes the interconnected microstructure resulting from the spinodal decomposition in a series of aging for the Fe-Cr system whose size and amplitude in composition are analyzed. The third, computer simulation using the Monte Carlo method and a numerical solution based on the Cahn-Hilliard-Cook theory.

Figure 2. Ion microscope micrographs of Fe-Cr alloys aged for 500h at 500°C as a function of Cr content –(a) 19% Cr, (b) 24% Cr, (c) 32% Cr and (d) 45% Cr. The bright regions are enriched in Cr and the dark regions lacking Cr (Miller *et al.* 1995)

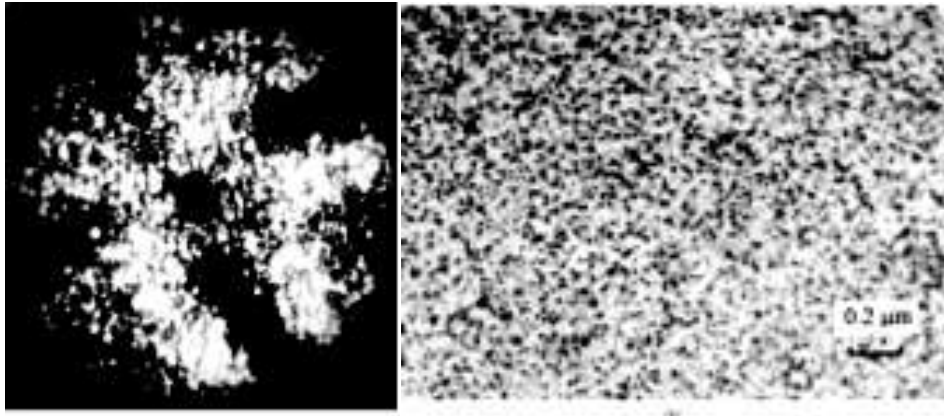


Source (Miller *et al.* 1995)

Miller *et al.* 1995 studied the phase decomposition at aging temperatures of 400 and 500 °C in Fe-45% Cr alloys. The examined microstructure turned out to be formed by spinodal decomposition. It was found that, at the aging temperature of 500 °C, the activation energy for diffusion was approximately 2.3 eV. However, a similar comparison could not be made for heat treatments of 400 °C, since the transformation kinetics is much slower; but the simulation predicts that the size depends on time, exhibiting a law of behavior with an exponent of time, 0.25.

Ustinovshikov *et al.* 1996 analyzed the formation of phase separation in solid solutions of Fe-Cr alloys. Using transmission electron microscopy and selected area electron diffraction patterns of Fe-(10; 20; 30; 40; 47) wt% Cr alloys treated isothermally at 500 °C (see Figure 3). The solubilized treatments were carried out at a temperature of 1200 °C. They reported some of the structural features, which are not considered for the phase diagram of the Fe-Cr system. These characteristics are the following:

Figure 3 (a) Fe-20%Cr alloy treated at 1200 °C for 1 h and quenched in water. Ion microscopy image showing Cr-rich clusters. (b) Fe-30% Cr alloy thermally treated at 1200°C for 1 h and quenched in water; the sequence of heat treatment at 550°C for 8 h; microstructure separation at low temperature.



Source (Ustinovshikov *et al.* 2005)

(A) Many researchers believe that the high-temperature region (1200-1400 °C) of the Fe-Cr diagram is a region of disordered solid solution. However, thermodynamic studies performed at high temperatures (1040-1400 °C) showed that the solid solution has a positive deviation from Raoult's law in all study compositions. Therefore, they exhibit a tendency to break down. The different types of microstructures formed under the phase decomposition showed Cr-enriched clusters located in a Cr-depleted matrix. These clusters are of different morphology depending on the thermal treatment and composition. For the 20% Cr and 30% Cr compositions, the embryos have a periodic distribution in the form called “microstructure clusters” oriented along the directions of smooth deformation of the matrix.

(B) When Fe-(30-47) wt% Cr alloys are heat treated in the high temperature region (1200-1400°C) and quenched in water, and subsequently aged in the region of phase formation σ at 600-830° C for different times, the two types of high temperature microstructural separation: $\alpha_1+\alpha_2$ and phase J dissolve completely.

In summary, it can be said that the analysis of spinodal decomposition experimentally has been difficult to perform in the early stages of aging for Fe-Cr alloys. Likewise, the comparison with simulation results has not been an easy task to carry out.

1.2 Phase Field Model

The phase field model was originally developed to study the phenomenon of solidification and other growth processes (Koyama *et al.*, 2006). Unlike the other approaches, the phase field model describes a microstructure by means of a group of field variables from which the spatial distribution of the grains or domains of the different phases and the limits between them can be analyzed. Typical examples of field variables are concentration and the long-range order parameter, which characterize compositional and structural heterogeneities, respectively. To overcome the problems inherent to a moving boundary, the phase field model uses the approximation of a diffuse interface for microstructural evolution (Bhadeshia, 2000).

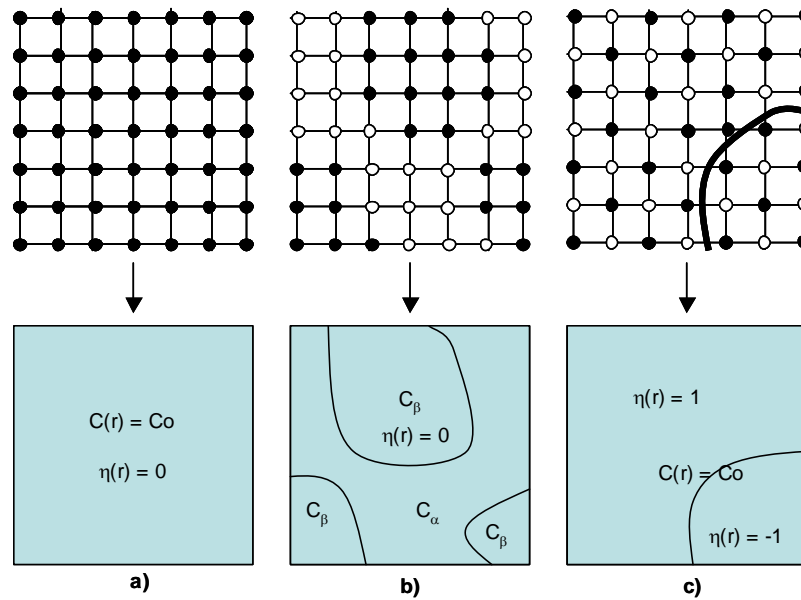
Three simple examples are presented in Figures 4(a-c) to illustrate the use of field variables that describe different morphologies. In the upper and lower part of the figure, the different morphologies and their corresponding field variable are presented. For example, figure 4(a) to a homogeneous disordered phase with field variable c_0 . Figure 4 (b) shows a mixture of two structurally sized phases described by a non-homogeneous composition field C . Finally, there is a monophasic with antiphase domain boundaries characterized by a long-range order parameter η (r). The variables C and η are continuous through the interface between phases or domains.

In the kinetic field model of phases with diffuse interface, the microstructural evolution is described by the spatial and temporal evolution of the field variables moving toward thermodynamic equilibrium, governed by the nonlinear diffusion equation of Cahn and Hilliard and the equation of Allen and Cahn (Cahn *et al.*, 1971, Allen *et al.*, 1979):

$$\frac{\partial c(r,t)}{\partial t} = -M\nabla^2 \left[\frac{\partial F}{\partial c(r,t)} \right] \quad (1)$$

$$\frac{\partial \eta_p(r,t)}{\partial t} = -L_{pq} \nabla^2 \frac{\partial F}{\partial \eta_q(r,t)} \quad (2)$$

Figure 4 Schematic representation of different morphologies and their corresponding field variables



Source (Melo, 2006)

where L_{pq} and M are kinetic coefficients. F is the free energy function in terms of the field variables. The solutions of these equations provide the morphology as well as the kinetic characteristics of the microstructural evolution for a given alloy system. The interfacial boundaries do not need to be specified in advance, but rather emerge with part of the numerical solution. Therefore, the fuzzy interface model offers the flexibility and generality to favorably solve the difficulties faced by the definite interface approach. In the Cahn and Hilliard theory, the interfacial energy is introduced through energy terms due to the compositional gradient. The total free energy F of the inhomogeneous system is given as:

$$F = \int_V \left[f(c) + \frac{1}{2} k \nabla^2 c \right] dV \quad (3)$$

where $f(c)$ is the local energy density and k is the gradient energy coefficient, which can be related to the atomic interaction parameters. The derivative of F with respect to C is as follows:

$$\frac{\partial F}{\partial c} = \frac{\partial f}{\partial c} - k \nabla^2 c \quad (4)$$

Substituting equation (4) into equation (1), the nonlinear Cahn and Hilliard equation is obtained:

$$\frac{\partial c(r,t)}{\partial t} = \nabla \cdot M \nabla \left[\frac{\partial f}{\partial c} - k \nabla^2 c \right] \quad (5)$$

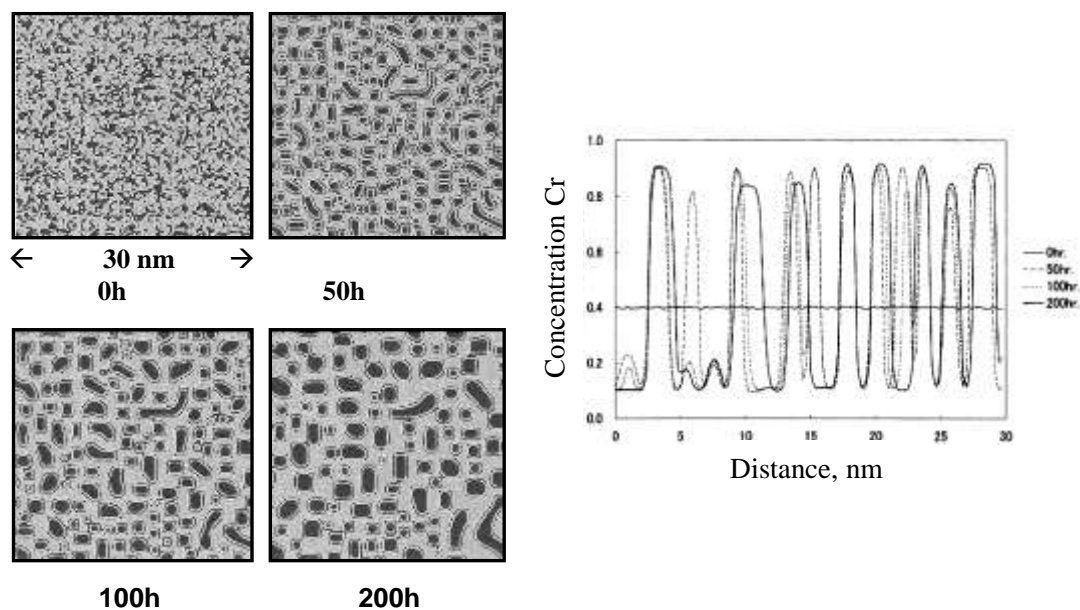
this equation can be solved by finite differences.

Spinodal decomposition in Fe-Cr alloys was studied in Fe-24, 32 and 45% at alloys. Cr, performed by computer simulation by Monte Carlo algorithm methods and by a numerical solution of the Cahn-Hilliard-Cook theory analyzed by Hyde and collaborators (Ustinovshikov *et al.*, 1995). The problem with the Monte Carlo method lies in the ambiguity of time and size measurement. This is a limiting factor in phase decomposition kinetic studies.

Honjo *et al.*, 2000 used a numerical model based on the Cahn and Hilliard linear equation for multicomponent systems that was applied to the prediction of microstructural evolution and phase decomposition in Fe-Cr and Fe-Cr-Mo systems. Figure 5(a) shows the microstructural evolution based on Cr concentration in a Fe-40% at binary alloy. Cr aged at 527°C. The formation of Cr-rich regions by phase decomposition is clearly seen. Their size and interdistance increased with aging time. The Cr concentration profile is shown in Fig. 18(b). The peak amplitudes are equivalent to the Cr equilibrium concentration at 527°C, which was evaluated by Thermo-Calc.

In this study, a numerical simulation model based on the linear, nonlinear, and modified Cahn and Hilliard strain energy equations for the Fe-Cr alloy system at different compositions and temperatures is proposed.

Figure 5 a) Microstructural evolution in a binary alloy Fe-40 % at. Cr aged at 527°C. b) Variation of the Cr concentration profile over time in the Fe-40% at binary alloy. Cr aged at 527°C



Source (Honjo *et al.*, 2000)

2. Methodology

2.1 Numerical Modeling

In the kinetic field model of phases with diffuse interface, the microstructural evolution is described by the spatial and temporal evolution of the field variables moving towards thermodynamic equilibrium, governed by the Cahn and Hilliard nonlinear diffusion equation in one dimension is the following (Honjo *et al.*, 2000):

$$\frac{\partial c(x,t)}{\partial t} = \nabla \cdot M \nabla \left[\frac{\partial f}{\partial c} - k \nabla^2 c \right] \quad (6)$$

where c is the atomic concentration as a function of position x , f is the local free energy, k is the energy coefficient of the compositional gradient, and M is the atomic mobility. This nonlinear equation has been widely used to simulate microstructural evolution in spinodally decomposing alloy systems such as Fe-Cr and Fe-Cr-Mo (Honjo *et al.*, 2000). However, this study does not present the comparison of simulated results with experimental ones.

The Cahn and Hilliard theory for spinodal decomposition is based on the analytical solution of the linear Cahn and Hilliard equation (Cahn *et al.*, 1971):

$$\frac{\partial c(x,t)}{\partial t} = M \left[\left(\frac{\partial^2 f}{\partial c^2} + 2\eta^2 Y \right) \nabla^2 c - 2\kappa \nabla^4 c \right] \quad (7)$$

where η is a measure of the mismatch in the lattice parameter a of the decomposed phases and Y is a parameter involving the elastic constants. This linear equation has also been used to follow microstructural evolution and is considered very useful for analyzing the early stages of spinodal decomposition.

For the numerical simulation, the free energy of the Fe-Cr alloy was determined using the model for a regular solution (Honjo *et al.*, 2000):

$$f = f_{Cr} c_{Cr} + f_{Fe} c_{Fe} + \Omega_{Fe-Cr} c_{Cr} c_{Fe} + RT [c_{Cr} \ln c_{Cr} + c_{Fe} \ln c_{Fe}] \quad (8)$$

where f_{Cr} , and f_{Fe} , c_{Cr} and c_{Fe} are the free energies in the pure state and the mole fraction of Cr and Fe, respectively. T is the temperature and R is the gas constant. Ω_{Fe-Cr} is the interaction parameter. Table 1 presents the value of the interaction parameter Ω as a function of T .

Table 1. Values of the lattice, diffusion, thermodynamic and elastic constants

Constants	Fe-Cr	
Parameter lattice (nm)	$a = 0.2866$	
Diffusion Coefficient ($\text{cm}^2 \text{s}^{-1}$)	$D_{Fe} = 1.2 \exp(-294000 \text{ Jmol}^{-1})/RT$ [63]	
	$D_{Cr} = 0.2 \exp(-308000 \text{ Jmol}^{-1})/RT$ [63]	
Ω_{Fe-Cr} (J mol^{-1})	$(18600.0+0.1T)$ [9]	
c_{ij} (J m^{-3}) Fe/Cr	$c_{11}=23.10 \times 10^{10}$	$c_{11}=35.00 \times 10^{10}$ [64]
	$c_{12}=13.54 \times 10^{10}$	$c_{12}=67.80 \times 10^{10}$
	$c_{44}=11.78 \times 10^{10}$	$c_{44}= 10.08 \times 10^{10}$
η	0.00614 [63]	

Source: Own Elaboration

Atomic mobility M was evaluated according to the following equation (Honjo *et al.*, 2000):

$$\bar{D} = M_i \left(\frac{\partial^2 f_o}{\partial c_i^2} \right) \quad (9)$$

where the interdiffusion coefficient \bar{D} was defined as (Cahn *et al.*, 1971):

$$\bar{D} = D_{Fe} c_{Cr} + (1 - c_{Cr}) D_{Cr} \quad (10)$$

The values of the diffusion coefficient D_{Fe} and D_{Cr} are also presented in table 1.

On the other hand, the energy coefficient due to the compositional gradient is defined in the spinodal decomposition theory of Cahn and Hilliard (Cahn *et al.*, 1971) as:

$$K = \left(\frac{2}{3} \right) h_{0.5}^M r_0^2 \quad (11)$$

where $h_{0.5}^M$ is the enthalpy of mixing at $c = 0.5$ and r_0 is the nearest neighbor distance and is defined as a function of the lattice parameter (a) shown in Table 1.

The elastic strain energy f_{el} was defined, according to the spinodal decomposition theory (Cahn *et al.*, 1971), as follows:

$$f_{el} = A \int \eta^2 Y (c - c_0)^2 dx \quad (12)$$

where A is the cross-sectional area corresponding to atomic flow, Y is an elastic constant defined by the elastic stiffness constants, c_{11} , c_{12} and c_{44} for the phases rich in Cr and Fe, shown in Table 1. As the difference between the lattice parameters of Fe and Cr is small ($a = (a_{Cr} - a_{Fe})/a_{Fe} = 0.00614$), the elastic strain energy is small and can be approximated to that of an isotropic phase decomposition for which Y was defined (Ustinovshikov *et al.*, 1998) as:

$$Y = c_{11} + c_{12} - 2 \left(\frac{c_{12}^2}{c_{11}} \right) \quad (13)$$

The elastic constants, c_{ij} , were defined as follows:

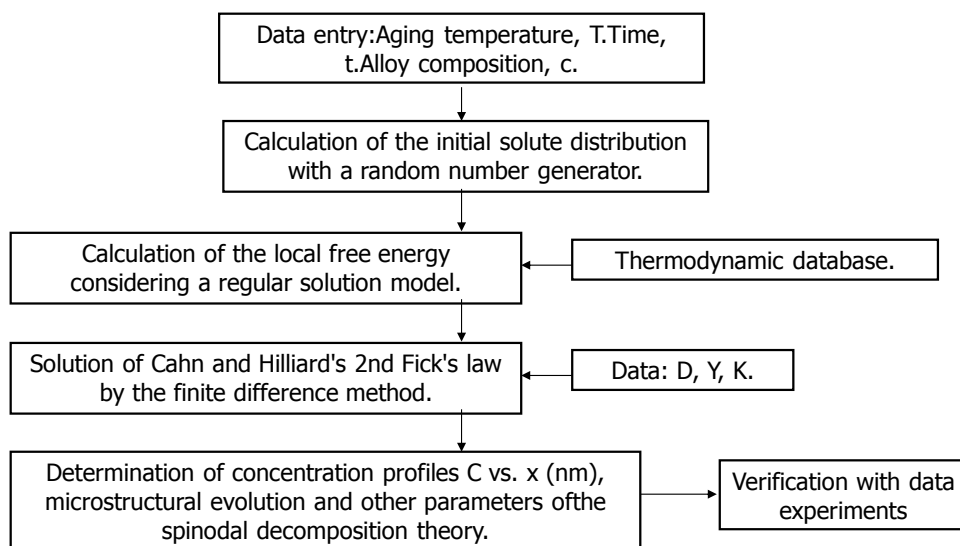
$$c_{ij} = c_{ij}^{Cr} c_{Cr} + c_{ij}^{Fe} (1 - c_{Cr}) \quad (14)$$

The partial differential equation (14) was solved using the explicit finite difference method (Ustinovshikov *et al.*, 1998) using a computer program in FORTRAN 95 language. A 101 x 101 mesh with a spacing of 0.25 nm was used. The time increment was 10 seconds. The composition of the alloy was Fe-32% at. Cr and that of Fe-40% at. Cr, the aging temperature was 500°C for periods of time in the range of 0 to 1000 h.

Figure 6 shows the diagram of the numerical model of the spinodal decomposition. The data input is the composition of the alloy (conditional on not leaving the miscibility zone characteristic of spinodal decomposition), temperature in Kelvin (K) and time in seconds (s) of the aging treatment. Next, the program calculates the initial solute distribution with the help of a random number generator that allowed obtaining a solute distribution closer to the one that occurs in an alloy in the solubilized and tempered state.

Subsequently, the free energy was calculated based on a regular solution model and with the supplied thermodynamic data. Including the diffusion data, it solves the Cahn and Hilliard linear and nonlinear equation in two dimensions by means of the finite difference method, using a FORTRAN computer program. The data output is the distribution of solute in spatial and temporal form, which allowed obtaining one-dimensional graphs of concentration and precipitation profiles after making two-dimensional graphs of the concentration profiles.

Figure 6 Numerical modeling diagram of the spinodal decomposition



Source: Own Elaboration

3. Results

3.1. Simulation with the Cahn and Hilliard Nonlinear Equation

3.1.1 Concentration Profiles

Figures 7 and 8 show the graphs obtained from the simulation using the nonlinear Cahn-Hilliard equation for Cr concentration vs. distance (concentration profiles) for Fe-32% at alloys. Cr and Fe-40% at. Cr at temperatures of 477, 500 and 527°C for different times, respectively.

The profiles for the time of 0 h correspond to the supersaturated solid solution; that is, the alloy in the solution quenched state. A slight fluctuation in the composition for this solubilized condition is observed in the concentration profiles. As the aging time progresses, the increase in the amplitude of the modulation in composition is detected. This behavior clearly indicates that the formation of the phases was carried out by the spinodal decomposition mechanism. Likewise, it can be concluded that the phase decomposition was carried out according to the following reaction:

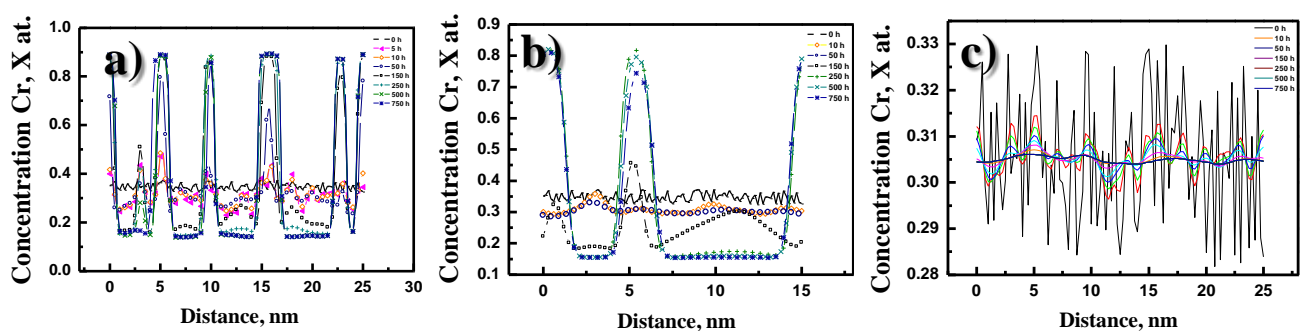


That is, the supersaturated solid solution α_{SS} decomposes spinodally into a mixture of α_1 Fe-rich and α_2 Cr-rich phases, as predicted by the Fe-Cr equilibrium diagram (Ustinovshikov *et al.*, 1998).

Figure 7 shows the Cr concentration profiles in the Fe-32% at alloy. Cr in this graph is observed for the time of 750 h (figure 7a) a maximum amplitude of the modulation, equilibrium composition. For the concentration profile of the temperature of 500°C (figure 7b) the maximum of the amplitude is observed after 500 h of aging. For the case of the temperature of 527°C (figure 7c), the composition of Fe-32% at. Cr is at the end of the immiscibility gap and is known as an asymmetric alloy. The fluctuation for the solubilized alloy (0 h) decreases with aging time. This suggests that phase decomposition is not taking place, but that there is a homogenization of the composition, since the overall composition of the alloy is outside the spinodal curve for this temperature.

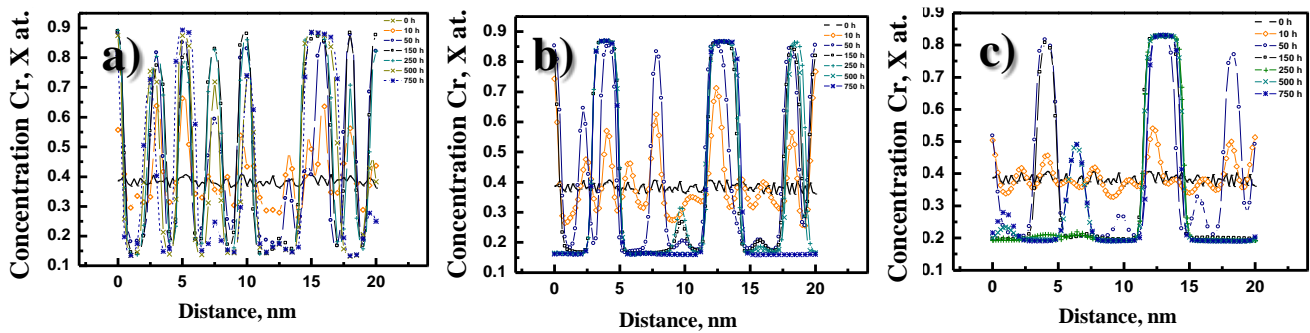
Figure 8 shows the Cr concentration profiles in the Fe-40% at alloy. Cr aged at 477°C, 500° and 527°C for different times. It is observed that there is a maximum amplitude of fluctuation after 750 hours of aging. That is, it approaches the equilibrium composition. For this case, at a temperature of 500°C (figure 8a), the maximum amplitude is observed to occur after 150 h of aging. Likewise, it is observed that the width of the maximum amplitude begins to increase after 500 h. This suggests that the thickening stage of the decomposed phases begins. Figure 8b shows the concentration profiles for the temperature of 527°C, which presents the maximum of the amplitude after 150 h of aging, equilibrium composition. There is still no broadening of amplitude, which indicates that the thickening stage has not yet occurred. It is also presented for the temperature of 500°C.

Figure 7 Cr concentration profiles calculated for the Fe-32%at alloy. Cr aged at 477, 500 and 527°C for different times



Source: Own Elaboration

Figure 8 Cr concentration profiles calculated for the Fe-40% at alloy. Cr aged at 477, 500 and 527°C for different times



Source: Own Elaboration

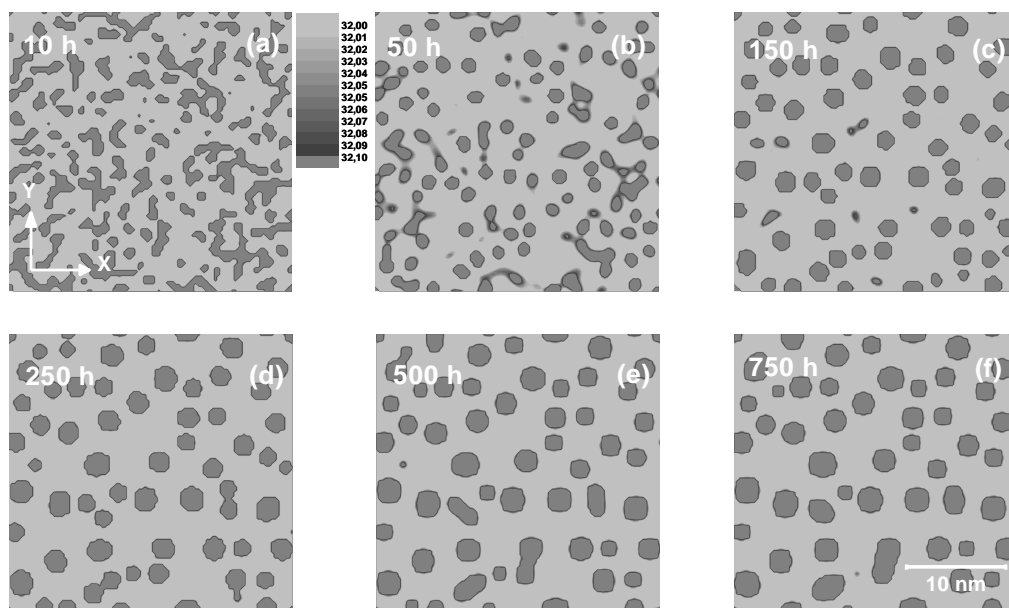
3.1.2 Microstructural Evolution

Figures 9 to 14 (a-f) show the simulated microstructural evolution, based on Cr concentration, for the Fe-32% at alloys. Cr and Fe-40% at. Cr aged at 477, 500 and 527 °C, respectively, for different times using the nonlinear equation of Cahn and Hilliard. The dark zones correspond to the phase rich in Cr and the clear ones to the phase rich in Fe. For the Fe-32% at. Cr aged at 477°C for 10 h, figures 9 (a) and (b), it is observed that the phase rich in Cr shows an interconnected morphology (percolation). As the aging continues, it is observed that the volumetric fraction and size of the phase rich in Cr increase and the morphology changes to rounded or ellipsoidal, figures 9 (c) and (f).

Figures 10 (a-f) show the microstructural evolution of the Cr concentration in the Fe-32% at binary alloy. Cr aged at 500°C for different times. Phase separation in the early stages shows the formation of isolated Cr-enriched islands; Figures 10 (a) and (b). Subsequently, a spheroidal shape is observed, figures 10 (c-f), for the final stages.

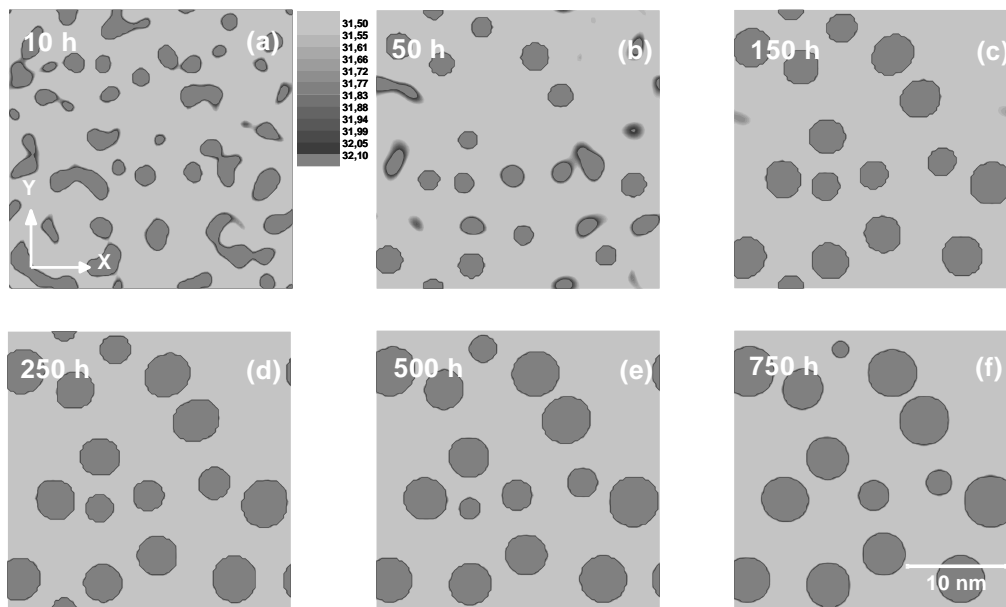
Figure 11 shows the microstructural evolution of the Fe-32% at binary alloy. Cr aged at 527°C for different times. Phase separation for the initial stages shows the formation of isolated islands enriched for Cr concentration; figure 11 (a), later the growth and coalescence of the phase enriched in Cr is observed, in the subsequent times (figure 11 (b-f)). Furthermore, the particles do not exhibit a preferential alignment.

Figure 9 Simulated microstructural evolution for the Fe-32% at binary alloy. Cr aged at 477°C for (a) 10h, (b)50h, (c) 150h, (d) 250h, (e) 500h and (f) 750h



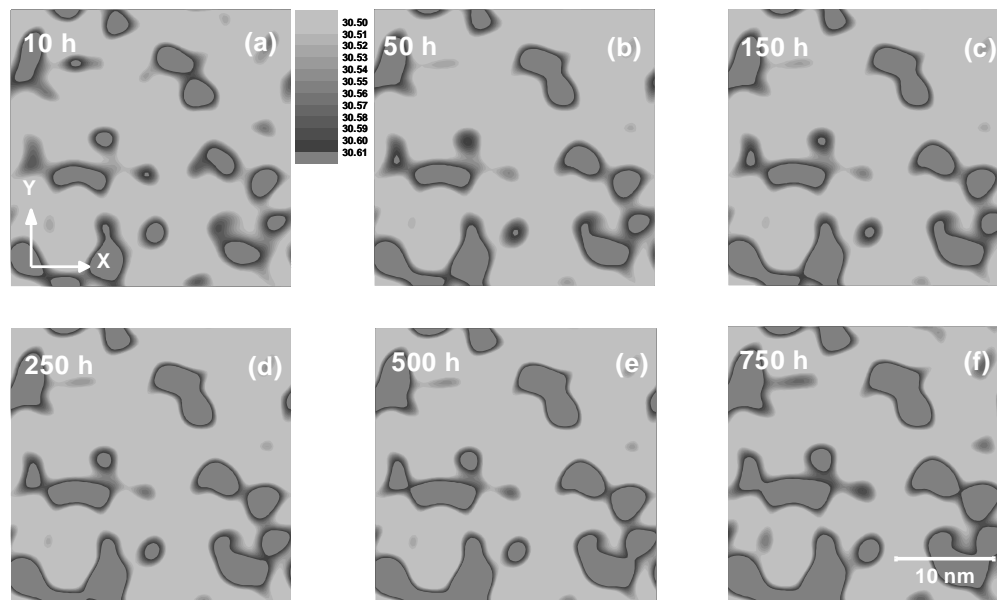
Source: Own Elaboration

Figura 10. Evolución microestructural simulada para la aleación Fe-32% at. Cr envejecida a 500°C por (a) 10 h, (b) 50 h, (c) 150 h., (d) 250 h, (e) 500 h y (f) 750 h



Source: Own Elaboration

Figure 11. Simulated microstructural evolution for the Fe-32% at alloy. Cr aged at 527°C for (a) 10h, (b) 50h, (c) 150h, (d) 250h, (e) 500h and (f) 750h



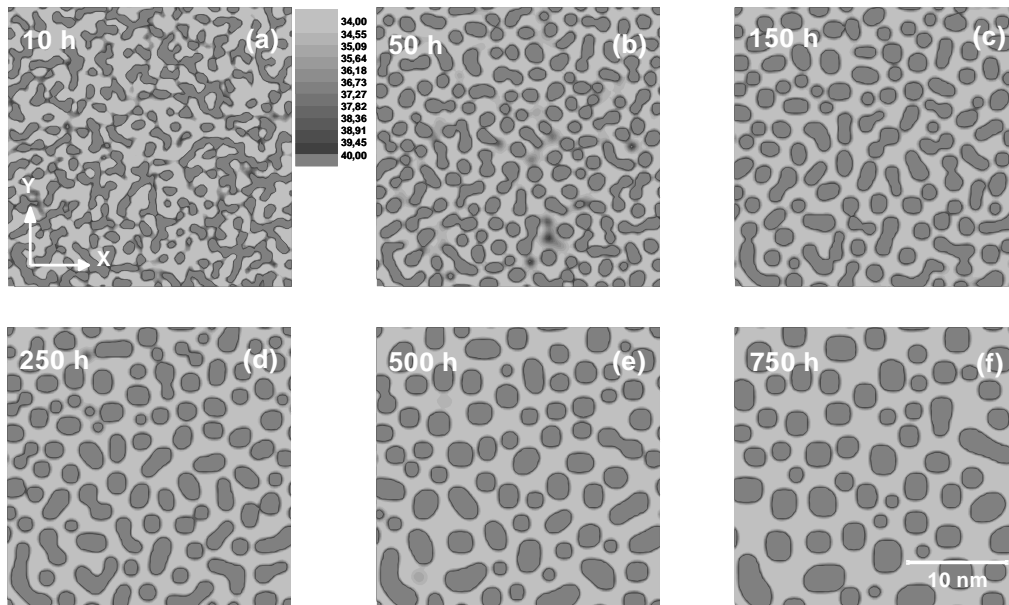
Source: Own Elaboration

Figure 12 shows the microstructural evolution for the Fe-40% at alloy. Cr aged at 477°C for different times. In the alloy aged for 10, 50 and 150 h, figures 12 (a-c), it is observed that the morphology of the phase rich in Cr shows an interconnected morphology (percolation). As aging continues, it is observed that the volume fraction and size of the Cr-rich phase increase, and the Cr-rich phase changes morphology to round or ellipsoidal, Figures 12 (d-f).

Figure 13 shows the microstructural evolution of the Cr concentration in the Fe-40% at binary alloy. Cr aged at 500 °C for different times. The phase separation in the initial stages presents a morphology of isolated islands enriched in Cr concentration, Figure 13 (a) and (b). Subsequently, a change in morphology to rounded or ellipsoid is observed in the final stages. Also, an increase in the volumetric fraction and in the size of the phase rich in Cr is observed.

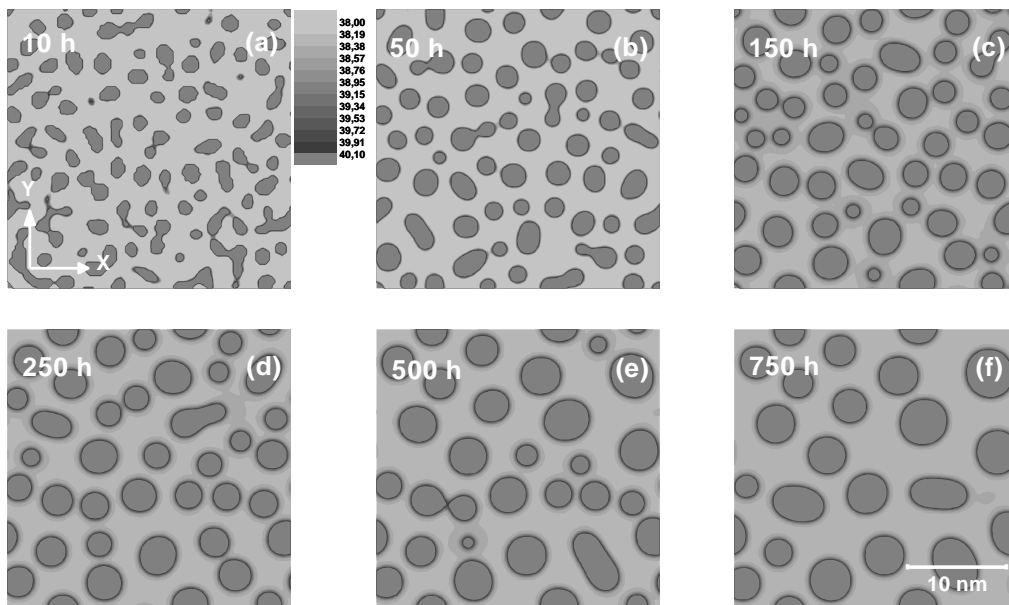
Figures 14 (a-f) show the microstructural evolution of the Fe-40% at alloy. Cr aged at 527 °C for different times. The phase decomposition in the initial stage, figure 14 (a), shows an interconnected morphology of the phase enriched in Cr, later to intermediate stages, figure 14 (b-d), the morphology is rounded or ellipsoidal, and in the final stages, Figures 14 (e) and (f), a spheroidal structure is observed. Also, a decrease in the volumetric fraction is observed, and an increase in the size of the phase rich in Cr.

Figure 12 Simulated microstructural evolution for the Fe-40% at alloy. Cr aged at 477°C for (a) 10h, (b)50h, (c) 150h, (d) 250h, (e) 500h and (f) 750h



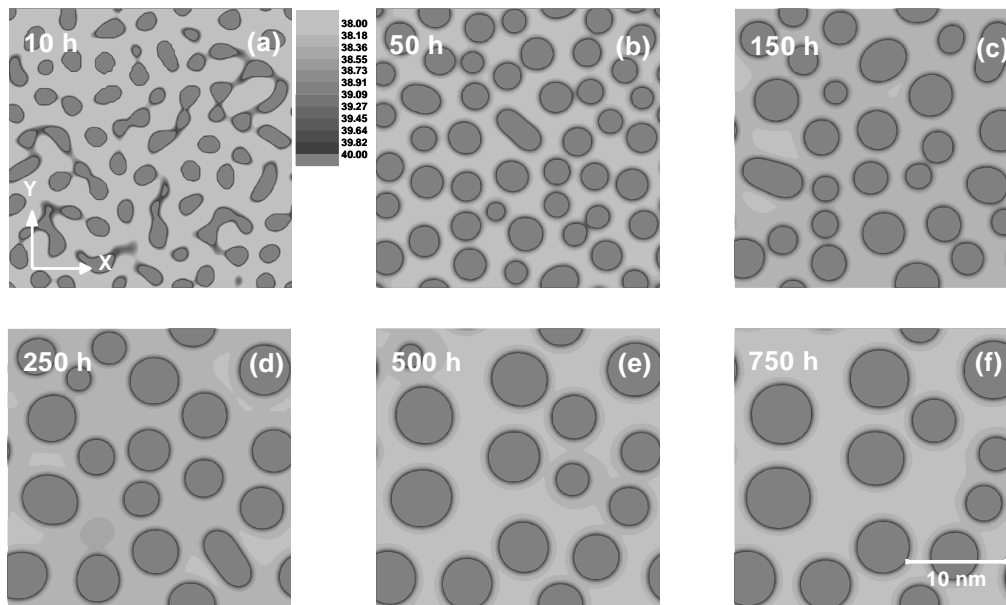
Source: Own Elaboration

Figure 13 Simulated microstructural evolution for the Fe-40% at alloy. Cr aged at 500°C for (a) 10h, (b) 50h, (c) 150h, (d) 250h, (e) 500h and (f) 750h



Source: Own Elaboration

Figure 14. Simulated microstructural evolution for the Fe-40% at alloy. Cr aged at 527°C for (a) 10h, (b) 50h, (c) 150h, (d) 250h, (e) 500h and (f) 750h.



Source: Own Elaboration

3.2. Simulation with the Cahn and Hilliard Linear Equation without Considering the Elastic Strain Energy

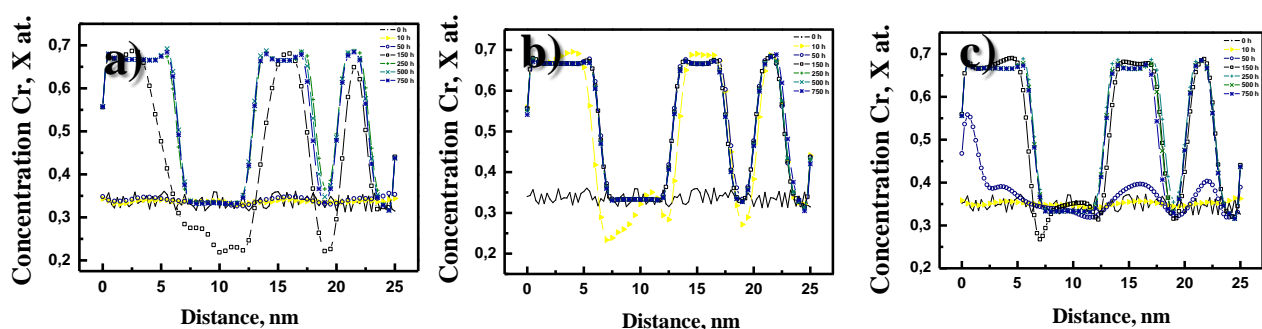
3.2.1 Concentration Profiles

Figures 15 and 16 show the concentration graphs of Cr vs. distance for Fe-32% at alloys. Cr and Fe-40% at. Cr at temperatures of 477°C, 500°C and 527°C for different times, using the Cahn-Hilliard linear equation without considering the strain energy.

Figures 15 a, b and c show the concentration profiles for the Fe-32% at alloy. Cr aged at 477, 500 and 527 °C, respectively. The profiles present the fluctuations in the composition of the enriched phase of Cr. A maximum in amplitude of concentration is observed in the profiles, which is reached at 150 h at 477°C (figure15a), for 150 h at 500°C (figure 15b) and 50 h at 527°C (figure 15c); balance composition.

From these aging times it is observed that the width of the amplitude begins to increase. So, the thickening stage begins. Also, it is observed for prolonged aging at the three temperatures, the bifurcation phenomenon occurs. That is, the formation of a minimum in the central part of the zone of maximum amplitude of the modulation.

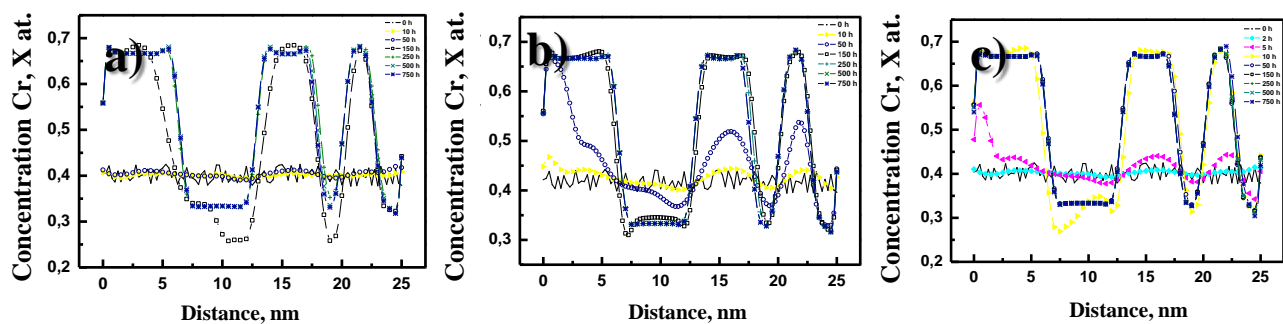
Figure 15 Cr concentration profiles calculated for the Fe-32%at alloy. Cr aged at a) 477°C, b) 500°C and c) 527°C for different times



Source: Own Elaboration

Figure 16 show the concentration profiles for the Fe-40% at alloy. Cr aged at 477, 500 and 527 °C, respectively. The profiles show the fluctuations in the composition of the Cr-enriched phase. A maximum in the amplitude of the modulation is observed in the profiles, which is reached at 150 h for 477°C (figure 16 a), 150 h for 500°C (figure 16b) and 10 h for 527°C (figure 16c), a composition close to that of equilibrium. From these aging times it is observed that the width of the amplitude begins to increase. This indicates, the beginning of the thickening stage. The profiles figures 16 a, b and c, also present the bifurcation phenomenon at prolonged aging times.

Figure 16 Cr concentration profiles calculated for the Fe-40% at alloy. Cr aged at a) 477°C, b) 500°C, and c) 527°C for different times



Source: Own Elaboration

3.2.2 Microstructural Evolution

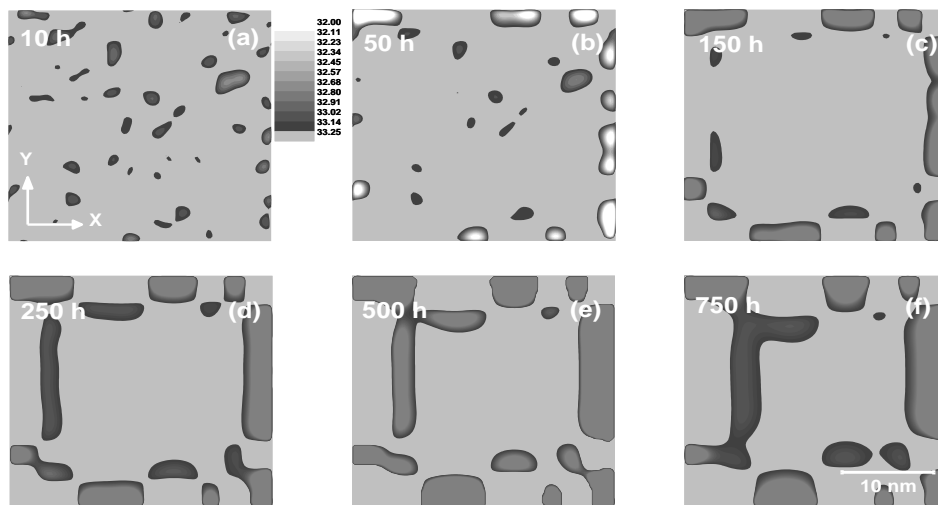
Figures 17 to 21 present the simulated microstructural evolution, based on Cr concentration, for Fe-32% at binary alloys. Cr and Fe-40% at. Cr at aging temperatures of 477°C, 500°C and 527°C, respectively, for different times. The dark zones correspond to the phase rich in Cr and the light zone to the phase rich in Fe. Figures 17 (a-f) show the microstructural evolution for the Fe-32% at alloy. Cr aged at 477°C. The morphology presented by the phase rich in Cr at initial times is in the form of isolated islands, figures 17 (a) and (b). Subsequently, the Cr-rich phase changes its morphology to round and elongated plates, which are preferentially aligned in directions parallel to the (x,y) coordinate axes. Also, it is observed that the volumetric fraction and size of the Cr-rich phase increase with aging time, figure 17 (f).

Figures 18 (a-f) show the microstructural evolution of the Cr concentration in the Fe-32% at. Cr aged at 500 °C for different times. The decomposition of phases in the initial stage, figure 18 (a), presents the formation of the enriched phase of the Cr concentration, which indicates a rounded or ellipsoidal morphology, and an apparent preferential alignment is observed. Subsequently, the intermediate and final stages present the formation of particles with a morphology of elongated plates and preferentially aligned on the directions parallel to the coordinate axes (x, y). Also, it is observed that the volumetric fraction and size of the Cr-rich phase increase with increasing aging time.

Figures 19 (a-f) show the microstructural evolution of the Fe-32% at alloy. Cr aged at 527 °C for different times. The phase decomposition in the initial stage, figure 19 (a), shows a rounded or ellipsoidal morphology and presents a preferential alignment on the directions parallel to the coordinate axes (x, y). Subsequently, in the intermediate and final stages, the formation of particles with a plate morphology and preferentially aligned is observed. Also, it is observed that the volumetric fraction and size of the phase rich in Cr increase with time.

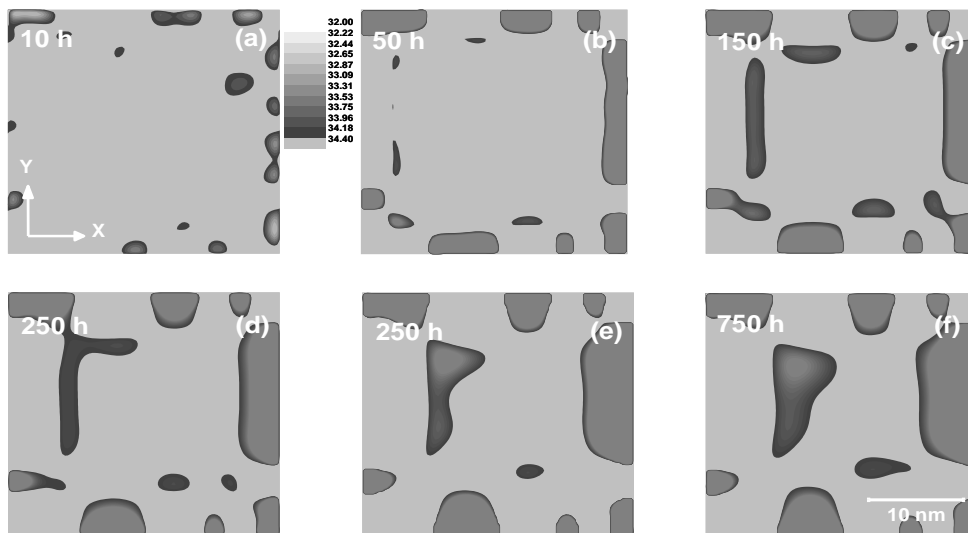
Figures 20, 21 and 22 present the microstructural evolution of the Fe-40% at alloy. Cr, aged at 477, 500 and 527°C for different times. The morphology observed in the initial stages (figures 20, 21 and 22 (a) and (b), respectively) is like that of the Fe-32% at alloy. Cr for the initial stages. That is, it is rounded and ellipsoidal with an apparent preferential alignment in directions parallel to the (x, y) coordinate axes. Likewise, the morphology that occurs over long periods of time (figures 20, 21 and 22 (c-f), respectively) is rounded and platelike, with an apparent preferential alignment. Also, it is observed that the volumetric fraction, as well as the size of the phase rich in Cr, increase with time.

Figure 17. Simulated microstructural evolution for the Fe-32% at alloy. Cr aged at 477°C for 10 h, (b) 50 h, (c) 150 h, (d) 250 h, (e) 500 h and (f) 750 h.



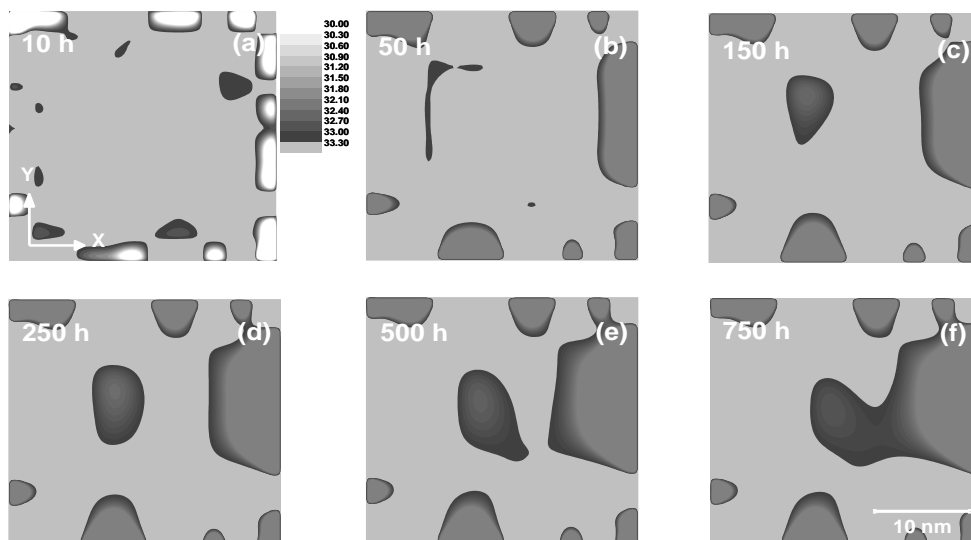
Source: Own Elaboration

Figure 18. Simulated microstructural evolution for the Fe-32% at alloy. Cr aged at 500°C for 10 h, (b) 50 h, (c) 150 h, (d) 250 h, (e) 500 h and (f) 750 h



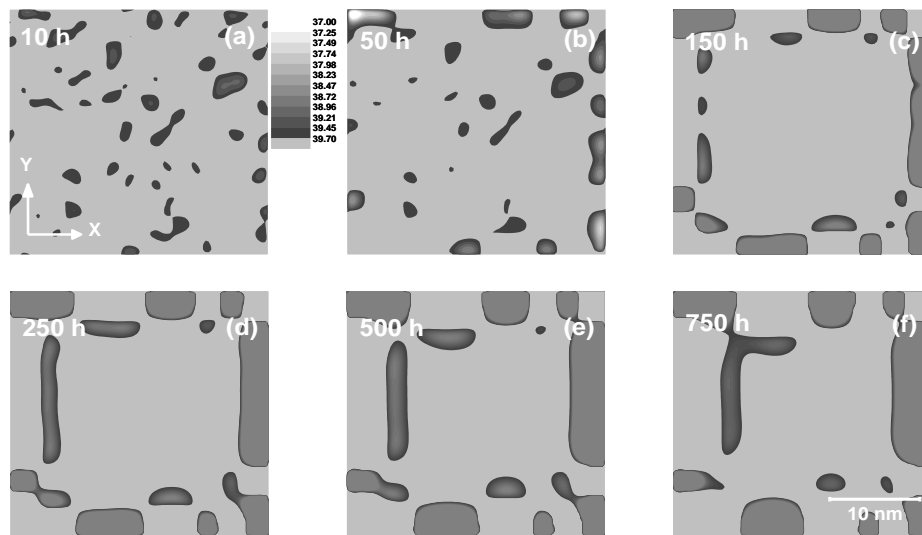
Source: Own Elaboration

Figure 19. Simulated microstructural evolution for the Fe-32% at alloy. Cr aged at 527°C for 10 h, (b) 50 h, (c) 150 h, (d) 250 h, (e) 500 h and (f) 750 h



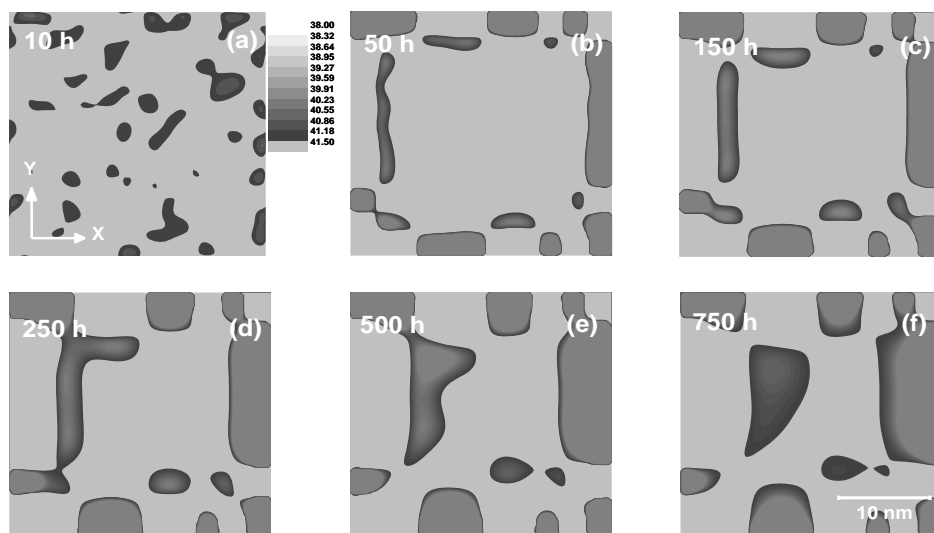
Source: Own Elaboration

Figure 20. Simulated microstructural evolution for the Fe-40% at alloy. Cr aged at 477°C for 10 h, (b) 50 h, (c) 150 h, (d) 250 h, (e) 500 h and (f) 750 h.



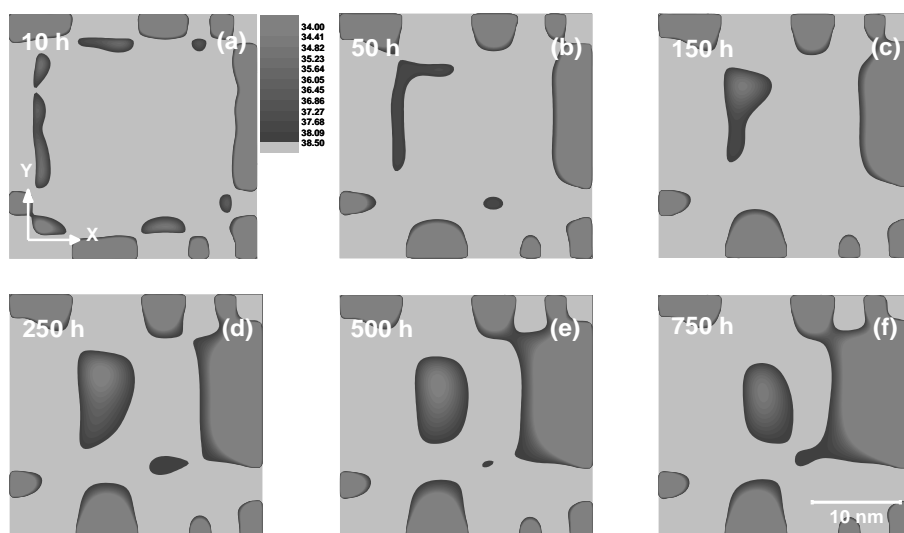
Source: Own Elaboration

Figure 21. Simulated microstructural evolution for the Fe-40% at alloy. Cr aged at 500°C for 10 h, (b) 50 h, (c) 150 h, (d) 250 h, (e) 500 h and (f) 750 h.



Source: Own Elaboration

Figure 22. Simulated microstructural evolution for the Fe-40% at alloy. Cr aged at 527°C for 10 h, (b) 50 h, (c) 150 h, (d) 250 h, (e) 500 h and (f) 750 h.



Source: Own Elaboration

4. Discussion of Results

4.1. Transformation Mechanisms

The evidence of the fluctuations in composition for the concentration profiles obtained by numerical simulation using the linear equation without considering, and considering the elastic deformation energy, and the non-linear equation of Cahn and Hilliard for the Fe-32% at alloys. Cr and Fe-40% at. Cr aged at 477, 500 and 527 °C for different times, detected the increase in the amplitude of the modulation in composition with the increase in aging time (Meshkov, 2022). This behavior clearly indicates that the formation of the phases was carried out by the spinodal decomposition mechanism (Honjo *et al.*, 2000, Ustinovshikov *et al.*, 2002, Cahn, 1962). Likewise, it can be concluded that the phase decomposition was carried out according to the following reaction:



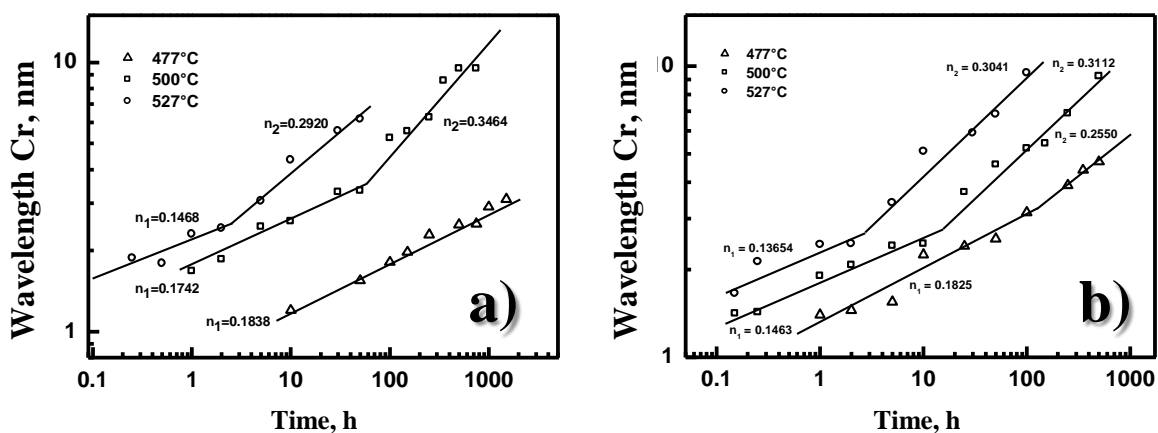
That is, the supersaturated solid solution α_{SS} decomposes spinodally into a mixture of α_1 Fe-rich and α_2 Cr-rich phases, as predicted by the Fe-Cr equilibrium diagram (Ustinovshikov *et al.*, 1998).

4.2 Phase Decomposition Kinetics

The results of graph 23 a) and b) of the variation of the wavelength, λ , with the aging time that was obtained for the decomposition kinetics using the linear equation of Cahn and Hilliard considering the energy of elastic deformation. The kinetics of evolution of the modulation in composition indicates that it is faster in the Fe-40% at alloy. Cr than in Fe-32% at. Cr. This is attributed to the fact that the first is located more to the center of the immiscibility gap. It is well known that the driving force for spinodal decomposition is the second derivative of the free energy with respect to composition, d^2G/dx^2 or G'' , and this is more negative for a composition located more in the center of the immiscibility gap, see figure 1. This driving force is what causes the decomposition kinetics to be faster (Hosford, 2005, Cahn, 1968).

Figure 23 also indicates the values of the two slopes that are clearly observed in the decomposition kinetics of Fe-32% at alloys. Cr and Fe-40% at. Cr, see figures 23 a) and 23 b). That is, there is first a slow stage with slopes or time exponent n between 0.13 and 0.19, which is a unique feature in phase decomposition via the spinodal decomposition mechanism. This slow kinetics is attributed to a type of cluster thickening during the early stages and a time growth exponent of 0.16 has been reported (Hirata, 1982), which agrees with the values determined in this study. In contrast, the slope of the kinetics increases to approximately 0.3 for long aging times. According to the thickening theory of Lifshitz, Slyosov, 1961 and Wagner, 1961 (LSW), an exponent of 0.333 is expected for diffusion-controlled thickening (Voorhees, 1992, Cahn, 1992). This suggests that the second stage observed corresponds to the thickening of the decomposed phases. It is important to highlight that this stage is not yet observed for the Fe.32% at alloy. Cr aged at a temperature of 477°C since the decomposition kinetics is slower.

Figure 23 Variation of λ with aging time for alloy a) Fe-32% at. and b) 40%at. Cr aged at 477, 500 and 527°C



Source: Own Elaboration

5. Acknowledgments

We thank the authors to TecNM-TEJJo Proyecto 10210.21-PD and participating institutions.

6. Conclusions

Analysis of the spinodal decomposition in Fe-Cr alloys using the nonlinear and linear Cahn-Hilliard equations shows that both equations reproduce the main features of the spinodal decomposition expected in aged Fe-Cr alloys according to the spinodal decomposition theory. However, the morphology of decomposed phases for linear equation simulation is more representative of phase decomposition in the early stages of aging. On the contrary, the nonlinear equation reproduces both the first and the last stages of aging in the aged Fe-Cr alloys.

7. Reference

Baker H. (1992). Alloy Phase Diagrams, ASM Metals Handbook, Vol. 03, 152.

Cahn J. W. (1966). The later stages of spinodal decomposition and the beginnings of particle coarsening, *Acta Metallurgica*, 14, 1685-1691.
<https://www.sciencedirect.com/science/article/abs/pii/0001616066900216?via%3Dihub>,
[https://doi.org/10.1016/0001-6160\(66\)90021-6](https://doi.org/10.1016/0001-6160(66)90021-6)

Cahn J.W. and Hilliard J.E. (1971). Spinodal decomposition: A reprise, *Acta Metallurgica*, 19(2), 151-161.
<https://www.sciencedirect.com/science/article/abs/pii/0001616071901271?via%3Dihub>,
[https://doi.org/10.1016/0001-6160\(71\)90127-1](https://doi.org/10.1016/0001-6160(71)90127-1)

Cahn J. W. (1962). On spinodal decomposition in cubic crystals, *Acta Metallurgica*, Vol.10, 179-183.
<https://www.sciencedirect.com/science/article/abs/pii/0001616062901141?via%3Dihub>,
[https://doi.org/10.1016/0001-6160\(62\)90114-1](https://doi.org/10.1016/0001-6160(62)90114-1)

Cahn J. W. (1968). Spinodal Decomposition, *Transactions of the Metallurgical Society of AIME*, Vol. 242, 166-180. <https://onlinelibrary.wiley.com/doi/abs/10.1002/9781118788295.ch10>

Hirata V. M. L. (1982) Ph.D. Thesis, Tohoku University, Japan.

Hyde J. M., Hetherington M. G., Cerezo A. and Smith G. D. W. and Elliott C. M. y Miller M. K. (1995). Spinodal decomposition in Fe-Cr alloys: experimental study at the atomic level and comparison with computer models--I. Introduction and methodology, *Acta Metallurgica et Materialia*, 43(9), 3385-3401.
<https://www.sciencedirect.com/science/article/abs/pii/0956715195000403?via%3Dihub>,
[https://doi.org/10.1016/0956-7151\(95\)00040-3](https://doi.org/10.1016/0956-7151(95)00040-3)

Honjo M. and Saito Y., Numerical simulation of phase separation in Fe-Cr binary and Fe-Cr-Mo ternary alloys with use of the Cahn-Hilliard equation, *ISIJ Internacional*, Vol. 40, No.9, 2000, 914-919.
https://www.jstage.jst.go.jp/article/isijinternational1989/40/9/40_9_914/_article,
 DOI:10.2355/ISIJINTERNATIONAL.40.914

Hosford. W. F. (2005) *Physical Metallurgy*, Taylor & Francis, EE.UU, 49-69.
<https://www.taylorfrancis.com/books/mono/10.1201/b15858/physical-metallurgy-william-hosford>,
<https://doi.org/10.1201/b15858>

Koyama T. and Onodera H. (2006). Modeling of microstructure changes in Fe-Cr-Co magnetic alloy using the phase-field method, *Journal of Phase Equilibrium and Diffusion*, 27(1) 22-29.
<https://link.springer.com/article/10.1361/105497106X92763>, DOI: 10.1361/105497106X92763

Lifshitz I. M. and Slyosov V.V. (1961). The kinetics of precipitation from supersaturated solid solutions", *J. Phys. Chem. Solids*, 19, 35-50.
<https://www.sciencedirect.com/science/article/abs/pii/0022369761900543?via%3Dihub>,
[https://doi.org/10.1016/0022-3697\(61\)90054-3](https://doi.org/10.1016/0022-3697(61)90054-3)

- Meshkov E.A., and Yanilkin A.V., New method of atomistic modeling of α - α' phase transition in Fe–Cr alloy with effective accounting for vibrational entropy, *Computational Materials Science*. Vol. 212, 2022. <https://www.sciencedirect.com/science/article/abs/pii/S0927025622003111?via%3Dihub>, <https://doi.org/10.1016/j.commatsci.2022.111563>
- Miller M. K., Hyde J. Cerezo M., A. and Smith G. D. W., Comparison of low temperature decomposition in Fe-Cr and duplex stainless steels, *Applied Surface Science*, Vol. 87-88, 1995, 323-328. [https://doi.org/10.1016/0169-4332\(95\)00497-1](https://doi.org/10.1016/0169-4332(95)00497-1)
- Qin R. S. and Bhadeshia H. K. (2010) Phase Field Modelling. *Materials Science and Technology*, 26(7), 803-813. <https://www.tandfonline.com/doi/abs/10.1179/174328409X453190>, DOI 10.1179/174328409X453190
- Ustinovshikov Y. and Pushkarev B. (2005). Alloys of the Fe–Cr system: the relations between phase transitions “order–disorder” and “ordering-separation”, *Journal of Alloys and Compounds*, 389, 1-2, 95-101. <https://www.sciencedirect.com/science/article/abs/pii/S0925838804010370?via%3Dihub>, <https://doi.org/10.1016/j.jallcom.2004.07.050>
- Ustinovshikov Y., Pushkarev B. and Sapegina I. (2005). Conditions of existence of a disordered solid solution having chemical interactions between the atomic species Fe-Cr, *Journal of Alloys and Compounds*, 394 (1-2), 200-206. <https://www.sciencedirect.com/science/article/abs/pii/S0925838804014008?via%3Dihub>, <https://doi.org/10.1016/j.jallcom.2004.10.033>
- Ustinovshikov Y. and Pushkarev B. (1998). Morphology of Fe–Cr alloys, *Materials Science and Engineering A*, 241 (1-2), 159-168. <https://www.sciencedirect.com/science/article/abs/pii/S092150939700484X?via%3Dihub>, [https://doi.org/10.1016/S0921-5093\(97\)00484-X](https://doi.org/10.1016/S0921-5093(97)00484-X)
- Ustinovshikov Y., B Pushkarev. and Igumnov I., Fe-rich portion of the Fe-Cr phase diagram: electron microscopy study, *Journal of Materials Science*, Vol. 37, 2002, 2031-2042. <https://link.springer.com/article/10.1023/A:1015259517812>, <https://doi.org/10.1023/A:1015259517812>
- Y. Ustinovshikov, M. Shirobokova and B. Pushkarev, A structural study of the Fe-Cr system alloys, *Acta Materialia*, Vol. 44, No. 12, 1996, 5021-5032. <https://www.sciencedirect.com/science/article/abs/pii/S1359645496000882?via%3Dihub>, [https://doi.org/10.1016/S1359-6454\(96\)00088-2](https://doi.org/10.1016/S1359-6454(96)00088-2)
- Voorhees P. W., Ostwald ripening of two-phase mixtures, *Annu. Rev. Mater. Sci.*, Vol. 22, 1992, 197-215. <https://www.annualreviews.org/doi/10.1146/annurev.ms.22.080192.001213>, <https://doi.org/10.1146/annurev.ms.22.080192.001213>
- Wagner V. C. (1961). Theorie der Alterung von Niederschlägen durch Umlösen. *Z Elektrochemie*, 65, 581-591. <https://onlinelibrary.wiley.com/doi/10.1002/bbpc.19610650704>, <https://doi.org/10.1002/bbpc.19610650704>
- Weng, Chen and Yang (2003). The high-temperature and low-temperature aging embrittlement in a 2205 duplex stainless steel, *Bulletin of the College of Engineering, N.T.U.*, No. 89, 45-61. <https://www.nrc.gov/docs/ML1004/ML100491406.pdf>
- Zhu F., Haasen P. and Wagner R., An atom probe study of the decomposition of Fe-Cr-Co permanent magnet alloys, *Acta Metallurgica*. Vol. 34, 1986, 457-463. <https://www.sciencedirect.com/science/article/abs/pii/0001616086900817?via%3Dihub>, [https://doi.org/10.1016/0001-6160\(86\)90081-7](https://doi.org/10.1016/0001-6160(86)90081-7)

Chapter 6 Hot Spot Identification Systems for Wildfire Control

Capítulo 6 Sistemas de Identificación de Puntos de Calor para Control de Incendios Forestales

CABALLERO-HERNÁNDEZ, Héctor†*, MUÑOZ-JIMÉNEZ, Vianney, RAMOS-CORCHADO, Marco A. and LÓPEZ-GONZALEZ, Erika

*Universidad Autónoma del Estado de México
Tecnológico de Estudios Superiores de Jocotitlán*

ID 1st Author: *Hector, Caballero-Hernández* / **ORC ID:** 0000-0002-2790-833X, **CVU CONACYT ID:** 445998

ID 1st Co-author: *Vianney, Muñoz-Jiménez* / **ORC ID:** 0000-0003-2180-6743, **CVU CONACYT ID:** 44343

ID 2nd Co-author: *Marco A., Ramos-Corchado* / **CVU CONACYT ID:** 37345

ID 3rd Co-author: *Erika, López-González*

DOI: 10.35429/H.2022.3.84.94

H. Caballero, V. Muñoz, M. Ramos and E. López

*hcaballero045@alumno.uaemex.mx

A. Ledesma (AA.). Science of Technology and Innovation. Handbooks-TII-©ECORFAN-Mexico, 2022.

Abstract

One of the most common problems that today's society with climate change is the increase in forest fires in various parts of the world. The present investigation refers to a literary review of the investigations carried out on the development of proposals that allow the identification of fire situations in natural ecosystems. The presence of fire is identified using computational systems that combine computer vision, artificial intelligence, and sophisticated monitoring variables that may indicate the presence of fire in a natural area. According to the research carried out, interesting models have been developed for the recognition of fire and its early detection, through advanced statistical processes, regression systems, and constant monitoring of the variables that intervene in the generation of fire.

Computer vision, Artificial intelligence, Hot spots, Forest fires

Resumen

Uno de los problemas más comunes que enfrenta la sociedad actual con el cambio climático es el aumento de los incendios forestales en varias partes del mundo. El presente trabajo hace referencia a una revisión literaria de las investigaciones realizadas sobre el desarrollo de propuestas que permitan identificar situaciones de incendio en ecosistemas naturales. La presencia de fuego se identifica mediante sistemas computacionales que combinan visión por computadora, inteligencia artificial y variables de monitoreo sofisticadas que pueden indicar la presencia de fuego en un área natural. De acuerdo con las investigaciones realizadas, se han desarrollado interesantes modelos para el reconocimiento del fuego y su detección temprana, mediante procesos estadísticos avanzados, sistemas de regresión y monitoreo constante de las variables que intervienen en la generación del fuego.

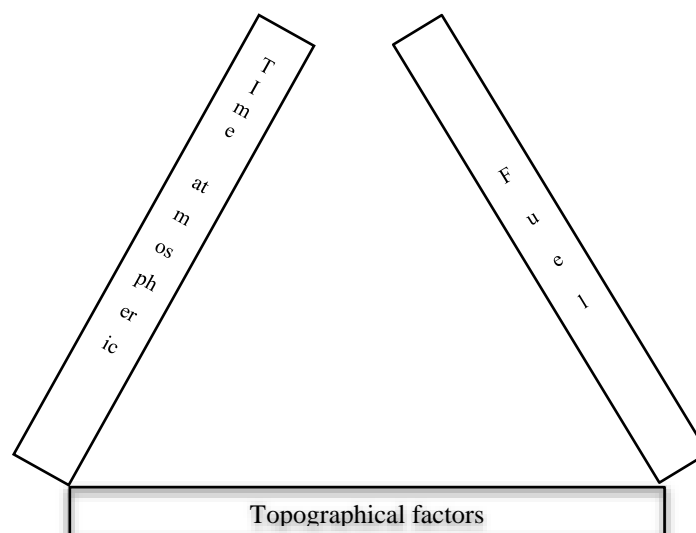
Visión por computadora, Inteligencia artificial, Puntos de calor, Incendios forestales

Introduction

Climate change, together with ground pollution and the uncontrolled release of garbage that contaminates water and subsoil, among other types of human carelessness are the main causes of forest fires in various parts of the world, being 96% of the causes of these events by activities carried out by man (Semarnat, 2018). Uncontrolled forest fires generate large losses of wild regions, destruction of human settlements and increased pollution at the atmospheric level (Cruz-Lopez, Manzano-Delado & Aguirre-Gómez, 2019). While it is true that the cycle of fire in ecosystems has to do with the renewal of these as a normal cycle of its existence (He et al., 2012), (Bowman et al., 2016), (Keeley et al., 2011), oversights and elements that do not belong to the fire cycle condition its stability (Villers-Ruíz, 2006).

Fuel, weather, and topographic factors are some of the main variables involved in the generation of fires.

Figure 1 Forest Fire Triangle



Source: Own Elaboration

Figure 1 represents the triangle of fire (Sutton, 2015), in which fuels are contemplated, which are the objects flammable, among them are trees and grasslands; the weather represents the conditions that are currently in the environment, taking into account that the weather conditions that favor high concentrations of oxygen and winds allow the fire to expand at a higher speed; finally, topographic factors are present, which determine whether or not there are natural barriers for the fire to spread or stop.

Globally, forest fires cause a release of 6.375 billion tons of carbon dioxide (CO₂) (Green Peace, 2019). Approximately more than 30 million km² are affected by forest fires worldwide (Randerson et al., 2012). The smoke released from wildfires contains hazardous particles such as PM₁₀ and PM_{2.5} (particles measured in microns) and are highly hazardous (Vicente et al., 2013), because when inhaled by humans can enter the bloodstream, causing lung and cardiovascular problems (Wettstein et al, 2018), (De Florio-Barker et al., 2019), (Adetona et al., 2016).

In the period between 2000 and 2010, only in Mexico more than 1.95 million hectares of forest were lost, while in the period from 2010 to 2020 the loss of 4.5 million hectares was reported losses due to more than 7,500 fires, which grew without control (CONAMER, 2013). The entities of Mexico that concentrate most of the forest fires are the State of Mexico, Mexico City, Chihuahua, and Michoacan which present more than 52% of the fires in the country (CONAFOR, 2021).

Due to the problems represented by forest fires, numerous works have been developed dedicated to the prevention, identification, and control of these. These works have focused on the use of technologies such as Wireless Sensor Networks, also known as *Wireless Sensor Network* (WSN) which are composed of tens or thousands of electronic sensors powered by batteries, called sensor nodes, which are distributed throughout an area of particular interest to monitor variables in the environment that indicate some important event (Chio Cho et al. , 2011).

Another technique used for the detection of forest fires is the identification of objects in images or video using *convolutional neural networks* (CNN), which are a variant of an artificial neural network where neurons correspond to receptive fields like neurons in the visual cortex. primary brain of a living being (Cruz et al., 2021), being one of the most common applications of deep learning (DL) (Bacoiu et al., 2019). Networks are trained with pure data or with characteristics obtained manually.

Another technology that allows locating events in geographical spaces are geographic information system (GIS), which are an organized set of hardware, software, and geographic data, oriented to capture, store, manipulate, analyze, and display geographically referenced information to solve complex problems that are related to the planning and management of a process (Moreira, 1996).

The following section presents a compilation of proposals that have been developed in Mexico and other countries to detect hot spots that represent forest fires, as well as studies on the effectiveness of currently available tools.

Fire identification: Proposals in the state of the art

In the analysis of hot spots there is a diverse range of research that addresses different methodologies and technologies to determine if a forest fire is developing, as well as the efficiency of these. One of the investigations that address the efficiency of forest fire detection systems using satellite technology is González-Gutiérrez et al. (2019), which performs an analysis on the reliability in the identification of hot spots in the state of Michoacán, Mexico.

This research shows the evaluation of the effectiveness of the *Early Warning System for Forest Fires*, this system has been in operation for approximately 34 years, however, the effectiveness of the system had not been proven, as a result of the investigation the authors point out that the CONAFOR (National Forestry Commission) system only detects fires that exceed 50 ha (hectares), therefore, authors suggest a change in the way fires are detected, so that technology included in focused points for a more efficient detection of forest fires.

In Pompa-García & González (2011) evaluated the fires that occur in the state of Durango and Mexico to detect which fires had greater proliferation, discovered that in the ecosystems where trees such as pine, oak and grasslands proliferate, different behaviors were detected. The authors detected that a fire where there was pine and oak this was presented in a group, while in areas where there is grassland, the fire occurs randomly.

Convolutional neural networks have high performance at object detection, but computationally come at a high cost. When implementing this type of network models in mobile devices or in low-cost *Internet of Things* (IoT) devices for object detection, the detection process is slow, as noted in the work of Lawrence & Zhang (2019), for this reason, the authors propose a model called IoTNet for resource-limited devices in object recognition using CNN. In Jardon, Varshney & Ansari (2020) propose an efficient fire detection method integrated and compatible with mobile devices. The results obtained in several standard fire datasets with the proposed method were superior to all existing methods in terms of most evaluation metrics such as accuracy, precision, recovery, and measurement, as noted in the paper. The proposed method is based on the CNN architecture called MobileNetV2.

In the investigation of Camacho, Díaz-Ramírez & Figuero (2015) exposes a network of sensors, which collected information on the environmental temperature and relative humidity under normal conditions, the authors realized that, when the temperature increased, the value of humidity decreased. The authors present the techniques of interpolation and the use of the Dempster-Shaner theory, to determine if there is a fire, although indicate that its effectiveness is low, given the variations provided by the model. Finally, the authors chose to use regression functions, taking time as an independent variable, and variables such as temperature and humidity were taken as dependent. The model proposed by the authors was evaluated in a middleware based on Java, and the sensor network platform used was IRIS. The result that authors obtained was 100% detection when the sensor nodes are not directly exposed to the sun.

Another application of a sensor network is observed in Hernández-Hostaller (2017), where propose the integration of temperature, carbon monoxide (CO), smoke, and infrared sensors. The acquired data is compared with a knowledge base to determine if there is a fire according to the data obtained by the sensor network, detecting the variations expected when simulating a fire.

The sensor networks require a series of considerations that allow them to effectively detect the variables are monitoring, in the work of Kim et al. (2020) perform an optimization in the WSN for the reduction of energy consumption and signal detection, which is applied to fire detection, through Continuous Object Tracking Based on Origin (OCOT), emphasizing distributed data, allowing a 49% reduction in network energy consumption without losing effectiveness in the detection of elements.

Computer vision systems have benefited from deep neural network models such as YOLO (*You Only Look Once*) (Redmon et al., 2016), this pre-trained model was implemented for numerous applications that require identification of objects that are contained in digital images or video. One of the applications that exists for identifying forest fires through the YOLO network is found in the work of Zhao (2022), in which developed a dataset (collection of elements) of 370 images containing fire and smoke situations with dimensions of 1850 x 1850 pixels. The authors made a modification on the convolutional network and named it Fire-YOLO, to later compare it against YOLO-V3 and Faster R-CNN (Girshick, 2015). In the project achieved a detection percentage of 76%, considering that the fire sections do not occupy more than 10% of the total image, compared to other models that require large portions of the image to perform the detection. The method implemented for building Fire-YOLO was Efficient Net.

There are other proposals whose solution is based on the integration of drones (also called unmanned aerial vehicles or UAVs) as can be seen in the work of Kinaneva (2020) in which use a series of drones which have digital image processing capabilities to detect forest fires. Meanwhile in the work of Rajeshwari (2019) present a proposal for capturing thermal images for fire detection, successfully detecting the areas in which a forest fire is located.

In some other proposals, in Parajuli (2020) and Zhao et al. (2021), carried out work to identify forest fire risk areas in Nepal and Nanjing, respectively, where present a characterization model of areas where forest fires can occur using information from GIS, because these systems allow to include information such as altitude, coordinates, reliefs, demarcation of zones by temperatures, presence of ecosystems, among others, allowing to identify the areas of greatest risk, to carry out preventive monitoring and prevent the spread of forest fires. As can be seen, there are different proposals that, based on software implementations, obtain information from different types of hardware to determine if there is the presence of a forest fire for prompt attention.

Wildfire identification technologies

One of the primary challenges that exist to reduce forest fires is the process of raising people's awareness about actions not to throw garbage, as well as avoiding intentional burning activities to develop activities such as agriculture and livestock. On the other hand, the other challenge that exists is the early detection of a fire, as well as the prediction of its evolution to avoid a rapid spread. Some points that was analyzed from the information collected previously in the works of González-Gutiérrez et al. (2019), Pompa-García & González (2011), Lawrence & Zhang (2019), Hernandez-Hostaller, (2017) Zhao (2022) and Parajuli et al. (2020) is that forest fire detection systems should consider the following elements.

- Monitoring of variables such as temperature, humidity, and presence of combustion gases such as CO, CO₂, as well as PM10 and PM2.5 particles.
- Identification of geographic areas that contain the highest probability of a fire, such as places with a lot of fuel and lack of moisture.
- Control of false positives and false negatives for parameters not contemplated.
- Presentation of possible decisions to prevent, contain or extinguish fires.

Is possible identified that there are four current trends for fire identification, such as detection by satellite imagery, detection by sensor networks, detection by capture of digital images and video using machine learning and GIS based models. Table 1 presents the most important advantages and disadvantages for forest fire detection.

Table 1 Fire detection technology

Detection technology	Advantages	Disadvantages
Satellite reconnaissance	- These systems can collect a large amount of information related to reliefs, weather conditions, as well as capture vast extensions of territory in digital images.	-These systems present difficulties to detect fires with an extension of less than 50 ha. - To access the information captured by these systems it is necessary to have connections via the internet.
Sensor networks	- These networks can act in specific places because can cover areas of several hectares. - WSN can monitor many variables such as temperature, relative humidity, presence of harmful gases, among other elements.	- WSN depend on the configuration of the central system to establish the appropriate parameters of the detected variables, because cause false positives or late alerts.
Deep Learning Recognition	-DL is highly efficient for detecting specific elements that have been captured in digital images and video. -DL can process information from different color models, as well as events captured by infrared technology. - DL can be implemented on a wide range of hardware.	-DL depend highly on rigorous training based on information contained in databases with many elements that present different contexts. - CNN is generally characterized by a high consumption of computational resources for its training, as well as for its operation. - CNN are not suitable for deployment in devices with low computational resources or that depend on batteries, without a control of energy consumption.
GIS	- GIS contain a large amount of information about the geographical points where the fires occur, because have information on the reliefs, terrestrial coordinates, among other elements, which allows classifying the risk areas.	- GIS depend on relatively constant updating and support from other systems for operation.

The different technologies that are mentioned in a general way in Table 1, have allowed to attack the problem of fires from different points of view, but it is possible to note that none of them can face the problem with 100% effectiveness in real conditions, because the contexts that can be presented are highly varied, with many restrictions, which condition the mathematical models that are implemented, because variables such as luminosity, weather conditions, bodies that are obstructing the visibility of fires, among others, are present. As mentioned above, satellite technology presents one of the first solutions for the early detection of forest fires, but it is conditioned to areas that exceed 50 ha of extension, on the other hand, accessing this system requires stable internet connections and other types of permits (with government or private entities), for this reason, the recognition by deep learning based on CNN, whose algorithms are implemented in different types of hardware makes them versatile in situations where the budget is reduced, allow mobility and as well as effective communication with personnel dedicated to fighting forest fires. This technology is implemented in IoT devices and unmanned autonomous vehicles (UAVs), whose collected information is analyzed on site or on servers, although UAVs have the limitation of wide energy consumption and a late response in devices with low computational power. Figure 2 shows an example of fire detection in a CNN image, where the result is framed in violet.

Figure 2 Detection of the presence of fire in a wooded area. Image obtained from Kaggle dataset, own detection using YOLOv5



Source: Gamaleldin, et al. (2018)

In the case of using IoT devices, such as Raspberry (Figure 3), require a continuous and stable power supply, in addition to the fact that when working continuously requires an effective power system to avoid greater energy consumption, which presents a problem to be solved in continuous operation, because battery banks usually limit current consumption when demand is at the limit of its capacity.

Figure 3 Raspberry Pi 3 B, one of the most widely used IoT

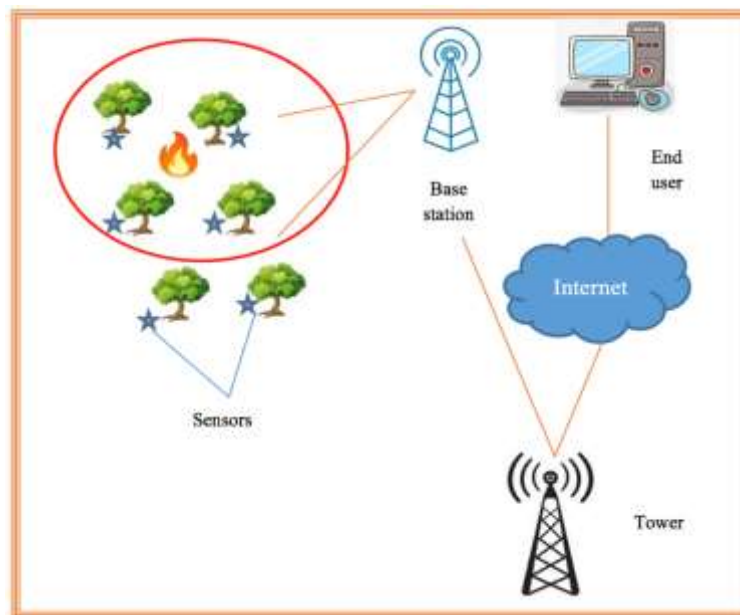


Source: Raspberry, (2018)

Sensor networks are an effective solution when monitoring the data that is captured from environments, especially when constantly monitoring temperature, humidity, and different types of gases, as well as the presence of PM10 and PM2.5 particles but depend extensively on the identification of thresholds that indicate the presence of a fire, as well as ensuring that the connection to the main base is stable.

Another challenge that sensor networks have is that nodes exposed to direct sunlight present problems due to the escalation of temperature, as well as the decrease in humidity, indicating that there is a fire, which is not present (false positive), and therefore, must consider different types of sensors. Figure 4 presents the basic scheme of a network of sensors for fire detection, where is possible see the basic components, such as sensors, the base station that is responsible for receiving the data, and the infrastructure available to make a link to the internet and send the data to the end user for decision making.

Figure 4 Schematic of a sensor network



Source: Zareei, et al., (2018)

One of the interesting developments that have been presented for computers is that of GIS systems, in which different types of geographic information are found, to identify the points of greatest incidence, these systems have the coordinates, and through GPS technology (*Global Positioning System*) it is possible to make tours with drones in an automated way for the early detection of forest fires.

Conclusions

Forest fire detection systems have a remarkable evolution in the last 15 years, because the development in technology with electronic components has allowed the computing capabilities of the hardware to rise and allow better processing capabilities and data transfer speed, this is essential when equipment of contained size and fast processing is required, this benefits the implementation of machine learning algorithms that allow recognizing early fire situations, especially in areas where available satellite technology has detection limitations.

Recognition systems based on machine learning, which use models based on CNN, have proven to be effective in detecting fire events, in addition to its implementation is possible carried out on different types of platforms, although have limitations such as high computational consumption in the training stage. Reconnaissance models based on deep learning can be implemented in servers, personal computers, portable devices, autonomous flight devices, among others, which gives a high versatility for the recognition of forest fire situations.

Sensor networks are highly effective when it is necessary to cover areas in which satellite technology is not able to quickly identify a fire, when it is in an area less than 50 ha, but knowledge bases are needed with very precise data that allow the implemented mathematical models to have an answer as accurate as possible, and an interpretation of the data obtained by the sensors with a series of perfectly defined ranges to avoid false positives or activation of alarms late. It is also important to note that the location of the sensors must be positioned in places where factors such as sunlight are not in direct contact with them, because alter its behavior.

Current GIS having a large amount of geographic information, allow the creation of models to identify fire risk areas in times of drought and high temperatures, are highly useful for the prevention of this type of event.

While it is true that the recognition models offered by artificial intelligence, as well as the recognition models implemented in sensor networks, can provide certainty that can reach more than 90% of the presence of a forest fire, both proposals need further development, which allows them to unify the most important characteristics of each one to offer robust systems that can attend with a greater effectiveness of its primary objectives.

Acknowledgment

We grateful to the Consejo Mexiquense de Ciencia y Tecnología for the support given in carrying out this project [CAT2022-0109].

References

- Adetona, O., Reinhardt, T. E., Domitrovich, J., Broyles, G., Adetona, A. M., Kleinman, M. T. Ottmar, R. D. and Naeher, L. P. (2016). Review of the health effects of wildland fire smoke on wildland firefighters and the public. *Inhal. Toxicol.* vol. 28, pp. 95-139, doi: 10.3109/08958378.2016.1145771, url: <https://pubmed.ncbi.nlm.nih.gov/26915822/>.
- Bacioiu, D., Melton, G., Papaelias, M. and Shaw, R. (2019). Automated defect classification of SS304 TIG welding process using visible spectrum camera and machine learning. *NDT E Int.*, vol. 107, doi: 10.1016/j.ndteint.2019.102139, url: <https://www.sciencedirect.com/science/article/abs/pii/S0963869518305942>.
- Bowman, D.M.J.S., Perry, G.L.W., Higgins, S.I. Johnson, C.N., Fuhlendorf, S.D. and Murphy, B.P. (2016). Pyrodiversity is the coupling of biodiversity and fire regimes in food webs. *Phil. Trans. R. Soc.* vol. 371. doi: 10.1098/rstb.2015.0169, url: <https://royalsocietypublishing.org/doi/full/10.1098/rstb.2015.0169>.
- Camacho, J., Díaz-Ramírez, A. and Figueroa, R. (2015). Redes de sensores inalámbricas para la detección de incendios forestales. *Research in Computing Science.* vol. 107, pp. 73-85, doi: 10.13053/rcs-107-1-7, url: https://www.rcs.cic.ipn.mx/2015_107/Red%20de%20sensores%20inalambrica%20para%20la%20deteccion%20de%20incendios%20forestales.pdf.
- Chio Cho, N., Tibaduiza Burgos, D. A., Aparicio Zafra, L. C. and Caro Ortiz, L. M. (2011). Redes de sensores inalámbricos. En Congreso Internacional de Ingeniería Mecatrónica-UNAB, vol. 1. url: http://ve.scielo.org/scielo.php?script=sci_arttext&pid=S1316-48212014000100002, url: https://d1wqtxts1xzle7.cloudfront.net/49325193/Redes_de_sensores_inalmbricos20161003-25940-1d0pa1f-with-cover-page-v2.pdf?Expires=1668224861&Signature=fuOc61Cc8jMqFBZhjmZ8x2AaAU6L7k2REZQxX0TEttZj24ILFNqAhaTk4zthF8Iy1ZAuHwIHkSWJrc-h6XZa-IBKHqrFs5TWGCSLXLwVAyEGyt4~w8h7BUzL~egXM8B2xs1MISK9iM4c1647hvABIsxtOefwrOIdZF~-bmootpQ~diJr-4kFh9bUORKdtVgANfcO9uXUV1VMnqWiogtuLKgtcRzU9RYbh~HTig1NnyTMDDg9AXH-KGWfJQ36Awj0f9UimyYPKz2wqMuL0POr~jhyXGpSuNgmE8UxEQXKs~ggTo6pQTPsisS6JqKiQGhtbkywdHjdecprFJysfRs0w__&Key-Pair-Id=APKAJLOHF5GGSLRBV4ZA.

Comisión Nacional Forestal, Gerencia del Manejo del Fuego (CONAFOR) (2021). Número de incendios [Base de datos]. Gobierno de México. Disponible en: http://dgeiawf.semarnat.gob.mx:8080/ibi_apps/WFServlet?IBIF_ex=D3_RFORESTA05_01&IBIC_user=dgeia_mce&IBIC_pass=dgeia_mce&NOMBREENTIDAD=* &NOMBREANIO=* [Consultado el: 15-05-2022].

CONAMER (2013). Plan Nacional de Desarrollo (PND) 2013-2018 (2013). Programa Nacional Forestal. Especial. [En línea] Disponible en: <https://conamer.gob.mx/documentos/marcojuridico/rev2016/PND%202013-2018.pdf>. [Consultado el: 15-05-2022].

Cruz, J. Y. J., Rivas, M., Quiza, R., Villalonga, A. Haber, R. E. and Beruvides, G. (2021). Ensemble of convolutional neural networks based on an evolutionary algorithm applied to an industrial welding process. *Computers in Industry*, vol. 133, doi: <https://doi.org/10.1016/j.compind.2021.103530>, url: <https://www.sciencedirect.com/science/article/pii/S0166361521001378>.

Cruz-Lopez, M.I., Manzano-Delado, L.L., Aguirre-Gómez, R., Chuvieco, E. and Equihua-Benítez, J.A. (2019). Spatial distribution of forest fire emissions: A case study in three Mexican ecoregions. *Remote Sensing*, vol. 11, doi: 1185, doi: <https://doi.org/10.3390/rs11101185>, url: <https://www.mdpi.com/2072-4292/11/10/1185>.

De Florio-Barker, S., Crooks, J., Reyes, J. and Rappold, A. G. (2019). Cardiopulmonary effects of fine particulate matter exposure among older adults, during wildfire and non-wildfire periods, in the United States 2008-2010. *Environ. Health Perspect.* vol. 127, doi: 10.1289/ehp3860, url: <https://pubmed.ncbi.nlm.nih.gov/30875246/>.

Gamaleldin, A., Atef, A., Sake, H. and Shaheen, A. (2018). Kaggle Fire dataset. Disponible en: <https://www.kaggle.com/datasets/phylake1337/fire-dataset>, [Consultado el: 20-07-2022].

Girshick, R. (2015) Fast R-CNN. arXiv:1504.08083, doi: <https://doi.org/10.48550/arXiv.1504.08083>, url: <https://arxiv.org/abs/1504.08083?so>.

González-Gutiérrez, I. et al. (2019). Thematic accuracy of hotspots and wildfires in Michoacán, Mexico. *Rev. Chapingo*, vol. 26 pp.17-35, doi: 10.5154/r.rchscfa.2019.01.011, url: https://www.scielo.org.mx/scielo.php?script=sci_arttext&pid=S2007-40182020000100017.

Green Peace, (2019). 2019: El año en el que los grandes incendios forestales han evidenciado la emergencia climática, 20-12-2019. [En línea]. Disponible en: <https://es.greenpeace.org/es/sala-de-prensa/comunicados/2019-el-ano-en-el-que-los-grandes-incendios-forestales-han-evidenciado-la-emergencia-climatica/>. [Consultado el: 15-05-2022].

He, T. Pausas, J. G., Belcher, C.M., Schwilk, D.W. and Lamont, B.B (2012). Fire-adapted traits of *Pinus arbuscula* in the fiery Cretaceous. *New Phytol.* vol. 194, pp. 751–759, doi: 10.1111/j.1469-8137.2012.04079.x, url: <https://nph.onlinelibrary.wiley.com/doi/10.1111/j.1469-8137.2012.04079.x>.

Hernandez-Hostaller, N. (2017). Indicador PER para fuego forestal y red de sensores para la detección temprana de incendios forestales en Costa Rica. *Revista Tecnología en Marcha*, vol. 30(2), pp. 48-57, doi: <http://dx.doi.org/10.18845/tm.v30i2.3196>, url: https://www.scielo.sa.cr/scielo.php?script=sci_arttext&pid=S0379-39822017000200048.

Jardon, A., Varshney, A. and Ansari, M. S. (2020). Low-Complexity High-Performance Deep Learning Model for Real-Time Low-Cost Embedded Fire Detection Systems. *Procedia Computer Science*, vol. 171, pp. 418-426, doi: <https://doi.org/10.1016/j.procs.2020.04.044>, url: <https://www.sciencedirect.com/science/article/pii/S1877050920310103>.

Keeley, J.E., Pausas, J.G., Rundel, P.W., Bond, W.J. and Bradstock, R. A. (2011). Fire as an evolutionary pressure shaping plant traits. *Trends Plant Sci.* vol. 16, pp. 406–411, doi: 10.1016/j.tplants.2011.04.002, url: <https://pubmed.ncbi.nlm.nih.gov/21571573/>.

- Kim, C., Kim, S., Cho, H., Kim, S. and Oh, S. (2020). An Energy Efficient Sink Location Service for Continuous Objects in Wireless Sensor Networks. *Sensors* vol. 20. doi: <https://doi.org/10.3390/s20247282>, url: <https://www.mdpi.com/1424-8220/20/24/7282>.
- Kinaneva, D., Hristov, G., Raychev, J. and Zahariev, P. (2020). Early Forest Fire Detection Using Drones and Artificial Intelligence. 2019 42nd International Convention on Information and Communication Technology, Electronics and Microelectronics (MIPRO), pp. 1060-1065, doi: 10.23919/MIPRO.2019.8756696, url: <https://ieeexplore.ieee.org/document/8756696>.
- Lawrence, T. and Zhang, L. (2019). IoTNet: An Efficient and Accurate Convolutional Neural Network for IoT Devices. *Sensors*, vol. 19, doi: <https://doi.org/10.3390/s19245541>, url: <https://www.mdpi.com/1424-8220/19/24/5541>.
- Moreira, M. A. (1996). Los Sistemas de Información Geográfica y sus aplicaciones en la diversidad biológica. *Revista: CIENCIA Y AMBIENTE*, pp. 80-86, doi: <http://repositorioslatinoamericanos.uchile.cl/handle/2250/3154329>, url: <https://www.redalyc.org/journal/5717/571760747003/html/>.
- Parajuli, A., Gautam, A., Sharma, S., Bhujel, K., Sharma, G., Thapa, P., Bist, B. and Poudel, S. (2020). Forest fire risk mapping using GIS and remote sensing in two major landscapes of Nepal. *Geomatics, Natural Hazards and Risk*. vol. 1, pp- 2569-2586, doi: 10.1080/19475705.2020.1853251, url: <https://www.tandfonline.com/doi/full/10.1080/19475705.2020.1853251>.
- Pompa-García, M. and González, P. (2011). Determinación de la tendencia espacial de los puntos de calor como estrategia para monitorear los incendios forestales en Durango, México. *Bosque (Valdivia)*. vol. 33. pp. 63-68, doi:10.4067/S0717-92002012000100007, url: <https://www.redalyc.org/articulo.oa?id=173124027007>.
- Rajeshwari, S. (2019). Effective forest fire detection system using visual images and unmanned aerial vehicle. *IJARIII*, vol. 5, doi: 16.0415/IJARIII-10993, url: <https://ijariie.com/FormDetails.aspx?MenuScriptId=159867>.
- Randerson, J. T., Chen, Y. Van Der Werf, B. M., Rogers, and Morton, D. C. (2012). Global burned area and biomass burning emissions from small fires. *J. Geophys. Res. Biogeosci.* vol. 117. doi: 10.1029/2012JG002128, url: <https://agupubs.onlinelibrary.wiley.com/doi/full/10.1029/2012JG002128>.
- Raspberry, (2018). Disponible en: <https://www.raspberrypi.com/products/raspberry-pi-3-model-b-plus/>. [Consultado el: 20-07-2022].
- Redmon, J., Divvala, S., Goschick, R. and Farhdi, A. (2016). You Only Look Once: Unified, Real-Time Object Detection, 2016 IEEE Conference on Computer Vision and Pattern Recognition (CVPR), pp. 779-788, doi: 10.1109/CVPR.2016.91, url: <https://ieeexplore.ieee.org/document/7780460>.
- Semarnat (2018). Incendios forestales. Secretaría de Medio Ambiente y Recursos Naturales. [En línea] Disponible en: <https://www.gob.mx/semarnat/articulos/incendios-forestales-148160>. [Consultado el: 15-07-2022].
- Sutton, I. (2015). *Process, Risk and Reliability Management*. Gulf Professional Publishing, pp. 602-666, 2015, url: <https://www.elsevier.com/books/process-risk-and-reliability-management/sutton/978-0-12-801653-4>.
- Vicente, A. Alves, C. Calvo, A. I., Fernandes, A. P. Nunes, T. Monteiro, C. Almeida, S. M. and Pio, C. (2013). Emission factors and detailed chemical composition of smoke particles from the 2010 wildfire season. *Atmos. Environ.* vol. 73, pp. 295-303, doi: 10.1016/j.atmosenv.2013.01.062, url: <https://www.sciencedirect.com/science/article/abs/pii/S1352231013000873>.
- Villers Ruíz, María de Lourdes. (2006). Incendios forestales. *Ciencias* 81, enero-marzo, 60-66. [En línea]. Disponible en: <https://revistacienciasunam.com/es/54-revistas/revista-ciencias-81/350-incendios-forestales.html>. [Consultado el: 15-08-2022].

Wettstein, Z. S., Hoshiko, S., Fahimi, J., Harrison, R. J., Cascio, W. E. and Rappold, A. G. (2018). Cardiovascular and cerebrovascular emergency department visits associated with wildfire smoke exposure in California in 2015. *J. Am. Heart Assoc.* vol. 7, doi: 10.1161/jaha.117.007492, url: <https://pubmed.ncbi.nlm.nih.gov/29643111/>.

Zareei, M., Vargas-Rosales, C., Villalpando-Hernandez, R., Azpilicueta, L., Anisi, M. H. and Rehmani, M. H. (2018). The effects of an Adaptive and Distributed Transmission Power Control on the performance of energy harvesting sensor networks, *Computer Networks*, vol. 137, pp. 69-82, doi: <https://doi.org/10.1016/j.comnet.2018.03.016>, url: <https://www.sciencedirect.com/science/article/abs/pii/S1389128618301300>.

Zhao, L., Zhi, L., Zhao, C. and Zheng, W. (2022). Fire-YOLO: A Small Target Object Detection Method for Fire Inspection. *Sustainability*, vol. 14, doi: <https://doi.org/10.3390/su14094930>, url: <https://www.mdpi.com/2071-1050/14/9/4930/htm>.

Zhao, P., Zhang, F., Lin, H. and Xu, S. (2021). GIS-Based Forest Fire Risk Model: A Case Study in Laoshan National Forest Park, Nanjing. *Remote Sens.* vol. 13, doi: <https://doi.org/10.3390/rs13183704>, url: <https://www.mdpi.com/2072-4292/13/18/3704>.

Chapter 7 Influence of patents on economic growth: An empirical analysis Mexico-Brazil

Capítulo 7 Influencia de las patentes sobre el crecimiento económico: Un análisis empírico México-Brasil

VARGAS-GONZÁLEZ, Jaqueline†* & RODRIGUEZ-HERNÁNDEZ, Gloria Patricia

Tecnológico de Estudios Superiores de Jocotitlán- Business Management Engineering, Mexico.

ID 1st Author: *Jaqueline, Vargas-González* / **ORC ID:** 0000-0003-4672-7259

ID 1st Co-author: *Gloria Patricia, Rodríguez-Hernández* / **CVU CONACYT ID:** 1157260

DOI: 10.35429/H.2022.3.95.105

J. Vargas & G. Rodríguez

*vargas@tesjo.edu.m

A. Ledesma (AA.). Science of Technology and Innovation. Handbooks-TII-©ECORFAN-Mexico, 2022.

Abstract

This article presents an empirical analysis to observe the influence of industrial property, measured as Patents, on the Gross Domestic Product (GDP) of two Latin American countries: Mexico - Brazil in the period 2000 - 2015 as phase I on study on patents and their effects. A unit root test is applied. The results show the existence of a positive relationship between the level of innovation and GDP.

Economic growth, Patents, Gross domestic product, Innovation

Resumen

Este artículo presenta un análisis empírico para observar la influencia de la propiedad industrial, medida como Patentes, en el Producto Interno Bruto (PIB) de dos países latinoamericanos: México - Brasil en el período 2000 - 2015 como fase I de estudio sobre patentes y sus efectos. Se aplica una prueba de raíz unitaria. Los resultados muestran la existencia de una relación positiva entre el nivel de innovación y el PIB.

Crecimiento económico, Patentes, Producto interno bruto, Innovación

1. Introducción

According to ECLAC reports, it is indicated that in order to sustain economic and social advances and respond effectively to the challenges that arise, it is essential to build capacities in the countries. The future requires very rapid and significant increases in productivity, as well as productive diversification that makes it possible to go beyond specialization in basic products. These increases will not occur spontaneously. Investment in basic and higher education, in science and technology, and in technical capacities for production becomes essential to bring about a new stage of growth with greater equality in Latin America and the Caribbean. Productive diversification and the incorporation of capacities must go hand in hand with a more intense and equitable effort to extend education to sectors that have been marginalized until now. ECLAC, 2015

When a country is in full employment of its factors of production, Capital and Labor, the Solow residual indicates that the growth of the Product is due to technological changes since the factors of production cannot be increased. This hypothesis has been studied empirically by numerous researchers over the last 20 years since the publication of the works, Barro (1991).

In this order of ideas, the increases in GDP explained by the residual contain, among other factors, innovation and industrial property, which in turn have positive effects on labor and capital, and therefore on GDP. Accordingly, Stern, Porter and Furman (2000) point out that the level of innovation in a region can be estimated with the number of patents generated.

This paper aims to study the relationship between Patents and economic growth using a panel data model for some Latin American countries, specifically: Mexico and Brazil. Through an econometric analysis for non-stationary panel data, the long-term relationship between production factors (Patents, Capital and Labor) and GDP is estimated, emphasizing the effect that the increase in Patents has on economic growth. of the countries. The analysis will be carried out through the use of GRETL, an econometric software.

In order to determine the order of integration of the series, apply the unit root test. It is necessary to know if there is a long-term relationship between GDP and the number of Patents, in order to know the causality that exists between these two series, which is supposed to be bidirectional, that is, there is a certain feedback between the increase in Patents and economic growth.

This text is organized as follows. The second part presents an overview of empirical studies that have been carried out at the international level on the relationship between patents and economic growth. The third part presents the model and the methodology to estimate. In the fourth part, the results of the unit root and Co-integration tests are presented and analyzed. In the last part, the final considerations are found.

2. Relationship Patents and Economic Growth

The relationship between patents and economic growth has been a well-studied topic in recent years. This section seeks to present international studies that have focused on this relationship, that is, the relationship between patents and economic growth of countries.

The study by (Griliches, 1990), where trends in time series of patents granted in the US are examined and their decline in 1970, is interpreted as a reflection of the changing meaning of these data over time. Therefore, it concludes that patent data remains a unique resource for the study of technical change. For his part, Keller (2004) mentions that differences in productivity explain a large part of the variation in income from one country to another, and technology plays a key role in determining productivity.

The authors Furman et al. (2002), present an empirical analysis of the determinants of the production of international patents at the national level.

The analysis of Acs et al. (2002), focuses on the problem of measuring economically useful knowledge, thus providing an exploratory study and a regression-based comparison of innovation count data and patent count data at the lowest levels. low possible geographical aggregation.

On the other hand, the work of Segerstrom (1998), explains why patent statistics have been more or less constant despite the fact that R&D employment has increased considerably in the last 30 years. In addition to showing through a model that an ever-increasing R&D effort has not led to any upward trend in economic growth rates, as predicted by early R&D-driven endogenous growth models with the "scale effect" property.

In the study by (Kortum, 1997) a theoretical model is developed - search for technological change that accounts for some disturbing trends in industrial research, patents and productivity growth. In the model presented, the researchers show the probability distributions of the possible new production techniques for each good in the economy.

On the other hand, Atz et al. (2010), within the focus on increasing levels of competition and decreasing products, mentions that the ability of a company to generate a continuous flow of innovations may be more important than ever in what allows a company to improve profitability and maintain a competitive advantage, and investigates several questions that are central to an examination of the productivity of innovation in a company.

The existing literature allows these studies to be grouped into two areas, those that determine a direct effect that goes from patents to economic growth, and those that determine an indirect effect between them. Indirectly, when they affect economic growth through another factor of production, such as capital or labor, for example, Gould & Gruben (1996), through a cross-sectional model on patent protection, study the role played by rights of intellectual property on the economic growth of a country.

Their results present empirical evidence that is on the way to ensure that intellectual property is a determinant of economic growth, and the effect of patents is greater in more open countries, in relative terms. The article examines the role of intellectual property rights in economic growth, using data from different countries on patent protection, the trade regime and the specific characteristics of each country. Evidence suggests that intellectual property protection is a significant determinant of economic growth. These effects appear to be slightly stronger in relatively open economies and are robust both to the openness measure and to other alternative model specifications..

Additionally, Park & Ginarte (1997), show that patents have a positive impact on capital accumulation, and therefore, by increasing fixed capital, they have a positive effect on the economic growth of economies.

Koléda (2004) shows that the effect of novel patent requirements on GDP growth can exhibit an inverted U-shape, implying that a stronger intellectual property protection policy can slow down the economic growth of an economy, and demonstrating that there is an optimal level of requirements which maximizes economic growth.

According to the study by Fink & Maskus (2005), the possibility that the effect of intellectual property rights on the economic growth of countries depends on the level of economic development is high. Added to this finding are the results of Schneider (2005), obtained through a panel data model of 47 developed and developing countries between 1970 and 1990, which argue that legally stronger patent rights have a positive effect on innovation, and therefore on economic growth, only in developed countries. On the other hand, Chen & Puttitanun (2005), using panel data from 64 developing countries, obtain results in favor of stronger patent rights having a positive effect on innovation in developing economies. Additionally, they present empirical evidence on the existence of a U-shaped relationship between intellectual property rights and economic growth, first it decreases and then it increases.

Futagami & Iwaisako (2007) show that a model with patents of infinite duration does not maximize social welfare, while an endogenous model of finite duration, which does not present scale effects in the production function, maximizes social welfare. In the case of Cysne & Turchick (2012), they study the optimal level of protection of intellectual property rights through a model of research and development (R&D) growth with an exogenous rate of imitation.

In the study by Kim et al. (2012), using two models, study the effect of patents and utility models on innovation and economic growth, controlling in turn for the level of economic (technological) development. They first study a country-level model, using a panel data model, for the period 1975-2003, and then a firm-level model in Korea, for the period 1970-1995 using 13,530 firms. Their conclusions ensure that patent protection contributes to innovation and economic growth in developed countries, however, the same does not happen with developing countries since they do not find statistical evidence.

3. Methodology and Econometric Model

The objective is to estimate the relationship between industrial property, measured as the number of patents, and real GDP for the countries: Mexico and Brazil, during the period between 2000 - 2015. During the last two decades, the panel data They have been used as an analysis tool by researchers from various areas to study the relationships between different variables. The main reason is that this methodology combines a dimension of time (time series) with another transversal dimension (Cross Section), which has greater benefits when making statistical inference.

In this order of ideas, when working with macroeconomic panel data, in which the time series is greater than the number of individuals, the existence of a long-term relationship between the variables that are analyzed for the group must be taken into account. of individuals. In other words, we must ensure that a co-integration relationship exists to avoid the problem of obtaining spurious results. Kao (1999) was one of the authors who introduced the term of spurious relationships in the use of panel data, when the time observations are greater than the number of individuals in a panel.

The model to be estimated is the following

$$\ln(Y)_{it} = \alpha_i + \beta_1 \ln(K)_{it} + \beta_2 \ln(L)_{it} + \beta_3 \ln(Pat)_{it} + e_{it} \quad (1)$$

where $\ln(Y)_{it}$ is the logarithm of the country's GDP (i) in the period (t), $\ln(K)_{it}$ is the logarithm of the country's gross fixed capital formation (FBC)(i) in the period (t), $\ln(L)_{it}$ is the logarithm of the labor force of each country (FLA) (i) in the period (t), $\ln(Pat)_{it}$ is the logarithm of the patent registrations of each country (PAT) (i) in the period (t).

3.1. Unit Root Test

It is interesting to ask why the unit root test is important. Because it is common for macroeconomic variables to grow or often decline over time. Variables that increase over time are examples of non-stationary variables. There are also series that do not increase over time, but where the effects of the innovations do not die out over time. These are also non-stationary. There is a major problem with regressions involving non-stationary variables, when the standard errors produced are biased. Bias means that the conventional criteria used to judge whether or not there is a causal relationship between the variables is not reliable. In many cases a significant relationship is discovered when in fact it does not exist. A regression where this occurs is called a spurious regression.

One problem with unit root tests is that they suffer from low power and distorted size. In the framework of classical hypothesis testing, the null and alternative hypotheses, the two competing conclusions that can be inferred from the data, are specified. Next, the data is examined, to see if we may be able to reject the null hypothesis and therefore accept the alternative. We are usually interested in rejecting the null hypothesis, so to be sure, we need to be completely confident that it is incorrect before rejecting it. Consequently, significance levels such as 90% or 95% are used. This means that using the data we feel more than 90% (or 95%) confident that the null hypothesis is wrong.

Two types of errors can be made: 1. incorrectly reject a true null hypothesis (this is often called a type I error), or 2. accept a null hypothesis as false (a type II error). The consequences of errors depend on the circumstances and the researcher must choose the level of significance appropriately. The size of the test is the probability of committing a type I error, which would be the level of significance chosen. The size is distorted if the true probability is not what one thinks one is testing for. This will occur if the true distribution of the test statistic is different from the one one is using. A major problem with unit root tests in general, and the Dickey-Fuller test in particular, is that the distribution of the test statistics is both nonstandard and conditional on the order of integration of the series, the time series properties of the errors, if the series has a trend, etc. This means that size distortion issues are common.

For example, you may want to test at the 95% level, but you don't know the correct distribution. Suppose the value of the test statistic at the 95th percentile is α for the distribution you are using, but α is at the 90th percentile for the true distribution. In this case, you would be rejecting more hypotheses than you expect and reducing your chances of making a Type I error. Although the reduction is at a cost, because the probability of making a Type II error is inversely related to the probability of making a Type I error. The power of a test is the probability of rejecting a false null hypothesis, that is, one minus the probability of making a type II error. Unit root tests are notoriously underpowered. Note that the size of the test and its power are not equal, since they are conditional probabilities based on different conditions: one is based on a true null hypothesis and the other is based on a false null hypothesis. When unit root tests are performed, the null hypothesis is usually: the variable has a unit root. The low power of unit root tests means that we are sometimes unable to reject the null hypothesis, wrongly concluding that the variable has a unit root.

3.3. Cointegration Test

After verifying that the series are integrated of order one, that is, that they contain a unit root in the panel, the co-integration test was continued, in order to find evidence of the existence of a relationship between the variables in the long-term. This is tested using the well-known Pedroni heterogeneous panel co-integration test (1999, 2000, 2004).

4. Empirical Data and Results

This section presents the data and results of the unit root and co-integration tests..

4.1. Data

The data of the countries: Mexico and Brazil, for this work were obtained from the World Bank, data are used on GDP (in millions of dollars), Gross Fixed Capital Formation (in millions of dollars), Labor force (in millions of people) and Patents (registration number). The database covers the period between 2000 and 2015.

4.2. Unit Root Test

According to Table 1, the unit root test applied to the time series indicates that in levels these series have a unit root since the probability of the tests does not allow rejecting the null hypothesis of the existence of a unit root, the null hypothesis is that the series is stationary, for which, as can be seen, it is rejected at 1% significance. The results of the applied tests are also presented in the Annex. In short, the results of the unit root test on the variables that are included in the model show that the series are I, that is, they are integrated of order one.

Table 1 Unit Root Test

México	Brasil
Contrastes aumentados de Dickey-Fuller, orden 3, para PIB: tamaño muestral 12 hipótesis nula de raíz unitaria: $\alpha = 1$	Contrastes aumentados de Dickey-Fuller, orden 3, para PIB: tamaño muestral 12 hipótesis nula de raíz unitaria: $\alpha = 1$

Source: Own Elaboration with GRETL Econometric Software

The model chosen for each series and country is shown. The test gives evidence to reject the null hypothesis of stationarity for each of the series.

In the case of Mexico, the variable that has the greatest impact on GDP is the variable corresponding to the country's gross fixed capital formation (FBC); in the case of Brazil, the variable with the greatest impact is the labor force of each country (FLA).).

Acknowledgements

The authors thank the National Council for Scientific and Technological Development (CNPq -Brazil), the State Agency for Research and Development (FAPEMIG-MG), the Technological Institute for Higher Studies of Jocotitlán and the Organization of American States (OAS-COINBRA) for financial support for the development of this study. This work has been also funded by Tecnológico de Estudios Superiores de Jocotitlán.

Conclusions

In this work, an empirical study was carried out on the relationship between Patents and economic growth for two Latin American countries Mexico-Brazil, using annual information on the number of patents and GDP, during the period 2000-2015, additionally, this relationship is observed with other factors of production such as Capital and Labor.

The unit root test is applied in order to determine the order of integration of the series. This test determines that the model series are integrated of order one. Los resultados presentan evidencia estadística sobre la existencia de una relación de largo plazo entre las Patentes, el Capital, el Trabajo y el PIB para los dos países considerados.

An interesting result is then presented, and it is the impact that Patents have on the GDP and on the economic growth of the countries. One possible explanation for the low elasticity of GDP with respect to patents is that, in most Latin American countries, the majority of patent registrations are carried out by non-residents, with the registration of residents being very small in terms of relative.

References

- Acset.al. (2002). Patents and innovation counts as measures of regional production of new knowledge. *Research Policy*, 1069-1085. [https://doi.org/10.1016/S0048-7333\(01\)00184-6](https://doi.org/10.1016/S0048-7333(01)00184-6)
- Atzet.al. (2010). A longitudinal of the impact of R&D Patents and Product Innovation on firm performance. *Journal of Product Innovation*, 725-740. <https://doi.org/10.1111/j.1540-5885.2010.00747.x>
- Barro. (1991). Economic Growth in a Cross Section of Countries. *The Quarterly Journal of economics*, 407-443. <https://doi.org/10.2307/2937943>
- Chen&Puttitanun. (2005). Intellectual property rights and innovation in developing countries. *Journal of Development Economics*, 474 – 493. <https://doi.org/10.1016/j.jdeveco.2004.11.005>

- Cysne&Turchick. (2012). Intellectual property rights protection and endogenous economic growth revisited. *Journal of Economic Dynamics and Control*, 851 – 861. <https://doi.org/10.1016/j.jedc.2011.12.005>
- Fink&Maschus. (2005). Intellectual Property and Development. *World Bank, Washington, DC*. <https://link.springer.com/book/10.1007/978-3-642-27907-2>
- Furman et al. (2002). The determinants of national innovative capacity. *Research Policy*, 899-933. [https://doi.org/10.1016/S0048-7333\(01\)00152-4](https://doi.org/10.1016/S0048-7333(01)00152-4)
- Futagami&Iwaisako. (2007). Dynamic analysis of patent policy in a endogenous growth model. *Journal of Economic Theory*, 306 – 334. <https://doi.org/10.1016/j.jet.2005.07.009>
- Gould&Gruben. (1996). The role of intellectual property rights in economic growth. *Journal of Development Economics*, 323-350. https://doi.org/10.1007/978-1-4615-6219-1_10
- Griliches. (1990). Patent Statistics as economic indicators- a Survey. *Journal of economic literature*, 1661-1707. <http://www.jstor.org/stable/2727442>
- Hadri&RAo. (2008). Panel Stationarity Test with Structural Break. *Oxford Bulletin of Economics and Statistics*, 245 - 269. DOI: 10.1111/j.1468-0084.2008.00502.x
- Kao. (1999). Spurious regression and residual-based test for cointegration in panel data. *Journal of Econometrics*, 1 – 44. [https://doi.org/10.1016/S0304-4076\(98\)00023-2](https://doi.org/10.1016/S0304-4076(98)00023-2)
- Keller. (2004). International technology diffusion. *Journal of Economic Literature*, 752-782. <https://www.jstor.org/stable/3217250>
- Kim, Y. L. (2012). Appropriate intellectual property protection and economic growth in countries at different levels of development. *Research Policy*, 358 – 375. <https://doi.org/10.1016/j.respol.2011.09.003>
- Koléda. (2004). Patents novelty requirement and endogenous growth. *Revue d'économie politique*, 201 – 221. https://doi.org/10.3917/redp.142.0201#xd_co_f=YjgzMzdiMDYtY2IwNC00ZWZkLTkwYWQtOWU0MWWhYTVkNTQw~
- Kortum. (1997). Research, patenting and technological change. *Econometrica*, 1389-1419. <https://doi.org/10.2307/2171741>
- Mahadeva&Robinson. (2000). *Prueba de raíz unitaria para ayudar a la construcción del un modelo*. México: Centro de Estudios Monetarios Latinoamericanos. <https://www.cemla.org/PDF/ensayos/pub-en-76.pdf>
- Park&Ginarte. (1997). Intellectual property rights and economic growth. *Contemporary Economic Policy*, 51 – 61. <https://www.jstor.org/stable/23622109>
- Pedroni. (2004). Panel Cointegration: asymptotic and finite sample properties of pooled time series with an application to the PPP hypothesis: New Results. *Econometric Theory*, 597 - 627. <https://doi.org/10.1017/S0266466604203073>
- Pedroni. (1999). Critical Values for Cointegration Test in Heterogeneous Panels with Multiple Regressors. *Oxford Bulletin of Economics and Statistics*. <https://doi.org/10.1111/1468-0084.0610s1653>
- Pedroni. (2000). Fully modified OLS for heterogeneous cointegrated panels. *Advances in Econometrics*, 93 – 130. [https://doi.org/10.1016/S0731-9053\(00\)15004-2](https://doi.org/10.1016/S0731-9053(00)15004-2)

Schneider. (2005). International trade, economic growth and intellectual property rights: A panel data study of developed and developing countries. *Journal of Development Economics*, 529 – 547. <https://doi.org/10.1016/j.jdeveco.2004.09.001>

Segerstrom. (1998). Endogenous growth without scale effects. *American Economic Review*, 1290-1310. <https://www.jstor.org/stable/116872>

SternPorter&Furman. (2000). The determinants of national innovative capacity. *Research Policy*, 899-933. [https://doi.org/10.1016/S0048-7333\(01\)00152-4](https://doi.org/10.1016/S0048-7333(01)00152-4)

Annexes

Table 2 Unit Root Test

Mexico	Brasil
<p>Contrastes aumentados de Dickey-Fuller, orden 3, para PIB: tamaño muestral 12 hipótesis nula de raíz unitaria: a = 1</p> <p>contraste con constante modelo: $(1 - L)y = b_0 + (a-1)y(-1) + \dots + e$ Coef. de autocorrelación de primer orden de e: -0.155 valor estimado de (a - 1): -0.241171 Estadístico de contraste: tau_c(1) = -1.15305 valor p asintótico 0.6968</p> <p>con constante y tendencia modelo: $(1 - L)y = b_0 + b_1*t + (a-1)y(-1) + \dots + e$ Coef. de autocorrelación de primer orden de e: -0.356 valor estimado de (a - 1): -2.97785 Estadístico de contraste: tau_ct(1) = -3.17972 valor p asintótico 0.08847</p>	<p>Contrastes aumentados de Dickey-Fuller, orden 3, para PIB: tamaño muestral 12 hipótesis nula de raíz unitaria: a = 1</p> <p>contraste con constante modelo: $(1 - L)y = b_0 + (a-1)y(-1) + \dots + e$ Coef. de autocorrelación de primer orden de e: -0.161 valor estimado de (a - 1): -0.330632 Estadístico de contraste: tau_c(1) = -3.72829 valor p asintótico 0.003751</p> <p>con constante y tendencia modelo: $(1 - L)y = b_0 + b_1*t + (a-1)y(-1) + \dots + e$ Coef. de autocorrelación de primer orden de e: -0.139 valor estimado de (a - 1): -0.339947 Estadístico de contraste: tau_ct(1) = -0.566914 valor p asintótico 0.9804</p> <p>con constante y tendencia cuadrática modelo: $(1 - L)y = b_0 + b_1*t + b_2*t^2 + (a-1)y(-1) + \dots + e$ Coef. de autocorrelación de primer orden de e: -0.102 valor estimado de (a - 1): 0.927866 Estadístico de contraste: tau_ctt(1) = 1.22083 valor p asintótico 1</p>

Source: Own Elaboration with GRETL Econometric Software

Table 3 Heteroskedasticity Test

Mexico	
Brasil	

Source: Own Elaboration with GRETL Econometric Software

Table 4 Autocorrelation

Mexico					Brasil				
Contraste de Breusch-Godfrey para autocorrelación hasta el orden 2 estimaciones MCO utilizando las 14 observaciones 2002-2015 Variable dependiente: uhat					Contraste de Breusch-Godfrey para autocorrelación hasta el orden 3 estimaciones MCO utilizando las 13 observaciones 2003-2015 Variable dependiente: uhat				
VARIABLE	COEFICIENTE	DESV.TIP.	ESTAD T	VALOR P	VARIABLE	COEFICIENTE	DESV.TIP.	ESTAD T	VALOR P
const	6.3998E+015	1.0592E+015	0.400	0.4648	const	1.3004E+012	1.3192E+012	0.458	0.6536
FAT	-9.1869E+07	3.4180E+08	-0.868	0.4322	FAT	3.8450E+07	1.7670E+08	0.208	0.7620
FBC	-2.3139E+010	4.5294E+010	-0.911	0.4226	FBC	-4.1311E+010	3.4547E+010	-0.121	0.4149
FLA	-1.3045E+09	2.4054E+09	-0.501	0.6299	FLA	-7.0794E+09	1.0404E+010	-0.680	0.5190
uhat_1	0.110972	0.420401	0.259	0.8012	uhat_1	0.229609	0.558662	0.429	0.6699
uhat_2	-5.431047	0.573092	-0.782	0.4732	uhat_2	0.0571010	0.313638	0.189	0.8543
					uhat_3	0.250344	0.398872	0.748	0.4543
R-cuadrado = 0.118955					R-cuadrado = 0.185193				
Estadístico de contraste: LM = 0.240096, con valor p = F(F(2,8)) > 0.540884) = 0.602					Estadístico de contraste: LM = 2.439740, con valor p = F(F(3,4)) > 0.433562) = 0.732				
Estadístico alternativo: TR ² = 1.665455, con valor p = F(Chi-cuadrado(2)) > 1.66543) = 0.435					Estadístico alternativo: TR ² = 0.943074, con valor p = F(Chi-cuadrado(3)) > 2.94239) = 0.504				
Ljung-Box Q' = 1.04408 con valor p = F(Chi-cuadrado(2)) > 1.04408) = 0.588					Ljung-Box Q' = 2.14338 con valor p = F(Chi-cuadrado(3)) > 2.14338) = 0.543				

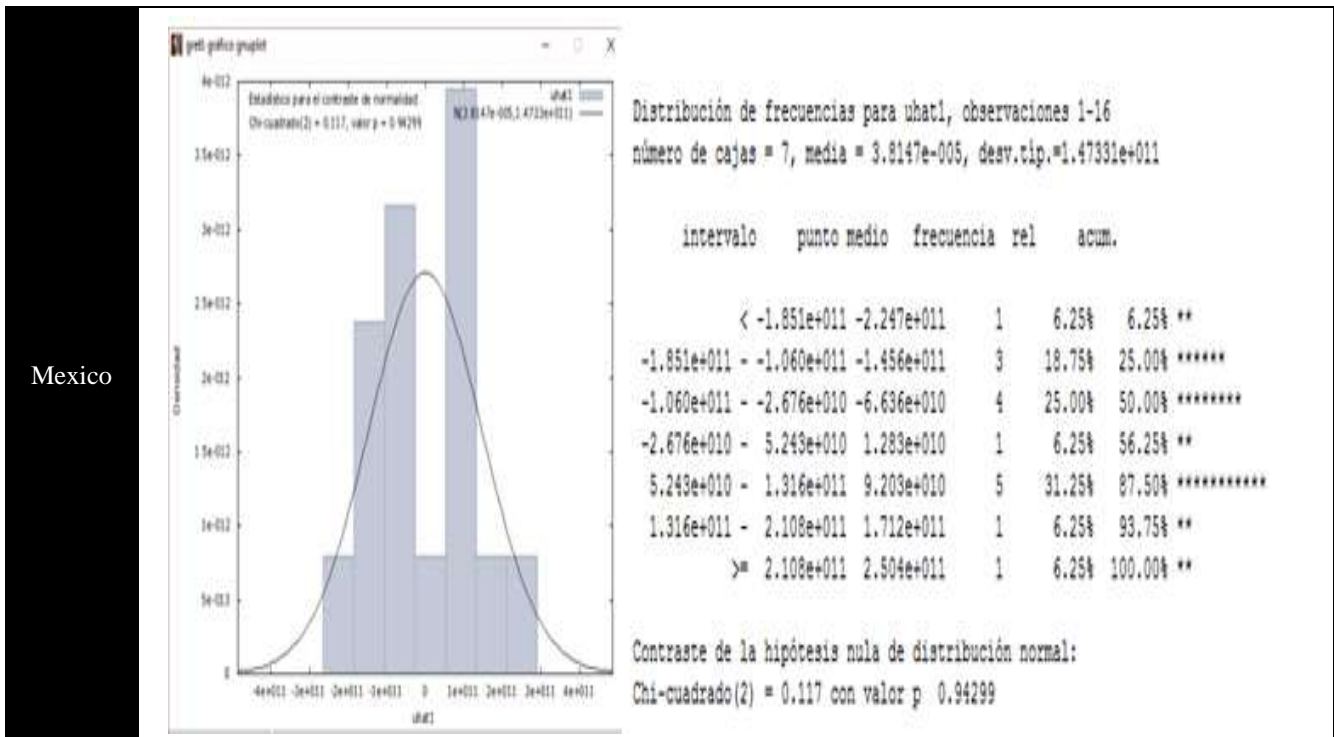
Source: Own Elaboration with GRETL Econometric Software

Table 5 Colineality

Mexico		Brasil	
Factores de inflación de varianzas (VIF)		Factores de inflación de varianzas (VIF)	
Mínimo valor posible = 1.0 Valores mayores que 10.0 pueden indicar un problema de colinealidad		Mínimo valor posible = 1.0 Valores mayores que 10.0 pueden indicar un problema de colinealidad	
2)	FAT 1.221	2)	FAT 1.410
3)	FBC 1.076	3)	FBC 1.593
4)	FLA 1.281	4)	FLA 1.423
VIF(j) = 1/(1 - R(j) ²), donde R(j) es el coeficiente de correlación múltiple entre la variable j y las demás variables independientes		VIF(j) = 1/(1 - R(j) ²), donde R(j) es el coeficiente de correlación múltiple entre la variable j y las demás variables independientes	
Propiedades de la matriz X'X:		Propiedades de la matriz X'X:	
norma-1 = 10800739		norma-1 = 2.6282781e+008	
Determinante = 4.3990816e+012		Determinante = 3.1739715e+013	
Número de condición recíproca = 2.5795489e-009		Número de condición recíproca = 3.8143868e-010	

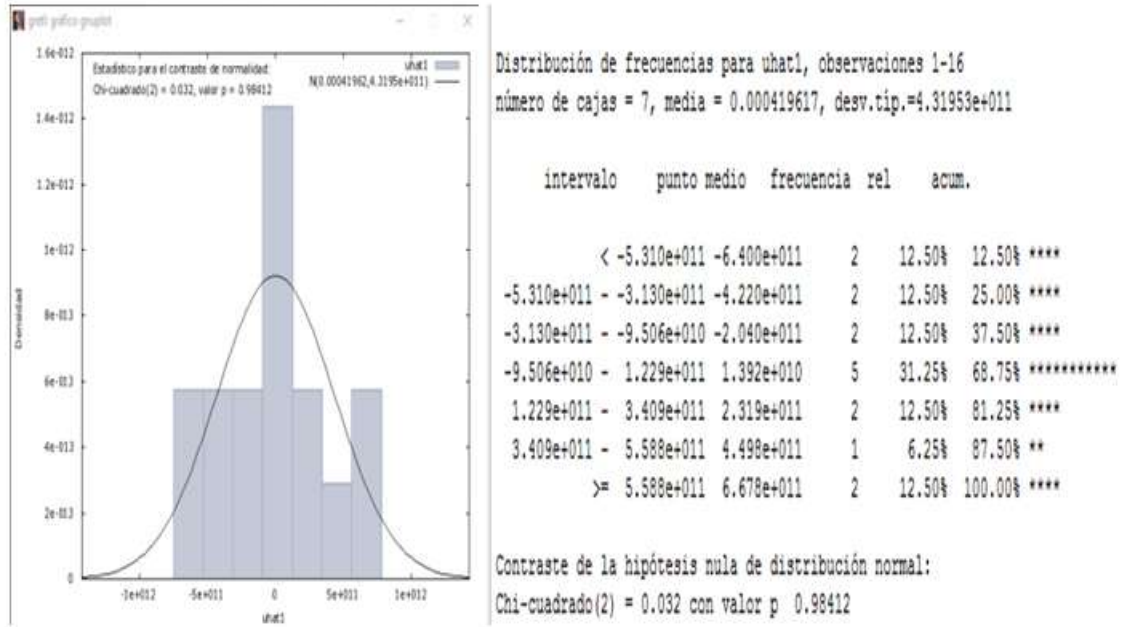
Source: Own Elaboration with GRETL Econometric Software

Table 6 Chi-Square



Mexico

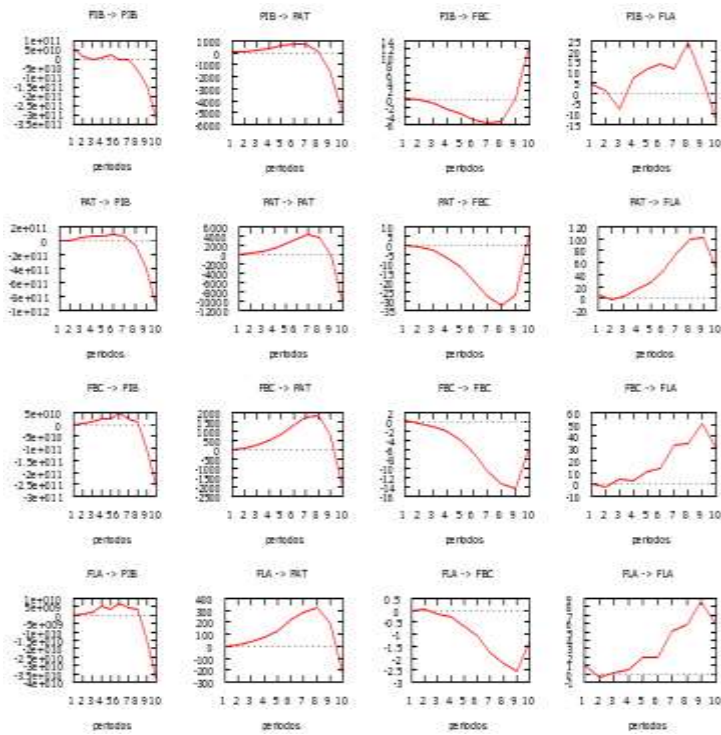
Brasil

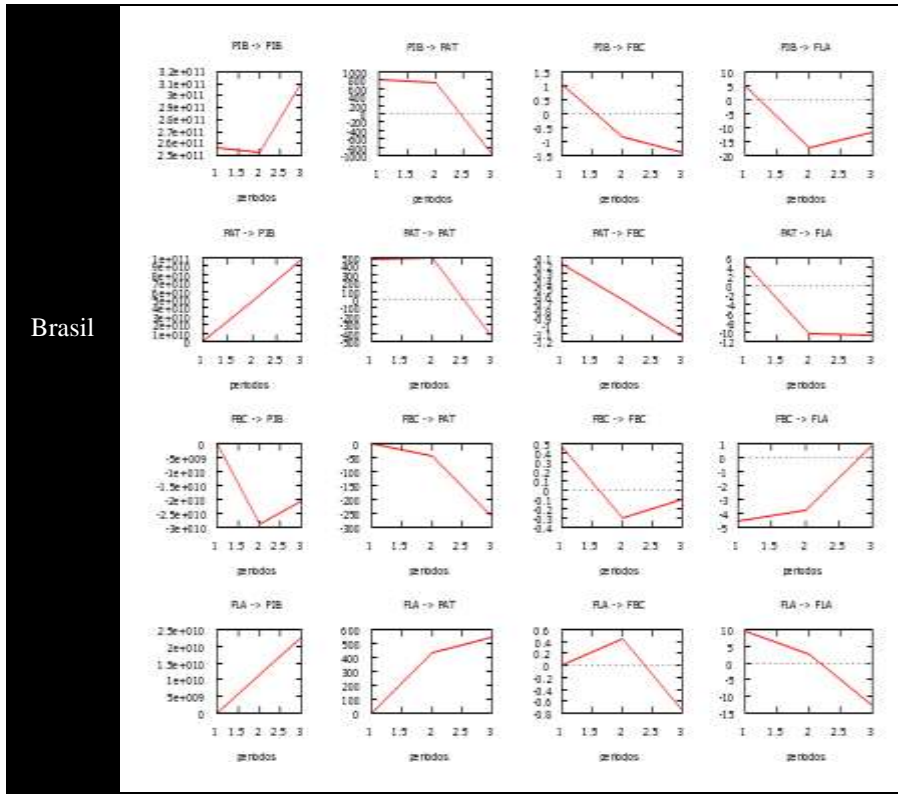


Source: Own Elaboration with GRETL Econometric Software

Table 7 Contrast of variables by country

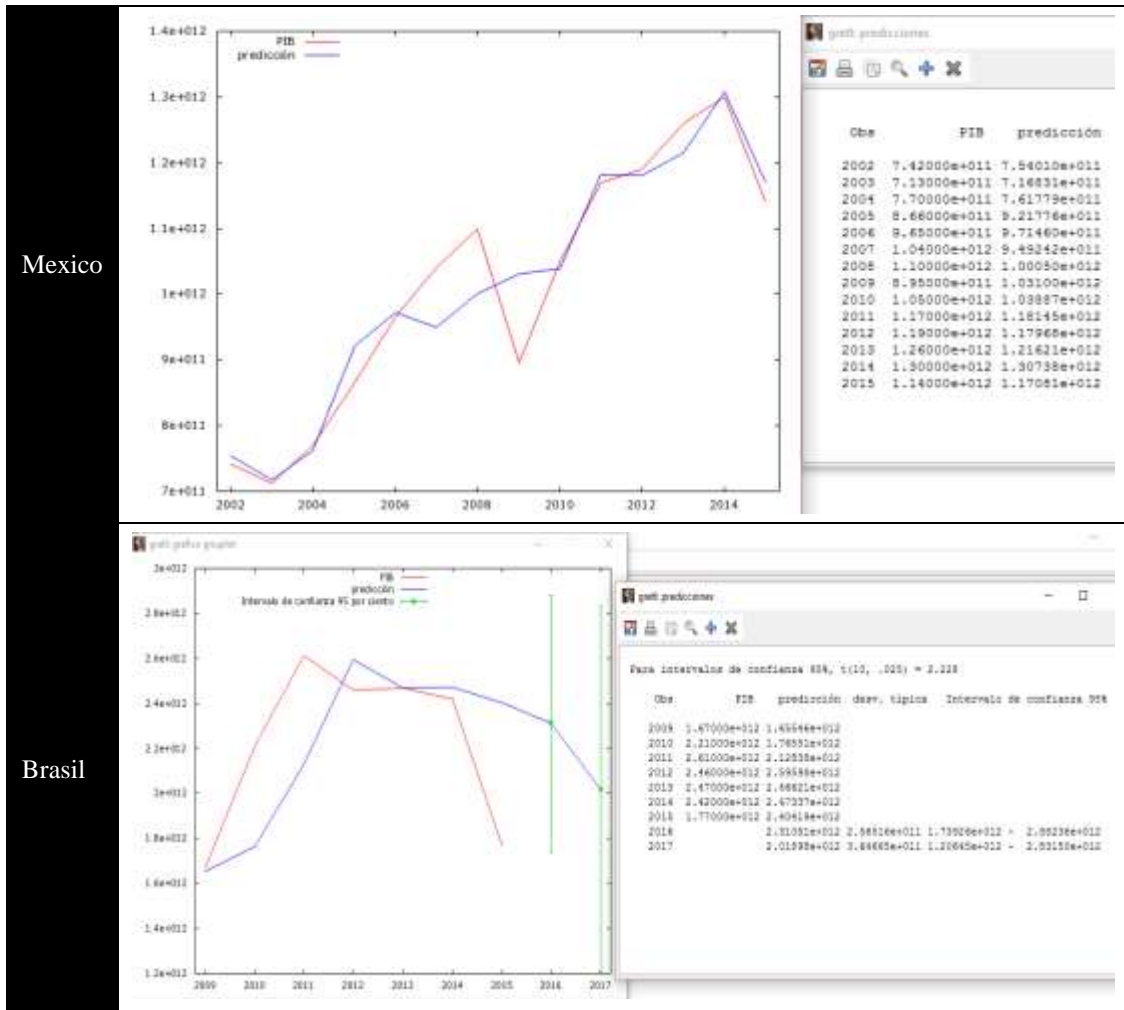
Mexico





Source: Own Elaboration with GRETL Econometric Software

Table 8 Predictions



Source: Own Elaboration with GRETL Econometric Software

Chapter 8 Introduction to Metallographic Study

Capítulo 8 Introducción al Estudio Metalográfico

SALAZAR-PERALTA, Araceli^{1†*}, PICHARDO-SALAZAR, José Alfredo², SÁNCHEZ-OROZCO Raymundo¹ and PICHARDO-SALAZAR Ulises³

¹*Tecnológico de Estudios Superiores de Jocotitlán, Carretera Toluca Atlacomulco km 44.8, Ejido de San Juan y San Agustín, Jocotitlán, México.*

²*Centro de Bachillerato Tecnológico Industrial y de Servicios No. 161, Exhacienda la Laguna s/n Barrio de Jesús 2ª Sección, San Pablo Autopan, Toluca. Estado de México.*

³*Centro de Estudios Tecnológicos Industrial y de Servicios No. 23. Avenida, Del Parque s/n, 52000 Lerma de Villada, México.*

ID 1st Author: *Araceli, Salazar-Peralta* / **ORC ID:** 0000-0001-5861-3748, **Researcher ID Thomson:** U-2933-2018, **CVU CONACYT ID:** 300357

ID 1st Co-author: *José Alfredo, Pichardo-Salazar* / **ORC ID:** 0000-0002-8939-9921

ID 2nd Co-author: *Raymundo, Sánchez-Orozco* / **ORC ID:** 0000-0003-0006-1711, **CVU CONACYT ID:** 169684

ID 3rd Co-author: *Ulises, Pichardo-Salazar* / **ORC ID:** 0000-0002-3758-2038

DOI: 10.35429/H.2022.3.106.129

A. Salazar, J.Pichardo, R. Sánchez and U.Pichardo

*araceli.salazar@tesjo.edu.mx

A. Ledesma (AA.). Science of Technology and Innovation. Handbooks-TII-©ECORFAN-Mexico, 2022.

Abstract

The quality assurance of materials in every process depends on materials science and engineering, since the characterization of materials is a fundamental process, for their control and innovation, as well as their proper functioning. In the synthesis of new materials, their properties depend not only on the type of raw material used (metal, polymer, ceramic, composite material), but also on the morphology acquired in the synthesis, structure, microstructure, etc. of the material obtained, hence the importance of metallographic characterization. Metallography is the science that deals with the microscopic study of the structural characteristics of a metal or an alloy, to study the microstructure, inclusions, as well as the thermal treatments to which the material has been subjected, in order to determine if the material complies with the specifications established in the Standards applicable to the design requirements for a specific use. The objective of this study was to present the basic techniques for the preparation of specimens to be evaluated metallographically, addressing the following topics: Generalities, Atomic structure: Nucleation and atoms, Crystal structure: Perfect crystals and crystals with imperfections. Substructure: Subgrains and other cellular structures, Microstructure: Grains of single metallic phases and configuration arrangements of alloys with multiple phase systems, Texture. Macrostructure. and Metallographic practice applicable to all metals. It is concluded that this study lays the foundations for subsequent and specific metallographic studies of ferrous and non-ferrous alloys.

Quality Assurance, Characterization, Microstructure, Properties

Resumen

El aseguramiento de calidad de los materiales en todo proceso depende de la ciencia e ingeniería en materiales, ya que la caracterización de los materiales es un proceso fundamental, para su control e innovación, así como del buen funcionamiento de los mismos. En la síntesis de nuevos materiales, las propiedades de los mismos dependen no solamente del tipo de materia prima utilizada (metal, polímero, cerámico, material compuesto), sino también de la morfología adquirida en la síntesis, estructura, microestructura, etc. del material obtenido, de ahí la importancia de la caracterización metalográfica. La metalografía es la ciencia que se encarga del estudio microscópico de las características estructurales de un metal o de una aleación, para estudiar la microestructura, inclusiones, así como los tratamientos térmicos a los que haya sido sometido el material, con la finalidad de determinar si el material cumple con las especificaciones establecidas en las Normas aplicables a los requisitos de diseño para un uso específico. El objetivo de este estudio consistió en dar a conocer las técnicas básicas para la preparación de especímenes a evaluar metalográficamente, abordando los siguientes temas: Generalidades, Estructura atómica: Nucleación y átomos, Estructura cristalina: Cristales perfectos y cristales con imperfecciones. Subestructura: Subgranos y otras estructuras celulares, Microestructura: Granos de fases metálicas sencillas y arreglos de la configuración de aleaciones con sistemas de fases múltiples, Textura. Macroestructura. y Práctica metalográfica aplicable a todos los metales. Se concluye que este estudio sienta las bases para estudios metalográficos posteriores y específicos de aleaciones ferrosas y no ferrosas.

Aseguramiento de Calidad, Caracterización, Microestructura, Propiedades

1. Introduction

The quality assurance of materials in every process depends on materials science and engineering, since the characterization of materials is a fundamental process, for their control and improvement, as well as their proper functioning. Now, the development and innovation of materials requires knowledge of the characteristics of the material, in order to choose the most suitable for a specific application. In the synthesis of new materials, their properties depend not only on the type of raw material used (metal, polymer, ceramic, composite material), but also on the morphology acquired in the synthesis, structure, microstructure, etc. of the material obtained, hence the importance of metallographic characterization. Metallography is responsible for the study of the structure, chemical composition and physical properties of metals and their alloys, for which it uses Microscopy, Polarimetry, and Radiography, studying the surface of metal specimens previously polished and subsequently attacked with chemical solutions. To reveal the microconstituents under study. Due to the great importance that metallography has for carrying out metallographic tests and problem solving in the industry, it is of great interest to know the basic techniques for the preparation of specimens to be evaluated, hence the relevance of this study.

The chapter has been compiled into 8 sections, which will serve as an auxiliary tool for students of Materials Engineering, Chemical Engineering, Industrial Engineering, and in general for all those people who, within the field, perform functions related to Quality Assurance of Metallic Materials, as well as for those who are interested in the Metallographic Study and wish to solve practical problems. Topics are addressed as follows:

Section 1. Generalities

1.1 Historical Background

Metallography began more than 200 years ago. One of the first initiators was R. A. F de Reaumur (1683-1757) who gave indications on how to differentiate steel gates through macroattack. At that time, its macro-development was carried out without the help of optical means.

Another initiator was S. Rimman (1) who by means of acid attack differentiated authentic Damascus steels from imitations, he wrote in 1774 “The attack is an appropriate means of which one can be valid to distinguish iron and steel gates in terms of differences in hardness, homogeneity and non-homogeneity”.

N. G. Sefstrom (2) in 1825 found that acid etching was a good means of seeing the homogeneity of the rolled iron structure.

The development of the structure of ground and polished iron is due to A. de Widmanstätten (3) 1808, who observed structural characteristics of iron, non-annealed gray iron and hardened steel which is known as Widmanstätten'sche structure.

In 1887 C.H. Sorby (4) reported the printing test on ground steels treated with strong acids. These age-old methods were macroetches that could be seen with the naked eye and did not require a mirror-polished specimen. Later use of the microscope required better surface preparation of the specimen and a special etching medium to differentiate metals.

Especially in the years 1870 to 1880 a series of microetching methods for iron and steel were used by the pioneers of metal microscopy. H. C. Sorby (5), A. Martens (6), and F. Osmond (7), who used dilute solutions of iodine in alcohol as etching media.

Years later the attack methods were further improved. Other researchers who also took part in these studies were:

H. Weddings (8), E. Hayn (9), H. Le Chatelier (10), I. E. Stead (11), W. Ischewsky (12), and Kourbatoff (13).

Day by day the era marked a new path, new methods of analysis that are innovated every day.

Metallography as a classic method is used to verify the development of structures in metallic alloys, mirror polishing metallic surfaces called metallographic specimens and observing them in an incident light microscope (14).

The structure of metals comprises very extensive features of varying degrees of complexity. In increasing order these magnitudes are:

- a) Atomic structure: Nucleation and atoms
- b) Crystal structure: Perfect crystals and crystals with imperfections
- c) Substructure: Subgrains and other cellular structures
- d) Microstructure: Grains of simple metallic phases and configuration arrangements of alloys with multiple phase systems.
- e) Texture
- f) Macrostructure.

Section 2. Atomic Structure: Nucleation and Atoms

Atom. It is the basic unit that can intervene in a chemical combination. It is made up of subatomic particles, of which the most important are electrons, protons and neutrons. Electrons are negatively charged particles that are found in energetic places known as *rempe*s or orbitals. Its mass is 9.1×10^{-28} g. Protons are positively charged particles found in the atomic nucleus and whose mass is 1.67×10^{-24} g. Neutrons are electrically neutral particles, found in the nucleus and having a mass slightly greater than that of protons 1.675×10^{-24} g. The number of protons in the nucleus of an element is known as the atomic number (Z). The number of protons and neutrons present in the nucleus of an atom of an element is known as the mass number. When measured in amu (atomic mass units), referred to the mass of a carbon 12 atom), it is called atomic mass (A). Some elements have more than one atomic mass, depending on the number of neutrons in their nucleus. These atoms are called isotopes (elements with the same atomic number but different masses). The atomic weight of an element is the average of the masses of the natural isotopes expressed in atomic mass units (amu).

2.1 Atomic models

At the beginning of the 20th century, Bohr proposed a planetary model to explain the atomic structure: in the center of the atom was the nucleus where the protons and neutrons are and surrounding said nucleus, the electrons rotated distributed in shells or energy levels. The closer they were to the nucleus, the less energy they had. This model did not explain some experimental results and therefore, in the late 1920s, Schrödinger and Heisenberg proposed a quantum mechanical model. Heisenberg said that it is impossible to know exactly the position and speed of an electron at a given time (Principle of uncertainty), so statistical regions of greater electronic probability (*rempe*) were described that define the possible position of an electron at a given time. moment. These regions are also known as atomic orbitals and have some sublevels. The position of an electron can be defined by 4 quantum numbers: **n**, **l**, **m** and **s**.

Bohr's postulates

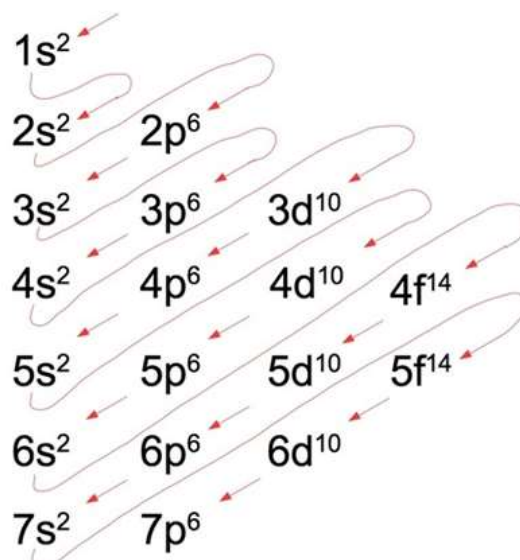
1. The electron revolves around the nucleus in a fixed set of allowed orbits, called stationary states: in them it rotates without absorbing or emitting energy.
2. Only those orbits in which the angular momentum of the electron is an integer multiple of $h/2\pi$ are allowed.
3. Electrons can jump from one allowed orbit to another by absorbing (if the final orbit is farther from the nucleus) or emitting (if the final orbit is closer to the nucleus) energy in the form of electromagnetic radiation. The Bohr model of the atom was unable to explain the following: The spectra of atoms more complex than the hydrogen atom. The variation of the intensity of the spectral lines, the arrangement and distribution of the electrons in various orbits, the fine structure of the spectral lines of hydrogen. And the effects of Stark and Zeeman.

2.2 Electronic configuration

The arrangement of the electrons in the various atomic orbitals is known as the electron configuration and it follows some basic rules:

1. An orbital cannot have more than two electrons, which must rotate in opposite directions.
2. Electrons do not gather in an orbital if there is another available with the same energy. There is an order in which the orbitals are filled and it is described in Figure 1. Following the direction indicated by each of the diagonals, the order of filling of the sublevels in the respective levels is determined.

Figure 1 Arrangement of electrons in the various atomic orbitals.



Source: <https://www.shutterstock.com/es/search/configuraci%C3%B3n-electr%C3%B3nica>

Electronic configuration examples: Helium (He₂: 1S²), Neon (Ne₁₀: 1S² 2S² 2 P⁶), Krypton (Kr₃₆: 1S² 2S² 2P⁶ 3S² 3P⁶ 4S² 3d¹⁰ 4P⁶). Thompson model. In 1904, before protons and neutrons were discovered, J.J. Thompson proposed a model for the atomic structure.

Thompson model

Sir Joseph Thompson (1856-1940). This English physicist at the age of 28 had the honor of being elected as a member of the Royal Society. In the same year he became Cavendish Professor of Experimental Physics at Cambridge. In 1897, he announced that he had identified cathode rays as streams of negatively charged particles, which he called corpuscles; which were later called electrons. He received the Nobel Prize for Physics in 1906. His model was referred to by others as "raisin pudding". According to this reasoning, an atom must have enough of a positive charge somewhere to neutralize the negative charges of the electrons present.

Rutherford's model

Many features of Thompson's model were examined and criticized, for example, some of them leading to certain predictions regarding the behavior of very thin metallic foils against atomic-sized projectiles, such as alpha particles. The streams of alpha particles come from uranium or radium, in bundles initially called alpha rays, because no one knew their nature it was necessary to give them a name. Ernest Rutherford identified alpha rays by defining them as atomic-sized particles with a mass of 4 amu and a charge of 2+.

Rutherford proposed that all of an atom's mass and all of its positive charge were concentrated in a small, dense bundle at the center of the atom (the nucleus). Surrounding this nucleus at some distance from it were the electrons that made the particle electrically neutral, although he did not explain how they could be outside and not be attracted to the nucleus.

2.3 Types of Bonds

Chemical bonds are the forces that hold atoms together in compounds. They are divided into several classes, depending on the properties of the compounds. The three main types are:

- 1) Ionic bonds, formed by the transfer of one or more electrons from one atom or group of atoms to another.
- 2) Covalent bonds that appear when one or more pairs of electrons are shared between two atoms. Both of these types of links are extreme and all links have some of them. Compounds in which the ionic character predominates are called ionic compounds; those in which the covalent character predominates are called covalent compounds.

- 3) Metallic bonds are found in solid metals such as copper, iron, and aluminum. In metals, each atom is bonded to several neighboring atoms, the bonding electrons are relatively free to move through the three-dimensional structure forming an electron cloud or sea of electrons, which give rise to typical metallic properties, such as high conductivity, electric and brightness.

Section 3. Crystal structure: Perfect crystals and crystals with imperfections.

Imperfections in crystals include defects such as atomic impurities, interstitial voids and aggregates, line defects (dislocations), and area defects (paired interfaces, subboundaries, and grain boundaries).

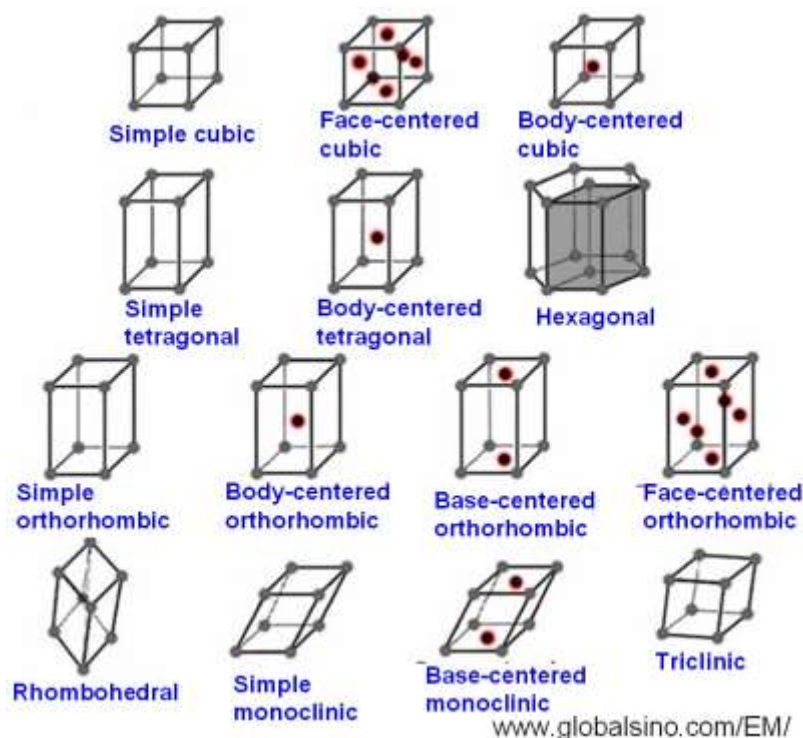
A common solid contains an order of 10^{23} atoms/cm³. To communicate the spatial arrangements of the atoms in a crystal, it is clearly not necessary to specify the position of each atom. Two complementary methodologies will be explained to describe in a simple way the three-dimensional arrangements of the atoms of a crystal. They will be referred to as the lattice and base concept and the unit cell concept, concepts linked to the principles of crystallography. An atom consists of a nucleus of protons and neutrons surrounded by electrons, but for the purpose of describing the arrangements of atoms in a solid, we will visualize the atoms as rigid spheres, similar to ping pong balls, starting with the concept of network and base.

3.1 Network

A network is a collection of points called network points, which are arranged in a periodic pattern such that the neighborhoods of each point in the network are identical. A network is a purely mathematical construction whose extension is infinite. A network can be one-dimensional, two-dimensional, or three-dimensional. In one dimension there is only one possible network: It is a line of points separated from each other by an equal distance. A group of one or more atoms located in a particular way with respect to one another and associated with each lattice point is known as a motif or base.

The base must have at least one atom, but it can contain many atoms of one or more types. To obtain a crystal structure, the base atoms must be placed at each lattice point (i.e., the crystal structure will be equal to the lattice plus the base). There are five different ways to arrange the points in two dimensions, so that each point has identical neighborhoods: Therefore there are five two-dimensional networks. There are only 14 unique ways to arrange the points in three dimensions. These unique three-dimensional arrangements of lattice points are known as Bravais lattices, named after Auguste Bravais (1811-1863), who was one of the first French crystallographers. Figure 2 shows Bravais networks. The 14 Bravais lattices Figure 2, are grouped into seven crystal systems, which are known as cubic, tetragonal, orthorhombic, rhombohedral (trigonal), hexagonal, monoclinic, and triclinic.

Figure 2 Bravais networks



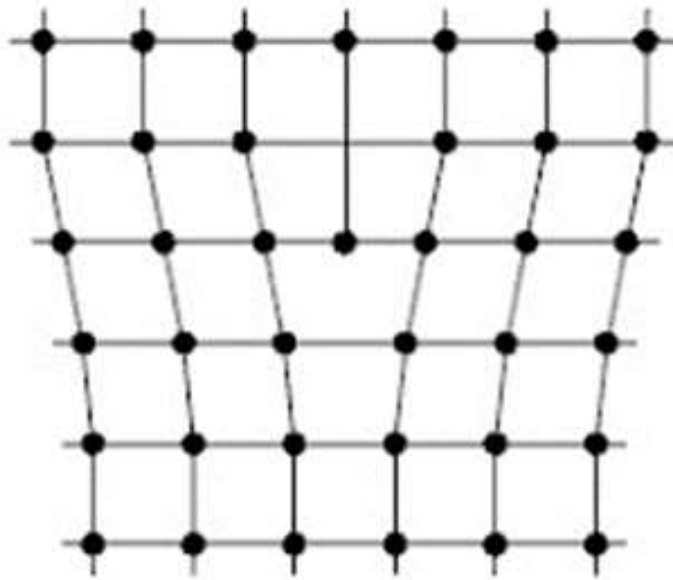
3.2 Imperfections in the crystals

The arrangement of atoms or ions in engineering materials contains imperfections or defects, defects that have a large effect on the properties of the materials. There are 3 basic types of imperfections: point defects, linear defects (dislocations), and surface defects.

3.2.1 Point Defects

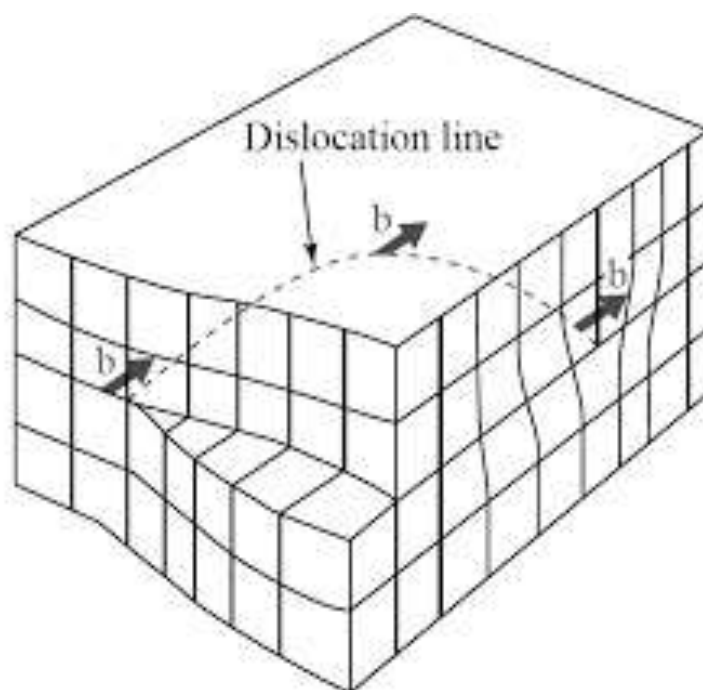
They are localized disturbances in the ionic or atomic arrangements of a crystal structure. The disturbance affects a region involving several atoms or ions; Examples of such imperfections are dislocations (misplaced atoms), vacancies, interstitial atoms, substitutional atoms: Figures 3, 4, 5, 6, 7.

Figure 3 Edge Dislocation

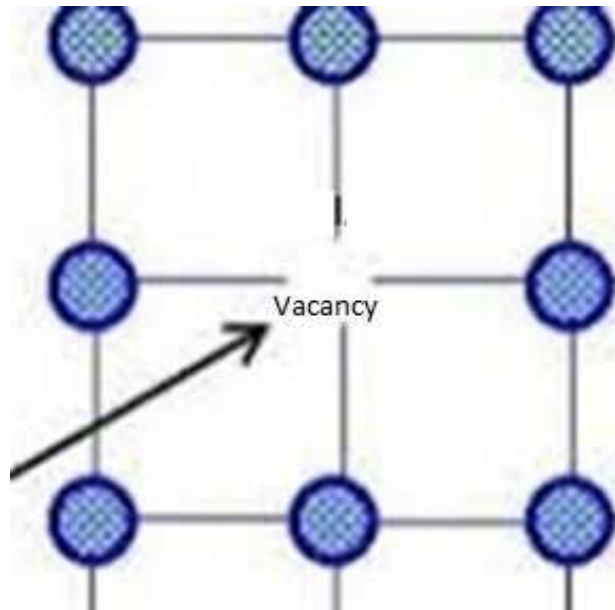


Source: Own Elaboration

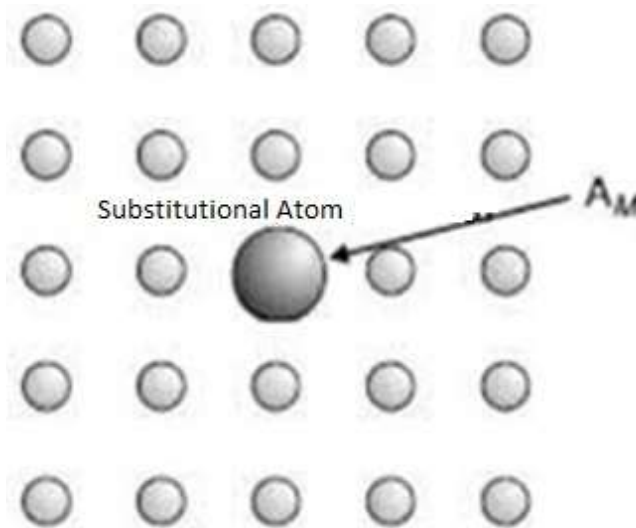
Figure. 4 Mixed dislocation



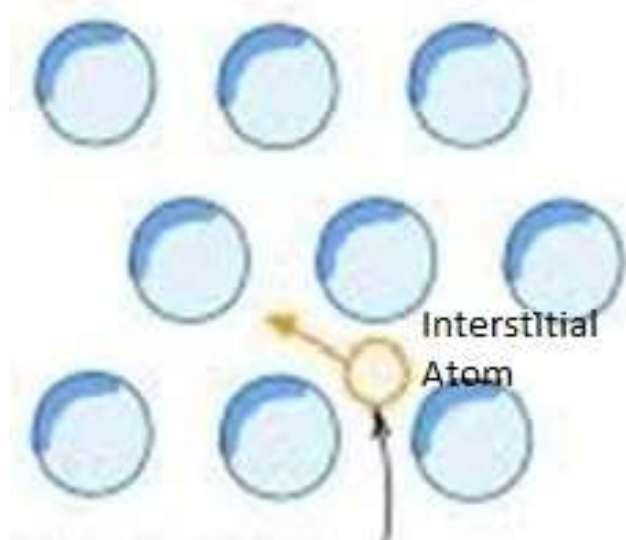
Source: Own Elaboration

Figure. 5 Vacancy

Source: Own Elaboration

Figure. 6. Substitutional Gold Atom

Source: Own Elaboration

Figure 7 Interstitial atom

Source: Own Elaboration

These imperfections can be caused by the movement of atoms or ions as they gain energy by heating during material processing or by the intentional or unintentional introduction of impurities. Impurities are usually elements or compounds contained in raw materials or during processing. For example, silicon crystals grow in quartz crucibles whose impurity is oxygen. In the case of dopants, they are elements or compounds that are added intentionally, in known concentrations, at specific places in the microstructure, with a desired beneficial effect on properties or processing. In general, the effect of impurities is detrimental, while in the case of dopants it is beneficial to obtain desired properties for a specific use of the material.

Section 4. Substructure

Subgrains and other cellular structures. Subgrains or cellular structures are formed by means of subboundaries (boundaries with small angles). The simplest of these boundaries consists of periodically spaced dislocations, dislocations can form cellular structures particularly in structures resulting from deformation. All kinds of imperfections in crystals can be found in single crystals or between grains of polycrystalline metals. Twins are an example of this. A twin is the symmetric grouping of identical crystals. The symmetry can be mirror with respect to the twin plane or by the rotation of its elements around the twin axis by 60° , 90° , 120° or 180° . A plastic deformation is produced on an annealed copper sample, performing a microstructural analysis represented in figures 8, 9, twins are observed. Twins are microstructurally identified as narrow subgrains with fairly rectilinear and parallel edges dividing the initial single crystal.

Figure 8 Twins within the grains of the copper matrix, due to deformation. Metals Handbook

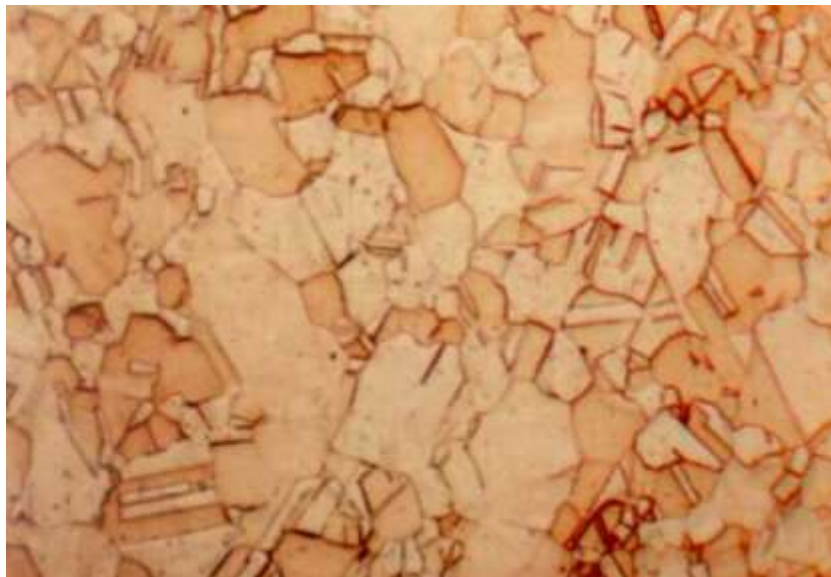
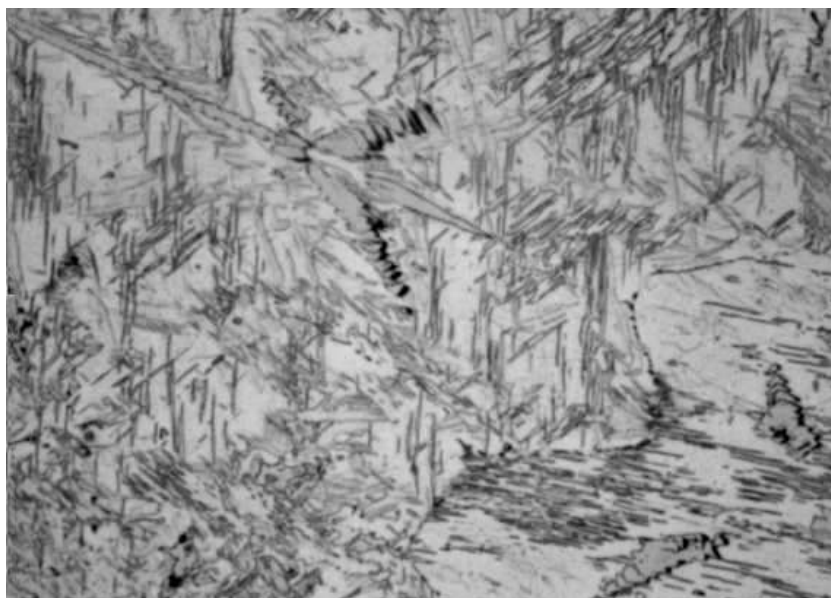


Figure. 9. Strain twins in a pure zinc crystal. Metals Handbook



Section 5. Microstructure

Grains of single metallic phases and configuration arrangements of alloys with multiple phase systems. Imperfections in crystals include defects such as atomic impurities, holes (vacancies), and interstitial aggregates, as well as substitutional atoms, linear defects (dislocations), and area defects (paired interfaces, subboundaries, and grain boundaries). The grain structure of single-phase polycrystalline metals is the most salient feature in the microstructure.

5.1 Pairs

They are imperfections that can originate during the development process; example: during annealing of cold-worked metal, or during grain deformation.

5.2 Structure with multiphase

It is that configurational arrangement of two or more phases to form a multifaceted structure, which highlights certain microstructural characteristics.

Section 6. Texture

It combines the strengths of lattice oriented crystallography with the microstructural strengths of grain structure. In a metal that has a preferred texture or orientation, the crystal takes over the grains and they are arranged in a correlated and organized manner.

Usually the metallic material is a polycrystal composed of a lot of crystal beads. When the grain orientation of a polycrystal is concentrated around a certain reference plane (or direction) of a macroscopic material, it is called preferred orientation, and texture is the preferred orientation of polycrystals. In a broad sense, the phenomenon that the grain orientation deviates from the random distribution in the polycrystal can be called texture.

In metallic materials, the existence of texture phenomena is universal. The external temperature field, electromagnetic field, strain field, and anisotropy within the crystal can cause texture. For example, the preferred grain orientation during deformation is slip surface, crystal slip, and moment effect during stretching. Industrial materials commonly have casting texture, deformation texture, recrystallization texture and phase change texture, among which deformation texture and recrystallization texture are most studied.

6.1 Description of crystal orientation and common types of texture.

The so-called crystal orientation refers to the three crystal axes (such as [100], [010], [001] axis) in a given reference coordinate system (such as rolling direction RD, lateral TD, and normal ND in rolling plate). When the orientation of the crystal is actually described, different reference frames are established due to different deformation conditions. For example, for the most common rolling deformation, the three reference frame axes are generally set to the rolling direction (RD) and the rolling surface. The direction (ND) and the transverse direction of the rolled sheet, that is, the direction perpendicular to the rolling direction (TD), assuming an orientation, is expressed as (110) [112], indicating the (110) plane of the unit cell at this time, parallel to the rolling surface, the [112] direction is parallel to the rolling direction.

The type of texture mainly depends on the nature of the metal and the processing method, etc. Among them, there are rolling texture, drawing texture and the like. Rolling texture is the texture that occurs during rolling deformation. It is characterized in that a certain crystal plane {hkl} of each grain is parallel to the rolling surface, and one direction is parallel to the rolling direction. The tread texture is usually expressed as {hkl}. Unidirectional stretching and pattern deformation cause a certain direction of the polycrystalline grains to be parallel to the stretching or pattern direction. The texture thus formed is called silk texture, also called fiber texture, parallel to stretching.

Or the glass orientation of the drawing direction. The presence of texture is universal in metallic materials. The essence of texture is that many grains are not distributed in a random orientation, which naturally leads to anisotropy in material properties. The effect of texture on material properties is studied to better utilize the texture in the material and to be able to regulate the related properties of the material.

Section 7. Macrostructure

The macrostructure of metals and alloys deals with those characteristics on a larger scale than that of the constituents of the microstructure (14).

A macrostructure comprises gas holes or porosities in molten metal which originate during solidification, such as flow lines in forging which originate during the deformation process.

Flow lines in the forged can be caused by elongated inclusions or by inhomogeneities in the alignment of the shape of the grains.

7.1 Origins of the structure

The structural characteristics of metals and alloys are produced by:

- a. transformations in which one or more phases are converted into one or more new phases.
- b. Mechanical processes
- c. Thermal processes or
- d. Diffusion processes (14).

Cold working is a typical mechanical process. The annealing of a cold worked metal is the main example of a thermal process. The fundamental principles that govern these principles are under the jurisdiction of Physical Metallurgy (15).

The transformations and processes that result in typical structures encompass basic mechanical characteristics. The transformation that produces solidification structures and solid-state transformation structures encompasses several mechanisms, the most important of which are: diffusion, nucleation, and growth; some more complex mechanisms are handled in martensitic and bainitic transformations (15).

The basic mechanical deformation includes mating and displacement and annealing processes, mainly recrystallization and grain growth processes by the mechanism of polygonization, nucleation, grain boundary growth and migration.

7.2 Single phase microstructure

Micrographic examination aims to reveal the structure of the metal and its non-metallic inclusions through observation through the optical microscope.

The definition of the microstructure of metallic materials is of overriding importance in the characterization of their composition and properties.

The main types are: solidification structures, solid state transformation structures, and annealing deformation structures, which are shown schematically in diagrams 1, 2, 3 (14, 20).

Diagram 1 Solidification Structures

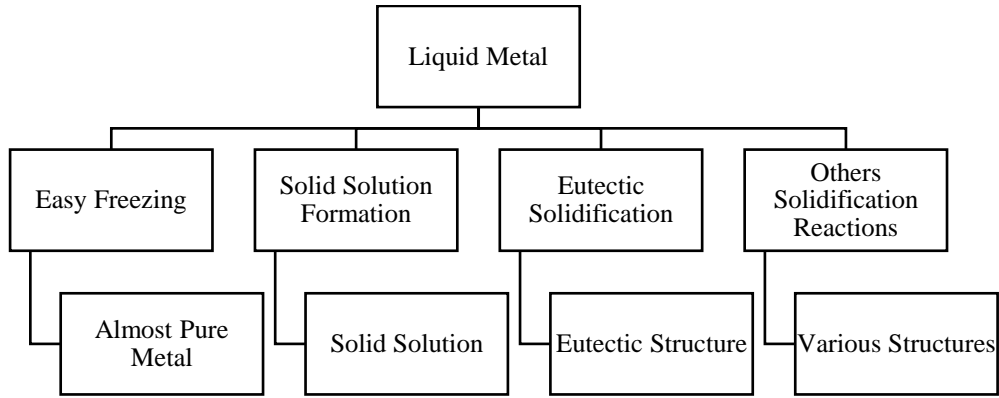


Diagram 2 Solid State Transformation Structures

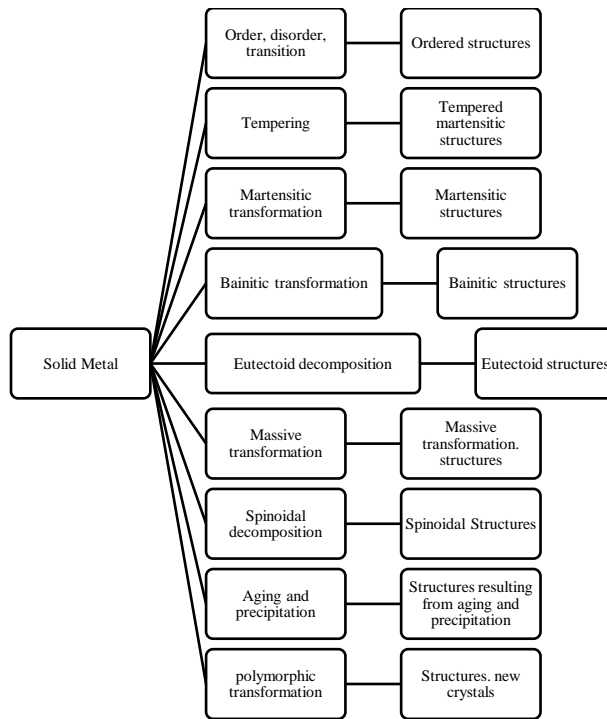
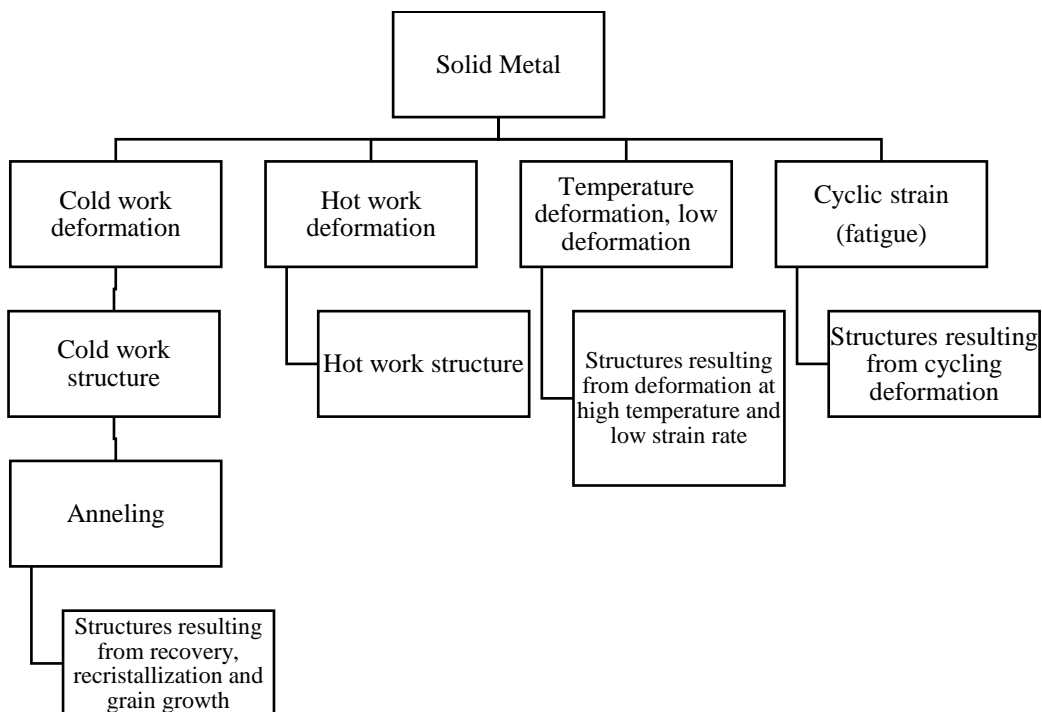


Diagram 3 Annealing Deformation Structures



The most notable structural features of single phase metals and alloys such as: grain structure and substructure are discussed below:

7.2.1 Grain structure

The grains are small crystals called crystallites that form a three-dimensional aggregate. The main characteristics of a grain structure are: grain size and anisotropic grain shape.

7.2.2 Types of grain structures

Typical grain structures include the following: affected structure, columnar structure, equiaxed grain structure, mature grain structure, deformed grain structure, inhibited recrystallization structure, and duplex grain structure (14, 18).

7.2.2.1 Structure affected

This type of structure is formed when grains grow to clump together or affect each other producing broken interfacial features. This type of structure is very rarely seen because the interfaces are generally flattened while the specimen is still at high temperatures. Affected grains are seen after secondary recrystallization.

7.2.2.2 Columnar structure

It is formed by processes in which there is unidirectional growth, especially during solidification, and also by aggregation processes including diffusion accompanied by a solid-state transformation. A columnar structure is shown in figures 10, 11 (14, 20).

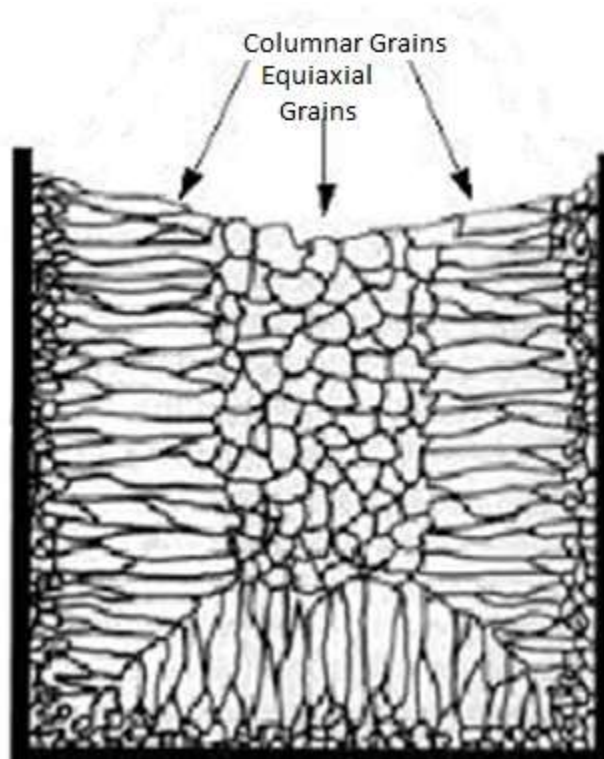
Figure 10 Columnar structure Metals Handbook



7.2.2.3 Equiaxed grain structure

This type of structure is formed in severe processes such as solidification and recrystallization Figure 12.

Figure 11 Columnar and equiaxial grains



Source: Own Elaboration

7.2.2.4 Mature grain structure

It forms when interfaces (i.e. those resulting from grain affection) adjust under the force of surface tension action.

7.2.2.5 Deformed grain structure

It is the result of cold working. In this structure the shape of the grains is anisotropic (Figs. 12-17).

Figure 12 Steel 1008 to 250X, with 10% of reduction. Metals Handbook

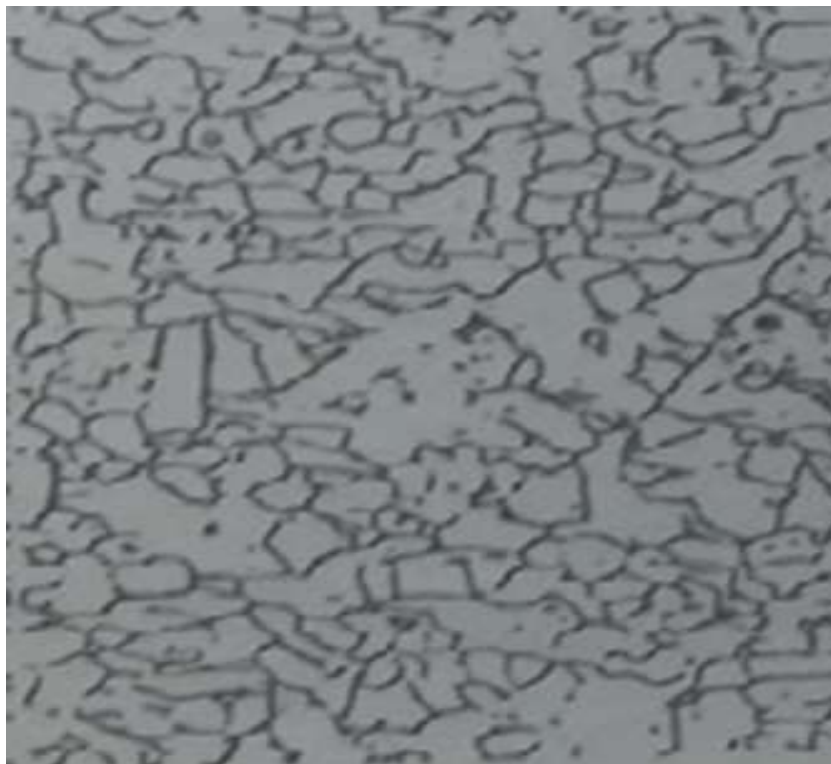


Figure. 13 Steel1008 a 250X, with 20% of reduction. Metals Handbook



Figure 14 Steel 1008 a 250X, with 30% of reduction. Metals Handbook



Figure. 15 Steel 1008 a 250X, with 40% of reduction. Metals Handbook

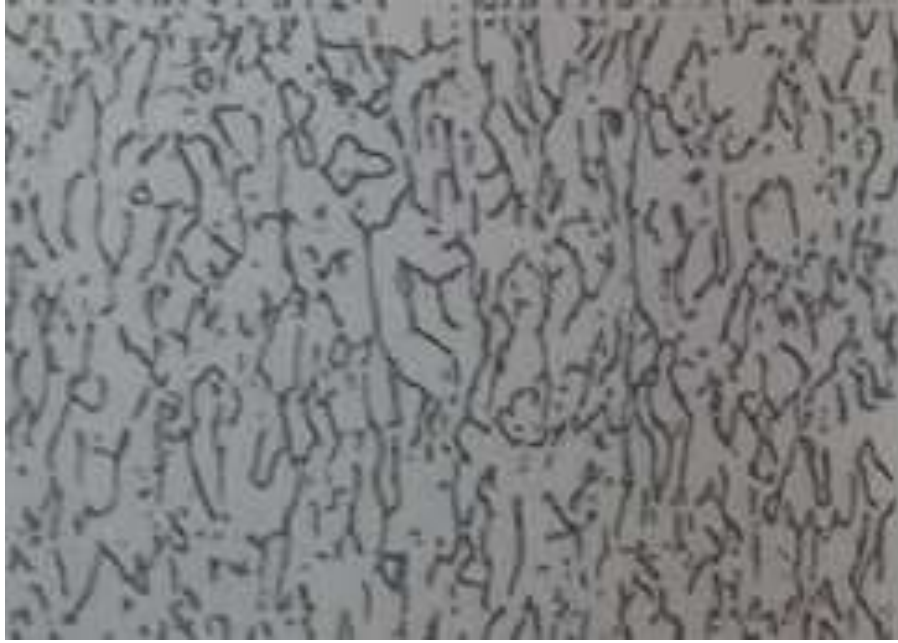


Figure. 16 Steel 1008 to 250X, with 50% of reduction. Metals Handbook

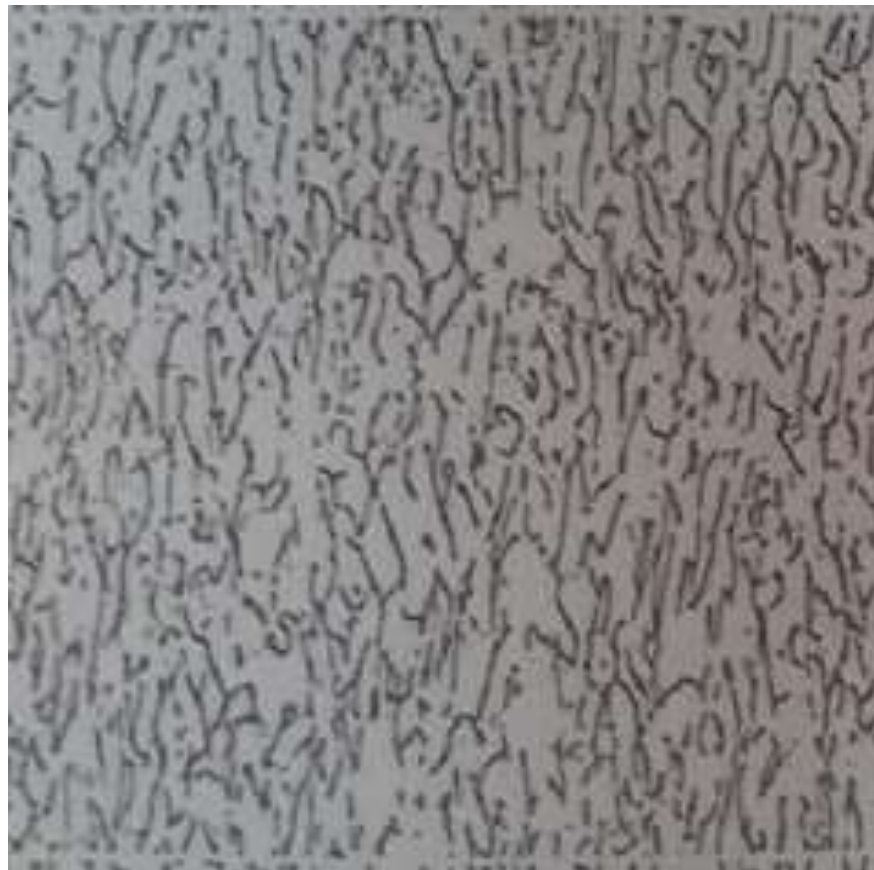


Figure 17 Steel 1008 to 250X, with 60% of reduction by cold rolled. Metals Handbook



7.2.2.6 Inhibited recrystallization structure

This type of microstructure is formed when the particles of secondary phases arrange themselves in a well-defined shape, preventing the movement of grain boundaries and imposing their specific shape on the resulting recrystallized structure (micrographs 18, 19, 20).

Figure 18 Low carbon Steel to 100X. Coarse ferrite. Grain 5. Metals Handbook



Figure. 19 Low carbon Steel to 100X. Grain 7. Metals Handbook



Fig. 20 Low carbon Steel to 100X. Grain 9. Metals Handbook



7.2.2.7 Duplex grain structure

It is one that consists of discrete regions with larger or smaller grain sizes (bimodal grain size distribution (Fig. 21).

Figure. 21 Steel with 0.013% of carbon to 100X. Dúplex ferrite. Metals Handbook



7.2.2.8 Three-dimensional grain structure

The grain structure exists in three dimensions. In a typical structure when two grains are separated by an interface, three interfaces join along a line or edge, and four edges join at a join point. These joints can be connected in countless ways without structural symmetry or exact repetition of details.

7.3 Grain shape

The grain shape for some purposes can be approximated to that of a sphere when the grains are equiaxial Fig. 22 Similarly non-equiaxial grains can be represented by ellipsoids. (14, 18).

Figure. 22 Equiaxed grains. Brass 260 to 75X. Size of grain 0.035 mm annealing to 482°C. Metals Handbook



Section 8. Metallographic Practice Applicable to All Metals

8.1 Methodology

It is worth mentioning that many of the steps described here for the preparation of specimens for metallographic study can also be used for other types of metallographic tests such as: electron microscopy, microhardness test, quantitative measurement of structure constituents and microtest analysis. electronics.

A properly prepared sample is one that meets the following requirements:

- a. Representative sample. The size of the sample will depend on what you want to evaluate.
- b. Sectioning, encapsulation (which is optional) can be done cold with resin and catalyst, or hot by means of a pressure encapsulator.
- c. Polished. Free from scratches, pinholes, and liquid stains or surface oxidation, this operation should be done as much as necessary to minimize distortion or flow of metal on the surface, caused by mechanical deformation, and thereby allow the true microstructure to be revealed by etching. later. It must be done in such a way that non-metallic inclusions are considered intact.

In general, the preparation of samples for metallographic analysis requires 5 operations, which are described below:

8.1.1 Sectioned

It is the operation by which a piece to be tested is sectioned to have a representative sample for the metallographic study, according to the characteristics that are to be evaluated; for example: for a deformation study, two sections are generally required; one perpendicular and one parallel to the major axis of the deformation direction. In the case of failed parts, they can be studied to find the cause of the failure; Selecting a specimen that intersects the origin of the fault zone, if the origin can be identified on the surface of the part, depending on the type of fault it may be necessary to take several samples from the fault area and from areas adjacent to the fault.

The sectioning operation can be done in three main ways:

8.1.1.1 Due to Fracture

Fracture tests can be done by means of controlled fractures, which can be produced by means of impact tests or tensile tests where the location of the fracture can be controlled by marking the material.

8.1.1.2 By Sawing

It is the oldest method used in the metallographic laboratory to section a material using a manual hacksaw. Saw blades are generally made of hard steel and are used to cut materials whose hardness is less than that of the saw blade or serrote. It is necessary to use oil or water-soluble oil as the cutting fluid to minimize frictional heating, which can soften or harden the tooth or age the microstructure of the specimen below the cut surface.

8.1.1.3. Cut with abrasive disc

Most of the cutting methods currently used in various laboratories is sectioning using abrasive disc cutting machines. All abrasive wheel cuts should be made wet using either water flow or a coolant (water soluble oil), which should flow directly into the cutting machine.

8.1.2 Mounting of Specimens

The main purpose of mounting the specimens for the metallographic study is to facilitate their handling, especially those that, because they are so small in size, cannot be handled properly for their preparation and study. Another additional benefit of mounting is the ease of being able to identify by name, alloy number or laboratory code for storage, writing on the surface of the specimen without damaging the sample.

8.1.2.1 Compression mounting

This is the most common method of mounting and is done by heating and pressing with molding materials such as bakelite, dialkyl phthalate resins, and acrylic resins. Bakelite and phthalate are thermosets and acrylic resins are thermoplastics. Both thermoset and thermoplastic materials require heating and pressure during the molding cycle, but after curing, assemblies made from thermoset materials can be ejected from the mold at the maximum molding temperature, whereas thermoplastics remain molten at the maximum molding temperature, for which it is necessary to allow it to cool under pressure before expelling the sample from the mold.

8.1.2.2 Materials for cold assembly

These materials are classified as polyesters, epoxies and acrylics, it is worth mentioning that these materials need a hardener (catalyst). The mixture of resin and hardener is prepared in the proportion that the manufacturer recommends, the mixture is made and poured into the mold which can be of any desired size or shape, according to the needs of each particular laboratory. Sometimes you can make your own molds with aluminum foil around blocks of wood of the desired size, since the aluminum foil can easily come off, it can also be prepared with silicone rubber.

8.1.3 Abrasion

It is one of the most important operations in sample preparation. During roughing, the operator must eliminate mechanical damage to the surface of the specimen due to cutting, since even if sectioning is done carefully, severe damage to the surface results. Damage can be removed by prolonged roughing. Roughing is completed by polishing the surface through a sequence of operations with progressively finer abrasives, 40 to 150 grit size abrasives generally being considered as rough abrasives and 180 to 600 grit sizes as rough abrasives. fine abrasives.

8.1.4 Polished

It is the final step to produce a flat, scratch-free, mirror-like surface (a necessary condition for subsequent metallographic interpretation, either qualitative or quantitative).

The polishing technique should not introduce foreign structures, such as contaminating metals, holes, comet tails or stains.

8.1.4.1 Mechanical polishing

This term is often used to describe the wide variety of final polishing procedures, including the use of cloth covered discs, and suitable polishing abrasives (alumina, diamond paste, magnesia). The disks have a rotating and vibrating movement, and the specimens are held manually or with automatic devices that allow polishing more than one specimen at the same time. Polishing must be done in a dust-free area, separate from the sectioning, assembly and grinding area, any contamination of a cloth by abrasive particles carried by a preceding operation or by dust, dirt or other material should not be tolerated. There are automatic polishers in which several specimens can be prepared automatically at the same time.

8.1.4.1.1 Movement of the specimen

The specimen is held in one hand, or both, depending on the operator's preference, and rotated in the direction opposite to the rotation of the disk. In conclusion, the specimen continuously moves back and forth between the center and the corner of the disc, thereby ensuring distribution of the abrasive and uniform wear of the polishing cloth.

Some metallurgists use a small rotation while moving the specimen from the center to the corner of one side of the disk. The main reason for sample rotation is to prevent the formation of comet tails, a polishing defect that is illustrated in Figure 23.

Figure. 23. Steel 12L14 without attack to 100X. It shows Comet tails resulting from directional polishing. Metals Handbook



8.1.4.1.2 Polishing pressure

In general, the applied pressure is determined by experience, the specimen must be held firmly in the initial polishing steps with a certain pressure, which decreases proportionally as polishing progresses. For soft metals the required pressure is less.

8.1.5. Washing and drying

The sample should preferably be washed with running water, dried with methanol or any other alcohol that does not leave a residue, and finally dried in a stream of hot air. Alcohol in general can be used for washing when the abrasive used is not soluble in water. The above cleaning precautions must be strictly followed.

8.1.6 Attack

Metallographic attack comprises all the procedures used to reveal particular structural characteristics of a metal under study, which cannot be observed in the polished material alone. Examination of a polished material before etching is recommended as it may reveal some important aspects such as porosity, cracks and non-metallic inclusions. In some non-ferrous alloys the grain size can be revealed adequately, only with a well polished surface without etching, using polarized light, because the etching obscures the grain boundaries, whereas in other applications etching is necessary to reveal the grain structure.

The attacker is used for phase identification, pore attack, and for orientation studies. The principle of multiphase attack in alloys is based on attack preference (different solution proportions of the phases in the attack), or preferential staining of one or more phases, to differentiate discrepancies in chemical composition or orientation. However, in pure metals or in single-phase alloys, preferential attack is primarily a result of differences in grain orientation.

Before attack, all specimens must be inspected to verify that the polishing has been correct and thus avoid the presence of scratches, pores, polishing reliefs, comet tails, and inclusions caused by polishing. Chemical etching is carried out by immersion of the sample in the etching solution until the required structure is revealed. Said attack is carried out in Petri dishes or in other suitable containers provided with loose covers to prevent excessive evaporation of the solvent, especially in those solutions that contain alcohol.

Glass containers can be used for all attackers except those solutions containing Hydrofluoric Acid. For these, the container must be made of polyethylene or some other suitable material, with the help of tweezers or some other means of handling; the surface of the specimen is submerged on the attacker with some agitation to ensure that the attacker is in contact with the specimen at all times. During the attack most metals lose their brilliance thereby indicating that the attack has been made. In practice, one can guess by the degree of darkness of the surface when the attack should be considered finished. It is worth mentioning that the attack can also be carried out with a cotton saturated with the attack solution, passing it over the polished surface. Once the attack is complete, the surface is washed with running water and then with alcohol, dried with a current of hot air (like that of a manual hair dryer).

8.1.6.1. Attack for macrostructure (Macroattack)

Macroscopic examination differs from microscopic examination because it uses very low magnifications and is used for the investigation of defects and structure in a larger area, while for microscopic examination small areas are used and are observed at higher magnifications. The macroetching technique is used to reveal solidification structures, flow lines, segregations, changes in structure due to welding, general distributions, size of inclusions, porosity, ingot defects and manufacturing defects, as well as fissures or cracks. It is important for the researcher to be aware that macroetching can greatly exaggerate the size of differences and defects, which can lead to misinterpretations of the actual condition of the material, for which experience is needed to make decisions. Special care must be taken to control the attack time.

When the roughness of the surface of the specimen is high, a strong attack is necessary, instead a moderate attack should be used for surfaces that have a fine finish such as that obtained with a 400 grit abrasive. If after macro etching there are rough lines this indicates that a finer roughing should have been used. Virgin metal exposed to attack is generally susceptible to oxidation, so it is necessary to protect it with a finish of either clear oil, glycerol, or clear lacquer if surface preservation is to be desired.

8.1.6.2 Attack for microstructure (microetching)

When a sample has been properly prepared, microscopic examination will clearly reveal structural features such as grain size, segregation, shape and size, phase distribution, and inclusions that may be present. The microstructure also reveals the type of heat treatment the metal has received. The proper attack is just as important, as are the steps of sampling, sectioning, mounting, roughing and polishing.

For most applications the following attack rules should be followed.

- a. Attack for a fair time. This time should be sufficient to reveal significant details of the microstructure, as excessive etching will exaggerate or erase fine details of the material's structure.
- b. If you want to have an additional contrast as for micro photography, this should be obtained by means of photographic techniques or (in some metaloscopes sets of lenses are integrated which give the desired contrast), instead of using an over attack which we it is convenient.
- c. When a specimen has been insufficiently etched it should be re-polished to remove the etching from the surface (repeating the last polishing step is usually sufficient) and re-etched, as re-etching without re-polishing generally produces poor results.
- d. Low magnification examination generally requires a higher etching than that required for higher magnification examination.
- e. After etching the surface of the specimen shall not come into contact with anything. It should be examined or photographed immediately before it rusts or becomes contaminated.

Acknowledgments

To the Industry Academy Linking Center (CCAI) of the Technological Institute of Higher Studies of Jocotitlán. For the Industry Academy Link.

To all the Institutions of my collaborators for their support

Conclusions

1. This chapter will serve for the Engineering student to acquire the fundamental knowledge to carry out the preparation of specimens for the metallographic characterization of materials, which is directly related to their physical and chemical properties.
2. Quality assurance in all manufacturing processes requires a metallographic study to determine compliance with the parameters established in the regulations applicable to each type of material, hence the importance of metallography.
3. This introductory study to Metallography will serve as the basis for other specific studies later.

References

[1]Rimman, S, Vetensk. Akad. Hdl. 34 (1773), pag. 318.

[2]Sefstrom, N.G. Jernkont. Ann. (1825), pag. 14

[3]Widmannstätten, A.V. Cristallographie du Fer. París (1900), pag. 25

- [4]Sorby H.C.J Iron Steel Inst. (1887), I, pag.255
- [5]Sorby, H.C. Proc. Sheffield Lit. Phil. Soc. (18649; Brit. Assoc. Rep. 1864, II, pag. 189
- [6]Martens, A..Z VDI 22 (1878), pag. 11
- [7]Osmond F. Method générale pour l analyse micrographique des aciers au carbone. 1895. Deutsch von Heurich. Halle A.S. Knapp (1895).
- [8]Wedding, H. Stahl und Eisen 9 (1889), pag. 263
- [9]Heyn, E. Mitt. MaterialPrüfungsamt 24 (1906), pag.253
- [10]Le Chatelier, H. Rev. Metall. Mém. 2 (1905), pags. 528-537
- [11]Stead, I.E. Metallographist 3 (1900), pag.220
- [12]Ischewsky, W. Stahl und Eisen 23 (1903), pag. 120. <https://www.amazon.com.mx/Stahl-Eisen-1903-Vol-Eisenh%C3%BCttenwesen/dp/0666575797>
- [13]Kourbatoff, Rev. Metals Handbook, American Society for Metals 8, (1973). U.S.A, pags. 143-146. http://bibliotecadigital.ilce.edu.mx/sites/ciencia/volumen2/ciencia3/080/htm/sec_11.htm
- [14]Robert F. Mehl. Metals Handbook, American Society for Metals 7: (1973). U.S.A, pags. 8, 9, 283, 287. <https://www.amazon.com/-/es/Taylor-Lyman/dp/B0013ET3QO>
- [15] (1) ASM International, 2004. ASM HANDBOOK VOLUME 9 Metallography and Microstructures. 10^a ed. USA: ASM Handbook Committee. https://www.asminternational.org/bestsellers/-/journal_content/56/10192/06044G/PUBLICATION
- [16] (2) Askeland, D.R. & Phulé, P.P., 2004. Ciencia e ingeniería de los materiales. 4^a ed. International Thompson editores, S.A. <https://www.scribd.com/document/437777380/Ciencia-e-Ingenieria-de-Los-Materiales-4a-Ed>
- [17] (3) Callister, W.D., 2007. Materials science and engineering: an introduction. 7^a ed. USA: Jhon Wiley & Sons, Inc. <https://catatanabimanyu.files.wordpress.com/2011/09/callister-7th-edition.pdf>
- [18] Xavier-Celestino, H., Suárez-Torres, L., & Fernández-Columbié, T. (2022). Cuantificación de los microconstituyentes o fases metalográficas de un acero ASTM A 36 soldado con electrodo revestido. *Ciencia & Futuro*, 12(2), 208-224. http://revista.ismm.edu.cu/index.php/revista_estudiantil/article/view/2173
- [19] Paucar, J. C. Q., Pérez, R. G. M., Pérez, E. P. A., & Silva, C. F. C. (2022). Evaluación del PWHT en el acero ASTM A743 mediante el análisis de datos de microdureza y metalografía. *Alfa Publicaciones*, 4(3), 6-21. <https://alfapublicaciones.com/index.php/alfapublicaciones/article/view/220/631>
- [20]Rodríguez Pérez, M., Cruz Crespo, A., & Mesa Álvarez, A. L. (2022). EFECTO DEL PRECALENTAMIENTO SOBRE LA MICROSTRUCTURA Y DUREZA DEL RECARGUE DE MARTILLOS DESMENUZADORES CON ELECTRODOS AWS E FeCr-A1. *Centro Azúcar*, 49(1), 13-20. <http://scielo.sld.cu/pdf/caz/v49n1/2223-4861-caz-49-01-13.pdf>

Chapter 9 Obtaining Process of Zinc Oxide (ZnO) in laboratory with Evaporation and Thermal Oxidation

Capítulo 9 Proceso de Obtención de material Óxido de Zinc (ZnO) en laboratorio con Evaporación y Oxidación Térmica

MASTACHE-MASTACHE, Jorge Edmundo^{1,2,3,†*}, LÓPEZ-RAMÍREZ, Roberto², VIGUERAS-SANTIAGO, Enrique¹ and HERMENEGILDO-MEJÍA, Francisco Javier²

¹Univerisidad Autónoma del Estado de México, Laboratorio de Investigación y Desarrollo de Materiales Avanzados (LIDMA), Facultad de Química, km 14.5 Carretera Toluca-Atlacomulco, C.P. 50200, Estado de México, México

²Tecnológico de Estudios Superiores de Jocotitlán, División de Ingeniería Mecatrónica, Carretera Toluca-Atlacomulco KM 44.8 Ejido de San Juan y, San Agustín, C.P. 50700, Jocotitlán, Estado de México, México

³Universidad de Ixtlahuaca, Facultad de Ingeniería, Ixtlahuaca Jiquipilco, San Pedro, C.P. 50740 Ixtlahuaca de Rayón, Estado de México, México

ID 1st Author: *Jorge Edmundo, Mastache-Mastache* / **ORC ID:** 0000-0001-6104-6764, **CVU CONACYT ID:** 544943

ID 1st Co-author: *Roberto, López Ramírez* / **ORC ID:** 0000-0001-8341-3684, **CVU CONACYT ID:** 233228

ID 2nd Co-author: *Enrique, Viguera-Santiago* / **ORC ID:** 0000-0001-9403-8808, **CVU CONACYT ID:** 25387

ID 3rd Co-author: *Francisco Javier, Hermenegildo-Mejía* / **ORC ID:** 0000-0002-7319-3582

DOI: 10.35429/H.2022.3.130.143

J. Mastache, R. López, E. Viguera and F. Hermenegildo

*jorge.mastache@tesjo.edu.mx

A. Ledesma (AA.). Science of Technology and Innovation. Handbooks-TII-©ECORFAN-Mexico, 2022.

Abstract

The following project shows the results of experiments related to obtaining zinc (Zn) nanoparticles on glass substrates by the thermal evaporation process in a high-temperature tubular furnace at 800 ° C, with a flow of 400 sccm of inert gas (Argon) used as carrier gas, to deposit metallic Zn particles in the cold zone of the furnace, likewise the metallic Zn deposit samples were thermally treated with the intention of being used as a proposed n-type semiconductor material based on metallic oxides, which was formed through the thermal oxidation technique in the same high-temperature tubular furnace at 500°C, with air flow at 600 sccm to form an oxidizing environment and consequently form continuous layers of material Zinc Oxide (ZnO) and be analyzed morphologically with Scanning Electron Microscopy, structurally with X-ray Diffraction and electrically by placing metallic contacts. s to the samples to measure their Current-Voltage curves.

Zinc, Oxide, Evaporation, Oxidation

Resumen

El siguiente proyecto se muestran los resultados de experimentos relacionados con la obtención de nanopartículas de zinc (Zn), sobre substratos de vidrio o alúmina por el proceso de evaporación térmica en un horno tipo tubular de alta temperatura a 800°C, con un flujo de 400 sccm de gas inerte (Argón) utilizado como gas de arrastre, para depositar las partículas de Zn metálico en la zona fría del horno, así mismo se trató térmicamente las muestras de depósito de Zn metálico con la intención de ser utilizadas como una propuesta material semiconductor tipo n basado en óxidos metálicos, el cual fue formado a través de la técnica de Oxidación térmica en el mismo horno tubular de lata temperatura a 500°C, con flujo de aire a 600 sccm para formar un ambiente oxidante y en consecuencia formar capas continuas de material de Óxido de Zinc (ZnO) y ser analizadas morfológicamente con Microscopia electrónica de Barrido, estructuralmente con Difracción de rayos X y eléctricamente colocando contactos metálicos a las muestras para medir sus curvas de Corriente Voltaje.

Zinc, Oxido, Evaporación, Oxidación

1. Introduction

At present we live surrounded by diverse equipment and technological devices, based on different materials, one of the most outstanding being semiconductors, which offer us great advances in the constant development of electronics, leading to the miniaturization of faster and faster devices. and better, without a doubt impacting our quality of life, conventionally the materials used for the design of these devices are silicon and germanium.

A semiconductor is any material that can act as a conductor or insulator depending on the input excitation, such as temperature, luminescence, atomic structure or the electric field, allowing different operating states to be presented, such as the conduction state when switching is allowed. passage of an electrical current or as an insulator preventing the flow of electrical current, used for embedded device applications (Choudhury, 2020).

The process of obtaining these semiconductor materials is conventionally developed with techniques such as the Czochralski Method, photolithography, ion implantation or cathodic sputtering, which involve robust equipment and are carried out in specialized facilities. (Ali, 2020).

This paper deals with the use of metallic oxide materials which can emulate the behavior of conventional semiconductor materials, thanks to their structural defects and can be used as a contribution for future projects in the development of integrated devices with different types of materials. that can be generated in the laboratory with the techniques of evaporation and thermal oxidation (Mikhlif, 2021).

It was chosen to work with metallic oxides due to their easy obtaining and especially zinc oxide (ZnO) due to its N-type electrical characteristics and its wide availability, in order to contribute to the development of materials technology and the introduction of options for work different materials in applications such as semiconductor to nanotechnology, where the synthesis and characterization of micro and nano structures of zinc oxide (ZnO) (Alsultany F. H., 2016).

1.2 Zinc oxide

Metal oxides with structures in the nanometer range have been widely investigated for their potential applications in sectors such as electronics, optics, materials science and the biomedical sector. Among these, zinc oxide (ZnO) is a key material in the industry due to its versatility, high chemical stability, its high electron transport capacity and its optical, electronic, magnetic and mechanical properties derived from nanometric spatial confinement (Dev, 2021). It is a biocompatible and relatively cheap material and can be functionalized, which allows it to expand its potential medical applications. The most common crystalline phase of this material is hexagonal wurtzite and it has a band-gap of 3.37 eV, which makes it suitable for short-wavelength optoelectronic applications. The lack of center of symmetry in this phase of wurtzite (Bakhsheshi-Rad, 2017), in combination with its high electromechanical coupling, it results in strong piezoelectric and pyroelectric properties and consequently its use in a wide range of applications. Much of the applied research has been on dye-sensitized solar cells, piezoelectric nanogenerators, sensors, optoelectronic and emission devices, photocatalysts, actuators in biomedical sciences, energy, and spintronics. Current knowledge of the physical and chemical properties of zinc oxide has not revealed that doping ZnO with rare earths generates new ferromagnetic properties. (Bagga, 2018).

1.3 Thermal Evaporation

Thermal evaporation is a physical vapor deposition (PVD) process, usually in high vacuum (10⁻⁵ torr or higher vacuum values), (Hamelmann, 2016), in which atoms or molecules reach a substrate from a vaporizing heat source without collisions in the deposition chamber. This process is one of the simplest and oldest when it comes to thin film deposition, (Kamalianfar, 2021). The material is placed on a source which is heated by some thermal or electrical process, such as a resistor, high-temperature oven, eddy current, electron beam, laser beam, or arc discharge. The evaporated particles are transported and are deposited on a substrate that normally serves as a support to control the evaporated films (Mora Viquez, 2022). The vapor expands inside the chamber that contains the substrate, and subsequently condenses on the substrate that is kept at a lower temperature (Kumar R. K.-D., 2015). Vacuum evaporation involves thermodynamic considerations, such as phase transitions from which the equilibrium vapor pressure of materials is derived, and kinetic aspects of nucleation and growth. The latter is important in the evolution of the microstructure of the deposited layer. The understanding of the theory of the evaporation process is based on the kinetic theory of gases (Liu, 2018).

1.4 Materials and methods Thermal Evaporation

As the first part of this evaporation process, a commercial bar of zinc (Zn) with a purity of 99.999% was used, from which the target was obtained for thermal evaporation, roughing the bar in a controlled manner to obtain the zinc filings (Zn), for the zinc (Zn) evaporation process, a horizontal tube resistive furnace (CMOD-HAT-1100D25) was also used. To obtain and control the layers of evaporated metallic zinc (Zn), a support such as glass or alumina substrates was used, which were conditioned to adjust to the conditions of the quartz tube.

A quartz tube for the horizontal furnace whose length is 60 cm with a radius of 1 cm and a thickness of 1 mm was used as a reaction chamber for oxidation and thermal evaporation. In addition, 2 lids were printed with 3D printing. the flow of inert gases or air inside the reaction chamber for which they were designed with the help of SolidWorks software and later printed on a 3D printer (Anet A8 open source Prusa i3 3D printer).

The deposition of thin films by thermal evaporation is a technique that complements the thermal oxidation technique to obtain oxides. Zinc (Zn) filings with a purity of 99.999% were used in this deposition process. Zn is also an element of the transition metal family and has a compact Hexagonal structure and a melting point equal to 419.5°C. In this case, the deposition is carried out at a temperature of 800°C with a flow of Industrial Argon gas. This gas, being inert, was used to transport the evaporated white Zinc (Zn) and take it to a lower temperature zone within the reaction chamber, likewise it prevents oxidation due to the effect of temperature.

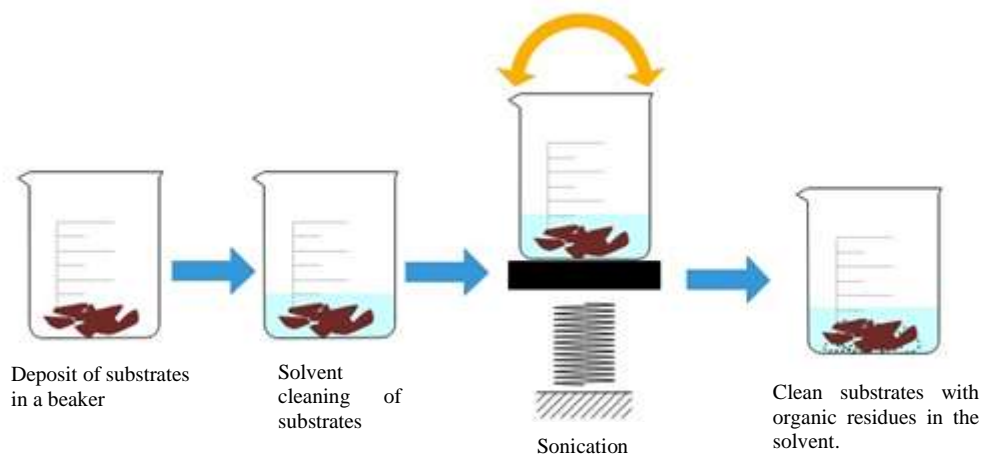
1.4.1 Substrate preparation, washing and degreasing

For this process, a sonicator equipment was used to facilitate the washing of the supports used, with the aim of eliminating organic and inorganic residues that it may have and with this, have surfaces free of parasitic elements. For this, the substrates were washed with three different solvents, which are:

1. Xylene $C_6H_4(CH_3)_2$: colorless and flammable liquid chemical compound, used in the process to remove organic residues from the samples.
2. Acetone $(CH_3)_2CO$: liquid, colorless, flammable and volatile organic compound, used to remove inorganic residues from substrates.
3. Methanol CH_3OH : colorless liquid used to remove xylene and acetone residues in the samples.

The substrates are deposited inside a 50ml glass beaker, in which 20ml of each solvent mentioned above are added, to subsequently sonicate the substrates in the solutions for 15 minutes at a power of 50 watts. At the end of the time, each of the residues of the different solvents were discarded. This process is repeated with each of the solvents; xylene, acetone and methanol respecting the order respectively shown in figure 1.1

Figure 1.1 Substrate preparation



Source of Consultation: Prepared by the work team

1.4.2 Oven preheat

In this step it is necessary to preheat to a temperature of $800^{\circ}C$ and wait until the temperature with the PID controller of the horizontal tube resistive furnace (CMOD-HAT-1100D25) is stable in order to start the thermal evaporation process, in the Figure 1.2 shows the horizontal tube furnace, which has a length of 40 cm, a width of 20 cm and a height of 20 cm.

Figure 1.2 Horizontal Tube Resistive Furnace (CMOD-HAT-1100D25)



Source of Consultation: Prepared by the work team

1.4.3 Preparation of the White of zinc filings (Zn)

In order to carry out the thermal evaporation of Zinc (Zn) it is necessary to obtain the target for evaporation, through a commercial zinc bar filing, in this process 120 mg of zinc (Zn) filings were used, which was deposited on a quartz canoe as shown in figure 1.3 to contain the evaporation target and withstand the evaporation temperature.

Figure 1.3 Zinc (Zn) filings on the quartz canoe

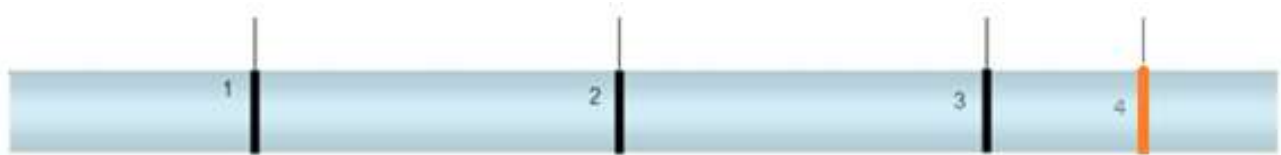


Source of Consultation: Prepared by the work team

1.4.4 Mounting of the zinc blank and substrate on the quartz tube

In this phase, the quartz tube was used that will serve as the reaction chamber, whose dimensions are 60 cm long with a radius of 1 cm and a thickness of 1 mm between the walls, in this tube the zinc filings are introduced (Zn) that was previously deposited on a quartz canoe, until the zone of highest temperature of the tubular furnace to be evaporated, this zinc (Zn) filings must remain in the middle of the quartz tube with the help of a stainless steel rod. In figure 1.4, marks 1 and 3 are shown, which indicate the limit of the walls of the horizontal tube resistive furnace, so the canoe containing the zinc (Zn) filings will be located at mark number 2, while at mark number 4 which is 25 cm from the center of the oven and is where the previously washed and degreased substrate will be placed.

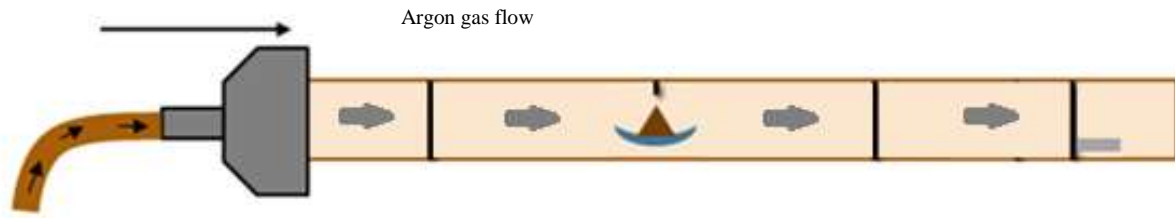
Figure 1.4 Quartz tube with markings for mounting the zinc filings and the substrate



Source of Consultation: Prepared by the work team

1.4.5 Coupling of the lid with the quartz tube

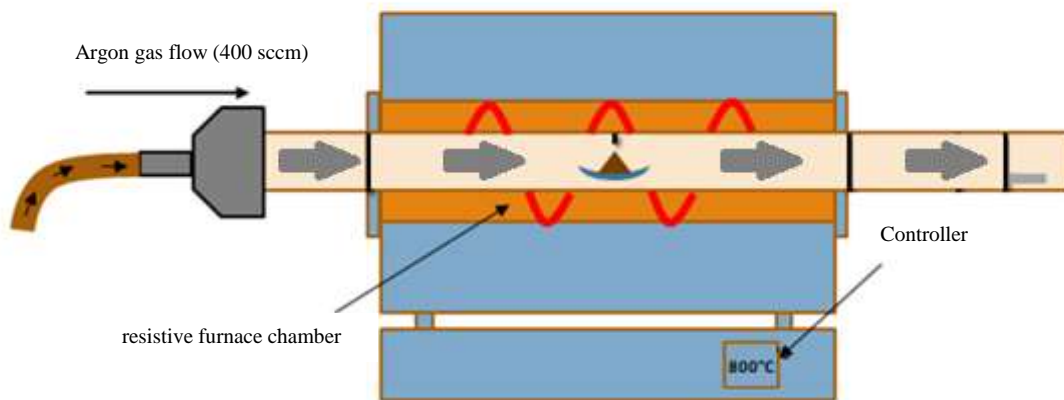
One of the printed covers is placed on the quartz tube at the left end, which has a hole with seals in the center that allows the access of gases to the tube as a chamber and a hose for the supply of carrier gas is placed. In this phase, a hose is connected to the lid coupled to the quartz tube so that it is supplied with argon gas, which is regulated with a flowmeter at 400 sccm as shown in figure 1.5.

Figure 1.5 Carrier gas supply (Argon)

Source of Consultation: Prepared by the work team

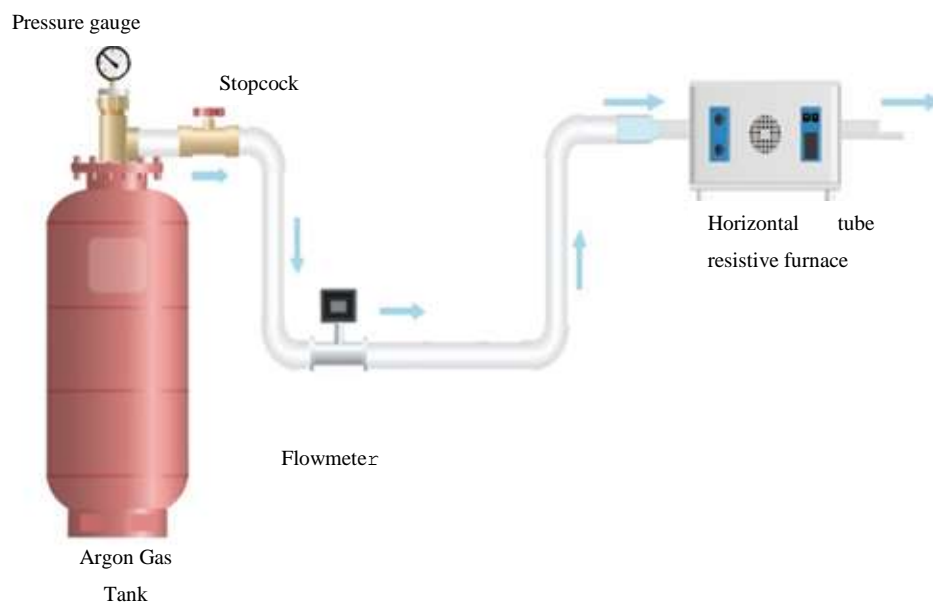
1.4.6 Thermal Evaporation Phase

In this phase, the quartz tube is placed inside the high-temperature resistive furnace with a horizontal tube previously heated to 800°C, and the canoe containing the zinc (Zn) shavings must already be placed inside the quartz tube, as well as the substrate on which the evaporated zinc (Zn) will be deposited, as shown in figure 1.6. Before the quartz tube is placed inside the furnace, the carrier gas (Argon) must already be flowing. Once the quartz tube is placed, the zinc (Zn) thermal evaporation process lasts 30 min with argon gas flow at 400sccm.

Figure 1.6 Thermal evaporation of zinc (Zn)

Source of Consultation: Prepared by the work team

Figure 1.7 schematically shows the interconnected equipment to carry out the thermal evaporation process of zinc, which must be calibrated and monitored by users trained in handling them to avoid wasting supplies or changes in the obtaining process.

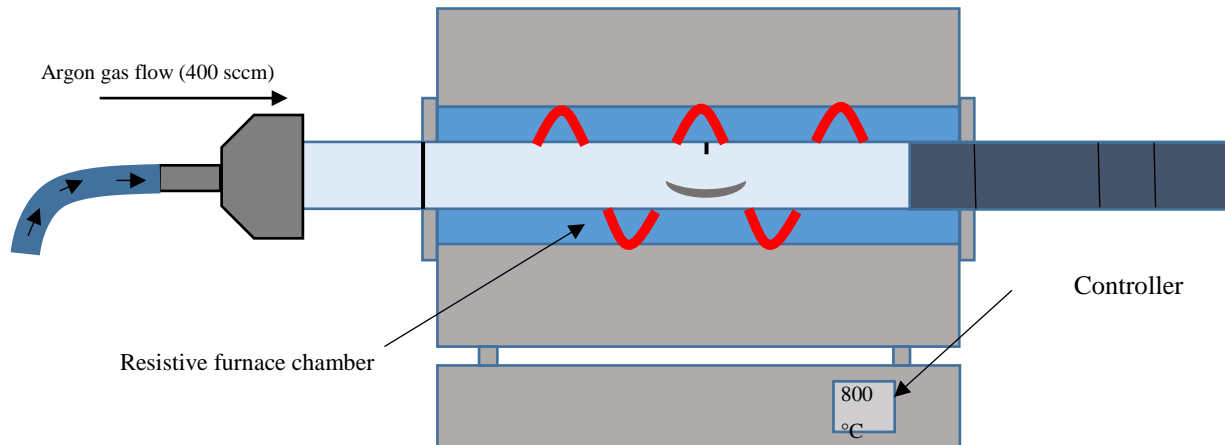
Figure 1.7 Thermal evaporation system for zinc (Zn).

Source of Consultation: Prepared by the work team

1.4.7 Disassembly of the quartz tube

Evaporation inside the quartz tube occurs as the blank is consumed in the flat area of the furnace and the evaporated particles are transported by the carrier gas to a lower temperature area, depositing the material in a metallic form on the walls of the furnace. the camera and at the same time on the previously placed substrate as shown in Figure 1.8. Once the thermal evaporation time is over, the cooling is abrupt, that is, the quartz tube is removed from the horizontal tube resistive furnace, once the quartz tube is out, it is necessary to close the flow of the carrier gas (Argon) and subsequently disassemble the substrate on which the evaporated zinc (Zn) was deposited.

Figure 1.8 Dismantling of the zinc (Zn) thermal evaporation system



Source of Consultation: Prepared by the work teamtrabajo

1.5 Thermal oxidation

Currently there are several proposals on the growth mechanism of the various structures for zinc oxide (ZnO). The vapor-solid mechanism is the most used to understand the formation of these, although the vapor-liquid-solid mechanism is also taken as a basis depending on the temperatures used in the formation of metal oxide. (Kumar R. K.-D., 2015). Reported temperatures for nanostructure formation in the literature range from 400 degrees to 1000 degrees Celsius based on the fact that zinc has a melting point of 420 degrees Celsius and a boiling point of 907 degrees Celsius. Depending on the temperature range used, it is the growth mechanism that tends to be used to explain the formation of the structures. The decomposition of ZnO happens at 1400 degrees, so it does not tend to exceed or reach these temperatures (Płóciennik, 2015).

1.5.1 Materials and methods Thermal Oxidation

For the thermal oxidation of metallic zinc, the same horizontal tube furnace was used to give a thermal treatment to the samples obtained in the evaporation process at 500 ° C for two hours and in the same way the quartz tube was used as a reaction chamber. to produce thermal oxidation and an air compressor was added to the production system to make an air flow flow inside the chamber and thus create an oxidizing environment for obtaining zinc oxide (ZnO).

1.5.2 Oven preheat

For this phase of thermal oxidation it is essential to preheat the horizontal tube resistive furnace to 500°C and wait for the PID controller of the furnace to reach the temperature and be stable to start the thermal oxidation process.

1.5.3 Mounting of the substrate in the quartz tube

In this phase of the process it is necessary to use a quartz tube similar to the one used in thermal evaporation, the tube has a length of 60 cm, a radius of 1 cm and a thickness of 1 mm between its walls, within In this quartz tube, the evaporated zinc sample was placed on the substrate, right in the middle of the tube. A lid was placed on the quartz tube at the left end, which was connected to a hose to supply air and achieve an oxidizing environment inside the reaction chamber and efficient thermal oxidation process, as shown in the figure. 1.9.

Figure 1.9 Mounting of the substrate in the quartz tube

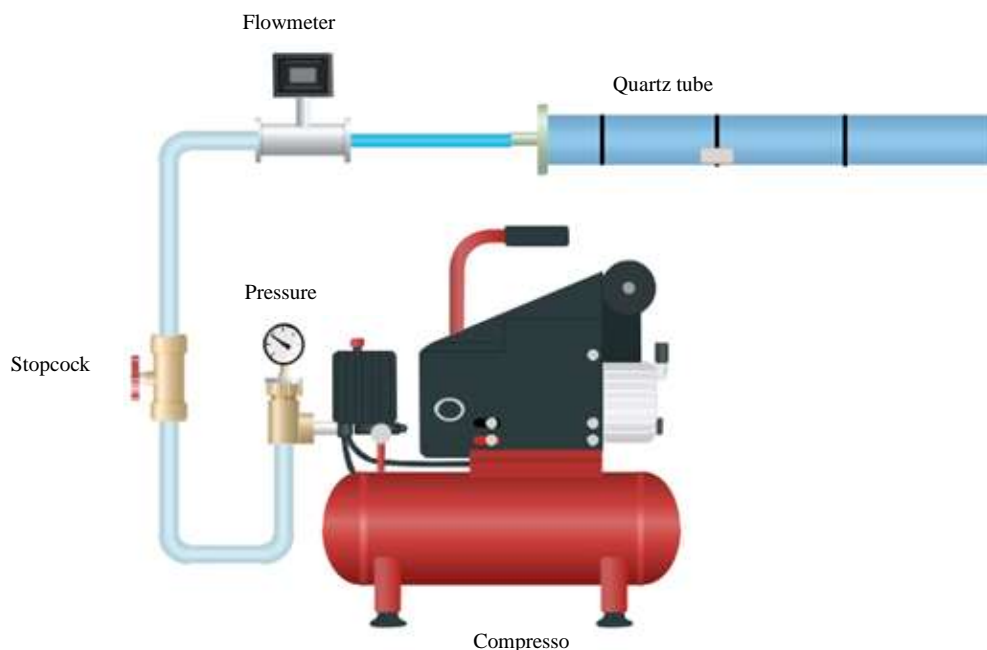


Source of Consultation: Prepared by the work team

1.5.4 Air Supply Coupling

Figure 1.10 schematically shows the interconnected equipment, to carry out the thermal oxidation process of zinc, where a commercial air compressor was incorporated, to maintain a constant flow and favor oxidation inside the chamber, all This equipment must be calibrated and monitored by users trained in handling it to avoid wasting supplies or changes in the procurement process.

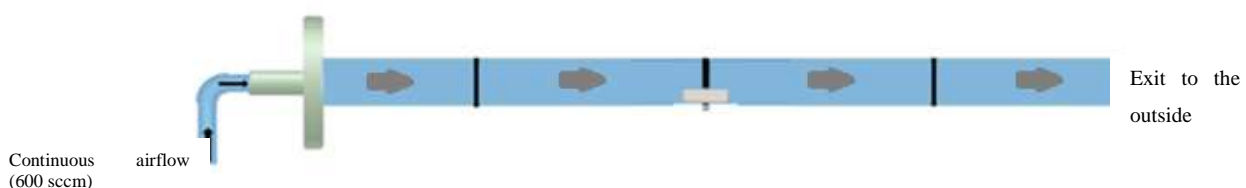
Figure 1.10 Thermal oxidation system of zinc (Zn)



Source of Consultation: Prepared by the work team

What shown in Figure 1.11, a hose is connected to the lid coupled to the quartz tube to be supplied with air, which is regulated with a flowmeter at 600 sccm.

Figure 1.11 Air supply

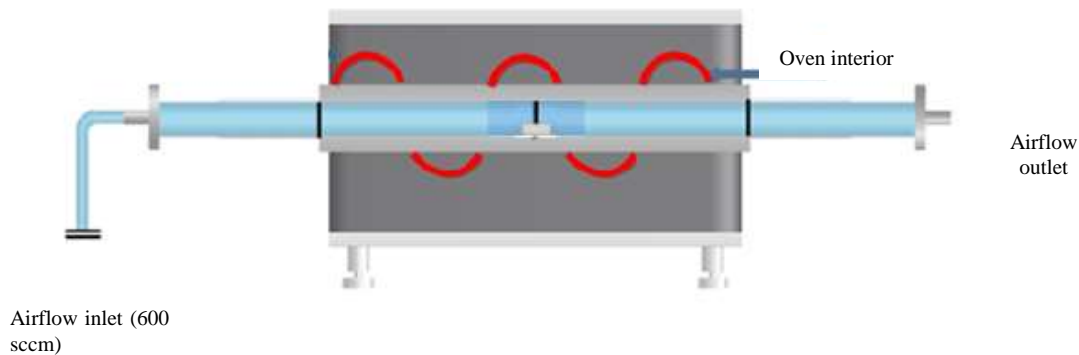


Source of Consultation: Prepared by the work team

1.5.5 Thermal Oxidation Phase

In this phase, the quartz tube is placed inside the horizontal tube resistive furnace previously heated to 500°C, inside the quartz tube the sample obtained in the process of thermal evaporation of zinc (Zn) must already be placed, as shown in Figure 1.12. Before the quartz tube is placed inside the oven, the air supply must already be flowing. Once the quartz tube is placed, the zinc (Zn) thermal oxidation process lasts 2 hours with air flow at 600 sccm. Once the thermal oxidation time is over, the air flow is closed and cooling is natural, that is, the quartz tube is removed from the horizontal tube resistive oven until the oven is at room temperature again once the cooling tube is out. quartz will disassemble the substrate, obtaining as a result the sample of zinc oxide (ZnO).

Figure 1.12 Thermal oxidation process



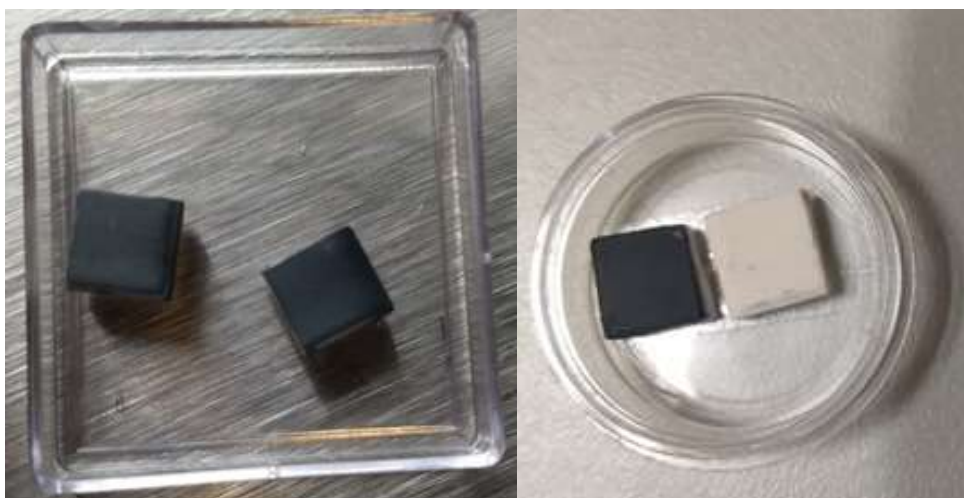
Source of Consultation: Prepared by the work team

1.6 Results

This section explains the results of the samples obtained with the previously described methodologies of evaporation and thermal oxidation, they were used to validate the technical results of characterization such as Scanning Electron Microscopy (SEM or SEM), X-Ray Diffraction Spectroscopy (XRD), characterization I-V, used to characterize oxides as semiconductors.

Figure 1.13 shows the physical results of the application of the methods used to obtain the Zinc Oxide material, where on the left side of the Figure the result of the deposition of the thermal evaporation of metallic Zinc on the substrates is observed. They serve as supports for the formation of the thin layer. On the right side of the Figure, the comparison and application of the second technique used, thermal oxidation, where the sample is observed before the oxidation process exhibits a dark grayish coloration and after thermal oxidation its coloration of the sample changes to whitish, typically as zinc oxide (ZnO) with large amounts of mass is known.

Figure 1.13 Results of the evaporation and thermal oxidation process.



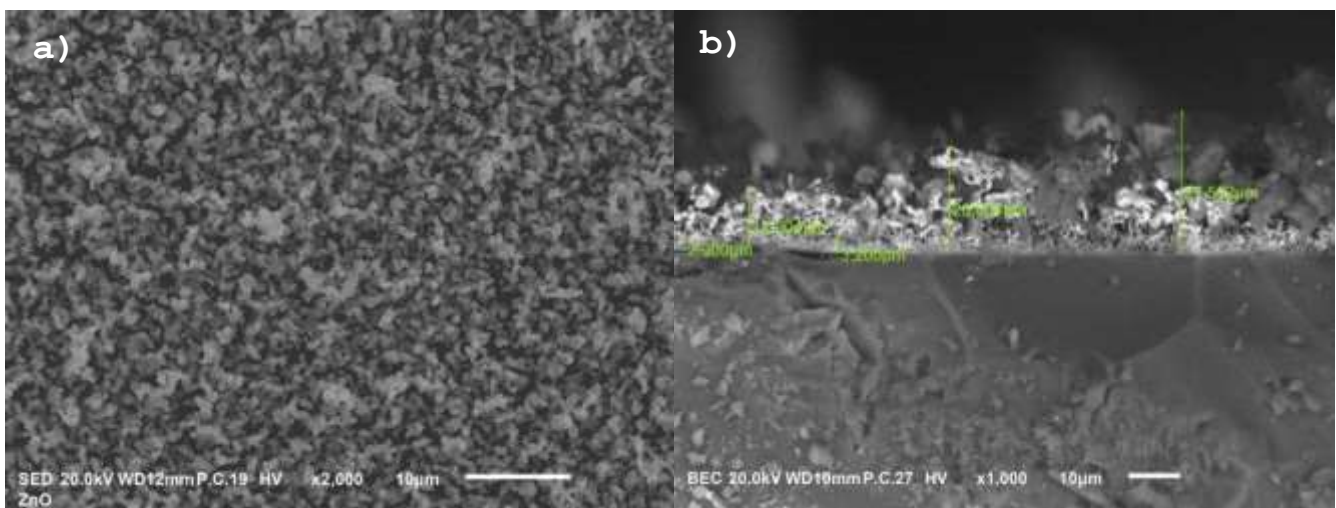
Source of Consultation: Prepared by the work team

1.6.1 Morphological characterization

The first scanning electron microscopy technique SEM for its acronym in English Scanning Electron Microscope, consists of making an electron beam fall on the sample that is analyzed to obtain a detailed image of the sample surface. In this way we can see if the surface is continuous, compact, rough, smooth or porous. Scanning electron microscopy images were obtained with the help of the SEM scanning electron microscope equipment (SEM, JEOL JSM-6510LV).

Figure 1.14 shows a surface and lateral image of the substrate with a thermally treated zinc oxide deposit, the measurement was made at a distance of 10 μm and it is operated with a 20 kV electron beam, with a working distance (WD) 12 mm, in the same way the way in which the ZnO film was formed is observed, which is continuous and grows on the substrate (a). In image (b) a micrograph of one side of the sample was taken to measure the thickness of the film, this micrograph allows us to see that the film has a base layer of 3 μm and from this the structure grows about 30 μm in the thickest edges and 12 μm at the thinnest edges, you can even notice that hexagonal structures begin to form at some points in the film.

Figure 1.14 Morphology (a) and thickness (b) of the film that forms



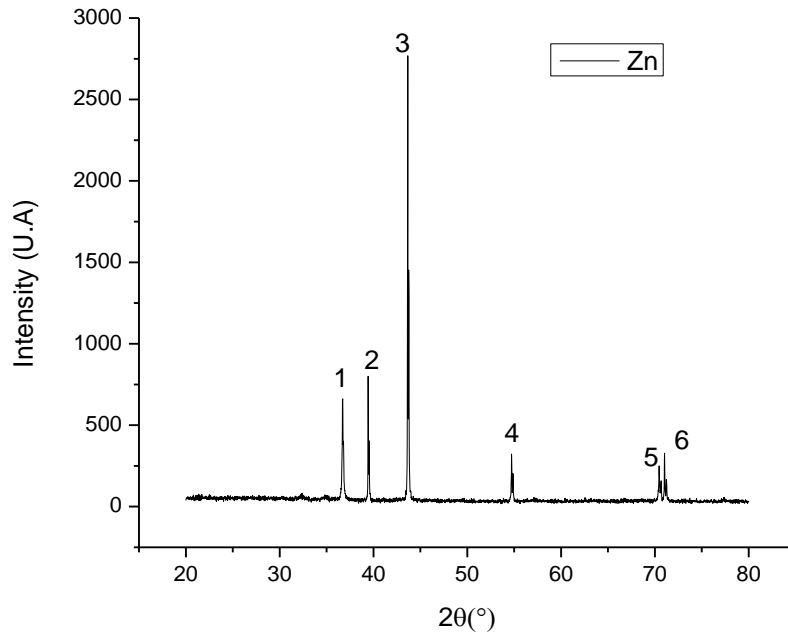
Source of Consultation: Prepared by the work team

1.6.2 Structural characterization

X-Ray Diffraction (XRD) characterization consists of an X-ray beam that penetrates the surface of a sample and is then diffracted by its crystal planes. The characteristic diffraction angle and intensity of a crystalline structure is unique for each material, so X-ray diffraction in polycrystalline samples allows identifying qualitative and quantitative aspects to determine physical and chemical properties (Van Khai, 2018).

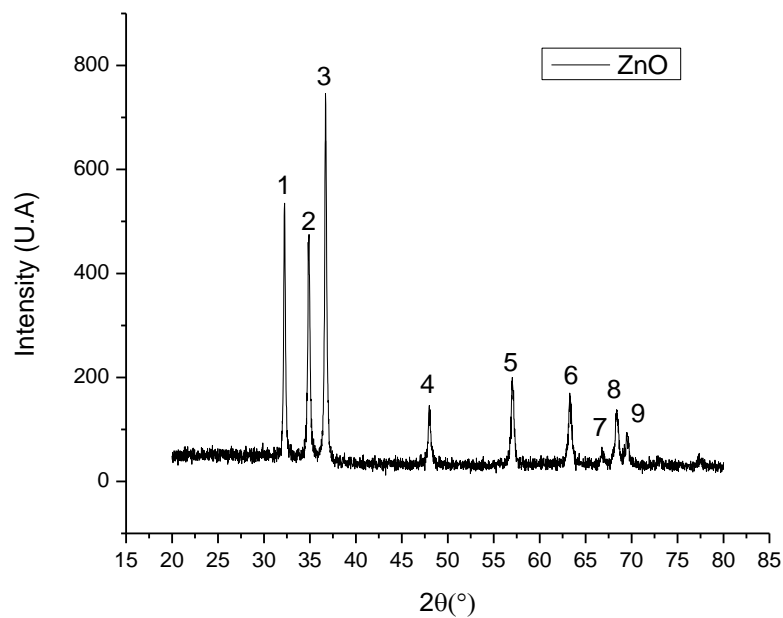
The samples obtained were analyzed before and after the thermal treatment by X-ray diffraction (XRD) with the help of the X-ray diffractometer measurement equipment (XRD, Bruker D8 discover), under the conditions; $\text{CuK}\alpha$ radiation (1.5418 \AA), 40 KV and 40 mA in a 2θ range from 20° to 80° with an increment of 0.0200° and an incidence time of 8s.

Graph 1.1 shows the result before the thermal oxidation process, showing the corresponding peaks of 1-6 at $2\theta = 36.7199^\circ, 39.4400^\circ, 43.6601^\circ, 54.7200^\circ, 54.8801^\circ, 70.4599^\circ, 70.6800^\circ, 71.0400^\circ$ and 71.2402° , which correspond to metallic zinc obtained thanks to thermal evaporation.

Graphic 1.1 Diffractogram of evaporated zinc (Zn)

Source of Consultation: Prepared by the work team

Graph 2 shows the results of the structural characterization once a sample is exposed to the thermal treatment to thermally oxidize, the result after the thermal oxidation process can be seen reflecting in the corresponding diffraction peaks of 1-9 at $2\theta = 32.2464^\circ$, 34.8206° , 34.8999° , 36.700° , 47.9793° , 48.0802° , 56.9834° , 63.2693° , 66.7539° , 68.3710° , 69.4300° , 69.6579° , 72.8738° , 77.3105° , these values were compared with the crystallographic table ZnO from PDF 00-036-1451, therefore, it is confirmed that the sample is only ZnO, where the orientations of the peaks were shown and are shown below peak 1: (1 0 0), peak 2: (0 0 2), Peak 3: (1 0 1), Peak 4: (1 0 2), Peak 5: (1 1 0), Peak 6: (1 0 3), Peak 7: (2 0 0), Peak 8: (2 0 1), peak 9: (2 0 1)

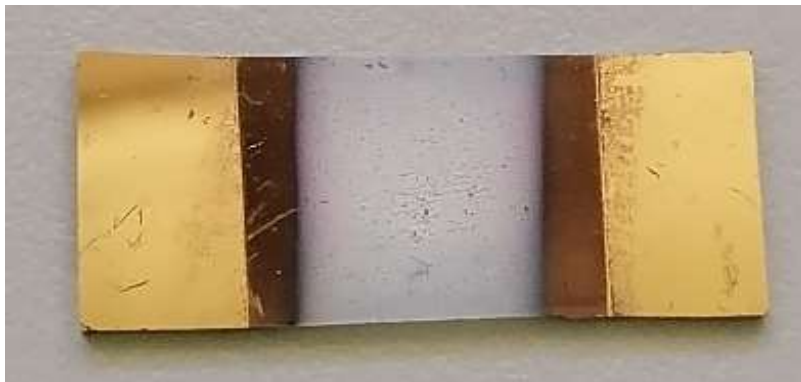
Graphic 1.2 Diffractogram of zinc oxide (Zno)

Source of Consultation: Prepared by the work team

1.6.3 Electrical Characterization I-V

The electrical characterization current and voltage I-V, is used to know the operation of the constructed ZnO device. However, in order to carry out the characterization it is necessary to add electrical contacts to the structure. These contacts must be ohmic, that is, they must offer a low resistance, and must be capable of conducting a current flow in both directions in order to be able to bias both forward and reverse (Van Khai, 2018). I-V characterization also serves to identify whether the junction that forms between the metal and the semiconductor forms an ohmic or rectifying contact. For our zinc oxide (ZnO) samples, it was necessary to add gold (Au) contacts by sputtering with the help of the Agar Auto Sputter Coater (Model.108A) equipment, starting from a 99.995% pure Gold target, a diameter of 57mm and thickness of 0.1mm, with 30 mA of current to generate the arc and a distance of 5 mm from the target to the base, leaving a distance of 1 cm between the gold (Au) contacts that were placed on the gold oxide. zinc (ZnO), as shown in Figure 1.15.

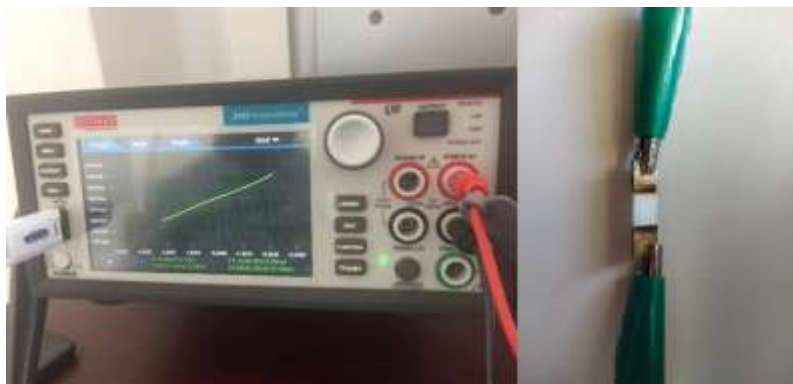
Figure 1.15 Sample of zinc oxide (ZnO) with gold (Au) contacts.



Source of Consultation: Prepared by the work team

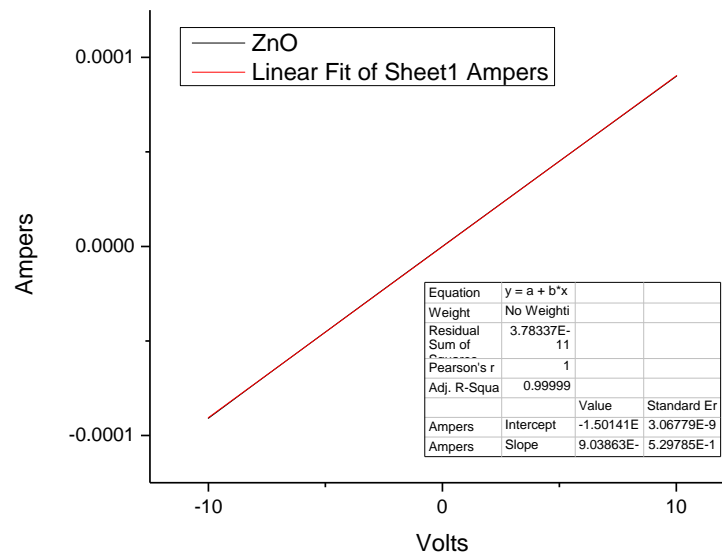
Figure 1.16 shows the electrical measurements made to the Au/Zinc Oxide/Au sample, which were made with the help of a KEITHLEY 2450 source with which a sweep was made in a range of -20 volts to 20 volts. , with a step of 10 mV and a current limit of 500 mA, in order to obtain the characteristic curve of the zinc oxide (ZnO) sample.

Figure 1.16 I-V measurement



Source of Consultation: Prepared by the work team

As shown in the IV curve of graph 1.3, it reflects an ohmic behavior of the sample, which exhibits a linear proportional form in both polarities and has a resistance $R=1.10636 \text{ M}\Omega$ per centimeter of sample, corresponding to zinc oxide. measured.

Graphic 1.3 Characteristic curve of this sample of zinc oxide (ZnO)

Source of Consultation: Prepared by the work team

1.7 Acknowledgments

The authors of this work are grateful for the support provided by the institutions and personnel of the Autonomous University of the State of Mexico, Laboratory for Research and Development of Advanced Materials (LIDMA), the Technological Institute of Higher Studies of Jocotitlán, Division of Mechatronics Engineering and the University from Ixtlahuaca CUI, Faculty of Engineering, who provided space, time, measurements and equipment to develop this product.

1.8 Conclusions

Using the two methodologies, it was possible to obtain controlled layers of Zinc Oxide where the process could be validated, characterizing the samples morphologically, structurally and electrically.

As a relevant fact to obtain metallic Zn films, it is necessary that the deposition is carried out in an inert environment where the carrier gas does not react with the target, in this way the films obtained are continuous and uniform, but porous. The thickness of the zinc (Zn) film is dependent on the gas flow, the distance between the target and the substrate, in addition this same thickness is related to the deposition time to which the sample is exposed, as well as dependent of the amount of Zinc that evaporates in the blank and of the evaporation temperature.

The choice of the electrical contacts that were coupled to the device to characterize it electrically must be ohmic so that the current flows without encountering resistance between the metal and the semiconductor, thus not affecting the I-V measurement.

1.9 References

- Ali, R. S. (2020). Characterization of ZnO Thin Film/p-Si Fabricated by Vacuum Evaporation Method for Solar Cell. *NeuroQuantology*, 1-6. doi:10.14704/nq.2020.18.1.NQ20103
URL: https://uomustansiriyah.edu.iq/media/attachments/221/221_2020_04_27!12_50_08_PM.pdf
- Alsultany, F. H. (2016). Control growth of catalyst-free ZnO tetrapods on glass substrate by thermal evaporation method. *Ceramics International*, 13144-13150. doi:https://doi.org/10.1016/j.ceramint.2016.05.102
URL: <https://www.sciencedirect.com/science/article/pii/S0272884216307118>
- Bagga, S. A. (2018). Synthesis and applications of ZnO nanowire: A review. *Conference Proceedings*, 2-15. doi:https://doi.org/10.1063/1.5047680
URL: <https://aip.scitation.org/doi/abs/10.1063/1.5047680>

- Bakhsheshi-Rad, H. H. (2017). Fabrication and characterisation of novel ZnO/MWCNT duplex coating deposited on Mg alloy by PVD coupled with dip-coating techniques. *Journal of Alloys and Compounds*, 159-168. doi: 10.1016/j.jallcom.2017.08.161
URL:<https://www.sciencedirect.com/science/article/abs/pii/S0925838817328906>
- Choudhury, T. y. (2020). FABRICATION AND CHARACTERIZATION OF Al DOPED ZnO THIN FILM BY PVD TECHNIQUE. *Journal of Advanced Scientific Research*, 403-405. Obtenido de URL:<https://www.sciensage.info/index.php/JASR/article/view/462/365>
- Dev, S. K. (2021). Development of indium doped ZnO thin films for highly sensitive acetylene (C₂H₂) gas sensing. *Superlattices and Microstructures*. doi: 10.1016/j.spmi.2020.106638
URL:<https://www.sciencedirect.com/science/article/abs/pii/S074960362030762X>
- Hamelmann, F. (. (2016). Thin film zinc oxide deposited by CVD and PVD. *En Journal of Physics: Conference Series*. doi:10.1088/1742-6596/764/1/012001
URL:<https://iopscience.iop.org/article/10.1088/1742-6596/764/1/012001/pdf>
- Kamalianfar, A. N. (2021). Hierarchical Sphere-Like ZnO–CuO Grown in a Controlled Boundary Layer for High-Performance H₂S Sensing. *Journal of Electronic Materials volume*, 5168-5176. doi: 10.1007/s11664-021-09005-4 URL:<https://link.springer.com/article/10.1007/s11664-021-09005-4>
- Kumar, R. K.-D. (2015). ZnO nanostructured thin films: Depositions, properties and applications A review. *Materials Express*, 3-23. doi:10.1166/mex.2015.1204
URL:<https://www.ingentaconnect.com/content/asp/me/2015/00000005/00000001/art00002>
- Liu, Y. (2018). Synthesis of AuPd alloy nanoparticles on ZnO nanorod arrays by sputtering for surface enhanced Raman scattering. *Materials Letters*, 26-28. doi:10.1016/j.matlet.2018.04.080
URL:<https://www.sciencedirect.com/science/article/abs/pii/S0167577X18306748>
- Mikhliif, H. D. (2021). Preparation of High-Performance Room Temperature ZnO Nanostructures Gas Sensor. *Acta Physica Polonica, A.*, 140 (4). doi: 10.12693/APhysPolA.140.320
URL:<http://przyrbwn.icm.edu.pl/APP/PDF/140/app140z4p06.pdf>
- Mora Viquez, J. R. (s.f.). Degradación fotocatalítica de RhB utilizando estructuras 1D de ZnO/Ce sintetizadas por el método de vapor sólido. URL:<https://repositorioinstitucional.buap.mx/handle/20.500.12371/16092>
- Plóciennik, P. Z. (2015). Estudio de película delgada de ZnO depositada por PVD. *2015 17th International Conference on Transparent Optical Networks (ICTON)*, 1-3. doi: 10.1109/ICTON.2015.7193661 URL:<https://ieeexplore.ieee.org/abstract/document/7193661>
- Van Khai, T. T. (2018). Structural, optical and gas sensing properties of vertically well-aligned ZnO nanowires grown on graphene/Si substrate by thermal evaporation method. *Materials Characterization*, 296-317. doi: 10.1016/j.matchar.2018.04.047
URL:<https://www.sciencedirect.com/science/article/abs/pii/S1044580317333594>

Chapter 10 Sensitivity analysis of ethanol production process using Aspen Plus

Capítulo 10 Análisis de sensibilidad del proceso de producción de etanol utilizando Aspen Plus

SÁNCHEZ-OROZCO, Raymundo†*, BERNAL-MARTÍNEZ, Lina Agustina and SALAZAR-PERALTA Araceli

Tecnológico de Estudios Superiores de Jocotitlán, Carretera Toluca-Atlacomulco Km 44.8, Ejido de San Juan y San Agustín, C.P. 50700, Jocotitlán, México

ID 1st Author: *Raymundo, Sánchez-Orozco* / **ORC ID:** 0000-0003-0006-1711, **CVU CONACYT ID:** 169684

ID 1st Co-author: *Lina-Agustina, Bernal-Martínez* / **ORC ID:** 0000-0002-4922-043X, **CVU CONACYT ID:** 173701

ID 2nd Co-author: *Araceli, Salazar-Peralta* / **ORC ID:** 0000-0001-5861-3748, **CVU CONACYT ID:** 300357

DOI: 10.35429/H.2022.3.144.160

R. Sánchez, L. Bernal, and A. Salazar

*r.sanchez@tesjo.edu.mx

A. Ledesma (AA.). Science of Technology and Innovation. Handbooks-TII-©ECORFAN-Mexico, 2022.

Abstract

In this work, a sustainable process for the production of ethanol from the monosaccharide glucose was simulated. The thermodynamic model used for the process was NRTL-RK (based on activity coefficients) due to the polar nature and non-ideal behavior of the species involved. The process was carried out in three steps. First, glucose in aqueous solution was subjected to a fermentation process using a stoichiometric reactor. The second stage consisted of carbon dioxide degassing using two flash tank systems. In the third stage, a RadFrac distillation column was used to facilitate the separation of ethanol and water. According to the results obtained, the molar flow rate of the distilled product stream was 5.04 kmol/h with a composition of 82.15% mol of ethanol, 15.37% mol of water and 2.47% mol of carbon dioxide, while the bottom stream whose molar flow rate was 143.39 kmol/h had a composition of 99.99% mol of water with traces of ethanol and carbon dioxide. The results obtained demonstrate that ethanol production from glucose is possible.

Bioethanol, Simulation, Sustainable

Resumen

En este trabajo, se simuló un proceso sostenible para la producción de etanol a partir del monosacárido glucosa. El modelo termodinámico utilizado para el proceso fue NRTL-RK (basado en coeficientes de actividad) debido a la naturaleza polar y al comportamiento no ideal de las especies involucradas. El proceso se llevó a cabo en tres etapas. En primer lugar, la glucosa en solución acuosa se sometió a un proceso de fermentación utilizando un reactor estequiométrico. La segunda etapa consistió en la desgasificación de dióxido de carbono utilizando dos sistemas de tanques flash. En la tercera etapa, se utilizó una columna de destilación RadFrac para facilitar la separación de etanol y agua. De acuerdo con los resultados obtenidos, el caudal molar de la corriente de producto destilado fue de 5.04 kmol/h con una composición de 82.15% mol de etanol, 15.37% mol de agua y 2.47% mol de dióxido de carbono, mientras que la corriente inferior cuyo caudal molar fue de 143.39 kmol/h tuvo una composición de 99.99% mol de agua con trazas de etanol y dióxido de carbono. Los resultados obtenidos demuestran que la producción de etanol a partir de glucosa es posible.

Bioetanol, Simulación, Sustentable

1. Introduction

Chemical compounds of renewable origin are coming to the forefront with the purpose of reducing pressure on oil reserves and above all, due to the lower environmental impacts caused compared to their fossil counterparts (Alio et al., 2019; Cardona et al., 2018; Kim et al., 2017). This trend is occurring as a result of several factors influencing human life and the economy worldwide: climate change, unstable oil prices, the search for alternative chemical sources, and the vision of ensuring security of energy supply due to ever-increasing global demand. However, stand-alone bioprocesses can present high operational costs, which can be reduced by process integration with a consolidated facility (Olofsson et al., 2017; Zhou et al., 2018; Sharma et al., 2020). In order to meet these supply needs while providing an economically viable option, the concept of biorefinery production was created (Abdou et al., 2020; Battista et al., 2019; Gil et al., 2014; Li et al., 2016; Morales et al., 2017; Morales et al., 2021).

In biorefineries, a number of different processes are used to fractionate biomass into various products, as in petroleum refineries, but working with a different and renewable feedstock. The purpose is also very similar to that of a petroleum refinery: to produce compounds for both the chemical industry and the fuel market (Tan et al., 2020; Zabed et al., 2016; Singh et al., 2017; Rodrigues et al., 2018; Kumar and Singh, 2016). Bioethanol, the most widespread chemical and fuel derived from renewable sources, has a consolidated market in the world and a large share in the Brazilian fuel market.

Bioethanol is one of the most promising alternative fuels to reduce fossil fuel consumption in the transportation sector (Kim et al., 2016; Isikgor and Becer, 2015; Chrysikou et al., 2018; Chandel et al., 2018). The economic viability of the bioethanol industry depends on a sufficient supply of high-quality, low-cost, bio-based renewable feedstocks and efficient biomass-to-bioethanol conversion technologies.

Consequently, biofuels, especially of the second generation, have gained great interest in the view of current environmental problems and oil dependence (Chin et al., 2020; Borand and Karaosmanoglu, 2018; Ardila et al., 2014; Bahry et al., 2017). Bioethanol used for commercial purposes is generally produced from edible feedstocks such as corn and sugarcane, which increases the cost of production. The high cost of these feedstocks is the driving force behind the search for second and third generation bioethanol produced from cheaper and more readily available feedstocks.

When bioethanol is produced from edible feedstocks such as corn and sugarcane, it is called first generation (1G) bioethanol and second generation (2G) 2G bioethanol if the feedstock is lignocellulose (Ashraf and Schmidt, 2018; Brown, 2015; Choi et al., 2019; Daylan and Ciliz, 2016). Examples of lignocellulosic biomass include corn stalks, wood, herbaceous crops, waste paper and paper products, agricultural and forestry residues, pulp and paper mill waste, municipal solid waste, and food industry waste. Lignocellulosic biomass consists of cellulose, hemicellulose, lignin, protein, ash and minor extractives (Hoang et al., 2020; Gnansounou and Dauriat, 2010; Vieira et al., 2020; Sarks et al., 2014; García-Velásquez et al., 2019). Lignocellulosic sources are the most promising feedstocks, have the highest potential and constitute an important part of most future emissions scenarios consistent with stringent climate change mitigation targets (Romaní et al., 2019; Tan et al., 2016; Zabed et al., 2017; Zhang et al., 2016; Devarapalli et al., 2017). Lignocellulosic feedstocks include woody (softwood and hardwood) and herbaceous (perennial grasses) energy crops, agricultural residues (cereal straw, stubble and bagasse), forest residues (sawdust, pruning and bark residues) and organic portions of municipal solid waste (Abdou et al., 2020; Cardona et al., 2018; Gil et al., 2014). Bioethanol production from lignocellulosic biomass materials typically has lower life-cycle greenhouse gas (GHG) emissions and lower risks to compete with food security than bioethanol production from food crops (Li et al., 2016; García-Velásquez et al., 2019).

Lignocellulosic biomass is being considered as a feedstock for bioethanol production due to the relatively low cost of acquisition, availability and sustainability of supply. 2G bioethanol has a greater potential to reduce greenhouse gas emissions compared to 1G bioethanol. Third generation (3G) bioethanol is obtained when algae are used as feedstock (Morales et al., 2021; Oliva et al., 2020). Algae bioethanol is possibly gaining ground due to the high carbohydrate content and the absence of lignin in most of the available algae. Despite efforts to reduce the cost of production by using various non-edible materials, the cost of processing the feedstock is still very high, making bioethanol uncompetitive with conventional gasoline (Romaní et al., 2019; Zhou et al., 2018). Life cycle assessment and techno-economic analyses are generally performed to evaluate the economic feasibility and environmental impact of bioethanol production processes (Cardona et al., 2018; Ardila et al., 2014; Hoang et al., 2020).

The chemical industry has long employed simulation strategies to design and optimize process operations. Initially simple models of unit operations (using multiple assumptions and simplifications to facilitate calculations) that could be solved by hand or mechanical calculators were employed, and later evolved to more sophisticated and rigorous models that can only be solved by computers (Nosrati-Ghods et al., 2020; Gil et al., 2014). The importance of computers in this context is that simplifying assumptions are no longer needed to facilitate computations. In addition, computers solve the operations of process units, so connecting several process streams (complete with recycles) and having the computer repeat the calculations until the matter and energy balances are balanced is relatively easy. Thus sequential modular process simulation for complete flowsheets was born (Gabhane and Kapoor, 2019).

Currently, the integration of simulation tools in process development is often used to analyze economic feasibility, performance, optimization and parameter estimation; therefore, it facilitates equipment design, sizing and cost evaluation (Daylan and Ciliz, 2016). Chemical process simulation provides unbiased material/energy data of production processes with reduced time and resource utilization for data collection (Gil et al., 2014). Simulations have the flexibility of effective process data predictions based on appropriate thermodynamic properties, design parameters, and actual plant conditions for individual plant designs. In addition, pre-production/modification process plants can be easily predicted using simulations to integrate/modify different alternative scenarios (Gabhane and Kapoor, 2019). For example, additions of new materials, technologies and recycling options in different processes can be easily realized, to evaluate their benefits and plan decisions for the industry (Chandel et al., 2018).

Several studies have been conducted to obtain ethanol from sugarcane juice (Vieira et al., 2020). It has also been reported that the use of this raw material represents 40% of the total cost of ethanol production and that this cost decreases when using sugarcane bagasse. However, the main limitation is the high degree of complexity associated with its processing and even more with its simulation.

In this work, the production of ethanol from glucose was simulated using Aspen Plus® version 11. The NRTL-RK thermodynamic model was used. The process was carried out in three stages, first, a fermentation process using a stoichiometric reactor. The second stage consisted of carbon dioxide degassing through flash tanks and finally, in the third stage, distillation in a RadFrac column to promote the separation of ethanol and water.

2. Methodology

2.1 General description of the process

For the design and simulation of the ethanol production process, a fermenter (FERM) was fed sugar (GLUCOSE in aqueous solution) along with yeast to produce ethanol and CO₂ as a by-product. The fermenter product was processed in two degassing stages (DEGAS1 and DEGAS2) to remove most of the CO₂ produced. The liquid product was fed to a RadFrac distillation column (COL1) to remove water and concentrate the ethanol. In the fermentation section for the transformation of glucose to ethanol, an aqueous glucose solution was fed to a fermenter along with an additional water stream to control the concentration. The fermenter product was degassed in a single-stage separator to remove most of the CO₂ produced by the fermentation process. The liquid product from the separator was pumped to a heater where it exchanged heat with the bottoms of the ethanol column prior to being fed to a second degassing tank. Additional CO₂ was removed in the second separator and the resulting liquid product was fed to the ethanol distillation column. The ethanol column removed most of the water in the bottom stream, concentrating the ethanol in the distillate. The distillation column, equipped with 38 stages, a reboiler and a total condenser, operated at a pressure of 50 psig. The distillate-to-feed column ratio specification was adjusted to maintain the ethanol purity specification in the column bottoms product. The specifications needed to construct the flowsheet are provided in Tables 1.1, Table 1.2 and Table 1.3.

Table 1.1 Component data and method of ownership

	ID	Type	Formula	Name
List of components	ETOH	CONV	C2H2O-2	ETHANOL
	WATER	CONV	H2O	WATER
	GLUCOSE	CONV	C6H12O6	DEXTROSE
	CO ₂	CONV	CO2	CARBON DIOXIDE
Method of ownership	NRTL-RK			
Henry's components	CO ₂			
Binary data	NRTL and Henry's binary forms			

Source: Own Elaboration

Table 1.2 Parameters of the feed streams

Parameter	Units	FERMFEED	H2OFEED
Mass flow			
GLUCOSE	kg/h	380	
WATER	kg/h	1150	
Temperature	°C	27	
Pressure	bar	2.5	
Mass fraction			
WATER			1
Temperature	°C		27
Pressure	bar		2.5
Mass flow	kg/h		1450

Source: Own Elaboration

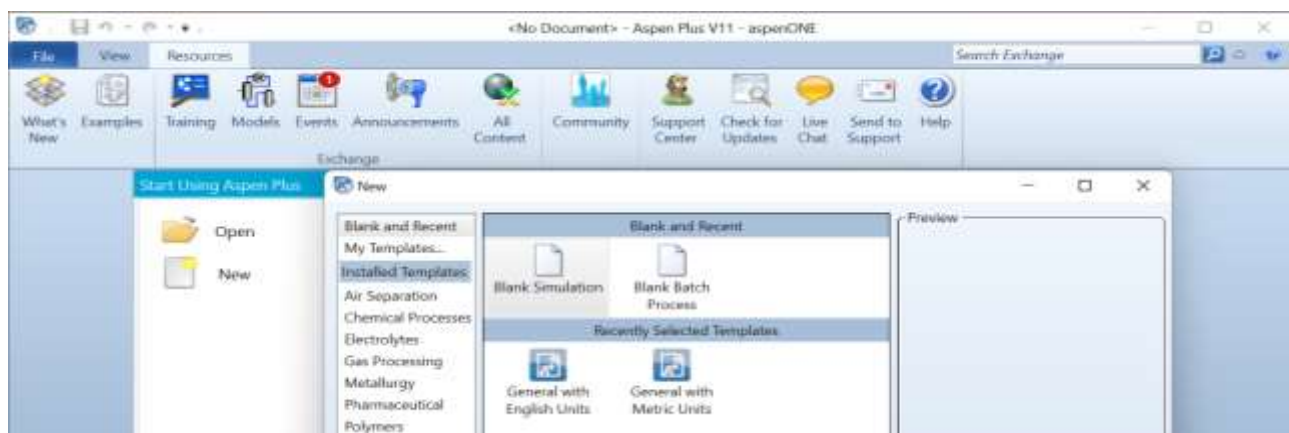
Table 1.3 Operating conditions of the process equipment

Process equipment	Units	Parameter and/or value
FERM		
Temperature	°C	32
Pressure drop	bar	0
Reaction		GLUCOSE → 2ETHANOL + 2CO ₂
Reaction conversion		1.0, key component: GLUCOSE
DEGAS1		
Pressure drop	bar	0
Heat requirement	cal/h	0
PUMP		
Increased pressure	bar	7
PREHEAT		
Calculation method		Short
Difference hot outlet-cold inlet	°F	10
DEGAS2		
Pressure drop	bar	0
Heat requirements	cal/h	0
COL1		
Number of stages		40 (including condenser and reboiler)
Condenser type		Total
Type of reboiler		Kettle
Convergence method		strongly non-ideal liquid
Reflux ratio		30
Distillate-to-food ratio		0.034
Column feed stage		30 (top stage)
Top stage pressure	bar	5

Source: Own Elaboration

2.2 Process modeling with Aspen Plus

To start the program and to perform a new simulation, it was necessary to select the New option in Figure 1.1, belonging to the Aspen Plus V11 program of the aspenONE® package, then click on Blank Simulation and then on Create.

Figure 1.1 Aspen Plus V11 home page

Source: Own Elaboration

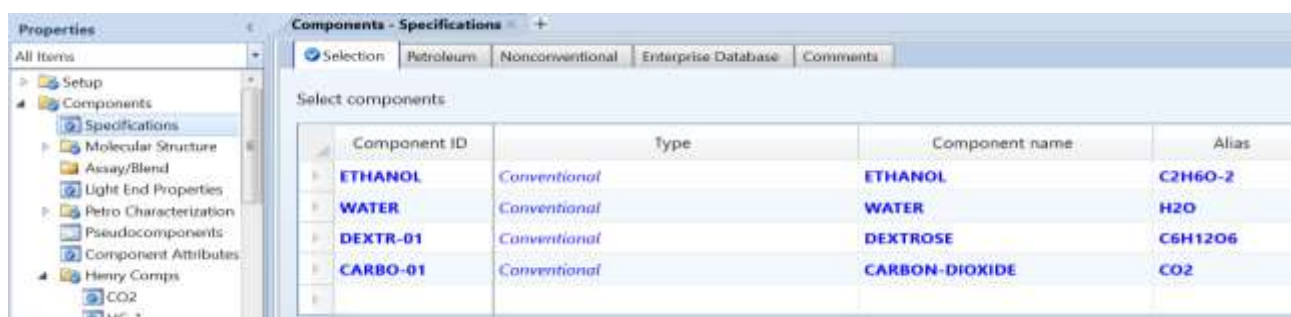
2.3 Specification of chemical components

The first step in preparing the process simulation was to establish the chemical basis for the model. This consisted of choosing the components to be included in the material balance and deciding which model to use for the prediction of physical properties and phase equilibrium. The program has an extensive list of components with their properties, and it was sufficient to select them (Figure 1.2). The components were chosen by double-clicking on them, or by highlighting the component and clicking on Add selected compounds. The name of each compound could also be typed directly into the corresponding boxes. Once all the compounds were selected, the thermodynamic model was defined.

2.4 Selection of the thermodynamic model

Once the components were specified, the thermodynamic model was chosen. This model was used to calculate the thermodynamic and transport properties of the components and their mixtures, such as enthalpy, entropy, density, specific heat, L-V equilibrium, etc. Therefore, the correct selection of the model was very important (Figure 1.3). In general, properties were calculated with equations of state (EOS), activity coefficient models (γ models) and special models (theoretical, empirical or hybrid correlations). The EOS models represented the liquid and vapor phases, while the gamma models represented only the liquid phase of the system. For this reason, they are used in conjunction with an equation of state to represent the vapor. Once the property specifications were completed, the property prediction by the proposed model was analyzed to ensure correct results. This was done using the Property Analysis function of Aspen Plus. The property analysis generated tables of physical property values, which were used to better visualize and understand the behavior of the properties as predicted by the property specifications.

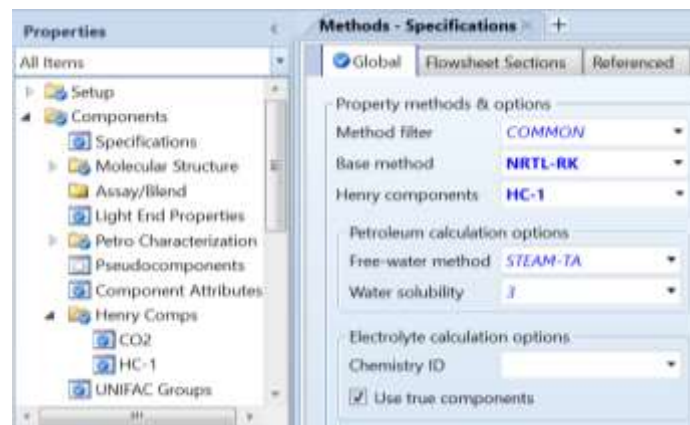
Figure 1.2 Component specification from the database



Component ID	Type	Component name	Alias
ETHANOL	Conventional	ETHANOL	C2H6O-2
WATER	Conventional	WATER	H2O
DEXTR-01	Conventional	DEXTROSE	C6H12O6
CARBO-01	Conventional	CARBON-DIOXIDE	CO2

Source: Own Elaboration

Figure 1.3 Specifications of the method for identifying thermodynamic properties

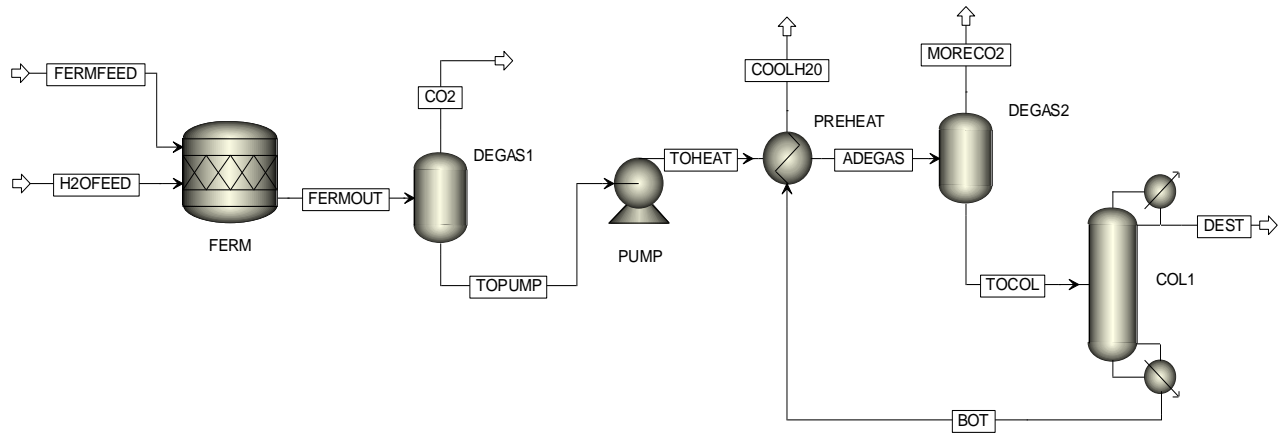


Source: Own Elaboration

2.5 Process flow diagram in Aspen Plus

The stages involved in ethanol production from dextrose included fermentation, gasification, syngas purging and methanol synthesis. The model was built using a general template with units in the metric system, adding the components and selecting the NRTL thermodynamic method (based on activity coefficients) in combination with the Redlich-Wong equation of state (NRTL-RK), and then performing the flow diagram in Aspen Plus as shown in Figure 1.4. Finally, the operating conditions of each process equipment were specified and the simulation was run. When the simulation converged it was possible to access the results through the toolbar in the Stream Summary option.

Figure 1.4 Process flow diagram for ethanol synthesis in Aspen Plus



Source: Own Elaboration

3. Results

3.1. Behavior of the ethanol-water system

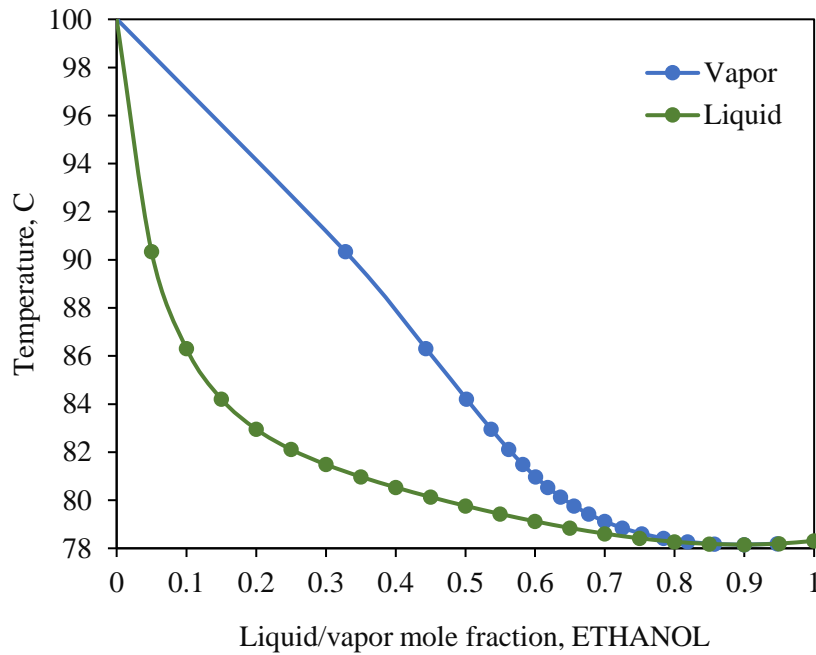
The vapor liquid equilibrium (VLE) curve of the ethanol-water system is shown in Figure 1.5. It can be seen that atmospheric distillation of this mixture is possible only to a certain extent. The maximum purity that can be achieved by atmospheric distillation is 95% by weight, because as soon as the composition reached 95.6% by weight (4.4% by weight of water) the azeotrope was formed. The mixture of ethanol and water forms a positive azeotrope. Ethanol boils at 78.4 °C and water at 100 °C. However, the boiling point of the azeotrope was 78.2 °C, which is lower than its two components.

Generally a positive azeotrope bubbles at a lower temperature than some other proportion of its constituents. For the binary ethanol/water system, 78.2 °C was the base temperature for the mixture to bubble at atmospheric pressure. Positive azeotropes are also known as lower boiling mixtures or minimum boiling azeotropes (Gil et al., 2014). Figure 1.6 shows the x-y plot of liquid equilibrium data generated by regression with the binary interaction parameters of the NRTL-RK thermodynamic model.

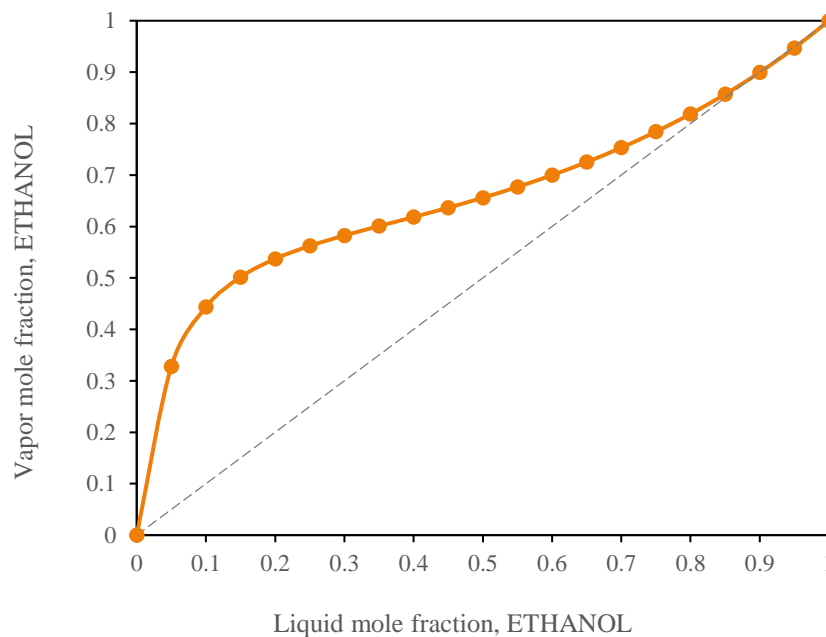
3.2 Composition profiles and molar flows

Figure 1.7 shows the profile of ethanol and water compositions through the distillation column. It can be observed that in stage 1 (condenser) the maximum concentration of ethanol and a small percentage of water was reached due to the azeotropic behavior of the mixture, likewise, it is notable that in stage 40 (boiler) it is almost entirely made up of water, there is only a small fraction of ethanol that was not recovered by the concentrator column. In addition, the liquid phase composition profile showed that the ethanol concentration decreased from stage 30 due to the feed stream.

Thus, also, the observed change in ethanol composition was due to the presence of an azeotrope in the mixture. The ethanol composition increased in the upper stages of the column, while the water composition was concentrated in the bottom stream of the column.

Figure 1.5 T-x-y diagram for ETHANOL/WATER

Source: Own Elaboration

Figure 1.6. x-y diagram for ETHANOL/WATER

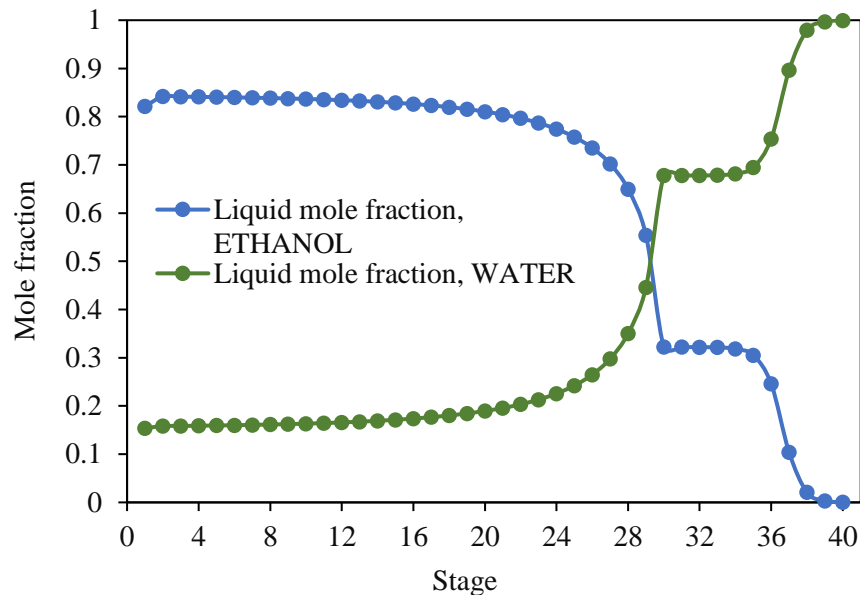
Source: Own Elaboration

The molar flow profiles of the vapor and liquid phases as a function of the number of stages in the distillation column are shown in Figure 1.8. It can be seen that the dilute ethanol feed is introduced starting at stage 30 where it comes in contact with the vapor which is at very high temperature and immediately begins to change phase. It then moves to the condenser where the steam is extracted as condensate and the ethanol mixture as distillate. The significant change in the liquid molar flux is primarily attributed to the feed stream of the azeotropic mixture.

This change was caused by the liquid phase vaporization due to the inlet temperature of water. Meanwhile, the vapor phase molar flux remained constant throughout the column. Moreover, as the distillation progressed, the composition of the distillate became richer in the less volatile component (ethanol), therefore the composition richest in ethanol corresponded to the first drop of distillate obtained. At this point it was also possible to analyze the distillation yield, i.e., when a greater mass of distillate was obtained, the ethanol composition tended to decrease.

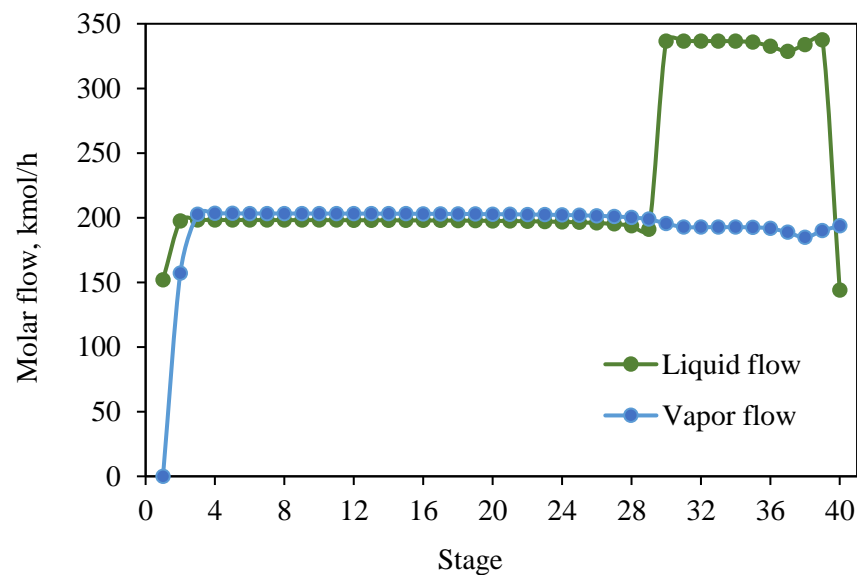
In some processes a purer distillate is required, which is in contrast to the amount that can be obtained. In general, the longer the column and the larger the contact surface within the column, the more effective the separation of the components will be, although it also depends on other factors (Abdou et al., 2020).

Figure 1.7. Profile of compositions in the distillation column for ETHANOL/WATER



Source: Own Elaboration

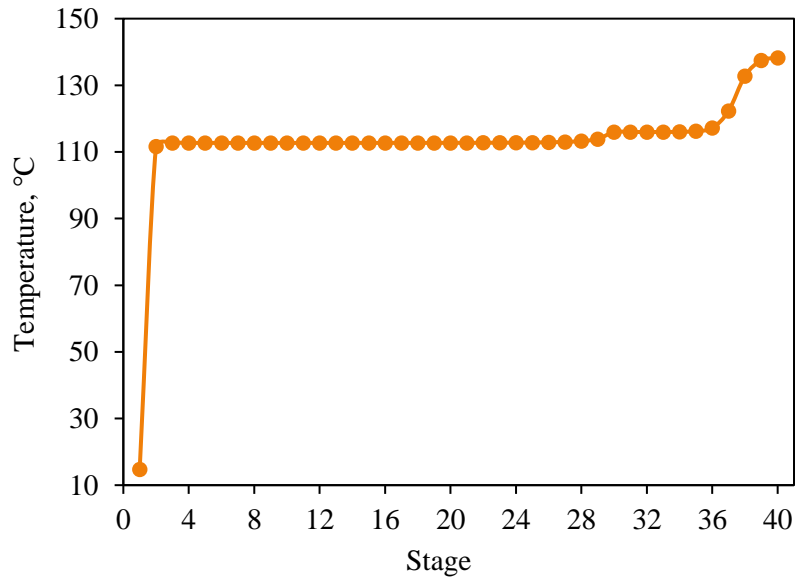
Figure 1.8 Vapor-liquid molar flow profile in the distillation column



Source: Own Elaboration

3.3 Temperature profiles through the distillation column

The behavior of the temperature profile in the column showed changes starting at stage 30 due to the feed stream of the azeotropic mixture. A significant increase in temperature was observed from stages 36 to 40 due to the proximity to the kettle (Figure 1.9). The temperature profile is of great help in controlling the purity of the column products since generally the composition is usually complicated and time consuming to measure, whereas the temperature offered a quick and simple measurement that being related to the composition at each stage of the column facilitates column control.

Figure 1.9 Temperature profile in the distillation column for ETHANOL/WATER

Source: Own Elaboration

3.4 Composition and conditions in process streams

After the simulation, process data such as mass flow, mole fractions of the components, final thermodynamic data, as well as the feed and outlet conditions of the reactor, flash separation tank and distiller were determined. Table 1.4 and Table 1.5 summarize the results according to each process equipment and stream involved. It is observed that the conversion of glucose is total and that the flow at the outlet of the stoichiometric reactor is constituted by 194.34 kg/hr of ethanol, 2600 kg/hr of water and 185.65 kg/hr of carbon dioxide. After this stream passes through the first flash separator, the mass flow of the outlet stream contains 173.09 kg/hr of carbon dioxide, 0.69 kg/hr of ethanol and 0.93 kg/hr of water. Since the gas generated in the fermentation process was not completely eliminated, it was necessary to place a second flash separator to separate the remaining carbon dioxide, which is equivalent to 7.06 kg/h. Subsequently, the mixture of ethanol and water was sent to a distillation column, where it separated the ethanol in the distillate stream and the water in the bottoms stream.

Table 1.4 Overall results of the process simulation (Part 1)

		FERMFEED	H2OFEED	FERMOUT	CO ₂	TOHEAT
Phase		Liquid	Liquid	Liquid	Vapor	Liquid
Temperature	C	27	27	32	25.3547	25.8016
Pressure	bar	2.5	2.5	2.5	2.5	9.5
Mole frac vapor		0	0	0	1	0
Mole frac liquid		1	1	1	0	1
Molar Enthalpy	cal/mol	-75782.6505	-68226.4504	-68934.8065	-93393.2488	-68266.2224
Mass Enthalpy	cal/gm	-3266.2800	-3787.1435	-3533.6950	-2138.0999	-3620.0425
Molar Entropy	cal/mol-K	-46.1415	-38.8489	-39.1185	-1.3066	-40.0025
Mass Entropy	cal/gm-K	-1.9887	-2.1564	-2.0053	-0.0299	-2.1213
Molar density	mol/cc	0.0472	0.0551	0.0504	0.0001	0.0519
Mass density	gm/cc	1.0954	0.9920	0.9833	0.0045	0.9783
Average PM		23.2015	18.0153	19.5079	43.6805	18.8579
Molar flows	kmol/hr	65.9440	80.4872	152.7590	4.0001	148.7589
ETHANOL	kmol/hr	0.0000	0.0000	4.2185	0.0151	4.2034
WATER	kmol/hr	63.8347	80.4872	144.3219	0.0519	144.2701
DEXTR-01	kmol/hr	2.1093	0	0	0	0
CARBO-01	kmol/hr	0	0	4.2185	3.9331	0.2854
Mole fractions						
ETHANOL		0	0	0.0276	0.0038	0.0283
WATER		0.9680	1	0.9448	0.0130	0.9698
DEXTR-01		0.0320	0	0	0	0
CARBO-01		0	0	0.0276	0.9832	0.0019
Mass flows	kg/hr	1530	1450	2980.0000	174.7278	2805.2722
ETHANOL	kg/hr	0	0	194.3435	0.6977	193.6457

WATER	kg/hr	1150	1450	2600	0.9345	2599.0655
DEXTR-01	kg/hr	380	0	0	0	0
CARBO-01	kg/hr	0	0	185.6565	173.0955	12.5611
Mass fractions						
ETHANOL		0	0	0.0652	0.0040	0.0690
WATER		0.7516	1	0.8725	0.0053	0.9265
DEXTR-01		0.2484	0	0	0	0
CARBO-01		0	0	0.0623	0.9907	0.0045
Volumetric flow	L/min	23.2802	24.3609	50.5076	653.5067	47.7908

Source: Own Elaboration

Table 1.5 Overall results of the process simulation (Part 2)

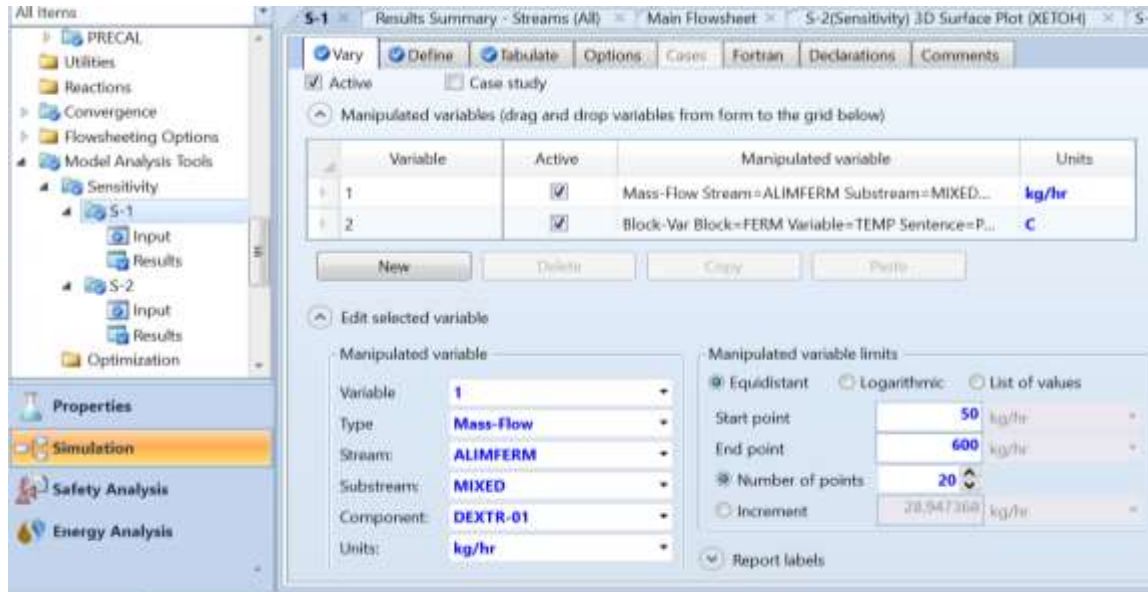
		COOLH2O	MORECO2	TOCOL	DEST	BOT
Phase		Liquid	Vapor	Liquid	Liquid	Liquid
Temperature	C	31.3572	139.4568	139.4568	40.2237	151.8516
Pressure	bar	5	9.5	9.5	5	5
Mole frac vapor		0	1	0	0	0
Mole frac liquid		1	0	1	1	1
Mole frac vapor		0	1	0	0	0
Molar Enthalpy	cal/mol	-68147.9486	-74985.7582	-66037.4053	-66943.8275	-65855.4427
Mass Enthalpy	cal/gm	-3781.9021	-2177.4567	-3508.0010	-1605.1766	-3654.6784
Molar Entropy	cal/mol-K	-38.5986	-9.2021	-33.8624	-72.3739	-32.3353
Mass Entropy	cal/gm-K	-2.1420	-0.2672	-1.7988	-1.7354	-1.7945
Molar density	mol/cc	0.0548	0.0003	0.0455	0.0191	0.0478
Mass density	gm/cc	0.9877	0.0099	0.8564	0.7962	0.8609
Average PM		18.0195	34.4373	18.8248	41.7050	18.0195
Molar flows	kmol/h	143.3968	0.3149	148.4439	5.0471	143.3968
ETHANOL	kmol/h	0.0215	0.0356	4.1677	4.1462	0.0215
WATER	kmol/h	143.3753	0.1188	144.1513	0.7760	143.3753
DEXTR-01	kmol/h	0	0	0	0	0
CARBO-01	kmol/h	0	0.1605	0.1249	0.1249	0.0000
Mole fractions						
ETHANOL		0.0002	0.1132	0.0281	0.8215	0.0002
WATER		0.9998	0.3772	0.9711	0.1537	0.9998
DEXTR-01		0	0	0	0	0
CARBO-01		0	0.5096	0.0008	0.0248	0.0000
Mass flows	kg/h	2583.9375	10.8459	2794.4264	210.4888	2583.9375
ETHANOL	kg/h	0.9915	1.6422	192.0036	191.0120	0.9915
WATER	kg/h	2582.9460	2.1403	2596.9252	13.9792	2582.9460
DEXTR-01	kg/h	0	0	0	0	0
CARBO-01	kg/h	0	7.0635	5.4976	5.4976	0
Mass fractions						
ETHANOL		0.0004	0.1514	0.0687	0.9075	0.0004
WATER		0.9996	0.1973	0.9293	0.0664	0.9996
DEXTR-01		0	0	0	0	0
CARBO-01		0	0.6513	0.0020	0.0261	0
Volumetric flow	l/min	43.6013	18.2609	54.3808	4.4063	50.0216

Source: Own Elaboration

3.5 Sensitivity analysis

One of the advantages of the simulation of the proposed system was that the performance sensitivity of the process to changes in the operating variables could be studied. With Aspen, the inputs were manipulated, and the effect was tabulated in a set of results according to the chosen variables. In general, the sensitivity analysis was performed to evaluate the parametric conditions of the process. The initial value for molar flux (glucose in aqueous solution) in the stoichiometric reactor was selected based on literature review (Cardona et al., 201; Gil et al., 2014) and subsequently investigated with sensitivity analysis (Figure 1.10).

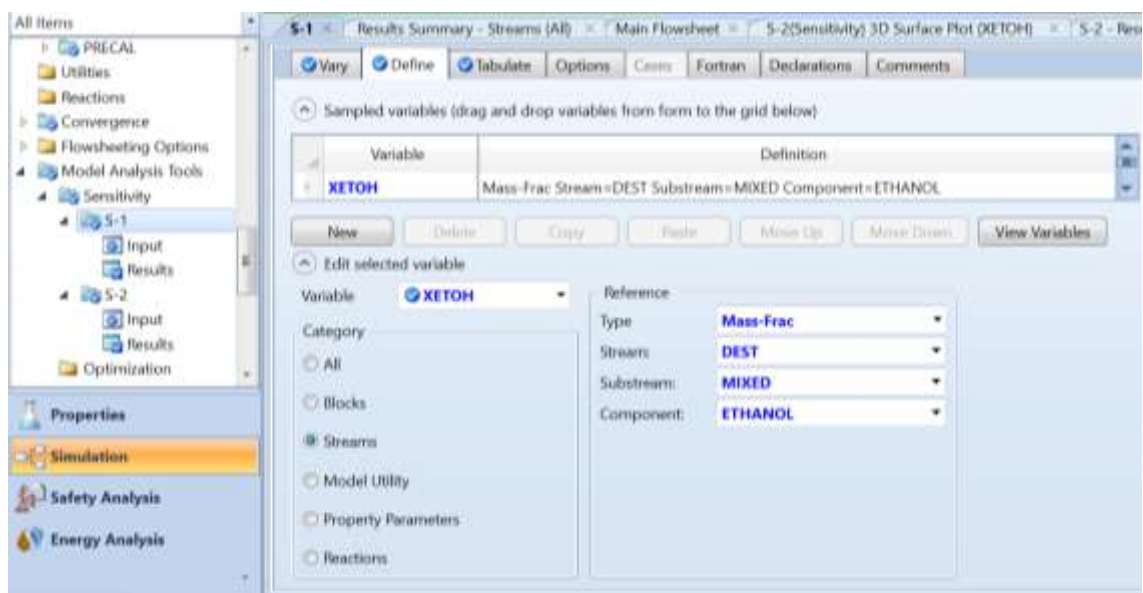
Figure 1.10 Sensitivity analysis of the manipulated variable



Source: Own Elaboration

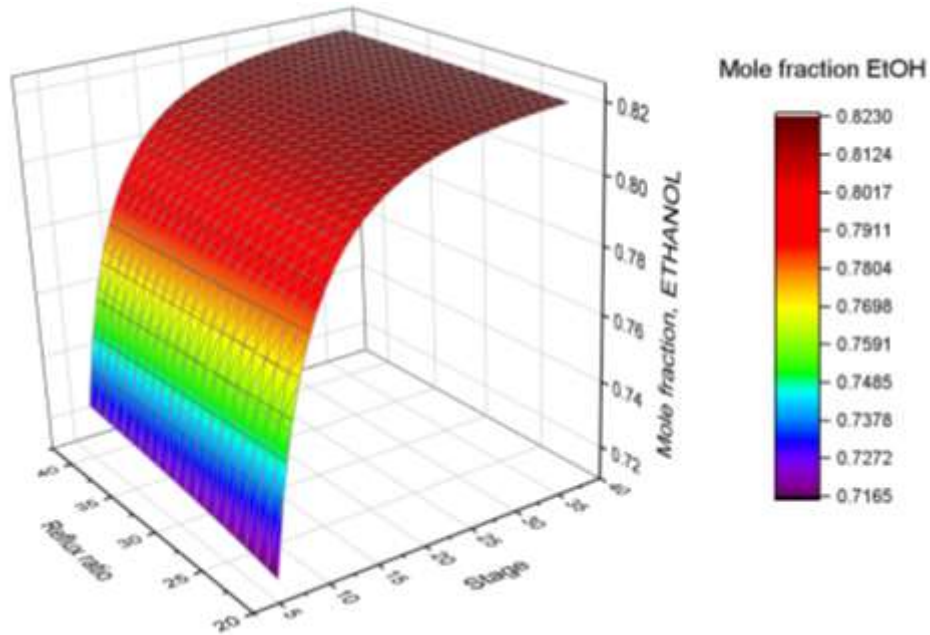
The influence of the molar flow rate in the reactor feed stream, the number of theoretical stages, as well as the reflux ratio required in the distillation column was analyzed with the purpose of maximizing ethanol production and making the process as cost-effective as possible. The sensitivity analysis was performed in the range of 50 to 600 kg/h of glucose in the reactor feed stream, while the reflux ratio was evaluated in the range of 20 to 40. For this analysis, the non-manipulable variable was the ethanol mass fraction in the upper stream of the distillation column (distillate) as shown in Figure 1.11. Thus, the process performance was evaluated through the manipulation of three independent variables (feed flow, column reflux ratio and number of caps) and one dependent variable (ethanol mass fraction). To analyze the influence of variables such as reflux ratio and feed stage on the distillation column, sensitivity analyses were developed using a surface plot (Figure 1.12). Through this tool, the reflux ratio values were varied from 20 to 40 and the feed stage from 5 to 40 to evaluate how the composition of anhydrous ethanol in the distillate stream changed. It is observed that as the feed stage approaches the kettle, the mole fraction of anhydrous ethanol increases, indicating that higher stages promote greater vaporization of the liquid fraction. This represents a benefit for the process because the objective is to obtain the highest possible purity in the separation of anhydrous ethanol. Regarding the reflux ratio, it was observed that it does not have a significant influence on the ethanol composition, i.e. an increase from 20 to 40 did not promote greater purity in the distillate composition.

Figure 1.11 Definition of parameters for sensitivity analysis as a function of the ethanol composition in the distilled product



Source: Own Elaboration

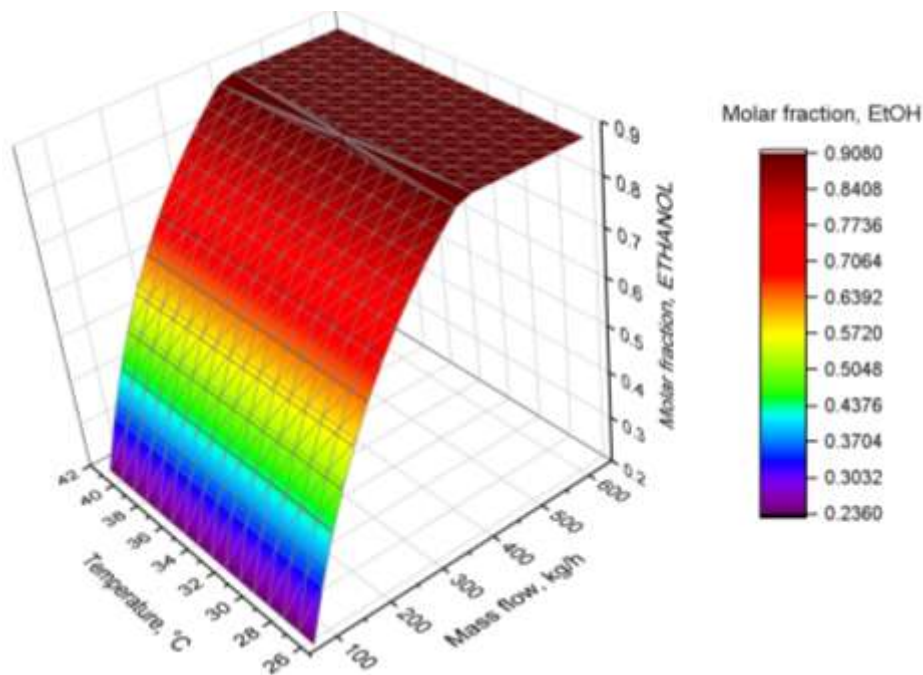
Figure 1.12 Influence of reflux ratio and number of stages on ETHANOL composition



Source: Own Elaboration

Additionally, the dependence of the ethanol mole fraction on the temperature and mass flow rate of the reactor feed stream was evaluated. Figure 1.13 shows that the temperature of the feed stream in the range of 25 to 40 °C has no effect on the ethanol mole composition. Therefore, operating the process with a temperature of 25 °C would be sufficient to achieve a maximum purity of 90% molar ethanol. Likewise, the mass flow of the feed stream evaluated in the range of 50 to 600 kg/h showed that a flow rate of 400 kg/h is sufficient to achieve maximum ethanol purity because at higher flow rates, the molar composition remains constant.

Figure 1.13 Temperature profile in the distillation column for ETHANOL/WATER



Source: Own Elaboration

4. Acknowledgment

The authors would like to thank the Technology of Superior Studies of Jocotitlán for the their kind supports provided for the realization of this research.

5. Conclusions

After evaluating the proposed process in Aspen Plus, we proceeded to the simulation of ethanol production from a stream of 380 kg/h of glucose and 1550 kg/h of water, also knowing that the temperature at which they enter the reactor was 27 °C, reactor temperature of 32 °C without pressure drop, and the distillation column was known to contain 40 plates, a reflux of 30, a flow rate of 148.44 kmol/h, the feed entered through plate 30 and the pressure of plate 1 was 5 bar.

Derived from the above, it was determined that the variables introduced are adequate for the process, this was evidenced by the execution of the simulation, otherwise it would not have achieved convergence. Thus, the distilled product stream with a total molar flow of 5.04 kmol/h had a composition of 82.15% mol of ethanol, 15.37% mol of water and 2.47% mol of carbon dioxide, while the bottoms stream with a total molar flow of 143.39 kmol/h had a composition of 99.99% mol of water with traces of ethanol and carbon dioxide.

Finally, one of the characteristics that stand out in the use of software is that they provide sufficiently reliable data for their application in professional engineering life, on the other hand, although the development of the calculations in an analytical way by an engineer is very good, it is always useful to use computational tools to facilitate the analysis of a process.

References

- Abdou Alio, M., Tugui, O.C., Rusu, L., Pons, A., Vial, C. 2020. Hydrolysis and fermentation steps of a pretreated sawmill mixed feedstock for bioethanol production in a wood biorefinery. *Bioresour. Technol.* 310, 123412. DOI: 10.1016/j.biortech.2020.123412. Retrieved July 4, 2022, from <https://pubmed.ncbi.nlm.nih.gov/32361645/>
- Alio, M.A., Tugui, O.C., Vial, C., Pons, A. 2019. Microwave-assisted Organosolv pretreatment of a sawmill mixed feedstock for bioethanol production in a wood biorefinery. *Bioresour. Technol.* 276, 170–176. DOI: 10.1016/j.biortech.2018.12.078. Retrieved July 4, 2022, from <https://www.sciencedirect.com/science/article/pii/S0960852418317498>
- Ardila, Y., Efren, J., Figueroa, J., Lunelli, B., Maciel Filho, R., Maciel, M. 2014. Simulation of ethanol production via fermentation of the synthesis gas using Aspen Plus TM. *Chem. Eng. Trans.*, 37 (2), 637-642. DOI: 10.3303/CET1437107. Retrieved July 4, 2022, from <https://www.aidic.it/cet/14/37/107.pdf>
- Ashraf, M.T., Schmidt, J.E. 2018. Process simulation and economic assessment of hydrothermal pretreatment and enzymatic hydrolysis of multi-feedstock lignocellulose – Separate vs combined processing. *Bioresour. Technol.* 249, 835–843. DOI: 10.1016/j.biortech.2017.10.088. Retrieved August 12, 2022, from <https://www.sciencedirect.com/science/article/pii/S0960852417319193>
- Bahry, H., Pons, A., Abdallah, R., Pierre, G., Delattre, C., Fayad, N., Taha, S., Vial, C. 2017. Valorization of carob waste: Definition of a second-generation bioethanol production process. *Bioresour. Technol.* 235, 25–34. DOI: 10.1016/j.biortech.2017.03.056. Retrieved August 12, 2022, from <https://www.sciencedirect.com/science/article/pii/S0960852417303267>
- Battista, F., Gomez Almendros, M., Rousset, R., Bouillon, P.-A. 2019. Enzymatic hydrolysis at high lignocellulosic content: Optimization of the mixing system geometry and of a fed-batch strategy to increase glucose concentration. *Renewable Energy* 131, 152–158. Retrieved August 12, 2022, from <https://doi.org/10.1016/j.renene.2018.07.038>
- Borand, M.N., Karaosmanoglu, F. 2018. Effects of organosolv pretreatment conditions for lignocellulosic biomass in biorefinery applications: A review. *J. Renewable Sustainable Energy* 10 (3), 033104. DOI: 10.1063/1.5025876
- Brown, T.R. 2015. A techno-economic review of thermochemical cellulosic biofuel pathways. *Bioresour Technol.* 178 166-176. DOI: 10.1016/j.biortech.2014.09.053. Retrieved May 18, 2022, from <https://pubmed.ncbi.nlm.nih.gov/25266684/>

- Cardona E., Llano B., Peñuela M., Peña J., Rios L.A. 2018. Liquid-hot-water pretreatment of palm-oil residues for ethanol production: an economic approach to the selection of the processing conditions. *Energy*, 160: 441-451. DOI: 10.1016/j.energy.2018.07.045. Retrieved May 18, 2022, from <https://www.sciencedirect.com/science/article/pii/S0360544218313409>
- Chandel, A.K., Garlapati, V.K., Singh, A.K., Antunes, F.A.F., da Silva, S.S. 2018. The path forward for lignocellulose biorefineries: bottlenecks, solutions, and perspective on commercialization. *Bioresour. Technol.* 264, 370–381. DOI: 10.1016/j.biortech.2018.06.004. Retrieved May 18, 2022, from <https://www.sciencedirect.com/science/article/pii/S0960852418307831>
- Chin, D.W.K., Lim, S., Pang, Y.L., Lam, M.K. 2020. Fundamental review of organosolv pretreatment and its challenges in emerging consolidated bioprocessing. *Biofuels, Bioprod. Bioref.* 14 (4), 808–829. DOI: 10.1002/bbb.2096. Retrieved May 18, 2022, from <https://onlinelibrary.wiley.com/doi/abs/10.1002/bbb.2096>
- Choi, J.-H., Jang, S.-K., Kim, J.-H., Park, S.-Y., Kim, J.-C., Jeong, H., Kim, H.-Y., Choi, I.- G. 2019. Simultaneous production of glucose, furfural, and ethanol organosolv lignin for total utilization of high recalcitrant biomass by organosolv pretreatment. *Renewable Energy* 130, 952–960. DOI: 10.1016/j.renene.2018.05.052. Retrieved August 12, 2022, from <https://www.sciencedirect.com/science/article/abs/pii/S0960148118305731>
- Chrysikou, L.P., Bezergianni, S., Kiparissides, C. 2018. Environmental analysis of a lignocellulosic-based biorefinery producing bioethanol and high-added value chemicals. *Sustain. Energy Technol. Assess.* 28, 103–109. DOI: 10.1016/j.seta.2018.06.010. Retrieved August 12, 2022, from <https://www.sciencedirect.com/science/article/abs/pii/S2213138817302679>
- Daylan, B., Ciliz, N. 2016. Life cycle assessment and environmental life cycle costing analysis of lignocellulosic bioethanol as an alternative transportation fuel. *Renew. Energy* 89, 578–587. DOI: 10.1016/j.renene.2015.11.059. Retrieved June 18, 2022, from <https://www.sciencedirect.com/science/article/pii/S0960148115304754>
- Devarapalli, M., Lewis, R.S., Atiyeh, H.K. 2017. Continuous ethanol production from synthesis gas by *Clostridium ragsdalei* in a trickle-bed reactor. *Fermentation* 3 (2), 1-13. DOI: 10.3390/fermentation3020023. Retrieved June 18, 2022, from <https://www.mdpi.com/2311-5637/3/2/23>
- Gabhane M. and Kapoor A., 2019. Simulation of ethanol production process using Aspen plus and optimization based on response surface methodology. *Res. J. Chem. Environ.* 23 (4), 80-89.
- García-Velásquez, Carlos A., Cardona, Carlos A. 2019. Comparison of the biochemical and thermochemical routes for bioenergy production: a techno-economic (TEA), energetic and environmental assessment. *Energy* 172, 232–242. DOI: 10.1016/j.energy.2019.01.073. Retrieved June 18, 2022, from <https://www.sciencedirect.com/science/article/abs/pii/S0360544219300751>
- Gil I.D., Gracia L.C., Rodriguez G. 2014. Simulation of ethanol extractive distillation with mixed glycerol as separating agent. *Braz. J. Chem. Eng.* 31(1): 259-270. DOI: 10.1590/S0104-66322014000100024. Retrieved May 22, 2022, from <https://www.scielo.br/j/bjce/a/CBzxwTCMZnvQmNTt9dGhHwr/>
- Gnansounou, E., Dauriat, A. 2010. Techno-economic analysis of lignocellulosic ethanol: A review. *Bioresour. Technol.* 101 (13), 4980–4991. DOI: 10.1016/j.biortech.2010.02.009 Retrieved July 4, 2022, from <https://www.sciencedirect.com/science/article/abs/pii/S0960852410002804>
- Hoang, P., Ko, J.K., Gong, G., Um, Y., Lee, S.M. 2020. Improved simultaneous co-fermentation of glucose and xylose by *Saccharomyces cerevisiae* for efficient lignocellulosic biorefinery. *Biotechnol. Biofuels* 13 (1). DOI: 10.1186/s13068-019-1641-2. Retrieved June 18, 2022, from <https://biotechnologyforbiofuels.biomedcentral.com/articles/10.1186/s13068-019-1641-2>

- Isikgor, F.H., Becer, C.R. 2015. Lignocellulosic biomass: a sustainable platform for the production of bio-based chemicals and polymers. *Polym. Chem.* 6, 4497–4559. DOI: 10.1039/C5PY00263J Retrieved May 22, 2022, from <https://pubs.rsc.org/en/content/articlelanding/2015/py/c5py00263j>
- Kim, S.M., Dien, B.S., Tumbleson, M., Rausch, K.D., Singh, V. 2016. Improvement of sugar yields from corn stover using sequential hot water pretreatment and disk milling. *Bioresour. Technol.* 216, 706–713. DOI: 10.1016/j.biortech.2016.06.003. Retrieved May 22, 2022, from <https://www.sciencedirect.com/science/article/pii/S096085241630801X>
- Kim, S.M., Tumbleson, M., Rausch, K.D., Singh, V. 2017. Impact of disk milling on corn stover pretreated at commercial scale. *Bioresour. Technol.* 232, 297–303. DOI: 10.1016/j.biortech.2017.02.005 Retrieved July 4, 2022, from <https://www.sciencedirect.com/science/article/abs/pii/S0960852417301104>
- Kumar, D., Singh, V. 2016. Dry-grind processing using amylase corn and superior yeast to reduce the exogenous enzyme requirements in bioethanol production. *Biotechnol. Biofuels* 9, 228. DOI: 10.1186/s13068-016-0648-1. Retrieved June 18, 2022, from <https://biotechnologyforbiofuels.biomedcentral.com/articles/10.1186/s13068-016-0648-1>
- Li K., Qin J.C., Liu C.G., Bai F.W. 2016. Optimization of pretreatment, enzymatic hydrolysis, and fermentation for more efficient ethanol production by jerusalem artichoke stalk. *Bioresour. Technol.*, 221: 188–194. DOI: 10.1016/j.biortech.2016.09.021. Retrieved July 4, 2022, from <https://www.sciencedirect.com/science/article/pii/S0960852416312767>
- Morales M., Arvesen A., Cherubini F. 2021. Integrated process simulation for bioethanol production: Effects of varying lignocellulosic feedstocks on technical performance. *Bioresource Technology* 328:124833. DOI: 10.1016/j.biortech.2021.124833. Retrieved May 16, 2022, from <https://www.sciencedirect.com/science/article/pii/S0960852421001723>
- Morales, M., Quintero, J., Aroca, G. 2017. Environmental assessment of the production and addition of bioethanol produced from *Eucalyptus globulus* to gasoline in Chile. *Int. J. Life Cycle Assess.* 22 (4), 525–536. DOI: 10.1007/s11367-016-1119-4. Retrieved July 4, 2022, from <https://link.springer.com/article/10.1007/s11367-016-1119-4>
- Nosrati-Ghods N., Naidoo M., Harrison S.T.L., Isafiade A.J., Tai S.L. 2020. Embedding Aspen Custom Modeller for Bioethanol Fermentation Into the Aspen Plus Flowsheet Simulator. *Chem. Eng. Transactions* 80, 289–294. DOI: 10.3303/CET2080049. Retrieved July 4, 2022, from <https://www.cetjournal.it/index.php/cet/article/view/CET2080049>
- Oliva, J.M., Negro, M.J., Alvarez, C., Manzanares, P., Moreno, A.D. 2020. Fermentation strategies for the efficient use of olive tree pruning biomass from a flexible biorefinery approach. *Fuel* 277, 118171. DOI: 10.1016/j.fuel.2020.118171. Retrieved May 16, 2022, from <https://www.sciencedirect.com/science/article/abs/pii/S0016236120311674>
- Olofsson J., Barta Z., Börjesson P. and Wallberg O. 2017. Integrating enzyme fermentation in lignocellulosic ethanol production: lifecycle assessment and techno-economic analysis. *Biotechnol Biofuels* 10(1), 51. DOI: 10.1186/s13068-017-0733-0. Retrieved May 16, 2022, from <https://biotechnologyforbiofuels.biomedcentral.com/articles/10.1186/s13068-017-0733-0>
- Rodrigues G., Errico, M., Rong, B.G. 2018. Techno-economic analysis of organosolv pretreatment process from lignocellulosic biomass. *Clean Technol. Environ. Policy* 20, 1401–1412. DOI: 10.1007/s10098-017-1389-y. Retrieved May 16, 2022, from <https://link.springer.com/article/10.1007/s10098-017-1389-y>
- Romaní, A., Larramendi, A., Yáñez, R., Cancela, A., Sánchez, A., Teixeira, J.A., Domínguez, L. 2019. Valorization of *Eucalyptus nitens* bark by organosolv pretreatment for the production of advanced biofuels. *Ind. Crops Prod.* 132, 327–335. DOI: 10.1016/j.indcrop.2019.02.040. Retrieved May 16, 2022, from <https://www.sciencedirect.com/science/article/abs/pii/S0926669019301414>

Sarks, C., Jin, M., Sato, T.K., Balan, V., Dale, B.E. 2014. Studying the rapid bioconversion of lignocellulosic sugars into ethanol using high cell density fermentations with cell recycle. *Biotechnol. Biofuels* 7 (1), 73. DOI: 10.1186/1754-6834-7-73. Retrieved May 16, 2022, from <https://biotechnologyforbiofuels.biomedcentral.com/articles/10.1186/1754-6834-7-73>

Sharma, B., Larroche, C., Dussap, C.-G. 2020. Comprehensive assessment of 2G bioethanol production. *Bioresour. Technol.* 313, 123630. DOI: 10.1016/j.biortech.2020.123630. Retrieved June 20, 2022, from <https://www.sciencedirect.com/science/article/abs/pii/S0960852420309020>

Singh, A. and Rangaiah, G.P. 2017. Review of technological advances in bioethanol recovery and dehydration. *Ind. Eng. Chem. Res.* 56 (18): 5147-5163. DOI: 10.1021/acs.iecr.7b00273. Retrieved June 20, 2022, from <https://pubs.acs.org/doi/10.1021/acs.iecr.7b00273>

Tan, L.i., Zhong, J., Jin, Y.-L., Sun, Z.-Y., Tang, Y.-Q., Kida, K. 2020. Production of bioethanol from unwashed-pretreated rapeseed straw at high solid loading. *Bioresour. Technol.* 303, 122949. DOI: 10.1016/j.biortech.2020.122949. Retrieved June 20, 2022, from <https://www.sciencedirect.com/science/article/abs/pii/S0960852420302182>

Vieira, S., Barros, M.V., Sydney, A.C.N., Piekarski, C.M., de Francisco, A.C., Vandenberghe, L.P.D.S., Sydney, E.B. 2020. Sustainability of sugarcane lignocellulosic biomass pretreatment for the production of bioethanol. *Bioresour. Technol.* 299, 122635. Retrieved June 20, 2022, from <https://www.sciencedirect.com/science/article/pii/S0960852419318656>

Zabed, H., Sahu, J., Suely, A., Boyce, A., Faruq, G. 2017. Bioethanol production from renewable sources: current perspectives and technological progress. *Renew. Sust. Energ. Rev.* 71, 475–501. DOI: 10.1016/j.rser.2016.12.076. Retrieved May 18, 2022, from <https://www.sciencedirect.com/science/article/abs/pii/S1364032116311339>

Zabed, H., Sahu, J.N., Boyce, A.N. and Faruq, G. 2016. Fuel ethanol production from lignocellulosic biomass: An overview on feedstocks and technological approaches. *Renewable Sustainable Energy Rev.* 66, 751-774. DOI: 10.1016/j.rser.2016.08.038. Retrieved May 18, 2022, from <https://www.sciencedirect.com/science/article/abs/pii/S1364032116304695>

Zhang, K.e., Pei, Z., Wang, D. 2016. Organic solvent pretreatment of lignocellulosic biomass for biofuels and biochemicals: A review. *Bioresour. Technol.* 199, 21–33. DOI: 10.1016/j.biortech.2015.08.102 Retrieved May 18, 2022, from <https://www.sciencedirect.com/science/article/pii/S0960852415012080>

Zhou, Z., Lei, F., Li, P., Jiang, J. 2018. Lignocellulosic biomass to biofuels and biochemicals: A comprehensive review with a focus on ethanol organosolv pretreatment technology. *Biotechnol. Bioeng.* 115 (11), 2683–2702. DOI: 10.1002/bit.26788. Retrieved May 18, 2022, from <https://onlinelibrary.wiley.com/doi/abs/10.1002/bit.26788>

Instructions for Scientific, Technological and Innovation Publication

[[Title in Times New Roman and Bold No. 14 in English and Spanish]

Surname (IN UPPERCASE), Name 1st Author†*, Surname (IN UPPERCASE), Name 1st Coauthor, Surname (IN UPPERCASE), Name 2nd Coauthor and Surname (IN UPPERCASE), Name 3rd Coauthor

Institution of Affiliation of the Author including dependency (in Times New Roman No.10 and Italics)

International Identification of Science - Technology and Innovation

ID 1st Author: (ORC ID - Researcher ID Thomson, arXiv Author ID - PubMed Author ID - Open ID) and CVU 1st author: (Scholar-PNPC or SNI-CONACYT) (No.10 Times New Roman)

ID 1st Coauthor: (ORC ID - Researcher ID Thomson, arXiv Author ID - PubMed Author ID - Open ID) and CVU 1st coauthor: (Scholar or SNI) (No.10 Times New Roman)

ID 2nd Coauthor: (ORC ID - Researcher ID Thomson, arXiv Author ID - PubMed Author ID - Open ID) and CVU 2nd coauthor: (Scholar or SNI) (No.10 Times New Roman)

ID 3rd Coauthor: (ORC ID - Researcher ID Thomson, arXiv Author ID - PubMed Author ID - Open ID) and CVU 3rd coauthor: (Scholar or SNI) (No.10 Times New Roman)

(Report Submission Date: Month, Day, and Year); Accepted (Insert date of Acceptance: Use Only ECORFAN)

Citation: First letter (IN UPPERCASE) of the Name of the 1st Author. Surname, First letter (IN UPPERCASE) of the First Coauthor's Name. Surname, First letter (IN UPPERCASE) of the Name of the 2nd Co-author. Surname, First letter (IN UPPERCASE) of the Name of the 3rd Co-author. Last name

Institutional mail [Times New Roman No.10]

First letter (IN UPPERCASE) of the Name Publishers. Surnames (eds.) Title of the Handbook [Times New Roman No.10], Selected Topics of the corresponding area © ECORFAN- Subsidiary, Year.

Instructions for Scientific, Technological and Innovation Publication

Abstract (In English, 150-200 words)

Text written in Times New Roman No.12, single space

Keywords (In English)

Indicate 3 keywords in Times New Roman and Bold No. 12

1 Introduction

Text in Times New Roman No.12, single space.

General explanation of the subject and explain why it is important.

What is your added value with respect to other techniques?

Clearly focus each of its features

Clearly explain the problem to be solved and the central hypothesis.

Explanation of sections Chapter.

Development of headings and subheadings of the chapter with subsequent numbers

[Title No.12 in Times New Roman, single spaced and bold]

Products in development No.12 Times New Roman, single spaced.

Including graphs, figures and tables-Editable

In the Chapter content any graphic, table and figure should be editable formats that can change size, type and number of letter, for the purposes of edition, these must be high quality, not pixelated and should be noticeable even reducing image scale.

[Indicating the title at the bottom with No.10 and Times New Roman Bold]

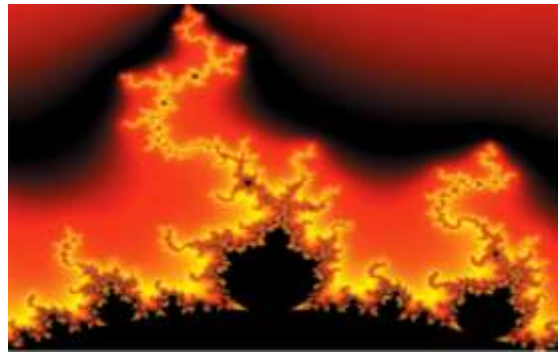
Table 1.1 Title

Variable	Descripción	Valor
V_V	Volumen de Venta	20000
P_V	Postura de venta	490.61
V_C	Volumen de Compra	20000
P_C	Postura de Compra	485.39
p^{Uh}	Precio último Hecho	491.61
V_o	Volumen Operado	1241979
P_u	Precio/Utilidad	0
p^{VL}	Precio/Valor Libro	0
U_a	Utilidad p/Acción	0
V^{La}	Valor Libro p/Acción	0

Source (in italics)

Should not be images-everything must be editable.

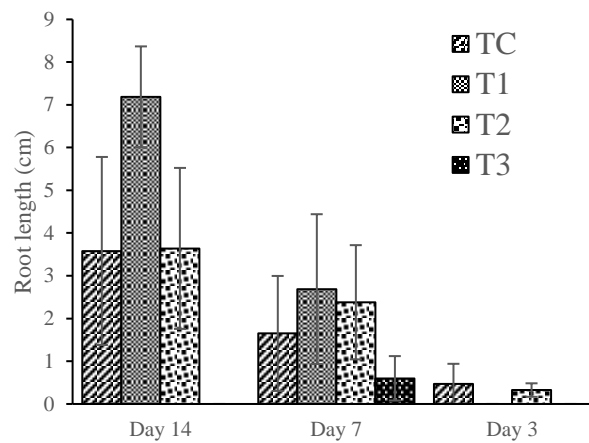
Figure 1.1 Title



Source (in italics)

Should not be images-everything must be editable.

Graphic 1.1 Title



Source (in italics)

Should not be images-everything must be editable.

Each chapter shall present separately in **3 folders**: a) Figures, b) Charts and c) Tables in .JPG format, indicating the number and sequential Bold Title.

For the use of equations, noted as follows:

$$\int_{lim^{-1}}^{lim^1} = \int \frac{lim^1}{lim^{-1}} = \left[\frac{1(-1)}{lim} \right]^2 = \frac{(0)^2}{lim} = \sqrt{lim} = 0 = 0 \rightarrow \infty \quad (1)$$

Must be editable and number aligned on the right side.

Methodology

Develop give the meaning of the variables in linear writing and important is the comparison of the used criteria.

Results

The results shall be by section of the Chapter.

Annexes

Tables and adequate sources

Instructions for Scientific, Technological and Innovation Publication

Thanks

Indicate if they were financed by any institution, University or company.

Conclusions

Explain clearly the results and possibilities of improvement.

References

Use APA system. Should not be numbered, nor with bullets, however if necessary numbering will be because reference or mention is made somewhere in the Chapter.

Use Roman Alphabet, all references you have used must be in the Roman Alphabet, even if you have quoted an Chapter, book in any of the official languages of the United Nations (English, French, German, Chinese, Russian, Portuguese, Italian, Spanish, Arabic), you must write the reference in Roman script and not in any of the official languages.

Technical Specifications

Each chapter must submit your dates into a Word document (.docx):

Handbooks title
Chapter title
Abstract
Keywords

Proceedings sections, for example:

1. *Introduction*
2. *Description of the method*
3. *Analysis from the regression demand curve*
4. *Results*
5. *Thanks*
6. *Conclusions*
7. *References*

Author Name (s)
Email Correspondence to Author
References

Intellectual Property Requirements for editing:

- Authentic Signature in Color of Originality Format Author and Coauthors
- Authentic Signature in Color of the Acceptance Format of Author and Coauthors
- Authentic Signature in Color of the Conflict of Interest Format of Author and Co-authors.

Reservation of Editorial Policy

ECORFAN Handbooks se reserva el derecho de hacer los cambios editoriales requeridos para adecuar la Obra Científica a la Política Editorial del ECORFAN Handbooks. Una vez aceptada la Obra Científica en su versión final, el ECORFAN Handbooks enviará al autor las pruebas para su revisión. ECORFAN® únicamente aceptará la corrección de erratas y errores u omisiones provenientes del proceso de edición de la revista reservándose en su totalidad los derechos de autor y difusión de contenido. No se aceptarán supresiones, sustituciones o añadidos que alteren la formación de la Obra Científica.

Code of Ethics - Good Practices and Declaration of Solution to Editorial Conflicts

Declaration of Originality and unpublished character of the Scientific Work, of Authorship, on the obtaining of data and interpretation of results, Acknowledgments, Conflict of interests, Assignment of rights and distribution

The ECORFAN-Mexico, S.C Directorate asserts to the Authors of the Scientific Work that its content must be original, unpublished and of Scientific, Technological and Innovation content to be submitted for evaluation.

The Authors signing the Scientific Work must be the same that have contributed to its conception, realization and development, as well as the obtaining of data, interpretation of the results, its writing and revision. The Correspondent Author of the proposed Scientific Work will request the form that follows.

Title of the Scientific Work:

- The sending of a Scientific Work to ECORFAN Handbooks emanates the commitment of the author not to submit it simultaneously to the consideration of other serial publications for it must complement the Format of Originality for its Scientific Work, unless it is rejected by the Arbitration Committee, may be withdrawn.
- None of the data presented in this Scientific Work has been plagiarized or invented. The original data are clearly distinguishable from those already published. And you have knowledge of the test in PLAGSCAN if a level of plagiarism is detected Positive will not proceed to arbitrate.
- References are cited on which the information contained in the Scientific Work is based, as well as theories and data from other previously published Scientific Works.
- The authors sign the Authorization Form for their Scientific Work to be disseminated by means that ECORFAN-Mexico, S.C. in its Holding Mexico consider relevant for the dissemination and dissemination of its Scientific Work by giving up its Scientific Work Rights.
- The consent of those who have provided unpublished data obtained by verbal or written communication has been obtained, and such communication and authorship are adequately identified.
- The Author and Co-Authors who sign this work have participated in its planning, design and execution, as well as in the interpretation of the results. They also critically reviewed the paper, approved its final version and agreed with its publication.
- No signature responsible for the work has been omitted and the criteria of Scientific Authorization are satisfied.
- The results of this Scientific Work have been interpreted objectively. Any result contrary to the point of view of those who sign is exposed and discussed in the Scientific Work.

Copyright and Access

The publication of this Scientific Work entails the transfer of the copyright to ECORFAN-Mexico, SC in its Mexico Holding for its ECORFAN Handbooks, which reserves the right to distribute on the Web the published version of the Scientific Work and the making available of the Scientific Work in this format supposes for its Authors the fulfillment of what is established in the Law of Science and Technology of the United States of Mexico, regarding the obligation to allow access to the results of Scientific Research.

Title of the Scientific Work:

Name and surnames of the Contact Author and the Coauthors	Signature
1.	
2.	
3.	
4.	

Principles of Ethics and Declaration of Solution to Editorial Conflicts

Publisher Responsibilities

The Publisher undertakes to guarantee the confidentiality of the evaluation process, it may not disclose to the Arbitrators the identity of the Authors, nor may it reveal the identity of the Arbitrators at any time.

The Editor assumes the responsibility of properly informing the Author of the phase of the editorial process in which the text is sent, as well as the resolutions of Double Blind Arbitration.

The Editor must evaluate the manuscripts and their intellectual content without distinction of race, gender, sexual orientation, religious beliefs, ethnicity, nationality, or the political philosophy of the Authors.

The Editor and his editing team of ECORFAN® Holdings will not disclose any information about the Scientific Work sent to anyone other than the corresponding Author.

The Editor must make fair and impartial decisions and ensure a fair peer arbitration process.

Responsibilities of the Editorial Board

The description of the processes of peer review is made known by the Editorial Board in order that the Authors know the evaluation criteria and will always be willing to justify any controversy in the evaluation process. In case of Detection of Plagiarism to the Scientific Work the Committee notifies the Authors for Violation to the Right of Scientific, Technological and Innovation Authorization.

Responsibilities of the Arbitration Committee

The Arbitrators undertake to notify about any unethical conduct by the Authors and to indicate all the information that may be reason to reject the publication of the Scientific Work. In addition, they must commit to keep confidential information related to the Scientific Work that they evaluate.

Any manuscript received for your arbitration must be treated as confidential, must not be displayed or discussed with other experts, except with the permission of the Editor.

The Referees should conduct themselves objectively, any personal criticism of the Author is inappropriate.

The Arbitrators must express their points of view with clear and valid arguments that contribute to the Scientific, Technological and Innovation of the Author.

The Arbitrators should not evaluate the manuscripts in which they have conflicts of interest and that they have been notified to the Editor before submitting the Scientific Work to evaluation.

Responsibilities of Authors

Authors must ensure that their Scientific Works are the product of their original work and that the data have been obtained in an ethical manner.

Authors must ensure they have not been previously published or are not being considered in another serial publication.

Authors must strictly follow the rules for the publication of Scientific Works defined by the Editorial Board.

Authors should consider that plagiarism in all its forms constitutes unethical editorial conduct and is unacceptable, consequently any manuscript that incurs plagiarism will be removed and not considered for publication.

Authors should cite publications that have been influential in the nature of the Scientific Work submitted to arbitration.

Information services

Indexing - Bases and Repositories

RESEARCH GATE (Germany)

MENDELEY (Bibliographic References Manager)

GOOGLE SCHOLAR (Citation indices-Google)

REDIB Ibero-American Network of Innovation and Scientific Knowledge-CSIC

Publishing Services

Citation and Index Identification H

Management of Originality Format and Authorization

Testing of Handbooks with PLAGSCAN

Evaluation of Scientific Work

Issuance of Certificate of Arbitration

Edition of Scientific Work

Web layout

Indexing and Repository

Publication of Scientific Work

Certificate of Scientific Work

Editing Service Billing

Editorial Policy and Management

143 – 50 Itzopan, Ecatepec de Morelos–Mexico. Phones: +52 1 55 6159 2296, +52 1 55 1260 0355, +52 1 55 6034 9181; Email: contact@ecorfan.org www.ecorfan.org

ECORFAN®

Chief Editor

VARGAS-DELGADO, Oscar. PhD

Executive Director

RAMOS-ESCAMILLA, María. PhD

Editorial Director

PERALTA-CASTRO, Enrique. MSc

Web Designer

ESCAMILLA-BOUCHAN, Imelda. PhD

Web Diagrammer

LUNA-SOTO, Vladimir. PhD

Editorial Assistant

REYES-VILLO, Angélica. BsC

Translator

DÍAZ-OCAMPO, Javier. BsC

Philologist

RAMOS-ARANCIBIA, Alejandra. BsC

Advertising & Sponsorship

(ECORFAN® -Mexico – Bolivia – Spain – Ecuador – Cameroon – Colombia - El Salvador – Guatemala -Nicaragua-Peru-Paraguay-Democratic Republic of The Congo, Taiwan), sponsorships@ecorfan.org

Site Licences

03-2010-032610094200-01-For printed material ,03-2010-031613323600-01-For Electronic material,03-2010-032610105200-01-For Photographic material,03-2010-032610115700-14-For the facts Compilation,04-2010-031613323600-01-For its Web page,19502-For the Iberoamerican and Caribbean Indexation,20-281 HB9-For its indexation in Latin-American in Social Sciences and Humanities,671-For its indexing in Electronic Scientific Journals Spanish and Latin-America,7045008-For its divulgation and edition in the Ministry of Education and Culture-Spain,25409-For its repository in the Biblioteca Universitaria-Madrid,16258-For its indexing in the Dialnet,20589-For its indexing in the edited Journals in the countries of Iberian-America and the Caribbean, 15048-For the international registration of Congress and Colloquiums. financingprograms@ecorfan.org

Management Offices

143 – 50 Itzopan, Ecatepec de Morelos–México.

21 Santa Lucía, CP-5220. Libertadores -Sucre–Bolivia.

38 Matacerquillas, CP-28411. Moralarzal –Madrid-España.

18 Marcial Romero, CP-241550. Avenue, Salinas 1 - Santa Elena-Ecuador.

1047 La Raza Avenue -Santa Ana, Cusco-Peru.

Boulevard de la Liberté, Immeuble Kassap, CP-5963.Akwa- Douala-Cameroon.

Southwest Avenue, San Sebastian – León-Nicaragua.

31 Kinshasa 6593 – République Démocratique du Congo.

San Quentin Avenue, R 1-17 Miralvalle - San Salvador-El Salvador.

16 Kilometro, American Highway, House Terra Alta, D7 Mixco Zona 1-Guatemala.

105 Alberdi Rivarola Captain, CP-2060. Luque City- Paraguay.

69 Street. YongHe district, ZhongXin. Taipei-Taiwan.

43 Street # 30 -90 B. El Triunfo CP.50001. Bogota Colombia



ISBN 978-607-8695-89-8



www.ecorfan.org